Seminar
on

Ice loads to marine structures in the Baltic Sea area

Building 116, Auditorium 82

DTU, Lyngby

3. June 2002

DANSK VANDBYGNINGSTEKNISK SELSKAB

DANISH SOCIETY OF HYDRAULIC ENGINEERING

v/ Helge Gravesen, Carl Bro as, Granskoven 8, 2600 Glostrup
Tlf. +45 4348 6328, Fax +45 4363 6567, email: hlg@carlbro.dk

DANSK VANDBYGNINGSTEKNISK SELSKAB
DANISH SOCIETY OF HYDRAULIC ENGINEERING

v/ Helge Gravesen, Carl Bro as, Granskoven 8, 2600 Glostrup
Tlf. +45 4348 6328, Fax +45 4363 6567, email: hlg@carlbro.dk

HSH

14.05.2002
HlG

Seminar on
Ice loads to marine structures in the Baltic Sea area

Time: Monday 3 June 2002, 14.30 – 18.00 hrs
Language: English
Bygning 116, Auditorum 82, Building 116, DTU, 2800 Lyngby

The main contents in the programme allows that the members of our society will get the opportunity to get an updated overview on design for ice loads been presented by one of the leading ice experts professor Mauri Määttänen, Helsinki University of Technology

14.30-15.15	Present design practice in Denmark. Experiences from recent ice model tests with wind turbine foundations by Helge Gravesen, Carl Bro and DTU
15.15-16.00	Experiences from field measurements of ice loads to light towers, professor Mauri Määttänen, HUT
16.00-16.15	Coffee break
16.15-17.00	Interpretation of results from ice model tests, professor Mauri Määttänen, HUT
17.00-17.45	Status of ice load estimate for wind turbine foundations in Baltic Sea area, professor Mauri Määttänen, HUT
18.00-19.30	Dinner Building 101
19.30-21.00	DVS Generalforsamling

Best regards
Helge Gravesen
chairman of DVS

Selected articles on ice loads will be available to the attendants

RESEARCH MEMO FOR DESIGN BASIS FOR ICE FORCES AT THE MIDDELGRUNDEN

Non-authorised translation by Rambøll, January 2000

1. INTRODUCTION

On behalf of SEAS, Helge Gravesen of Carl Bro has initiated a research of ice forces concerning preparation of design basis for the project regarding wind turbines at the Middelgrunden.

The research group consists of:

Helge Gravesen, Carl Bro A/S
Carsten Sørensen, RAMBØLL
N.-E. Ottesen Hansen, LIC Engineering A/S.

The research memo has been prepared within a limited time based upon the research group's existing knowledge on the basis of a draft from Carl Bro at an initial meeting 26 August 1999. The memo contains both comments and recommendations. The memo is primarily based upon a draft prepared by N.-E. Ottesen Hansen. Supplements and corrections are incorporated by Helge Gravesen, partly on the basis of comments from Carsten Sørensen and partly on the basis of a union meeting held 15 September 1999 at the premises of Carl Bro with participation of the research group and the following:

Lars Jørgensen and Per Vølund, SEAS
Sten Frandsen and Morten Lybech Thøgersen, Risø
René Zorn, DHI
Jørgen Pinholt, Elsamprojekt
Simon Green and Claus Gormsen, Niras
Torben Arnbjerg Nielsen, RAMBØLL
Jeppe Blak Nielsen, Carl Bro.

To the largest possible extent general demands to wind turbines in inner Danish waters have been worded.

2. SYMBOLS

U_{is}	velocity of the ice floes (m/s)
τ	shear tension on ice floe from air or water (pa)
c_D	drag coefficient on ice floe (= 0,004 and 0,006 for air and water, respectively) (-)
ρ	density of water and air, respectively (kg/m^3)/auxiliary parameter for ice load evaluation
V	water velocity 1 m below water surface or wind velocity at a height of 10 m (m/s)
c_u	compressive strength of the ice (pa)
σ_f	bending strength og the ice (pa)
t	thickness of the ice (m)
K_{max}	the total of the 24-hour mean of the frost period (<0°C)
ρ_{is}	density of the ice (900 kg/m^3)
Y_{is}	bulk density of the ice (8.84 kN/m^3)
γ_w	bulk density of the water (=ρ_wg) (N/m^3)
g	acceleration due to gravity (9.81 m/m^2)
E	elasticity module of the ice (2 GPa)
μ	friction coefficient (-)
F	ice load (N)
k	dimensionless factor on the ice load depending on the D/t ratio
D	diameter of the structure at the attack height of the ice, respectively the diameter of the conic structure at the water level line (m)
D_T	diameter at the top of the conic structure (m)
α	the angle with horizontal on the conic structure (°)
f_n	the eigenfrequency of the structure (s^{-1})
L	length of fissures in the ice (m)
ν	Poisson's ratio (-)
$\sigma_{c,lokal}$	local ice load (pa) on small area A_{lokal}
A_{lokal}	small area on the structure exposed to local ice load (m^2)
f_{is}	the frequency of the ice load (s^{-1})

3. DIMENSIONING FACTORS

In connection with the establishment of a wind farm a design basis will be prepared for ice loads.

The wind turbines are expected to have foundations with either vertical sides or being issued with a cone (directed upwards or downwards). Design basis shall comprise all these types. Ice load is not defined for structures dominated by fatigue loads.

In the design basis rules are to be specified for the following:

- The strength of the ice
- The friction between ice and turbine foundation
- The static load on the turbine foundation from ice floes
- The dynamic load on the turbine foundation from ice floes
- The load from icing up.

4. ICE FLOES

Ice loads on a structure result from the ice bumping against the structure or by the ice being pressed against the structure as a result of influence from current and wind. Thus there is an upper limit for the amount of ice loads, which may arise in the Øresund depending on forces of nature and the geography. The upper limit for the influences depend on:

a) The kinetic energy of the ice floes
b) Current and wind in the area
c) The size of the ice floes

The limit for the ice forces are evaluated by:

1. Maximum size of ice floe 2 × 2 km

2. Maximum current velocities and distributions of current velocities determinated for the area. It is assumed that the current line at the Drogden course is approx. twice the size of the current over the Middelgrunden. In connection with bid U_{is} = 1.0 m/s is estimated, since no correlation with wind is assumed

3. Wind and current load on ice floes are calculated on the basis of the formula:

   $\tau = 0.5\, c_D\, \rho\, V^2$
   where c_D = 0.004 and 0.006 for air and water, respectively
   ρ = density of water and air, respectively
   V = water velocity 1 m below the water surface or wind velocity at a height of 10 m, respectively.

The ice floes are assumed to have a shape so that the force initially is transferred to one wind turbine. As the ice floe is broken by a wind turbine, this will eventually come into contact with others.

As the basis for the above it may be noted that floes with a diameter of 500-2000 m and a thickness of up to 50 cm were observed in the waters opposite the Prøvestenen on a few days during the winter 1995/96. During the winter 1996/97 ice floes with a diameter of up to 20 m and a thickness of up to 5 cm were observed. SOK (1996 and 1997).

5. THE STRENGTH AND THE THICKNESS OF THE ICE

In the Øresundskonsortiet's Contract No. 2, Dredging & Reclamation, the following dimensioning ice thickness is stated in Design Requirement:

Recurrence period	5 years	10 years	50 years
t(m)	0.33	0.42	0.57

It is suggested to use the same basis for the Middelgrunden.

In the Elsam Project EFP-96 report about wind turbine foundations at sea the following strength parameters for the ice at a 50 years' ice situation at Rødsand are stated:

Compressive strength of the ice, σ_u	1.65 MpPa
Bending strength of the ice, σ_f	0.36 Mpa

It is suggested to use values for ice parameters approx. corresponding to those used by the Øresundskonsortiet for foundations for wind turbines situated at the Belts or further down towards the Baltic Sea, as these values are the newest for the area:

Return period	5 years	10 years	50 years	100 years	10,000 years
K_{max} (-°C 24 hours)	170	245	410	480	960
σ_u (Mpa)	1.0	1.5	1.9	2.0	2.6
σ_f (Mpa)	0.25	0.39	0.50	0.53	0.69
t (m)	0.33	0.42	0.57	0.63	0.91

where
σ_u = the thickness of the ice
σ_f = the bending strength of the ice
t = thickness of the ice = $0.032\ (0.9\ K_{max} - 50)^{0.5}$
K_{max} = the total of the 24 hours mean degree in the frost period (<0°C)

Other ice parameters:

Density of the ice, ρ_{is}	900 kg/m^3
Unit weight, Y_{is}	8.84 kN/m^3
Elasticity module, E	2 GPa
Friction coefficient between ice and ice is estimated to, μ	0.1

The 10,000 years' situation is included in case the ice load is treated as an accident load (without partial coefficients) and not as a natural load with characteristic parameters and appurtenant partial coefficients.

6. STATIC ICE LOADS

6.1 Structure with vertical sides

For determination of the ice load (crushing) on the wind turbines the application formulas stated in DS 410 for vertical structures are suggested. Structures are assumed to have vertical sides, the angle of which is less than 20°.

$$F = k\sigma_u Dt \qquad (6.2)$$

F	:	Horizontal ice force
k	:	Dimensionless factor depending on the D/t ratio
σ_u	:	The compressive strength of the ice
D	:	Diameter of the structure at the attack height of the ice
t	:	Thickness of the ice

$k = 1 + 3/(1 + D/t)$ for wind turbine foundations (with $D/t < 9$).

The above-mentioned formula originates from Tryde (1983).

6.2 Conic structures

For determination of the ice force (upbending ice, incl. share from crushing and ride-up) on the wind turbines the Ralston's formula for conic structures is used (API, Bul. 2N, 1995).

For an upward structure, see figure 1, the following formulas are used:

$$F_H = [A_1\sigma f t^2 + A_2\rho_w g\, t\, D^2 + A_3\rho_w g\, t\, (D^2-D_T^2)]A_4 \qquad (6.2)$$

$$F_v = B_1 F_H\, 0\, B_2\rho_w g\, t\, (D^2-D_T^2) \qquad (6.3)$$

F_H	:	Horizontal force on the conic structure
F_V	:	Vertical force on the conic structure
$\gamma_w=\rho_w g$	:	Unit weight of water
μ	:	Friction coefficient between ice and structure
σ_f	:	Bending strength of the ice
t	:	Thickness of the ice
D	:	Diameter of the conic structure in the water level line
D_T	:	Diameter at the top of the conic structure
α	:	Angle with horizontal on the conic structure

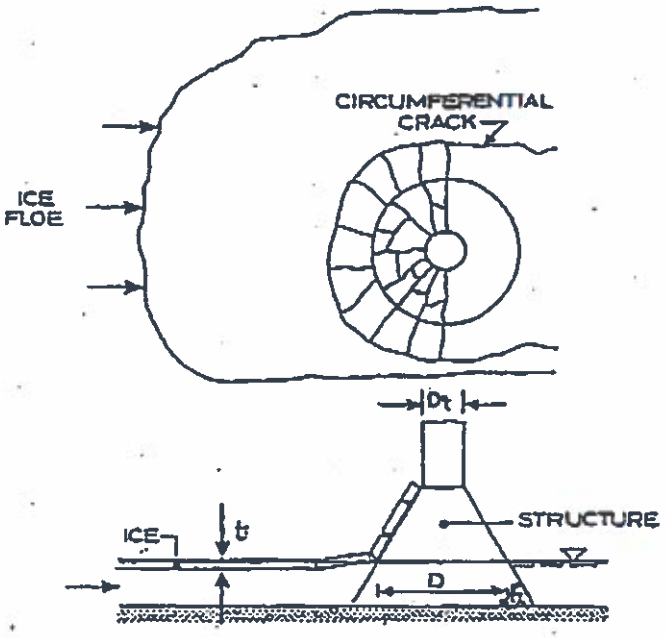

Figure 1. Ice floes pushed towards conic (upward) structure

The dimensionless coefficients, A_1, A_2, A_3, A_4, B_1, and B_2 are found from the figures in Enclosure 1. Often it will be more practical to use an auxiliary parameter ρ defined as a solution to the equation, cf. Thunbo Christensen (1988)

$$\rho - \ln(\rho) + 0.0830\,(2\rho + 1)\,(\rho - 1)^2\,(\gamma_w D^2/\sigma_f t) \tag{6.4}$$

Thus, A_1 and A_2 may be found analytically as

$$A_1 = (1 + 2.711\rho\,\ln(\rho))/(3(\rho - 1)) \tag{6.5}$$

$$A_2 = 0.075\,(\rho^2 + \rho - 2) \tag{6.6}$$

The correlation between ρ and $(\gamma_w D^2/\sigma_f t)$ is also shown on a figure in Enclosure 1.

If the conic structure is very steep ($\alpha > 70°$) the formulas (6.3) and (6.4) may be applied.

For a downward conic structure the formulas (6.3) and (6.4) may be applied with the correction that A_2, A_3, and B_2, read for an upward conic structure, are all multiplied by 1/9.

An attack point for the ice force is assumed between water level and 0.8 × ice thickness below the water level for a vertical construction. For an upward cone an attack point is estimated at the water level. For a downward cone an attack point 0.8 × ice thickness below the water level is estimated.

7. DYNAMIC LOADS

7.1 Vertical walls

It is suggested to use the method from LIC Engineering (1997).

By ice drift both dynamic and static influences arise. The natural vibrations of the structure will influence the breaking frequency of the ice, especially for structures with vertical sides, so that it is tuned to the eigenfrequency (lock-in). This means that the structure is influenced to vibrations in its eigenfrequency forms.

A conservative method for analysis of these vibrations is as follows.

The criterion for tuning is (cf. Singh et al (1990)):

$$U_{is}/t\, f_n > 0.3 \qquad (7.1)$$

U_{is} : The velocity of the ice floe
t : The thickness of the ice
f_n : The eigenfrequency of the structure

The load is applied as a serrate profile, see figure 2, where the maximum value is the static, horizontal ice load. After crushing of the ice the load is reduced to 20% of the maximum load. The load is applied with a frequency corresponding to the eigenfrequency of the structure. All eigenfrequencies fulfilling the tuning criterion shall be gone over.

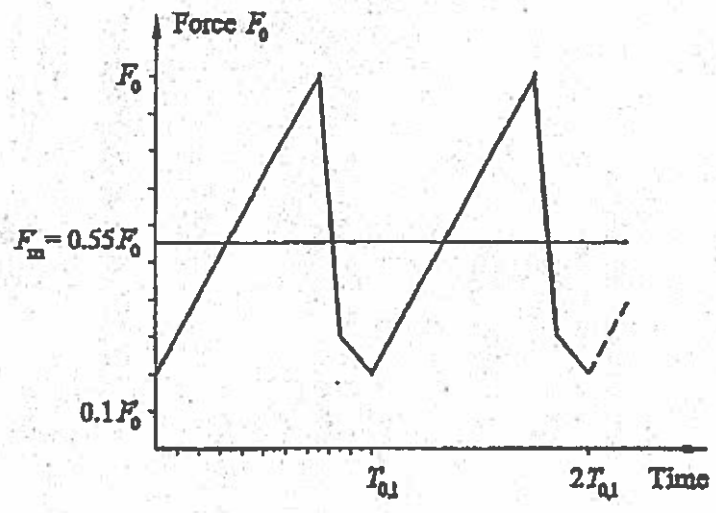

Figure 2. Serrate load profile

All subduing contributions in the structure are taken into account. Generalized contributions to be anticipated. Extra subduing as a consequence of the upfolding of the ice floes may be included if documentation therefore is available.

7.2 Conic structures

For conic structures the breaking frequency of the ice shall be calculated independent of the natural vibration of the structure. For all structures still applies that the frequency of

the ice load must not be close to the eigenfrequency of the structure / that the eigenfrequency of the structure must be minimum 20% outside the load frequency area for breaking ice.

The frequency from the ice load, f_{is}, may be determined as

$$f_{is} = U_{is}/L \qquad (7.2)$$

where
U_{is} is the velocity of the ice floe
L is the length of fissures in the ice

L is determined as

$$L = \rho\, D/2 \qquad (7.3)$$

where
D is the diameter of the cone at the water surface
ρ is determined from Enclosure 1, where ρ is given as function of $(Y_w D^2/\sigma_f t)$
σ_f = the bending strength of the ice
t = the thickness of the ice

The force is applied from the same assumed simplified model as shown in Figure 2 despite the breaking mechanism differs totally for conic structures compared to vertical structures.

The question regarding what is the best estimation for the length of the fissures and whether this changes from static to dynamic load case has been the subject of quite of few discussions.

Thunbo Christensen (1989) states

$$L = (0.5\, E\, t^3/(12\gamma_w(1-\nu^2)))^{0.25} \qquad (7.4)$$

This is also stated by Clough & Vinson (199x). In Tsinker (1991) Blanchet et al (1989) are quoted for the fact that the block typically is 4-5 times t.

Izumiyama et al (1991) quotes Tatinclaux (1986) for the following expression:

$$L/t = 0.26 - 0.54\, (\sigma_t/\gamma_w t)^{0.5} \qquad (7.5)$$

The fact that the velocity of the ice floe is included in the calculation expression for the length of the fissures is missing.

Carsten Sørensen has used a previous model for wedge-shaped structures (Sørensen, 1978), in which the velocity of the ice floe is included, for comparison of Ralston's (static) calculation with a wedge of approximately the same geometry, see Enclosure 2. It appears from the example that the dynamic calculation gives fissure lengths of 40% of Ralston's static calculation corresponding to a frequency of ice bumps of approx. 0.13 Hz.

It must be concluded that relatively wide limit of frequencies be assumed in order to give a safe design.

8. LOAD ON THE FOUNDATION FROM FROZEN ICE

In case the ice freezes on to the *foundation* a change of the water level will cause a vertical force on the pile.

The adhesion strength by shear breach for sea ice may be estimated to $\tau_0 < 0.1$ Mpa for structures of wood, steel, or concrete. The values correspond to an upper limit for the load.

Adhesion will appear only during quiet periods with neap tide.

It should be investigated whether the surrounding ice is able to absorb the force arisen in bending.

Values may be found in the literature Nakazawa et al (1994), Terashime et al (1999), and Tsinker (1991).

9. FRICTION ICE/WIND TURBINE FOUNDATION

The decisive factor for the friction between ice and wind turbines is the marine fouling on the wind turbines. A heavy fouling consisting of acorn barnacles and mussels increases the friction while a soft fouling consisting of plants does not increase the water resistance of the structure.

There will be sparse fouling of acorn barnacles below the ripple zone (lowest water level plus wave amplitude). Regarding ice forces the roughness from acorn barnacles is thus not taken into account. This means that normal roughness for concrete or steel will be used in the area where the ice attacks.

The value for friction coefficients is presented in for instance Nakazava et al, 1994.

By investigation of bridge piers and some of our own structures the hard marine fouling – acorn barnacles and mussels – appear below the ripple zone at low water. Some individuals may occur at the border but they will not contribute to a rough surface.

Besides, the few individuals that have settled at the water line are expected to be scoured off during building-up of an ice cover.

The following friction coefficients are used by calculation of ice forces.

Static: steel/ice: 0.2
concrete/ice: 0.3

Dynamic: steel/ice: 0.1
steel/concrete: 0.2

Marine fouling may be ignored.

The friction coefficients may be reduced if special covers are used, for which friction coefficients are given. The covers shall be of a nature so that at least they can be kept intact during an entire hard winter.

10. LOCAL ICE PRESSURE

The expression recommended by Thunbo Christensen et al (1995) is used:

$\sigma_{c,lokal} = \sigma_c(5t^2/A_{lokal} + 1)^{0.5}$

assuming that $\sigma_{c,lokal} < 20$ Mpa

At the same time the maximum load must be exceeded.

11. RAISING OF ICE

For a situation with a recurrence period of 50 years dimensioning for raising of ice to a minimum of level +7 m shall be used. Partial coefficient with earth pressure at rest from a large-grained mass with specific gravity 6 kN/m^3 should not be included.

12. ICING UP OF TURBINE TOWER

Norwegian standards state the following two load cases for icing up corresponding to 56° N latitude:

- spray from waves ice thickness max. 80 mm
- rain/snow ice thickness max. 10 mm

It is estimated that icing up is not a critical load case.

13. LITERATURE

Tryde, P. (1983): "Ice technique, the physical and mechanical properties of the sea ice. Ice forces on structures" (in Danish). Notes from 1983.

Nakazava, N., T. Terashima and H. Saeki, 1994: Ice Material Surface Interaction in Ice Friction and Ice-Adfreeze Bonding. Proceedings of the Fourth (1994) International Offshore and Polar Engineering Conference, Osaka, Japan, April 10-15, 1994.

Terashina, T., T. Kawai, A. Furya, K. Narita, N. Usani and H. Saeki, 1999: Experimental Study on Adfreeze Bound Strength between Ice and Pile Structures, Proceedings of the Ninth (1999) International Offshore and Polar Engineering Conference, Brest, France, May 40 – June 4, 1999.

SOK's Ice and navigation conditions in the Danish waters in winter 1995/96 and 1996/97, respectively (in Danish).

API (1995): "Recommended practice for planning, designing, and constructing structures and pipelines for arctic conditions", Bul. 2N, ed. 1995.

LIC Engineering (1997): "Mono-Pile Foundation. Wind turbine foundations at sea" (in Danish), EFP-96, J.nr. 1363/96-0006. Final report from 1997.

Thunbo Christensen (1988): "Calculation of Optimal Dimensionless Coefficients for Ralston's Plastic Limit Analysis Approach to Determination of Sheet Ice Loads on Conical Structures". Progress Report 66, ISVA, DTU, 1988.

Thunbo Christensen (1989): "Determination of extreme ice forces. Notes from a short course at University of Salford, with corrections from 1995.

Thunbo Christensen, F., Bruun, P. and sackinger, W.M. (1995): "Ice loading and pileup against vertical and inclined sea walls". ASCE task committee on inclined and vertical wall structures.

Ralston, T.D. (1977): "Ice force design considerations for conical offshore structures". Proc. 4th int. conf. on Port and Ocean Engng. under Arctic Conditions (POAC-77, vol. 2, pp. 13-31, Luleå, Sweden.

Ralston, T.D. (1979): "Plastic limit analyses of sheet ice load on conical structures". Physics and mechanics of ice. IUTAM symposium, Copenhagen, 1979.

Singh, S.K., Timeo, G.W., Frederking, R.M.W., and Jordan, L.J. (1990): "Test of ice crushing on a flexible structure". 9th Int. Conf. on Offshore Mechanics and Arctic Engng. Vol IV, pp. 89-94.

Clough & Vinson (199x): "Ice forces on fixed conical structures".

Tsinker (1995): "Marine structures engineering: Specialized applications". Chapman & Hall.

Blanchet, D., Churcher, A., Fitzpatrick, J., and Barda-Blanchet (1989): "An analysis of observed failure mechanics for laboratory first-year and multi-uear ice". In special report 89-5 by IAHR, edited by G.W. Timco.

Izumiyama, K., Kitagawa, H., Koyama, K., and Uto, S. (1991): "On the interaction between a conical structure and ice sheet". Proc. 11th int. conf. on Ports and Ocean Engng. under Arctic Cond., St. John's, Canada.

Tatinclaux (1986): Ice floe distribution in the wake of a simple wedge". Proc. OMAE'86, vol. 4.

Sørensen, C. (1978): Interaction between floating ice sheets and sloping structures. Series Paper 19, ISVA. DTU.

ENCLOSURE 1

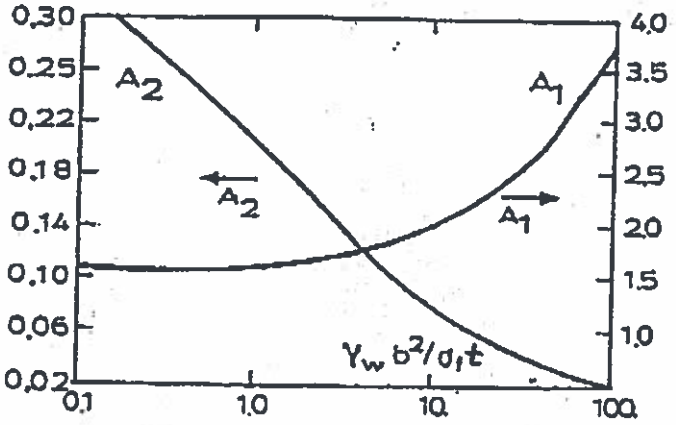
A2
A1
A2
A1
Yw b²/σ1t
0.30
0.25
0.22
0.18
0.14
0.10
0.06
0.02
4.0
3.5
3.0
2.5
2.0
1.5
1.0
0.1
1.0
10.
100.

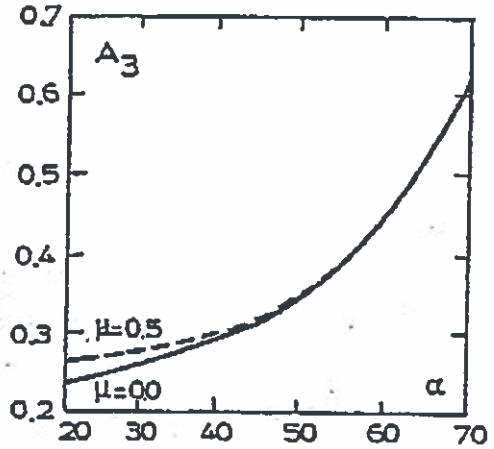
A3
μ=0.5
μ=0.0
α
0.7
0.6
0.5
0.4
0.3
0.2
20
30
40
50
60
70

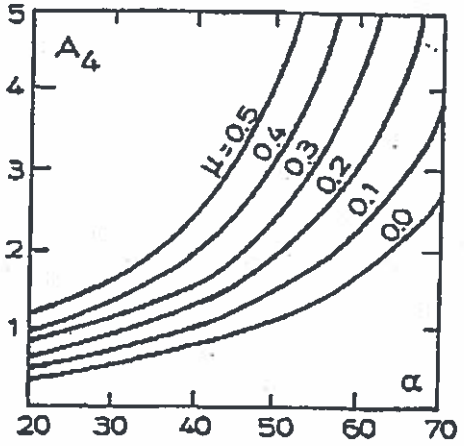
A4
μ=0.5
0.4
0.3
0.2
0.1
0.0
α
5
4
3
2
1
20
30
40
50
60
70

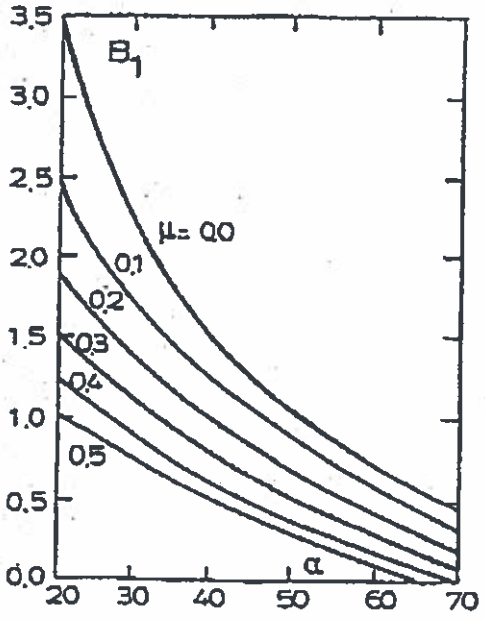
B1
μ= 0.0
0.1
0.2
0.3
0.4
0.5
α
3.5
3.0
2.5
2.0
1.5
1.0
0.5
0.0
20
30
40
50
60
70

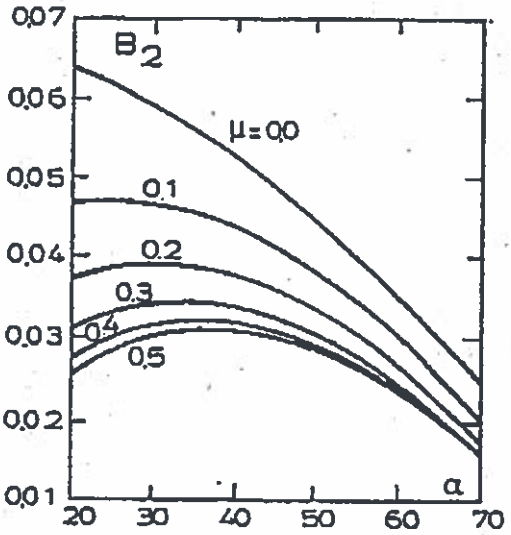
B2
μ=0.0
0.1
0.2
0.3
0.4
0.5
α
0.07
0.06
0.05
0.04
0.03
0.02
0.01
20
30
40
50
60
70

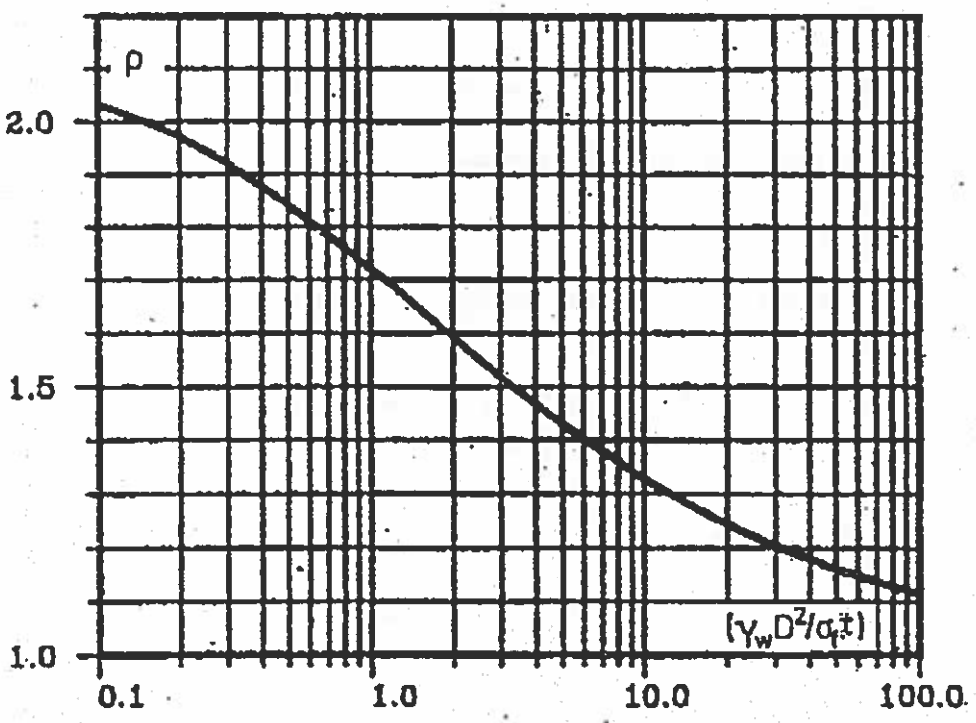
ρ
2.0
1.5
1.0
0.1
1.0
10.0
100.0
$(\gamma_w D^2/\sigma_t t)$

ENCLOSURE 2

Comparison of sundry formula expressions

A. CALCULATION ASSUMPTIONS

Structure with leaning front – Cone, cone angle = 45°, diameter = 8 m, tower diameter = 2 m.

Ice parameters: r_o = 1250 kN, r_f = 500 kN, h = 0.64m, velocity of floe u = 1 m/sec, friction factor = 0.2, crushing contact factor k = 0.7.

B. CALCULATION RESULTS

Load case	Horizontal ice movement				Vertical ice movement
Component	horizontal ice load (kN)	vertical ice load (kN)	ice breach, length (m)	ice bump frequency (Hz)	vertical ice load (kN)
method					
ref. 1	750	-680	7.9	0.13	
ref. 2	640	-520	3.1	0.32	

OMAE 1502

TEN YEARS OF ICE-INDUCED VIBRATION ISOLATION IN LIGHTHOUSES

M. Maattanen
University of Oulu
Department of Mechanical Engineering
Oulu, Finland

ABSTRACT

The concept of vibration isolation for slender fixed bottom-founded steel lighthouses was proposed in 1974 in order to avoid severe ice-induced vibrations during a level ice sheet crushing. After computer and scale-model simulations the first vibration isolated lighthouse was constructed in 1977 in the Gulf of Bothnia in Finland. Extensive telemetry measurement program in the first as well as in later models of the vibration isolated lighthouses has verified the operation of theoretical model also in the field. This far 9 steel lighthouses with the vibration isolation have been built offshore along the coast of Finland. A description of theoretical basis, technical solution, instrumentation and measurements are given, the newest lighthouse models are presented and the application possibilities of vibration isolation to other offshore structures are discussed.

INTRODUCTION

At the beginning of 1970's Finland extended its winter navigation by keeping the northernmost harbours open through the winter. In addition to increased ice breaker capability the shipping channels also had to be improved. Winding and narrow shipping channels in shallow seas required closely spaced aids-to-navigation. Due to the presence of moving ice floating buoys could not be used. In order to reduce the high cost of convetional caisson type fixed bottom-founded aids-to-navigation simple steel structures were developed.

The first steel aids-to-navigation were constructed in 1973 in the Gulf of Bothnia. Initial experiences were not promising: during crushing even thin ice sheets were inducing severe resonant vibrations in the superstructures of those slender steel structures. The adverse vibrations were especially persistent in lighthouses with a tall and heavy superstructure. Fatigue failures occured, and in some cases an overloading failure in foundation pile occured. On request by the Finnish Board of Navigation the University of Oulu started a research program to find out the origin of the adverse vibrations in steel lighthouses and to develop better design criteria.

The ice-induced vibrations were learnt to be self-excited by nature and the onset of vibrations dependent on the dynamic stability of the structure during dynamic ice-structure interaction. The concept of vibration isolated lighthouse was developed and the first structure completed in 1977. Field measurements have verified the expected behaviour both in the first and later models of the vibration isolated lighthouse. Now there are altogether 9 vibration isolated lighthouses in operation in the Finnish waters.

The vibration isolation in a lighthouse can be compared to that of a car. The excitation of the bumpy road is that of fluctuating ice loads, wheels, springs and shock absorbers have the counterpart of a vibration isolation section, and the car body is to be replaced by the superstructure of the lighthouse. With ice excitation there is an additional complication in the fact that the fluctuation of the ice load is dependent on the response of the structure. However, by observing the ice load dependence on the structural response in the design, adverse ice-induced resonant vibrations can be totally suppressed.

The development of steel lighthouses have been reported earlier (3, 4, 5). In this paper only a brief description of the development phase, theoretical models and laboratory testing is given. Highlights of the measurement data are presented and newest vibration isolated lighthouses introduced. Possibilities of utilizing the field proven vibration isolation concept to other offshore structures are considered. Promising application areas are structures in earthquake zones and arctic oil drilling or production platforms.

RESEARCH AND DEVELOPMENT

Compared to a gravity type caisson lighthouse the advantage of steel lighthouse is that the projectional area which is exposed to ice action can be made significantly smaller resulting in significantly reduced global ice loads. The disadvantage is that by fully utilizing the high strength of steel a slender bottom-founded structure becomes flexible and is prone to vibrations due to dynamic ice crushing loads. In-field observations have indicated resonant type vibrations.

The load of a moving ice sheet against a vertical

cantilever type bottom-founded structure will cause a structural deflection. With a flexible structure a lot of elastic energy will be stored before ice failure takes place. When the spring back of the structure occurs the elastic energy is released in ice crushing. As the spring back rate is added to the ice velocity, the relative velocity of the structure in relation to ice increases, and ice failure will occur at a higher strain rate in brittle mode. The result is a reduction in ice strength and an easier deflection rebound. The opposite takes places during the ice load build-up phase. The deflection rate reduces the relative velocity and strain rate yielding to a ductile ice behaviour and at a certain point to the maximum available ice strength.

During a complete ice load cycle there is an increase of ice strength during deflection build-up phase and a reduction during the deflection spring back phase. This promotes energy interchange from the ice to the structure and vice versa. Elastic energy is being first stored during the load build-up phase and later released during the spring back phase. Hence the structural response accelerates by itself during dynamic ice-structure interaction. The energy pumping into the structure can be regarded as negative damping which raises the question of dynamic stability. Indeed, in many cases flexible structures are dynamically unstable in ice crushing.

The analytical model for ice induced self-excited vibrations was presented by Määttänen, 1977, (4). The model is based on coupling the strain rate dependence of ice strength together with the dynamic equations of equilibrium of the structure. It is possible to predict which natural modes of the structure are dynamically unstable for the effects of laterally moving ice and then by numerical integration to solve the structural response, the limit cycles. Even though the model starts from an autonomous system of dynamic equations of equilibrium - with no time dependent ice load function - it predicts similar saw-tooth like ice force histories as what have been measured in field. Lately there has been other ice-induced vibration models that also take into account the effect of strain rate in ice crushing, (1, 7, 8).

The analytical model made it possible to vary structural properties in such a way that some of the natural modes could be made dynamically stable. The vibration isolated steel lighthouse is based on this concept. Structural stiffness and mass is adjusted in such a way that those natural modes which cause significant superstructure movements are made dynamically stable. In Fig. 1 there is an example. The superstructure modes 1, 2 and 4 are dynamically stable because less than 0.36 % of internal positive damping is enough to suppress the effect of ice induced negative damping. The third mode is aperiodically unstable, it would need 530 % modal damping to become stable. Hence there will be ice induced vibrations in the third mode and even resonance is highly likely. However, in the third mode there is practically no dynamic response in the superstructure and therefore it is no threat to the operation of the vibration isolated lighthouse. Due to the nature of the ice excitation the fifth or higher modes cannot contribute any significant vibration levels to the superstructue.

In 1974 the operation of lighthouse vibration isolation was simulated in a 1:2 scale model, (3), by using electro-hydraulic actuators to simulate the single pile foundation movement just under the vibration isolation section. As this model verified computer predictions a decision was made to construct a test lighthouse with the vibration isolation system. The Kokkola test lighthouse was completed in 1977 in the Gulf of Bothnia.

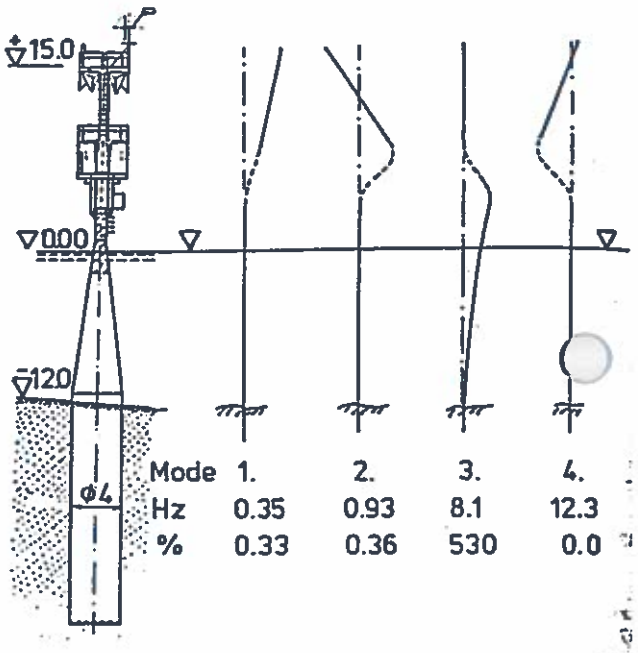

Fig. 1 The vibration isolated lighthouse Kemi-2, natural modes and frequencies, and modal damping required to suppress ice induced vibration

The operation of vibration isolation system was also tested in scale model tests in US Army CRREL ice tank in 1979. Again the vibration isolation system prevented resonant vibrations in superstructure natural modes, (6). Without a vibration isolation resonant vibrations always occured.

IN-FIELD EXPERIENCE

Environment

In summer 1986 there were 9 vibration isolated lighthouses in operation in Finnish waters. The total accumalated experience was 24 years. The oldest had functioned 9 years and the 4 newest were just installed. Most of the experience has been gathered from the northernmost part of the Gulf of Bothnia, around 65th latitude. Only one winter's experience was from south at 62nd latitude. The water depth in the lighthouse locations were from 8.7 to 17 m. The salinity of the brackish water was from 6 to 12 parts per thousand.

Air temperatures vary from +26 in summer to -35 in winter. During the last ten year period the maximum recorded wind speed was 39 m/s. Annual ice could be to 7 months. In landfast ice zone maximum ice thickness was 1.3 m, in the actively moving ice area level ice thickness has reached 0.9 m but there has been pressure ridges with sails over 2 m high and rafted together frozen ice with maximum thickness up to 1.5 m. At the location of Kemi-2 lighthouse, just outside the edge of landfast ice, maximum measured ice thickness was 1.2 and pressure ridge sail 2.0 m. Both these maximum tures had moved and loaded the lighthouse.

easuring system

To measure and monitor ice effects in vibration olated lighthouses a dedicated telemetery system was veloped in the Department of Electrical Engineering the University of Oulu, (2). Up to 5 transducers be measured simultaneously. The system is battery vered and it takes care of power and signal condi-ioning for strain gauges, accelerometers or LVDTs. ignals are amplified, multiplexed and transmitted quentially ashore to the receiving station. Scanning te is 79 Hz and all signals can be reproduced up to Hz frequency resolution in the demultiplexing unit the receiving station. At first signals were moni-red and plotted manually but later an automatic self-iggering remote tape recording system was added. The ceived signal could also be transferred, by using a lephone line and usual computer modem, to the Univer-ty of Oulu for real time monitoring or recording.

A usual measurement set-up included accelerometers h in the foundation and in the vibration isolated perstructure, relative displacement between the foun-tion and superstructure, and underwater strain gauges the foundation for global bending moment measure-nts. As the ice movement can take place from any rection two perpendicular components were measured a vector sum formed.

The deficiency of the telemetery system is that no formation of the ice velocity and thickness can be sured. However, ice thickness can be measured ctly after ice movements or estimated from ice maps.

asurement results

Some of the initial measurement data and experi-es is published in ref. (5). In the first vibration olated test lighthouse at Kokkola no significant ice fects were recorded by the telemetery system. A hanical pen plotter recorded usually only the move-nts due to wind action on the superstructure. One gle event induced a relative displacement of 89 mm peak to peak in the vibration isolation section. movement is 32 % from the displacement allowance. ording to computer simulation a 3.3 MN sudden ice relaxation could have caused the corresponding placement.

The second test application in 1978 was a vibra-isolated supestructure on top of an old foundation , Fig. 2. The most interesting results of these urements are published in (5). In this experiment old foundation was underdimensioned for existing conditions but it offered a stringent test for the ration isolation system. There were no shock ab-bers in the superstructure with most of the damping ced by special flexible beams in the vibration lation section. It was learnt that the net effect of induced negative damping was more than about 6 % for first natural mode at 0.48 Hz. Self-excited vibra-ns appeared but they were not severe. However, due the too flexible foundation the displacement allow-e between the foundation and the superstructure had e increased from initial 0.35 m to 0.55 m after to the arrest of movement were encountered in 1979. ay 1980, when the movement of landfast ice over-essed the foundation pile, which got a permanent linination, the vibration isolation saved the super-cture from any damage. Thereafter the superstruc-was installed on a new stiffer foundation at its ent location at Välikivikko about 10 nautical miles from the original location. Again measurements ified the existence of resonant type vibrations in first mode, (5). However, the dynamic response of superstructure is smooth with maximum accelerations than 0.3 g.

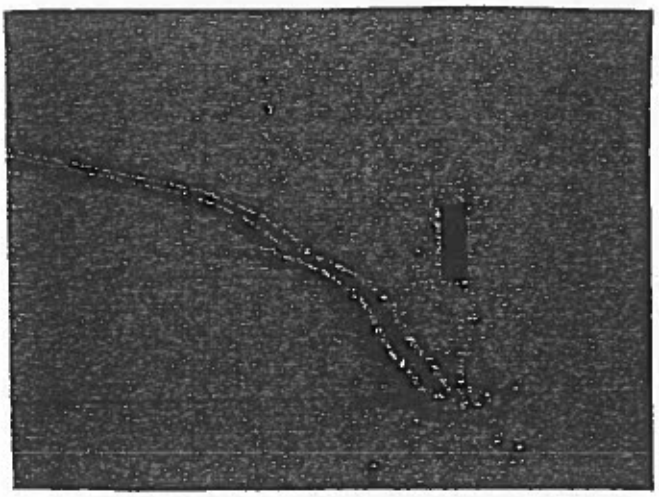

Fig. 2 The Välikivikko lighthouse.

The third application, lighthouse Kemi-2, Fig. 3, which was constructed in 1981, was the first one that was designed completely as a vibration isolated light-house. The location was the same where the 1973 con-structed first Kemi-2 steel lighthouse experienced fatigue failure in the superstructure due to resonant vibrations in 1973/74, (3), and later the collapse of the foundation pile in 1980, see the previous para-graph.

Fig. 3 The Kemi-2 lighthouse.

The cross section of the new Kemi-2 is shown in Fig. 1. The foundatin is a 4 m diameter single steel pile driven down to sea bottom. The superstructure has vibration isolation section starting 3.5 m above the

waterline. A 4 m diameter room for equipment and temporary occupation is 6.0 m above the sea level. A narrow shaft supports the top platform at 15 m level. On this platform there is a electrical lantern and a 150 W wind generator. Under the 15 m platform there are 6 large passive radar reflectors.

The superstructure natural modes are controlled by the stiffness of flexible beams in the vibration isolation section and by two concrete masses at 6 and 15 m level. The natural modes and frequencies are given in Fig. 1. The required damping - calculated according to the theory given in ref. (4), and based on Cook Inlet ice strength versus stress rate data - to make natural modes stable in relation to ice-induced vibrations, is also given. As the internal modal damping due to the vibration isolation section was already initially about 6 %, it can be seen that the superstructure modes are dynamically stable with a good margin. However, as the previous experiences indicated that over 6 % structural damping is required in the Gulf of Bothnia to totally avoid resonant type vibrations shock-absorbers were installed in the vibration isolation section to increase modal damping up to 15 %.

A lot of telemetery data has been recorded from Kemi-2. Depending on ice thickness and velocity different crushing frequencies have been recorded up to 9.2 Hz, 5.7 Hz in 0.3 m thick ice, Fig. 4, 2.5 Hz in 0.6 m thick ice, Fig. 5, and 1.1 Hz in 0.6 m thick ice, Fig. 6, which also indicates the stopping of ice movement. It is noteworthy that no resonant type vibrations in superstructure modes, e.g. at 0.35 Hz, have appeared. In some instances, Fig. 7 and 8, crushing frequency varied randomly from 0.1 to 0.5 Hz and was intermittently at 0.35 Hz but never persistedly locked to the lowermost natural mode frequency. This proves that this mode is dynamically stable. In structures with no vibration isolation crushing frequency was attracted and locked to the dynamically unstable natural mode in a wide ice velocity and frequency range. Even a 0.1 m thick sheet ice crushing could induce severe vibrations in the superstructure. Now with the vibration isolation the superstructure was always stable. A good proof is the smooth operation of the wind generator on top of the Kemi-2 lighthouse for over 5 years now.

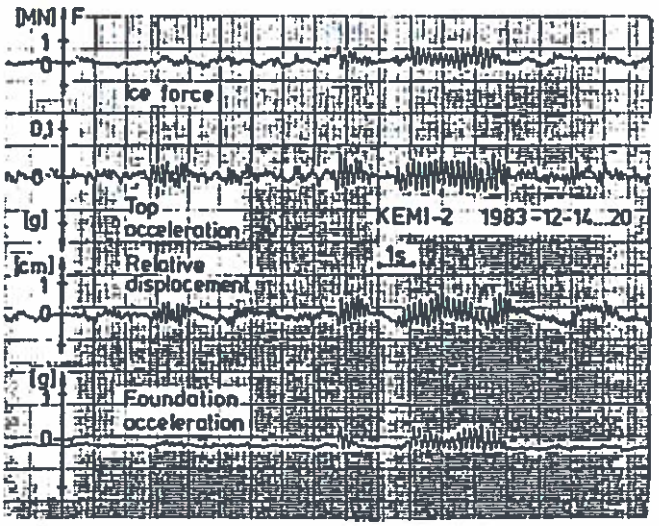

Fig. 4 Telemetery data, Kemi-2, ice thickness 30 cm.

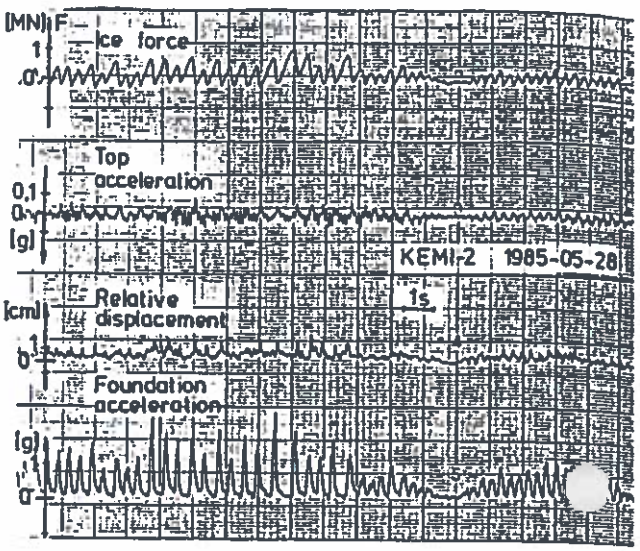

Fig. 5 Telemetery data, Kemi-2, ice thickness 0.5 m

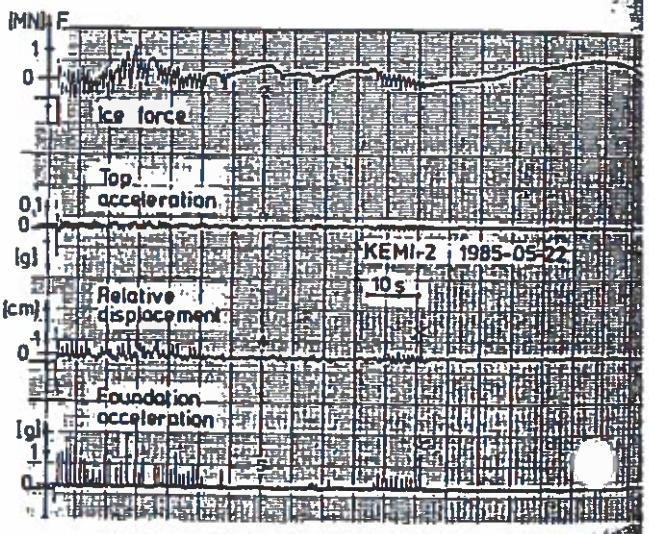

Fig. 6 Telemetery data, Kemi-2, ice thickness 0.6 m

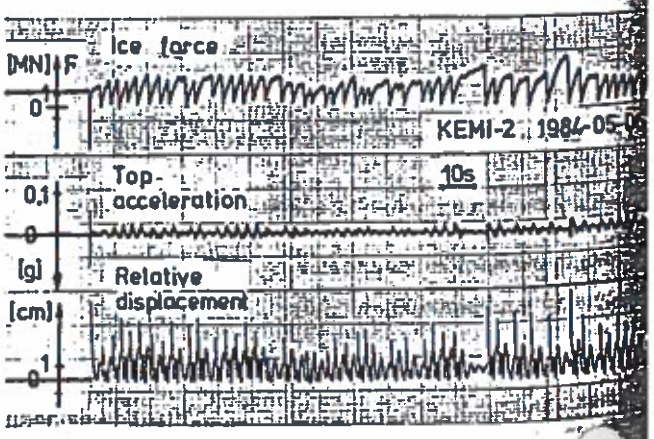

Fig. 7 Telemetery data, Kemi-2, ice thickness 0

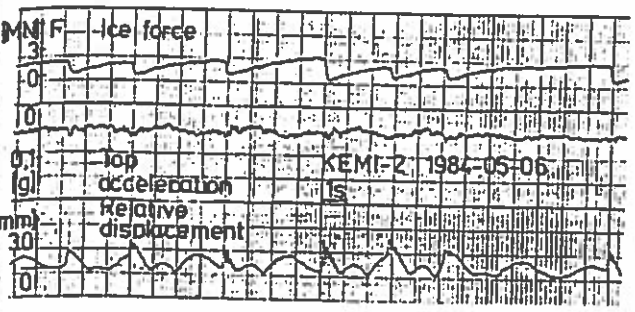

Fig. 8 Telemetery data, Kemi-2, ice thickness 0.6 m.

The maximum recorded ice load against Kemi-2 has been 3.9 MN, Fig. 7. At the instant of ice failure the superstructure acceleration has been only 0.07 g. Foundation accelerations up to 4 g have been recorded. Even higher static ice forces could have occured since the telemetery signal recording is triggered on only by the dynamic ice action. E.g., the Kemi-2 lighthouse has experienced a slow movement of 1.28 m thick level ice but the recording was not triggered. The nominal design level ice load was 6.4 MN in a 1.2 m thick ice. In pressure ridges even higher static type ice loads might have been encountered. In a first year pressure ridge with a 2 m high sail the keel has been down to sea bottom at 12 m waterdepth. Together with the parent level ice the total design pressure ridge load is 13 MN.

Wave loading

The advantage of slender foundation pile is that the wave loads are small. Usually wave loading is insignificant when compared to ice loads. However, if the wave crest is high enough to hit the superstructure that lies on weak beam springs the effect is different. The designed operation is such that the wave load pushes the superstructure against its movement limit and thereafter the whole superstructure behaves as a continuous structure. After the wave passes the springs rebound the superstructure back to center. However, the nominal design is such that the maximum waves should not reach to those parts of the superstructure that are supported by the springs.

In September 1984 a record south-west storm moved along the Gulf of Bothnia and caused the water level to rise 2.2 m just 20 km north from Kemi-2. It is estimated that the storm surge was about 2 m also at the location of Kemi-2. This is one meter above the design consideration, which made it possible for storm waves to hit the bottom of the superstructure at 6 m above the normal waterline. The only result was a burst rubber seal between the foundation and superstructure at the 6 m level. The vibration isolation performed as expected.

NEW LIGHTHOUSES

After the good experiences of the two test lighthouses and Kemi-2 the Finnish Board of Navigation fully accepted the vibration isolated lighthouse for its aids-to-navigation program. In 1985 two sister lighthouses for Kemi-2 were constructed, one to Pietarsaari and one to Pori. Experience from the first winter's operation was similar to that of Kemi-2 with no resonant superstructure vibrations and undisturbed smooth running of wind generators.

A new philosophy was emerging in the desing of aids-to-navigation. The radar was becoming more common in small crafts and it was realized that the visual range of even the most powerfull lighthouse lanterns was very limited in fog or in bad weather when aids-to-navigation are most badly needed. Hence lighthouses were developed to be better visible in radar screens and the lantern was becoming a secondary aid. Both passive large radar reflectors and active racons were installed. This approach made it possible to automate lighthouses and reduce significantly the required power. Small wind generators or solar cells are sufficient to run the racons and the small electrical lanterns.

In summer 1986 four new radar lighthouses, Fig. 9. a, were constructed to the south-western corner of Finnish waters near the Swedish border. The design includes a 20 m tall vibration isolated superstructure with a helicopter platform on top, passive radar reflectors with corner length 1.5 m, a racon and a small electrical lantern. Electronics are battery powered with solar cell recharging. The foundation steel pile is moulded in concrete in a rock pit at a water depth up to 17 m. The construction cost of these radar lighthouses was less than one third of a conventional gravity type lighthouse for the same ice conditions and water depth.

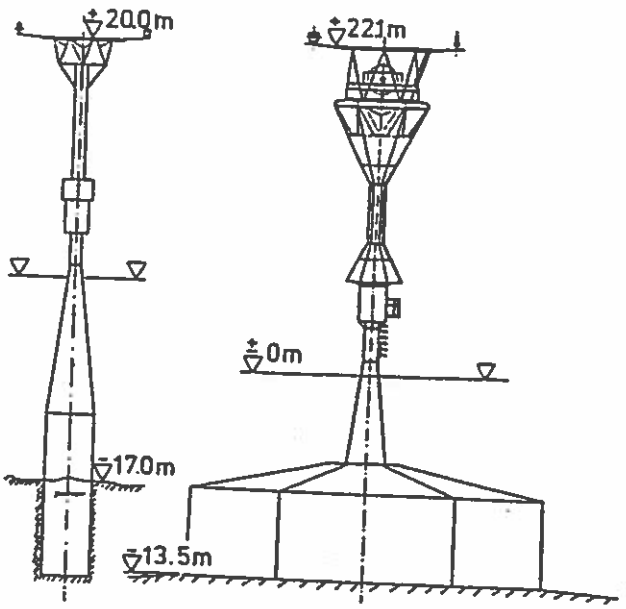

Fig. 9 a) A Radar lighthouse.
b) The Lion of Finland.

The largest of vibration isolated lighthouses thus far is now under construction and it will be completed in summer 1987. The Lion of Finland will be the first lighthouse when arriving to Finnish waters in the Baltic. The cross section of the Lion of Finland is presented in Fig. 9. b. The helicopter platform at 22 m level is supported above the wind generator by a trusswork. It is expected that the helicopter platform would protect the windgenerator from helicopter downwash. There are two rooms for equipment and temporary occupation at 15 and 17 m levels. Passive radar reflectors with a corner length of 1.5 m are embedded in the walls of the upper room. The racon and electrical lantern are 22.7 m above sea level on the helicopter platform. The vibration isolation section is between levels 3.7 and 8 m. Concrete masses at the 6 m level and on the helicopter platform are used to tune superstructure natural modes. The foundation is a concrete caisson at the 14 m

water depth and a steel pile up from the -6 m level. Superstructure modes are dynamically stable in relation to ice induced vibrations. As an additional safety precaution there are also shock absorbers in the vibrations isolation section.

APPLICATION POSSIBILITIES

The vibration isolated steel lighthouse has been proved to be a cost effective and reliable choice as an aid-to-navigation in the Northern Baltic. It is a minor step to extend the foundation design to withstand ice loads in future arctic shipping channels where level ice thickness can reach up to 2 m.

Another straightforward application is as an aid-to-navigation in earthquake zones. Then it is not the question of dynamic stability but of pure vibration isolation. The displacement allowance up to 0.55 m to any direction laterally between the foundation and the superstructure has been tested in-field. The effects of foundation movement due to ice excitation are more difficult to isolate in the superstructure than foundation movement in the earthquake case because the latter are random and the former tend to resonate with superstructure modes. Normally the foundation excitation frequencies are higher and amplitudes lower in earthquake excitations.

Some arctic offshore oil drilling or production platforms can also utilize the concept of vibration isolation. The possibility of severe ice-induced self-excited resonant vibrations is a risk for monopodes or multi-legged structures. By cutting the rigid connection between the foundation and superstructure and supporting the superstructure on spring elements, the superstructure natural modes can be made dynamically stable. Then significant ice-induced vibrations will occur only in foundation modes which are no threat for the superstructure. The vibrations isolation system can easily be designed to carry the total weight of the superstructure. Depending on the magnitude of ice induced movements on top of the foundation even a bridge bearing type isolation can be adequate.

CONCLUSIONS

In-field experiences have indicated that ice crushing againts slender offshore structures can induce severe resonant vibrations. Vibration isolation is an efficient method to prevent superstructure vibrations and to retain the cost effectiveness of steel structures in lighthouses and other offshore structures that have to withstand loads excerted by moving ice.

The origin of ice-induced vibrations is traced into the energy interchange between the structure and ice in dynamic interaction. By observing strain rate effects continuously in different phases of a structural vibration cycle a theoretical model is developed to predict the onset of ice-induced vibrations, dynamic stability and limit cycles.

In structural design natural modes can be tailored in such a way that those modes that exhibit significant superstructure movements will by dynamically stable for ice excitation. With a vibration isolation system this goal can be easily achieved.

Experiences and measurements of vibration isolated steel lighthouses in the Gulf of Bothnia have verified theoretical expectations. In dynamically stable natural modes no resonant vibrations have occured. However, the magnitude of ice induced negative damping has been larger than what was originally estimated from laboratory test data. Modal damping between 5 to 15 % is required to totally suppress ice induced resonant vibrations.

After good in-field experiences and due to low cost several new vibration isolated lighthouses have been built in Finnish waters. Now there are 9 units in operation and the tenth under construction. The newest design includes large passive radar reflector, racon, electrical lantern, wind generator or solar cells and helicopter platform.

The concept of vibration isolation can be extended to arctic offshore lighthouses and to lighthouses in earthquake zones. Also the superstructures of arctic offshore oil drilling or production monopodes or multi legged structures can be made dynamically stable with a vibration isolation system.

REFERENCES

1. Daoud, D. and Lee, F., "Ice-Induced Dynamic Lo on Offshore Structures." Proc. OMAE-86, pp. 212-218. ASME, New York 1986.
2. Leppänen, P., Myllylä, R. and Kostamovaara, J., "A Telemetery System for Measurement of Ice Load upo Aids-to-Navigation." Proc. POAC-83, pp. 1045-1054, Tech. Res. Centre of Finland, Espoo 1983.
3. Määttänen, M., "Experiences of Ice Forces agai a Steel Lighthouse Mounted on the Seabed and Constru tional Refinements." Proc. POAC-75, pp. 857-869. University of Alaska, Fairbanks 1975.
4. Määttänen, M., "Stability of Self-Excited Ice-Induced Structural Vibrations" Proc. POAC-77, pp. 6 694. Memorial University of Newfoundland, St. John' 1977.
5. Määttänen, M., "Experiences with Vibration Isolated Lighthouses." Proc. POAC-81, pp. 491-501. Universite Laval, Quebec City 1981.
6. Määttänen, M., "Dynamic Ice-Structure Interact During Continuous Crushing." CRREL Report 83-5, US Army CRREL, Hanover, NH, 1983.
7. Toyama, Y., Sensu, T., Minami, M. and Yashima, "Model Tests on Ice-Induced Self-Excited Vibration o Cylindrical Structures." Proc. POAC-83, pp. 834-844 Tech. Res. Centre of Finland, Espoo 1983.
8. Xu, J., Shi, Q. and Meng, Z., "Features of Fre quency and Amplitude in Ice-Induced Vibration of a Jacket Platform." Proc. POAC-83, pp. 952-959 ch Res. Centre of Finland, Espoo 1983.

IAHR Ice Symposium 1996
Beijing

ICE FAILURE AND ICE LOADS ON A CONICAL STRUCTURE – KEMI-I CONE FULL SCALE ICE FORCE MEASUREMENT DATA ANALYSIS

Mauri Määttänen[1] Anita Nortala Hoikkanen[2] John Avis[3]

ABSTRACT

Full scale ice force measurements were conducted through a joint Finnish industry project in 1984-87 with a conical test section at the Kemi-I lighthouse in the Northern Baltic. However, detailed data analysis results were not fully realized until late 1995, after a joint industry project with several North American oil companies. Kemi-I cone ice force data was analysed for average, maximum, standard deviation, peak load distribution shapes, and frequency content. Different ice loading scenarios include level ice, rafted ice and first year ridges. The results give, for the first time, a clear picture of different ice failure and clearing modes for a full scale conical structure. Ice failure in full scale occurs in multi-modal fashion by bending, shearing, and crushing. Rubble pile formation in front of the cone is common. Its geometry and volume were analysed. The measured ice force values were compared to existing theoretical model predictions. In general, the predicted loads are higher than those actually measured regardless of the rubble pile effect. In particular, dependence to ice thickness is significantly lower. This knowledge of ice failure modes, data analysis results, statistical distributions, and validated theoretical models give means for the reliable design of economical conical offshore structures in ice infested waters.

INTRODUCTION

The design of concical structures to withstand ice forces has been based on empirical models derived from small scale test results, (Edwards et al 1976, Brooks 1981), or on theoretical models with assumed ice failure and clearing modes, (Bercha et al 1975, Croasdale et al 1993, Izumiayama et al 1993, Nevel 1992, Ralston 1977). Many scale model tests have been conducted and reported. Theoretical cone ice force models have been developed for over twenty years but full-scale data is scarce. In-field full-scale measurements were conducted during the years 1984-1987 in the Gulf of Bothnia, as a joint Finnish industry project, by using an instrumented steel cone at Kemi-I lighthouse. The cone diameter at waterline was 10 m with a cone angle of 55°. Ice was of low salinity with all varieties of first year ice features.

Most of the project funding was expended during the test cone offshore installations thus what was remaining after the measurements did not allow a detailed analysis of results to be conducted. Hence only preliminary results of the data have been available thus far, (ie, ice force plots only).

In 1989, an International Joint Industry Project with five major American oil companies was formed to conduct more measurements at the Kemi-I cone. The plan was to have more instrumentation for vertical load component measurements, and for more comprehensive ice data measurement and monitoring. However weather conditions at sea delayed installations leaving the cone sections unsafe which resulted in gradual cone dismantling due to wave action before actual measurements were to start. As an alternative program, in early 1994 it was decided to carry out a more thorough analysis of the existing Kemi-I cone ice force data. The actual analysis work was conducted at the Helsinki University of Technology, with project management by Kvaerner Masa Marine Inc. in North America.

The objectives were to compile and evaluate the Kemi-I test cone data, carry out detailed data analysis, link measured ice force histories to factual information on environmental parameters, compare existing cone ice force theories to the measured cases, verify new findings, propose

[1]Professor, Helsinki University of Technology, Otakaari 4, SF-02150 Espoo,Finland.
[2]Research Engineer, Kvaerner Masa Yards, Kaanaantie 3, SF-00560 Helsinki,Finland
[3]Vice President, Kvaerner Masa Marine Inc., 201 Defense Hwy., Ste 202, Annapolis, MD 21401, USA

improvements for cone ice force calculations, and validate a reliable ice force design model. The data analysis was conducted during February-September 1994.

The full report was completed in March 1995, (Tam et al.). Access to the detailed data is limited to the partners of the project; however, this paper describes some of the most important findings of the data and results of the analysis that the partners have agreed to share.

MEASUREMENT DATA

Measurements were carried out to full extent during the winters 1984/85 and 1985/86, and with minimal instrumentation in 1986/87. The first winter was characterised with level ice and a lot of movement, and the second with many pressure ridges. Both these winters were more severe than average, with a probability less than once in 50 years.

Kemi-I measurement data include 65 different digital ice force history records, analog instrumentation tape recordings, strip chart records, some 50 hours video records, plenty of color prints and slides, and personal notes in addition to ice and meteorological data.

The original Kemi-I test cone instrumentation plan had provisions for both horizontal and vertic load component measurements. Problems during installation at sea caused the loss of vertical loa measurement capability. The most important and well functioning was the horizontal load measuring system. Its calibration is based on individual transducer laboratory calibration. Load resultant is calculated as a vector sum of individual transducer readings, and the total error is estimated to be less than 5 %. Other instrumentation included strain gauges, accelerometers and thermocouples.

Ice load transducer data was recorded in digital form by using a datalogger and computer. Redundant recordings were conducted in analog form by an 14 channel instrumentation tape recorder and a 2 channel strip chart recorder. A measurement log was written on formatted note sheets. Ice action was recorded continuously from above by video and intermittently, from any direction, by photographs.

Ice thickness was measured by drilling through the ice, either when the ice was stationary or, after measurmements, along the channel broken by the cone. However, local ice thickness data that can be related to measured individual ice force peaks could not be measured. Maximum level ice thickness was 0.86 m and maximum rafted ice 1.5 m thick. Ice index strength tests were made by uniaxial compression. At 10^{-3} strain rate, uniaxial compressive strength was from 1.7 to 2.4 MPa, Flexural strength from 0.44 to 0.56 MPa, and modulus of elasticity from 3.0 to 6.4 GPa, were measured b in-situ beam bending at close by locations. Also thin sections were made for ice crystallographic studies. The structure is typical for low salinity columnar grained ice with grain size from 2 to 20 mm.

The long time difference from measurements to data analysis complicated the work and somewhat degraded the quality. The data was stored for over seven years at the University of Oulu with the result that some documents, including videos, have disappeared. The personnel who did actual measurements have dispersed, and for others at least the memory of details has faded. As a consequence, very little data exists on the ice thickness, ice/structure friction coeficient and ice-ice friction coefficient as well as other potentially useful ice property information.

ICE CONE INTERACTION

Qualitative analysis gives information on phenomena in ice cone interaction that are essential to understand before any quantitative analysis or adaptation to theoretical models can be applied. There were two major findings: ice failure occurs in a multimodal way and rubble will pile up against the cone, Fig. 1.

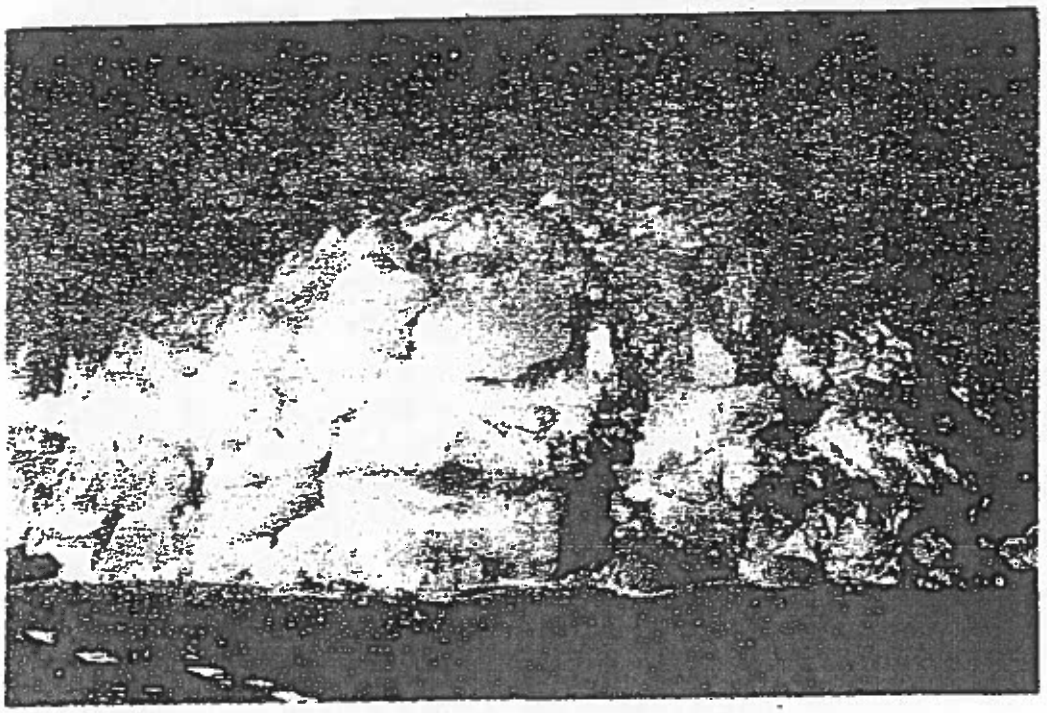

Figure 1. Rubble formation in level ice.

In sheet ice failure against the cone, there is first local ice edge crushing forming large a contact area that allows, in a later phase, high enough loads to cause radial cracking, and thereafter major ice edge failures either by bending or shearing. These three failure mechanisms do not normally occur simultaneously along the whole contact perimeter but more or less randomly. The last phase includes clearing mechanisms, raising and pushing aside broken floes and rubble.

The size and shape of floes in the rubble indicated that there has to be other simultaneous mechanisms in addition to generally assumed bending failure which was observed when rare snowless conditions allowed crack observations. The average size of the largest floes was only one to two times the sheet ice thickness, which cannot be a result of bending failure alone. A more likely explanation is shearing or splitting. The smallest ice pieces, starting from the one millimetre range, prove that crushing is also present.

In level ice, the clearing of broken ice occurs in such a way that most of the ice that is lifted up also slides down along the cone and falls into the broken channel. The channel is only slightly wider than the cone diameter at the waterline. Only a few floes or some rubble is left on the edges of the channel. Sometimes the weight of rubble in front of the cone breaks the underlying level ice downwards in a wide arc, to a distance of 2 to 4 times ice thickness from the cone, clearing the whole cone surface. It is a question whether the circumferential crack has formed earlier while the ice edge was lifted upwards, or later downwards by the weight of the rubble alone. Existence of multiple circumferential cracks suggests that wave action after ice edge failure can be the initiator, Fig.2.

Rubble pile formation in front of the cone is more of a rule than an exception. The rubble grows fast, after only a few meters of ice movement. Only in two cases was rubble formation insignificant; in winter during a very slow ice movement, and late in the spring when the ice was weak, the snow on top slushy, and the ride-up layer was single without a rubble pile. When there is continuous ice movement, velocity has little effect on rubble surcharge height after a threshold value. The most pronounced rubble piles accured when adfrozen snow was on top of the sheet ice. The friction between the rubble and underlying sheet ice is an important factor. At the beginning of the winter, when air temperatures were low and there was no snow on top of the ice, rubble formation was not as significant as when snow was present. A couple of times, as very cold ice pieces were forming the rubble, consolidation by adfreezing made the rubble pile intermittently stationary. In these cases, ice failure could occur against the rubble instead of the cone.

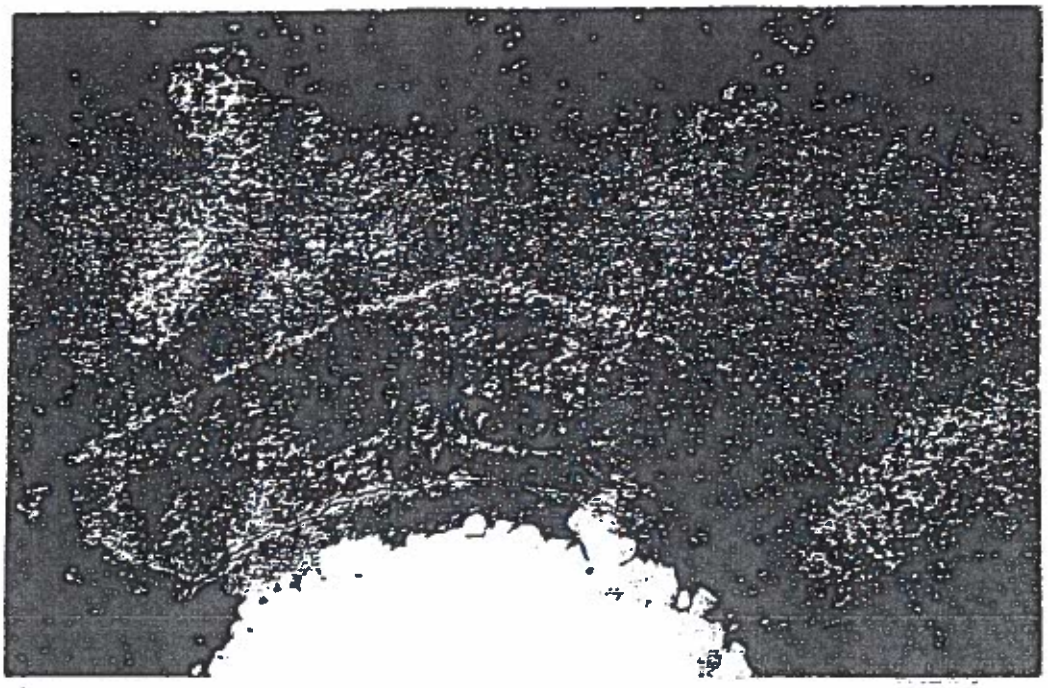

Figure 2. Multiple circumferential cracks.

The rubble first climbs up the cone surface. At the topmost location, floes start to roll down but due to cone angle also sideways in relation to ice movement, Fig. 3. From above, the rubble looks like an alive horseshoe shape that is winding inside out. During winding the floes that are forming the horseshoe, are gradually moving backwards. The highest point of the rubble is dominantly at the stagnation point. The height is decreasing first gradually and more abruptly towards the end of rubble horseshoe. The circumferential extent of rubble is about 100°.

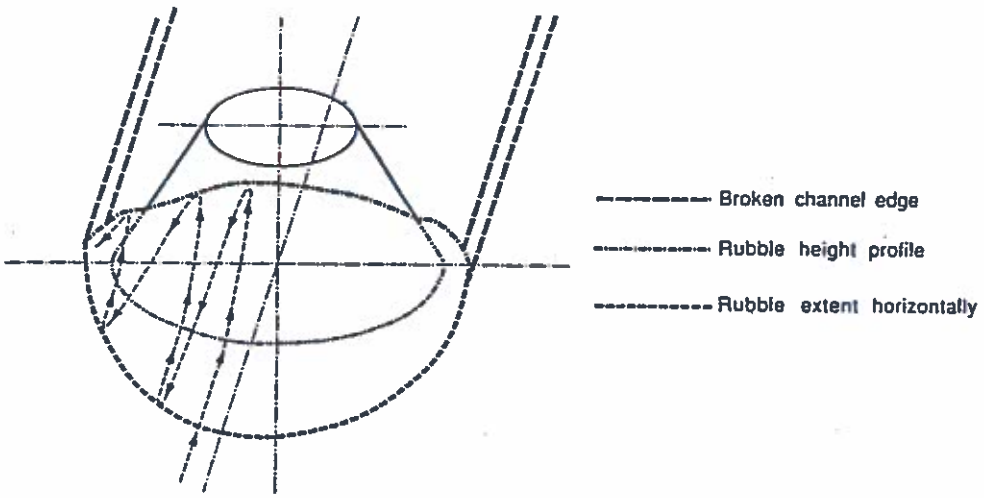

Figure 3. Rubble profile and ice particle path.

Viewing from the side, the rubble angle of repose is usually constant. In some instances, especially with big rubble formations, there is a hump in the profile. Floes are first falling steeply from the top of the rubble but may stop for awhile on a less slanting slope before falling the rest of their way down onto the level ice.

The failure mode of a pressure ridge is such that the uplifting effect of the cone dislodges easily the ridge consolidated thickness. Thereafter the clearing mechanism is similar to that of level ice. In conjunction with pressure ridges the rubble pile volume increased. This was especially true if the ridge keel was grounding on top of the caisson. In such case the surcharge height could be 9 m. But 9 m or even higher rubble piles are frequent on shallows, and indeed, on top of the Kemi-I caisson before the cone was present. A realistic case for cone ice force models is when the ridge keel

is not hitting the caisson, e.g a keel with depth less than 5.5 m. Then the observations indicated that the surcharge height does not increase but the extent of the rubble increases.

DATA ANALYSIS RESULTS

The first step in the data analysis was a critical evaluation and ranking of the existing data. Thereafter individual ice force plots were related to actual ice conditions and a versatile analysis conducted for ice load histories and statistics, Fig. 4. Analysis was conducted for all 65 cases, but for comparison with the most commonly used theoretical models only the most reliable data sets were chosen.

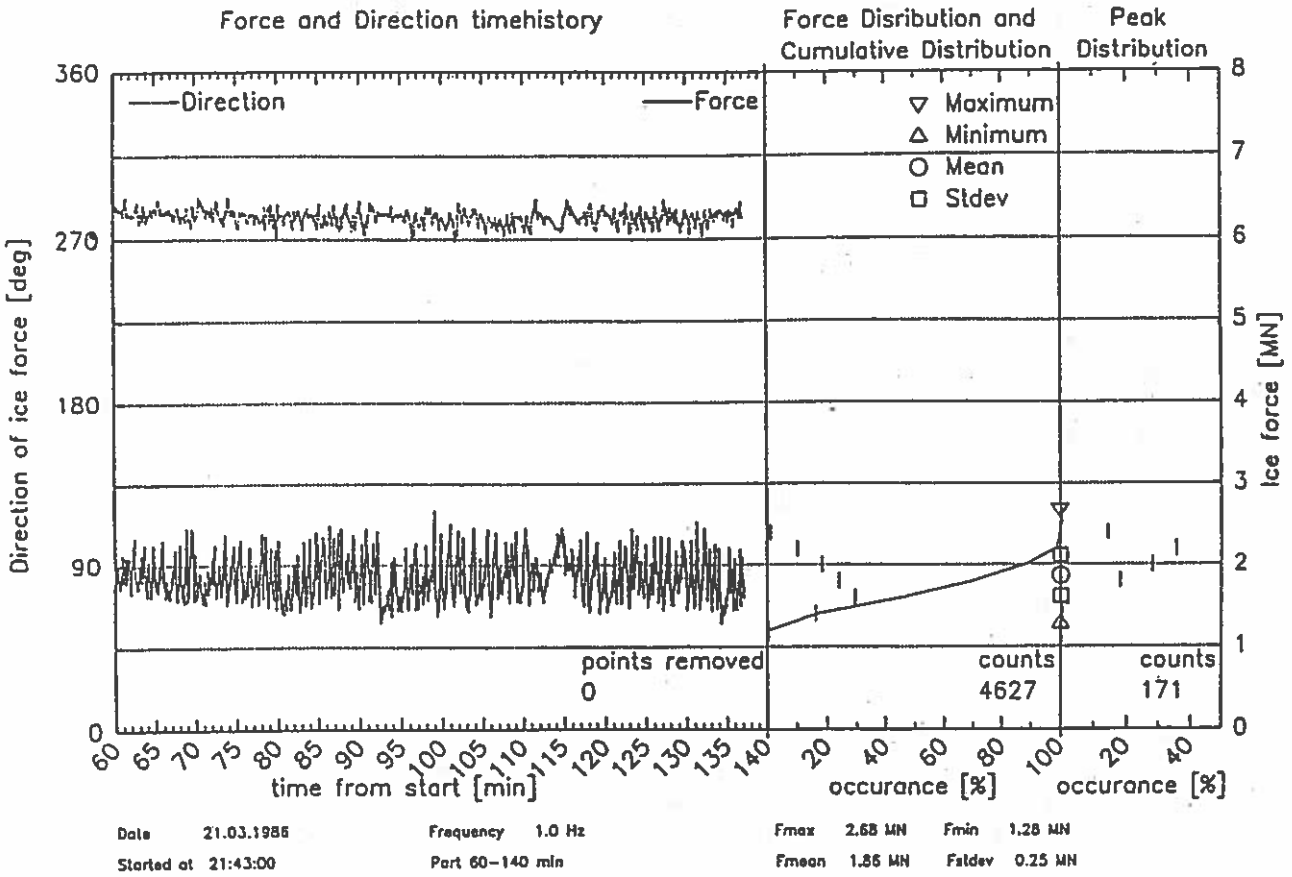

Figure 4. Horizontal ice load history and statistical analysis

Theoretically, ice thickness has an effect on cone ice forces both in ice breaking and clearing components. Depending on the failure mode, the dependence on breaking component is to power two in bending and to power one in shearing or crushing. In the clearing component a power one dependence is straightforward, but if the rubble volume is also dependent on ice thickness a higher power will result. In Kemi-I measurements there was no means to separate breaking and clearing components. The only indication in the ice force histories is that the peaks represent major ice failure events and lower levels in between peaks represent clearing dominated phases. Peak intervals are related to ice failure distance divided by ice velocity. Generally this distance is shorter than bending theory predicts. However, at the moment of ice force peak there is simultaneous clearing present, and in clearing dominated phases, a process of grinding larger floes into small rubble continues.

Ice force dependence on ice thickness is presented in Fig 5. It is not a purely one parameter presentation because ice temperatures have been different in different test cases. Thus also ice strength variation is embedded in these results. However, ice strength effect is small as indicated by the sensitivity analysis. Ten percent change in ice strength changes load only by three percent. A general trend is a fairly linear increase of ice force with ice thickness. A curve fit on ice force peaks indicates a lower than power one dependence. The reason may be the thick ice events of consolidated rafted ice which may have lower flexural strength than single layer parent ice in bending. But still the trend is

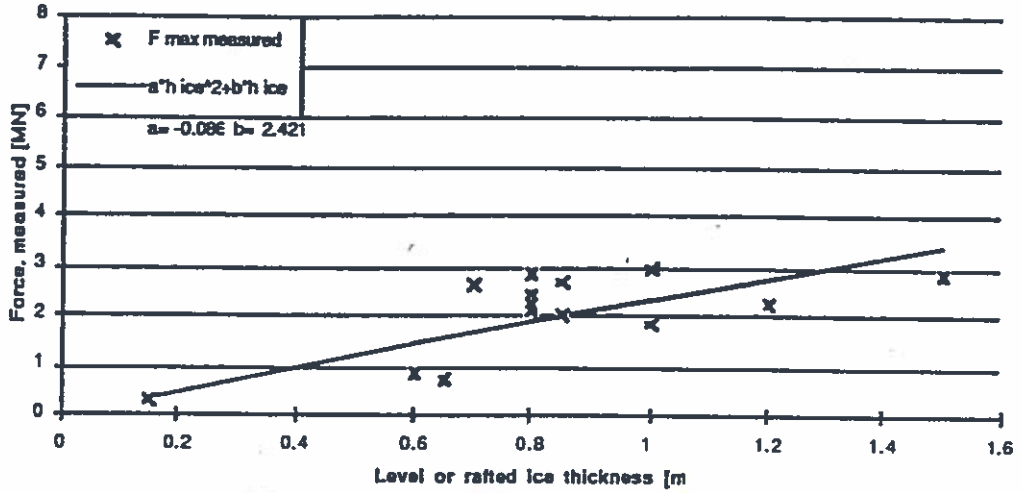

Figure 5. Maximum level ice force vs. ice thickness.

the same if cases with ice thicker than 0.90 m are omitted. In thin ice, flexural strength has been higher at lower air temperatures of about -15 °C, compared to 0.8 m thick ice with about 0 °C temperatures. Even though all these mitigating factors are observed, the cone ice force dependence o ice thickness is closer to power one than power two. This suggests that bending is not the decisive failure mode in maximum cone load. In design, rafted or consolidated thick ice is usually the decisive case. This data suggests that a design with flexural failure mode and power two dependence, may by overly conservative.

The average ice forces indicate a similar linear trend as with the maximums. Now the clearing component is more decisive. Thus the data trend is as expected.

In theoretical cone ice force models, ice velocity is not an independent parameter. Its effect is through ice strength which is loading rate dependent. In ductile range, ice strength is roughly proportional to power 0.33 in relation to strain rate. After transition from ductile to brittle range there is a decrease in strength both with compressive (crushing) and bending failure modes whereafter strength is rate independent. If ice velocity increases further, the clearing components will start to contribute due to inertia effects. Level ice data indicates that there is no dependence on velocity up to 0.25 m/s ice velocity. Evidently this is all in the brittle ice failure range but below such high velocities where inertia effects would be significant.

COMPARISON WITH THEORETICAL CONE ICE FORCE MODELS

A great many cone ice force models based on scale-model test results and either experimental or theoretical approach have been published. In full-scale, rubble formation in front of the cone has been common. Friction plays an important role both in ice failure and clearing phases. In the case of a first year pressure ridge action there is additional rubble to be cleared and possibly a consolidated layer inside the ridge in addition to the parent ice sheet. Ice breaking and clearing mechanisms are similar both for upwards and downwards breaking cones, but buoyancy dependent components are different.

A theoretical ice force model should be based on physical background including ice failure and broken ice clearing mechanisms. The model has to be general so that all normal first year ice-cone interaction modes can be simulated, as well as upwards and downwards breaking cones. Conical structures have finite dimensions which necessitates a requirement for 3-D modelling capability. Now, based on these requirements, only four models, out of the nine in the Reference list, are briefly described and compared to full-scale data. These models are presented in chronological order.

Ralston's model (1977) is one of the oldest, best known and most referred. It is based on ice bending failure by plastic limit analysis along sectorial wedges. The kinematics observe the rotation in plastic hinges between the wedges and along the circumferential yield line. Energy is simultaneously

dissipated for raising the ice sheet from the water, and pushing broken floes upwards for clearing the cone. The thickness of the rising broken layer can be chosen to observe rubble formation or presence of a pressure ridge. The maximum load is expected at the moment the yield line is fully developed along the whole circumferential perimeter.

The Määttänen and Hoikkanen model (1986, 1990) is based on elastic ice wedge failure. The model assumes radial cracks to form before maximum ice load occurs at the onset of circumferential ice failure. Wedge loads include vertical and axial cone reaction loads and moment at the wedge end, and distributed weight and friction of the varying thickness rubble above. The rubble load on the wedge and cone is calculated by assuming a passive soil pressure type model. Beam Finite Element model is used to solve the equilibrium of the wedge. Wedge failure load is the minimum of bending, shearing or cracking load. Wedge failure can occur either upwards due to cone reaction force, or downwards, due to the weight of the rubble.

Nevel's model (1992) is based on refined kinematics analysis for a wedge and its elastic bending failure. The wedge static equilibrium accounts for the breaking force by bending. Its end loads include cone reaction forces and a moment due to eccentricity, and ride-up force including rubble weight. The number of wedges is one parameter in the model. The model has choices for simultaneous or sequential wedge breaking, and active or passive ice action on the ride-up. Out of 8 different choices, one that assumes simultaneous wedge failures, active ice action and excludes ice standing against the neck was used in comparisons.

The Croasdale and Cammaert model (1993) is a 3-D extension of the earlier Croasdale 2-D model. Refinements include modification of ice sheet failure geometry to account for 3-D effects, rubble pile-up in front of the cone, and the elastic failure condition together with the effect of in-plane ice sheet compression. The total horizontal load is composed of five components: ice sheet failure load, load to push the ice sheet through the rubble and along the cone, load due to the weight of rubble, and load needed to turn ice blocks vertical at the top of the slope.

For the comparison of theoretical models, 14 different Kemi-I cone ice force measurement cases were selected to be used as input data. Ice thickness varies from 0.15 to 0.85 m in level ice and up to 1.5 m in rafted ice. No pressure ridges were included due to the lack of information on keel geometry. Ice moving velocity varied from 0.08 to 0.25 m/s. At this range ice behaviour is mostly elastic and inertia effects are insignificant. Ice was columnar grained with low salinity, from 0.036 to 0.158 %. Air temperatures during these test cases were from -1.2 to -16 °C but there was typically from 5 to 20 cm thick layer of snow on top that made ice temperature warmer. Based on in-situ cantilever tests, ice flexural strength values from 0.56 to 0.44 MPa from early winter to late spring were used in models. For all models an estimated common value of 3.1 MPa was used for ice Young's Modulus. It has only a small effect on results. Friction values were not measured. For all the models ice to ice friction coefficient was estimated to be 0.26 and ice to cone friction coefficient was estimated to be 0.15.

Theoretical models predict the maximum ice load value. Therefore from the measured data the peak values from each test case were chosen for comparison, Fig. 4. Rubble height was taken from measurement data and for each theoretical model rubble thickness parameters were adjusted to give the same total rubble weight.

The sensitivity of models to the most important input parameters was tested by giving a 10 % increase to the nominal value. It was learnt that there are differences between individual models even with most fundamental parameters. The change of cone angle induces highest changes in the ice load. An increase from 55 to 60 degrees increased ice loads in average about 30 %. Cone diameter 10 % increase increased ice loads less than 10 % in all but Nevel's model where increase was 17 %. A 10 % increase of ice thickness or rubble height increased ice loads about 7 %.

The Ralston model most often predicts too high ice loads, Fig. 6. This could be due to the nature of plastic limit analysis upper bound solution, and assumption of simultaneous yield lines both in radial and circumferential directions. A slight improvement is achieved if the radial yield lines are considered to have lost their moment capacity before circumferential yield line is fully developed. Note that Ralston's method predicts well a number of model test results.

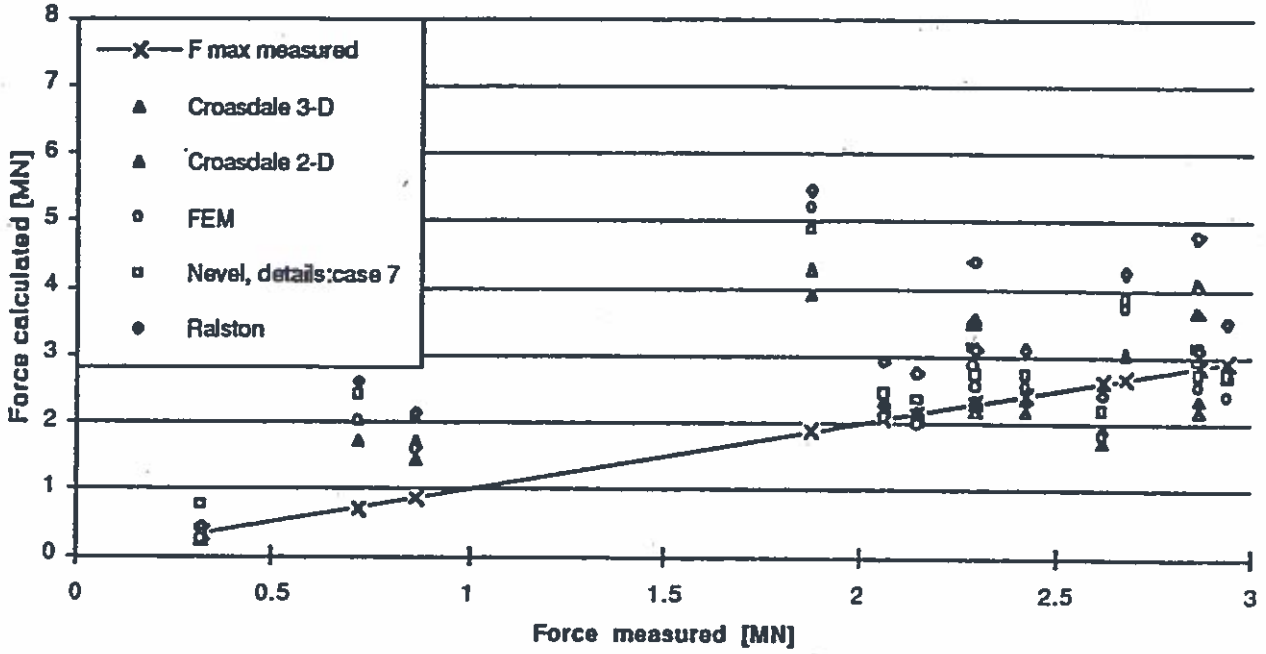

Figure 6. Horizontal ice force comparison for different models.

CONCLUSIONS

The full scale measurements have verified the existence of multimodal ice failure in front of the cone. Both bending, crushing, and shearing modes are present. The floe size is significantly smaller than what ice bending failure alone would predict.

A typical ice failure cycle includes first local crushing and shearing which increase contact area until a high enough ice edge load is possible to cause a major ice sheet failure. Both radial and circumferential cracks are present. Multiple circumferential cracks manifest wave action effects after ice edge failure. Circumferential cracks extend more in the direction of ice movement than sidewards. The broken channel is just slightly wider than the cone diameter.

Ice rubble formation is more common than the case of no rubble pile. Snow cover on top of the sheet ice and high ice velocity promote rubble formation. Slow ice movement velocity or low ice friction during high temperatures late in spring reduce rubble formation. Rubble is normally in continuous movement, turning inside out and clearing over the sides of the cone. Most of the rubble falls down into the broken channel, only few floes are left on top of the ice edge. The weight of the rubble can cause a downward ice edge failure and the collapse of the whole rubble pile.

Full scale measurement data analysis indicates that the overall dependency of cone ice force to ice thickness is less than to the first power. With thicker rafted ice the exponent is still lower. This implies significant reductions for design ice forces, especially in the case of maximum ice thickness with rafted consolidated ice. Ice velocity, flexural strength and modulus of elasticity have a small effect to the total ice load.

Four theoretical models were tested against Kemi-I full-scale level and rafted ice data. Present cone ice load prediction models take well into account the physical phenomena in ice-cone interaction. In macro-scale all the important aspects are covered. Results indicate that plastic limit analysis model is likely to overpredict while elastic analysis models give relatively good predictions at a wide range of ice thicknesses.

Model sensitivity analysis indicates that the cone angle is the most important parameter in cone ice forces. Next come cone diameter, ice thickness, density, ridge surcharge height, friction and flexural strength in decreasing order.

Plastic limit analysis model overpredicts, and it has been used to demonstrate that a conical shape is efficient in reducing ice loads from those of a vertical structure. Now the full scale data proves that cone is more efficient than what has been thought earlier, even with the presence of the rubble pile.

Kemi-I test cone full scale measurements give, for the first time, reliable full scale data for cone ice forces. A good qualitative view on ice failure, rubble formation, and clearing modes is available. Ice force peak measurements and theoretical model predictions correlate well with FEM and Nevel models. Together with ice forces statistical variations, a sound basis for cone ice force design is set. The data also proves the efficiency of a conical structure in reducing total ice forces.

ACKNOWLEDGEMENT

This Project was a Joint Industry Project, including Amoco Canada Petroleum Company, Conoco Inc., Exxon Production Research Company, Mobil Research and Development Company, Neste Oy, and Texaco Inc. The authors want to express their appreciation for the active involvement of the participant companies and for making this project possible.

REFERENCES

Bercha F.G. and Danys J.V. (1975): Prediction of Ice Forces on on Conical Offshore Structures. Proc. IAHR Symposium on Ice, p. 447-458. Hanover, NH, USA.

Brooks L.D. (1981): Ice Resistance Equations for Fixed Conical Offshore Structures. Proc. POAC 1981, Vol I, pp. 91-99. Quebec City, Canada.

Croasdale K., and Cammaert A. (1993): An improved method for the calculation of ice loads on sloping structures in first-year ice. Proc. First International Conference on Development of the Russian Arctic Offshore. St.Petersburg, Russia.

Edwards R.Y. and Croasdale K.R. (1976): Model Experiments to Determine Ice Forces on Conical Structures. Symposium on Applied Glaciology. Cambridge, England.

Izumiyama K., Irani M.B., and Timco G.W. (1993): Computation of Sheet Ice Forces on a Faceted Conical Structure. Proc. POAC, Vol 2, p 517-526. Hamburg, Germany.

Määttänen M. (1986): Ice Sheet Failure against an Inclined Wall. Proc. IAHR Symposium on Ice 1986, Vol I, pp. 149-158, University of Iowa, Iowa City, IO, USA.

Määttänen M. and Hoikkanen J. (1990): The Effect of Ice Pile-Up on the Ice Force of a Conical Structure. Proc. IAHR Symposium on Ice 1990, Vol. 2, pp.1010-1021. Helsinki University of Technology, Espoo, Finland.

Nevel D. (1992): Ice Forces on Cone from Floes. Proc. IAHR Symposium on Ice 1992, Vol 3, pp 1391-1404, Banff, Canada.

Ralston T. (1977): Ice Force Design Considerations for Conical Offshore Structures. POAC 1977, Vol II, pp. 741-752. Memorial University of Newfoundland, St.John's, Newfoundland, Canada.

Tam G., Määttänen, M., Hoikkanen J., Nortala-Hoikkanen A., Mäkinen E., and Kivelä J. (1995): Ice Force Measurement Analysis for the Kemi-I Cone - A Joint Industry Project. Volume I and II. 127 p + ~280 p Appendices + Video + Slides + Computer Program. Kvaerner-Masa Inc, Vancouver, Canada.

Wessels E. and Kato K. (1988): Ice Forces on Fixed and Floating Conical Stuctures. Proc. IAHR Symposium on Ice, Vol 2, p 666-691. Sapporo, Japan.

NUMERICAL SIMULATION OF ICE-INDUCED VIBRATIONS IN OFFSHORE STRUCTURES

Mauri Määttänen
Department of Mechanical Engineering
Helsinki University of Technology
mauri.maattanen@hut.fi

ABSTRACT

As moving ice fails against an offshore structure the resulting ice load is not constant. An evident reason for ice load fluctuations is the variation of oncoming ice properties. Transient loads are also caused by ice edge, floe or iceberg hitting the structure. Normally ice load fluctuations are resulting from a more or less random ice failure process. However the most severe dynamic ice load scenario can occur even though ice properties and ice velocity would be constant. Under certain conditions the ice failure becomes coupled with the dynamic response of the structure. Initially independent local ice failures at different locations at contact zone are likely to synchronise. The worst conditions are a resonance with one of the lowest natural modes. This paper gives a review of dynamic ice action scenarios, and methods to predict dynamic ice loads by numerical simulation. Such capabilities are dearly needed in near future while the projected offshore wind energy is being realised in Northern Europe.

1. INTRODUCTION

Adverse vibrations due to moving ice crushing against offshore structures were first reported in Cook Inlet oil drilling structures /2,25/. In Finland first experiences with single steel pile foundations for lighthouses in 1973 were disastrous. Severe resonant vibrations destroyed their superstructures during the first winter /16/. At Bohai Sea Chinese oil production platforms with jacket foundations were also damaged due to dynamic ice loads, /31,32/. Common to all these structures was that the construction included relatively narrow and flexible components that were directly under ice action. The opposite case was Molikpaq, an arctic caisson retained island, that is wide and very stiff structure. This drilling platform is a double walled steel ring, diameter 111 m, height 30 m, having the centre part filled with sand that enhances sliding resistance and damping capability. In 1986 while a multiyear ice floe was moving and crushing against the caisson, the whole structure vibrated continuously. Due to vibrations the pore pressure in the soil increased and the whole structure was close to be displaced /6/.

The problem of ice-induced vibrations in slender flexible structures that have to withstand the loads of moving ice fields has been under research over three decades but still a debate on the origin of vibrations continues. The main question is why the ice force is fluctuating periodically even though a constant thickness homogeneous ice field is moving at constant velocity and crushing against a vertical structure.

A number of approaches have been presented to predict dynamic ice loads during ice crushing /2,3,9,10,11,12,17,23,25,27,30,32/. If the loads are known then it is a straightforward process to numerically solve the dynamic equations of motion and to predict structural response. This kind of forced vibration analysis can readily be used to calculate transient response due to ice edge impacts or iceberg hits. Uncertainties come from assumptions on ice crushing pressure dependence on changing contact area and aspect ratio.

Theoretical explanations for dynamic ice structure interaction are based on forced or self-excited vibration models. In the former, ice is having a characteristic failure frequency, or ice is fractured into floes of certain size /25,23,11,13,28/. Hence ice force build-up and failure frequency is directly proportional to ice velocity. The interaction ice force depends only on the advancement of ice sheet. Ice force history is then known a priori when the ice velocity is known. If the dynamic response of the structure is insignificant there is no dynamic interaction, only dynamic reaction forces. A mechanical model for this kind of an interaction can be presented by breaking brittle cantilevers, Matlock /11/. In his model a moving chain of brittle elastic beams simulate ice contact. As a beam contacts the structure the load build-up is linear until the beam breaks and load returns to zero until a next beam makes the contact. "Ice" velocity controls the load build-up rate and the beam strength maximum load. The spacing of beams and ice velocity determine the load frequency. Matlock's model presents a predetermined forced vibration problem that well simulates the low ice velocity saw-tooth ice load history, and even the onset of a resonance condition but not the change into random response with further increasing ice velocity.

No physical reasoning exist to support characteristic ice failure length in crushing. Only in ice bending failure, the characteristic length of an elastic plate on Winkler foundation determines the size of broken floes. Indeed, at high ice velocities bending failures can excite a structure into resonance as has been witnessed in China, /33/.

In the self-excited ice-induced vibration model /2,17,22,30,32/, the interaction ice force is dependent on the dynamic response of the structure at the ice action point with no a priori known ice force time history. The model observes the dependence of ice strength on varying loading rate. Hence the feed-back - or coupling - variable is the dynamic response velocity. The system is autonomous and the only chance for vibrations to occur is then that the system is dynamically unstable, which yields to limit cycles in self-excited vibrations. An autonomous vibration system is one in which dynamic response and the interaction force originates from the system itself without need to know beforehand any loading history.

Scale model tests /18/ have indicated that the frequencies of natural modes of the structure control ice failure frequencies at a wide velocity range. Hence a lock-in to the natural mode frequency takes place. Thus in a multi-legged or wide structure independent ice failures at different locations are likely to synchronise. This is due to vibration velocity of a natural mode superimposing to the ice velocity, which promotes coherent ice failures at different locations.

A numerical model to simulate dynamic ice-structure interaction and ice-induced vibrations should be able to predict different velocity dependent ice failure patterns, saw tooth like at low ice velocities, frequency lock-in and synchronisation at increasing ice velocity, and random at high ice velocity. Both Sodhi /28/ and Määttänen /21/ give a review of different ice-structure interaction models. Thereafter further models have emerged that also observe multi-point ice load excitation /9,10,22/. Only the last represents results on predicted frequency lock-in and ice failure synchronisation.

This paper gives background information on such ice mechanics parameters that have significant effect on ice-structure interaction, and describes different approaches for numerical models. A brief description is given on ice impact loads. Vibrations that are caused by random variations of ice thickness, strength, etc. are not treated here. The presented self-excited model is based on ice crushing strength dependence on loading rate. The original model with single point ice action for beam structures has been used to predict ice-induced vibrations in Finnish steel lighthouses /20/, and later expanded for any three dimensional structure with multi-point ice excitation /22/. The theory behind the model is briefly described. Application examples are presented for both a multi-legged and a wide offshore structure to demonstrate the simulation

capabilities for varying ice thickness and velocity cases. Also ice-induced vibration analysis for offshore wind turbine foundations are discussed.

2. ICE MECHANICS BACKGROUND

Ice-structure interaction implies that both the ice and the structure are active partners. In the case of a rigid structure, the only contribution of the structure to ice failure process is the shape of the structure at the contact zone. Ice load fluctuations against rigid structures are caused by the properties of ice alone. Subsequent ice edge flaking failures is one explanation, tendency to fail into floes of certain size another, but also the dynamic response in the ice field together with the ice strength sensitivity to strain rate can contribute to resulting interaction ice force fluctuations. Instead of interaction a better expression in the case of a rigid structure would be ice action against a structure.

In the case of a flexible structure, the dynamic response of the structure plays an active role with the force originating from the ice failure process. Hence all structural properties, shape at the contact zone, stiffness, mass and damping will have their effect on the interactive forces between the ice and the structure. The distinction between a rigid or flexible structure is arbitrary, however. Even a solid rock undergoes elastic deformations when loaded by ice action. Also the ice field itself undergoes elastic deformations. From the practical point of view a structure can be considered flexible when its displacements are significant when compared to ice elastic deformations, e.g. of the same order as the ice grain diameter.

In dynamic ice structure interaction energy from the moving ice is being transferred and stored as elastic energy in the structure. After ice failure and at structural spring back phase stored energy is released. It is converted into breaking ice and into kinetic energy. Energy exchange implies also dynamic response to occur, either in the structure, in ice, or in both. As ice strength is strongly dependent on loading rate, dynamic response will alter the average loading rate, and hence interaction forces. Ice failure will occur at high loading rate with low ice strength, and load build up at low loading rate with high ice strength. This yields to the synchronisation of ice failure and structural response. It is more pronounced with flexible structures that exhibit significant displacements at the ice action point. Of course the stored kinetic and elastic energy in the ice cover itself can also activate and control ice crushing.

Ice velocity is the governing parameter in the character of ice load history. Velocity effects express themselves in stress or strain rate, which has a strong effect on the interaction ice force. Hence it is imperative to observe the relative velocity, which is a difference of ice edge and structure contact point velocities. At very low ice velocities, e.g. thermal expansion, ice behaviour is ductile and ice-structure interaction resembles viscous flow. Ice load is pseudo static. Ductile deformation may include cracking effects.

With increasing velocity cracking activity increases when interaction time becomes too short for ice stresses to be relaxed and bounded by creep. A damaged ice zone is forming. Ice load and stresses, as well as structural deflection build up until ice compressive strength level is reached. Ice starts to break into floes and small fragments. In certain conditions ice is practically being pulverised. The clearing mechanism of broken ice mass with ice floes or fragments are different to that of pulverised ice: the former pops out "explosively" while the latter is extruding. As ice major failure occurs the load level drops suddenly, and the deflection of the structure springs back. Often the spring-back stroke exceeds the zero state causing a gap between the ice edge and the structure. Thereafter the advancing ice edge makes contact to the structure and a new load cycle starts. This produces a saw tooth like ice force or displacement history.

At higher velocities the response history will gradually change. The frequency of ice failures increases with ice velocity until at a certain velocity range a natural mode of the structure may start to control the ice failure frequency: a lock-in resonant state occurs. At still higher ice velocities conditions for the resonance are lost. Ice failure turns into totally brittle and ice load fluctuations random. Stress or strain rate is directly proportional to relative velocity between ice and structure. It is at the transitional strain rate range from ductile to brittle, 10^{-3} - 10^{-2} 1/s, or stress rate around 0.2 - 0.6 MPa/s, where self-excited vibrations are most pronounced, Fig. 2.

Recent studies have found out how the actual ice failure is occurring at high loading rates. Studies by using high speed photographic techniques and transparent structure wall /7/, or tactile sensors /1,5/, indicate that there is only a narrow "contact line", in which high interaction pressure is acting and crushing the ice, while the rest of the contact zone is involved only in the clearing mechanism.

3. BASIC DYNAMIC ICE STRUCTURE INTERACTION MODEL

A schematic model of ice interaction with structures has three elements: structure, ice failure process, and ice sheet, Fig. 1. For the structure and ice there are well known governing differential equations, dynamic equations of equilibrium. The two interacting bodies are connected by the centre element, the ice failure process, which includes clearing mechanisms of broken ice mass. Also the conditions of continuity have to be taken care of in the centre element.

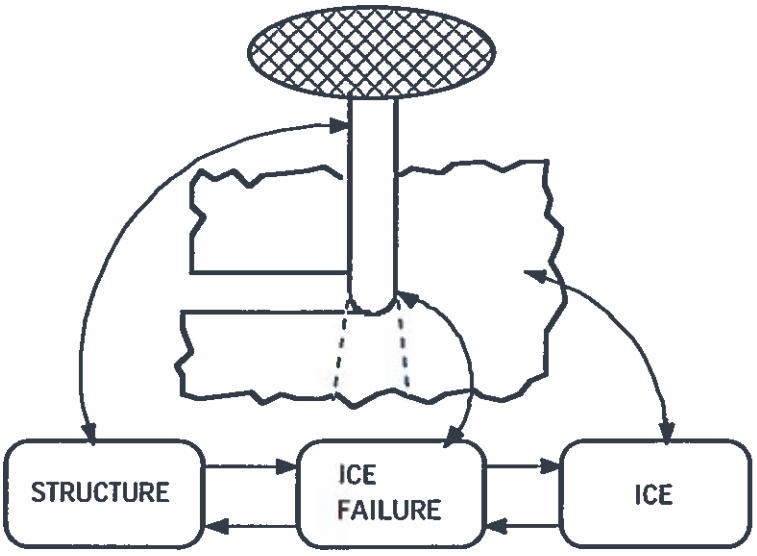

Figure 1. Elements in ice interaction with structures.

A schematic mathematical model of ice interaction with structures, Fig. 1, can be formulated with two coupled equations of equilibrium, Eq. 1 and 2,

$$[k]\{\delta\}+[d]\{\dot{\delta}\}+[m]\{\ddot{\delta}\}=\{f(\delta, \dot{\delta}, \ddot{\delta}, \Delta, \dot{\Delta}, \ddot{\Delta}, t, V)\} \quad (1)$$

$$[K]\{\Delta\}+[D]\{\dot{\Delta}\}+[M]\{\ddot{\Delta}\}=\{F(\delta, \dot{\delta}, \ddot{\delta}, \Delta, \dot{\Delta}, \ddot{\Delta}, t, V)\} \quad (2)$$

which represent the governing differential equations of the structure and ice in a discretized form. Symbols $\{\delta\}$ and $\{\Delta\}$ stand for the displacement vectors of the structure and ice, dot above means derivation in relation to time t giving velocities and accelerations, [k], [K], [d], [D], [m], and [M] are stiffness, damping and mass matrices respectively, V is the nominal ice velocity. The coupling is through non-linear functions $\{f\}$ and $\{F\}$ that describe interaction forces from the structure to ice failure process, and from ice failure process to the ice sheet.

Most problems could be analysed by means of computational mechanics if a mathematical model could correctly present all elements in Fig. 1. The main difficulty is in the ice constitutive model: elastic, viscous, and plastic behaviour including cracking should be modelled in three dimensions. Interaction forces in Eq. 1 and 2 are not known beforehand, they depend on the state of the system. The most common approach is to assume an interactive forcing function, which enables to separate the two systems. Physical interpretation of Eq. 1 is then ice with no response, and of Eq. 2, an infinitely rigid structure.

There are many simplifications in modelling ice behaviour and failure. The non-linear visco-elasto-plastic constitutive equations of ice are linearised and/or replaced by a simple constitutive law, which considers only one effect to be significant. This way it is possible to have a linear elastic material model for fast loading cases, reference stress method for slow loading cases, ideal plastic behaviour for limit load analysis, etc. Kärnä /9/ observes the ice behaviour at two scales: near field that observes ice damage, failure and extrusion during clearing, and far field that observe elastic only response including radiation damping.

Structural damping is important in suppressing ice-induced vibrations. In scale model, and full scale tests, it has been measured, that with a sufficiently high internal damping in the structure, resonant type self-excited vibrations can be totally avoided /20/.

Time is significant in two cases: if there is a characteristic failure frequency in the ice and if loading rate is so low that visco-plasticity becomes important. The latter can be considered insignificant if crushing frequency is higher than about 0.5 Hz, which is the normal case. When the ice failure occurs within a few seconds from the beginning of load build up, the ice failure is dominantly brittle with only an insignificant time dependent creep in the ice deformation response.

The effects of relative distance between the ice edge and the structure are also important. When there is a gap, the ice force is zero regardless of relative velocities. During crushing, normally more ice is crushed than the elastic rebound of the structure. During load build-up the uneven ice edge is being smoothened and there is some elastic indentation into the ice as well. All these displacement contributions have to be observed in the vibration model.

4. ICE IMPACT

The impact of ice against structure has different scenarios: transients during ice sheet edge hitting, splitting of floes, pushing aside floes, growler or iceberg impacts. These load cases are decisive in high arctic but of minor importance in the Baltic compared to resonant type crushing loads.

If a sufficiently large ice sheet is moving and its edge hitting a structure there will be a short duration transient after which continuous ice structure interaction will establish according to previous models. During the transient phase initial load build-up may induce higher dynamic response to the structure than in the continuous phase. If the laws for ice load build-up can be assumed, the calculation of dynamic response is straightforward. Typically dynamic amplification in the transient is less than twofold from that of the static loading. If a resonant

loading in dynamic ice structure interaction is possible, its dynamic amplification is much higher due to inherently low damping of structures.

Splitting of a small floe during an impact occurs easily. The interaction is just to initiate splitting. Theoretical models based on force equilibrium /13/ and on fracture mechanics /26/, explain the low load levels needed for splitting the ice. The latter model explains also the splitting of floes with a diameter of several kilometres.

The hit of an floe is rarely symmetric. Asymmetric contact causes the floe to rotate and then being pushed aside the structure. Interaction forces can be calculated according to laws of conserving energy and momentum /24/. The hit of a growler or iceberg can be treated like hit of an floe. However more emphasise is now in the load build-up history. It is dependent on the velocity, the size of contact area, and on aspect ratio. The velocity can be calculated from the energy balance and the rest from the geometry of impacting bodies /24/. An important factor is ice strength dependence on the contact area /26/.

5. SELF-EXCITED ICE-STRUCTURE INTERACTION MODEL

The first to propose self-excitation as the origin of ice-induced vibrations was Blenkarn /2/ who defined the dynamic stability condition for a single degree of freedom system. He used the concept of negative damping, which can be derived from the decreasing ice force versus loading rate.

Määttänen /17/ extended Blenkarn's model for a multi degree of freedom system and solved a stability condition for each natural mode of the structure. By using ice strength versus stress rate dependence as a starting point, limit cycles were also solved by numerical integration. Relative displacement effect was observed for gaps. Saw-tooth like ice force histories could be derived directly from the physical properties of ice and the structure without any a priori assumptions on time dependent ice forcing function. Ice force frequency lock-in with unstable natural modes is correctly predicted. A simple equation to predict the dynamic stability of a natural mode (sensitivity to ice-induced vibrations) and the frequency of saw tooth ice force frequency at low velocities was derived. Theoretical predictions were in good agreement with both scale model and full scale measurement data.

The structure is discretized by using Finite Element Method. Ice interaction is observed as a nodal load in those nodes that are under ice action. Ice load is simply ice crushing strength times the area that is controlled by the node in question. The crushing strength is dependent both on contact normal velocity and contact area.

$$\sigma_c = \sigma_c(v - \dot{u})\sqrt{\frac{A_0}{A}} \qquad (3)$$

Ice crushing strength against a wide structure is reduced according to the area dependence as defined by Sanderson /26/. Relative velocity at a contact node is ice velocity v minus nodal displacement velocity du/dt. Crushing strength dependence on relative velocity is based on the stress rate as defined by Blenkarn

$$\dot{\sigma} = (v - \dot{u})\frac{8\sigma_0}{\pi d} \qquad (4)$$

Here σ_0 is reference strength, now 2 MPa is used, and d the diameter of the structure. Equation 4 was originally intended for narrow structures and is not directly applicable for wide structures.

However, if non-simultaneous ice failure at different zones along the width of the structure is assumed a realistic value for d can be used. There is no definite answer for the width of an independent zone. E.g. a value of one or two times the ice thickness can be chosen. The effect of width d in the denominator is to scale velocity range. Thus ice velocity dependence comparisons can be made regardless of the correct width. In the following applications the real leg diameter is used for the multi-legged structure and d=1 m for the wide structure.

Based on the measurement data /25,2/, and combining Eq. 3, ice crushing strength vs. stress rate, is approximated by using a fourth degree polynomial,

$$\sigma_c = (2.00 + 7.80\dot{\sigma} - 18.57\dot{\sigma}^2 + 13.00\dot{\sigma}^3 - 2.91\dot{\sigma}^4)\sqrt{\frac{A_0}{A}}\ MPa \qquad (5)$$

in which $\dot{\sigma}$ is given in MPa/s and the reference area A_0=1 m^2. The polynomial part covers ice failure mode transition from ductile to brittle. At higher strain rates ice failure is brittle and strength is assumed to be constant, Fig. 2. At very low loading rate the ice behaves as a viscous fluid. However, as now the load build-up time is short, in order of a second or less, the viscous deformations in ice can be omitted. In reality there are always random variations in ice strength, now especially at the decreasing part. Hence the whole curve should be interpreted as a deterministic average presentation on ice crushing strength.

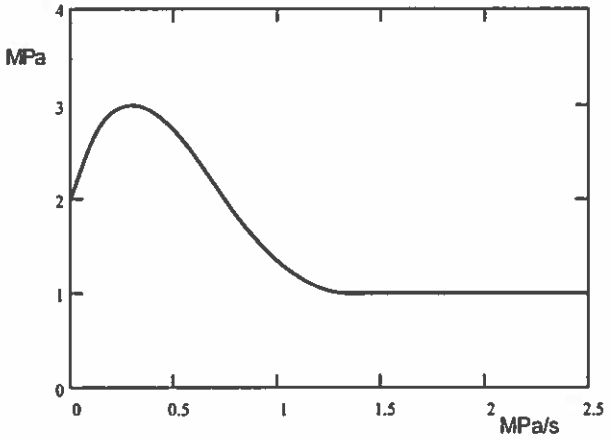

Figure 2. Ice crushing strength vs. stress rate.

Implementing ice crushing strength by Equation 4 and 5 into nodal loads in the dynamic equations of motion for the whole structure, Eq. 1 with δ replaced by u, yields

$$[k]\{u\} + [d]\{\dot{u}\} + [m]\{\ddot{u}\} = \{F(v,\{\dot{u}\})\} = \{F_0\} + [\phi]\{\dot{u}\} \qquad (6)$$

where [k], [d], and [m] are the stiffness, damping and mass matrices of the structure, $\{u\}$, $\{\dot{u}\}$, and $\{\ddot{u}\}$ are the nodal displacement, velocity and acceleration vectors. $\{F_0\}$ is the constant part of the load vector representing ice strength at the nominal stress rate corresponding to ice velocity v. Matrix $[\phi]$ has nonzero terms only at its diagonal corresponding to ice action nodes and resulting from the structural response velocity according to Equation 4 and 5. Each ice action node has its own ice load, which is independent from others. The coupling plays role only through the combined effect of all nodal loads to displacement and velocity response.

In initial state the structure is at rest with no vibrations. As both $\{\dot{u}\} = \{\ddot{u}\} = \{0\}$ only static displacements are caused by the loads $\{F_0\}$. In order to have vibrations the ice-structure system has to be dynamically unstable. Mathematically the autonomous system of equations 6 has then roots that have positive real part and make deviations from the equilibrium to grow with time.

This means that if there are any disturbances they tend to grow dynamically and develop into vibrations or into an aperiodic divergence. Considering the shape of the controlling curve, (Fig. 2), it is evident that disturbances will not grow without bounds but the vibrations have to develop into stable limit cycles. The reason is that energy is being pumped into the structure only at the decreasing part of Figure 2. Then with increasing vibration amplitudes increasing structural damping will eventually dissipate all the energy that is fed into system during each vibration cycle.

The Eq. 6 is highly non-linear both due to the shape of ice crushing strength curve and the possibility of contact loss between the ice edge and the structure. The response history of the structure can be solved by numerical integration. In order to get stable limit cycles as soon as possible, it is advantageous to use the static displacement of the average ice load as an initial condition. Another way to reduce CPU-time is to use principal mode presentation. Usually only a small number of the lowest modes are needed to model global structural vibration state. If ice velocity is such that the initial state will not fall into the decreasing part of the crushing strength curve, a sufficiently large disturbance is needed to make the structure to vibrate, allowing conditions for limit cycles either to develop or all vibrations to decay.

Any 3–D structure can be modelled by FEM. For ice-induced vibration analysis the needed output is natural modes and frequencies for the limit cycle program input. Number of ice action nodes are chosen according to the geometry of interaction, and nodal ice loads can have components to all co-ordinate directions. Each nodal load is calculated independently according to Equation 5.

6 APPLICATION STRUCTURES

Figure 3 presents the FEM-model of a generic three-legged jacket platform that is intended to operate in moderate first-year ice conditions. Water depth is 19 m and jacket legs go deep into sea bottom. Soil support is simply modelled by pinning the legs at -24 m depth. The diameter of jacket legs at waterline is 1.2 m. The structure is symmetric, each cross section forms an equilateral triangle. At the waterline the distance of legs is 10.2 m. The deck at +13 m level is hexagonal and has a mass of 300 Mg. The structural model includes only primary structures with the mass of secondary structures.

The first 16 natural modes are given in Table 1. Global modes that are most important in ice-structure interaction in global y-direction (from left to right) are presented in Figure 3. Due to structural symmetry many frequencies are repeated. The first and second bending modes are at 1.31 and 3.24 Hz, and twist modes at 1.44 and 3.70 Hz respectively. The structure is relatively flexible, especially in relation to ice load action at the waterline. The deck mass is a significant factor in the dynamic response of the structure.

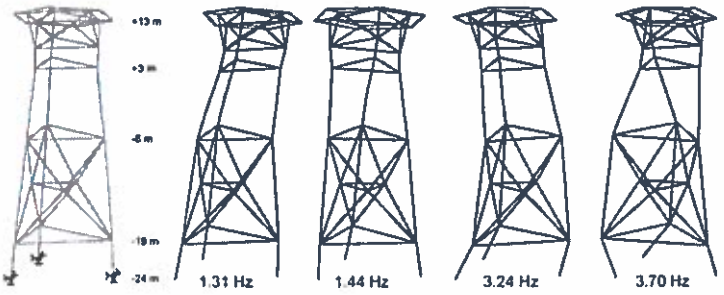

Figure 3. Three legged jacket platform and natural modes.

The wide application structure is a fictive caisson retained island (CRI) intended to withstand multi-year ice loads in 20 m water depth, Fig. 4. The retaining ring is made of steel. Wall height is 8 m above sea level. The deck rests freely on top of the ring. The planview is octagonal with longest sides 64 m at the waterline and total width 90 m. The base is 112 m wide and supported on soil. For vibration analysis soil stiffness including core sand is simply observed by linear spring elements at foundation nodes. Total horizontal spring coefficient is 29 GN/m. The total mass of the structure including core sand and added soil and water mass is 510 Gg. The foundation springs, ring cross section rigidity and total mass were adjusted to give natural frequencies roughly at the same range as what has been measured on an actual caisson retained islands /6/.

The first 16 natural frequencies are given in Table 1. The most important modes from the ice-structure interaction point of view are plotted in Figure 4. Even though the structure as a whole is very stiff against ice action, there are many low natural modes that contribute to deformations at ice action points. If the deck would have been fixed on the caisson ring to carry through loads, natural frequencies would have been higher, and many of the modes in Figure 4 totally different.

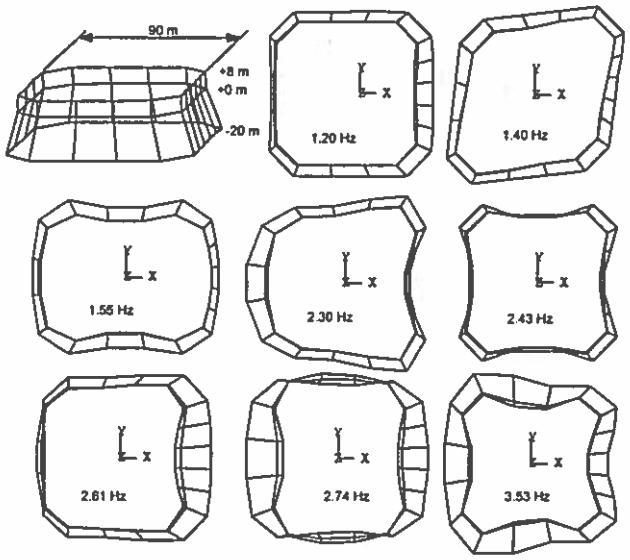

Figure 4. CRI natural modes.

Mode	CRI	3-leg
1	1.19	1.31
2	1.20	1.31
3	1.31	1.44
4	1.40	3.24
5	1.55	3.24
6	2.28	3.70
7	2.30	6.76
8	2.43	6.76
9	2.61	8.76
10	2.70	10.6
11	2.74	10.6
12	3.32	10.7
13	3.44	11.1
14	3.52	11.1
15	3.53	11.4
16	3.58	11.4

Table 1. Lowest natural frequencies (Hz)

Self-excited ice-structure interaction numerical simulation indicates that the 3-legged jacket platform in Figure 3 is highly sensitive for ice-induced vibrations. It would have needed over-critical structural damping to prevent ice-induced vibrations. Resonant lock-in type vibrations, synchronised at each leg, emerge at every practical ice thickness value. Limit cycles develop fast; at ice action point usually during the first cycle, (Fig. 5.a). On the other hand the deck mass takes several cycles before steady limit cycles are stabilised.

At very low ice velocities corresponding the nominal stress rate in the ductile range, left from the ice strength maximum in Figure 2, or at high velocities in the brittle range, no self-excited vibrations develop. If ice velocity makes the nominal stress rate just right from the ice strength maximum, the limit cycles predict saw tooth like structural response at the waterline, (Fig. 5.b). The frequency of repeating ice failures is well below the lowest natural frequency. With increasing velocity at certain point the first natural mode frequency starts to control the crushing frequency regardless of ice velocity, (Fig. 5.c). The lock-in can persist until a higher mode starts to control and makes a lock-in to another frequency, (Fig. 5.d). At velocity range in between,

there exist limit cycles that combine both natural modes, (Fig. 5.e). Partly this is a result of inertia loads from the deck mass.

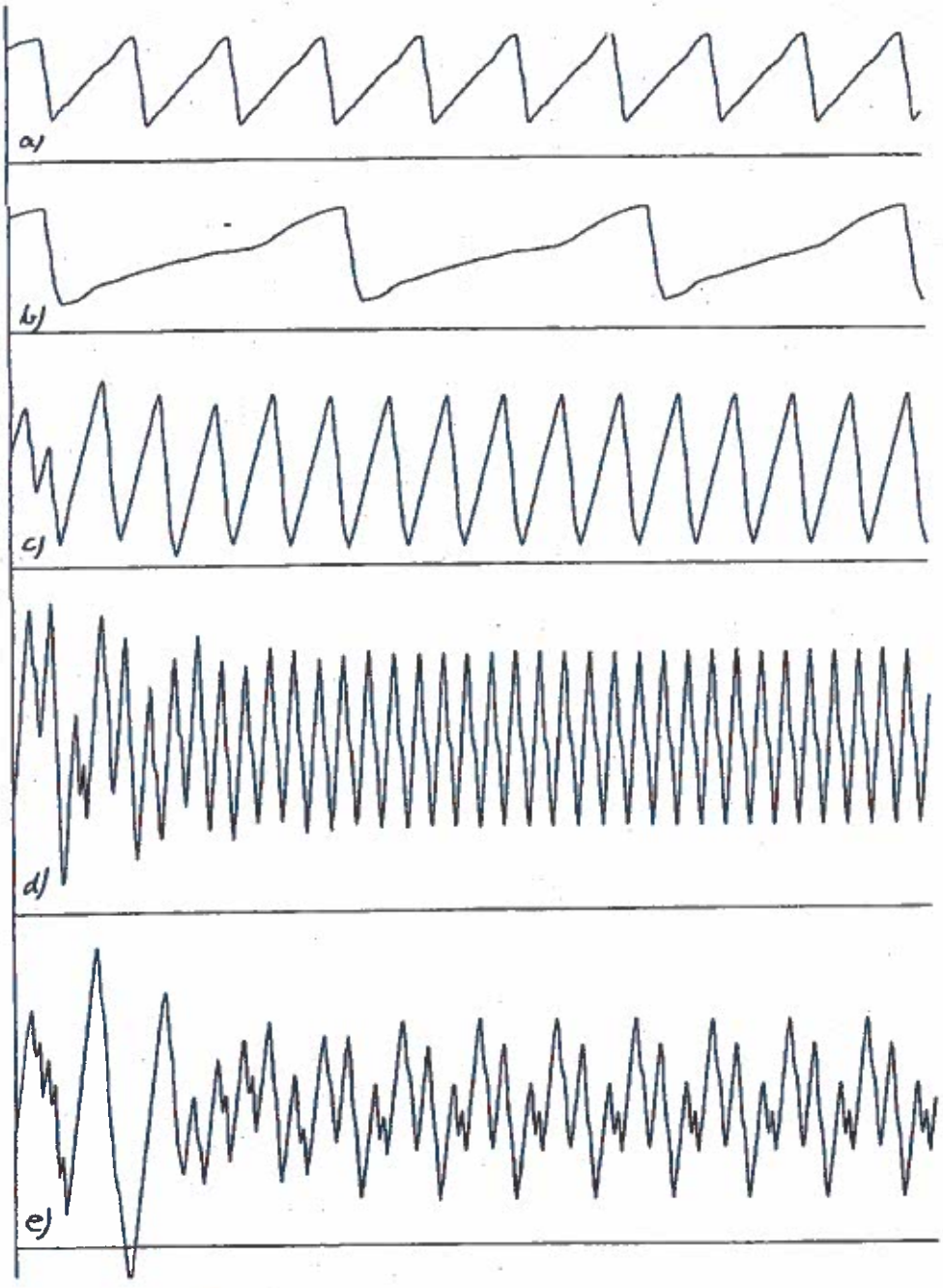

Figure 5. Jacket platform waterline node displacement history vs. time from 0 - 16 s at different ice velocity ratio r. f is limit cycle frequency and d is maximum displacement at ice action point.

a) h=1.0 m, r=0.5, f=0.78 Hz, d= 69 mm.
b) h=2.0 m, r=0.5, f=0.27 Hz, d=135 mm
c) h=1.0 m, r=1.0, f=1.32 Hz, d= 76 mm
d) h=1.0 m, r=1.7, f=3.06 Hz, d= 63 mm
e) h=1.0 m, r=1.4, f=-.-- Hz, d= 79 mm

If ice is thin, higher modes are likely to control the crushing frequency. E.g. in the case of a 0.1 – 0.2 m thick ice 11.1 Hz frequency is dominating and with 0.3 – 0.6 m thick ice 9.9 Hz respectively. With 0.7 m thick ice it is possible to have steady limit cycles at 6.84, 3.06 or 1.31 Hz frequency depending on ice velocity or whether all the three legs are under ice action. On contrary with thick ice, ice velocity directly controls the crushing frequency. Assuming an unrealistic high ice thickness of 2 m, steady saw tooth like limit cycles can be predicted from 0.27 Hz to about 1 Hz with increasing ice velocity. Thereafter the first mode at 1.31 Hz causes a lock-in to occur. Again at the brittle range no lock-in vibrations occur.

The displacement amplitudes of limit cycle vibrations were not simply related to ice velocity. The reason was the jump from one mode to another, and intermittent combination modes, that prevented distinct velocity dependence to show up.

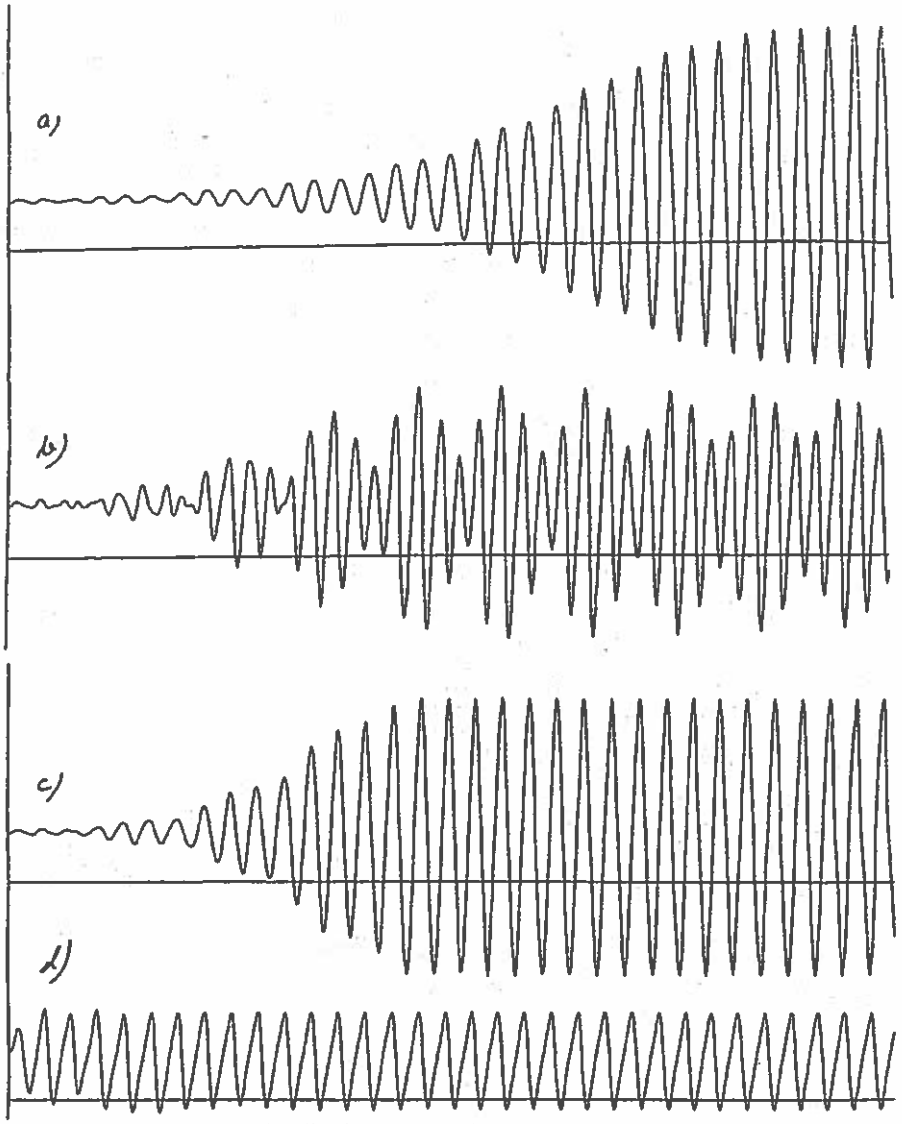

Figure 6. CRI centre node displacement history vs. time from 0 - 32.5 s at different ice thickness h. f is limit cycle frequency and d is maximum displacement at ice action point.

a) h=0.5 m, f=1.21 Hz, d=20 mm.
b) h=2.0 m, f=1.54 Hz, d=22 mm (ice action only at center 1/3-part)
c) h=1.0 m, f=1.18 Hz, d=26 mm
d) h=16. m, f=1.25 Hz, d=49 mm

It was not possible to predict the jacket structure in Figure 3 to exhibit asymmetric ice-induced vibrations, e.g. twisting along the vertical axis. Even if the initial state of deformation was that of a pure twist mode, and ice loads were acting only on two legs to allow 180 degree phase shift in excitation, the limit cycle lock-in response soon developed into a symmetric one controlled by the first mode. However, in another jacket platform with different mass and stiffness properties, persistent steady state lock-in twist mode limit cycles could be predicted

The wide caisson retained island was stiff and not very sensitive to exhibit ice-induced vibrations. By increasing structural damping it was possible to prevent resonant lock-in type ice-induced vibrations totally. In most cases it took many cycles before limit cycle amplitudes started to increase and a steady state to develop, (Fig. 6.a). Always the first mode at 1.2 Hz was the dominant one, and ice loads were synchronized at each ice action node. It was not possible to simulate such saw tooth like response history as was common with narrow structures. Also response, that would be a combination of different modes, Fig. 6.b, was unlikely. Steady state limit cycles were practically always controlled by the first natural mode frequency at 1.21 Hz regardless of ice thickness. Only small variations at 1.18 and 1.25 Hz appeared, Fig. 6.c – d.

With increasing velocity the crushing frequency was generally constant, close to the first natural frequency. The limit cycle displacement amplitude, on the other hand, has almost a linear dependence on velocity, Fig. 7. The non-dimensional velocity is scaled in relation to the center part of the decreasing range in Figure 1. Value r=0.5 corresponds to the peak value and r=1.5 the beginning of the brittle range.

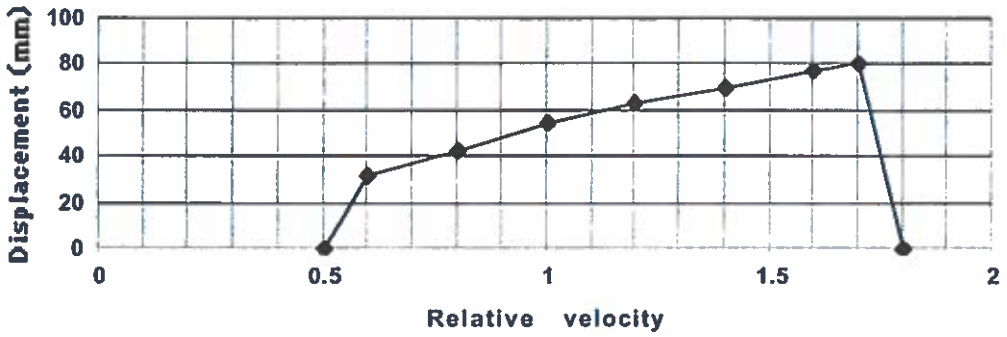

Figure 7. Limit cycle amplitude vs. velocity

It was not possible to achieve steady state limit cycles at asymmetric modes with the caisson-retained island. With symmetric modes it was easier to have lock-in vibrations if ice loads were only at the center part of the sidewall. This is to be expected when compared to the shape of natural modes. The nodes close to corner experience smaller displacement amplitudes and hence their interaction velocity differs from that of center part nodes. Thus corner nodes are in a sense out of phase of the center part and disturb the development of steady state limit cycles.

7. ICE LOADS ON WIND TURBINE FOUNDATIONS

European Commission has set a renewable energy goal to have 5 GW offshore wind energy by 2010 and 50 GW by 2020. Present wind turbine unit size is 2 MW and in design phase there are 3 to 5 MW units. Anyway the EC goal would require thousands of offshore foundations also in the Baltic at ice infested waters. Simultaneous wind and ice induced vibrations in tall structures is a combination with no in-field experience this far. Thus only computational mechanics simulations can give insight for proper design.

After the nature of ice-induced vibrations were learnt and vibration isolation for lighthouses were introduced, the steel foundation pile proved to be successful and replaced caisson foundations in Finland /20/. The same solution is not feasible for wind turbine foundations. Vibration isolation is intended to carry through high vertical and small horizontal loads between the tower and foundation. This function is hard to be combined with high horizontal wind loads.

Without vibration isolation there are two ways to mitigate the effects of dynamic ice forces. First the foundation can be made so stiff that foundation displacement response is insignificant. This requirement is likely to increase foundation cost even though with a caisson foundation the stiffness is naturally high. The second alternative is to use a conical section at the waterline that both changes ice failure from crushing to bending and reduces ice loads. Then the displacement response reduces as well. More important is that ice failure frequency is dependent on ice thickness. With thick ice the frequency falls well below the lowest natural frequencies of the complete structure. Thus the threat of resonant vibrations is avoided with thick ice. With thin ice resonance is possible but the resulting loads are small. The structure needs to be designed to withstand individual ice load pulses and random fluctuations.

In design the natural frequencies and modes of the complete structure has to solved first, and if needed, structural mass and stiffness changed in such a way that resonance due to propeller blade excitation is avoided. Load cases include transients due to ice edge hit or sudden ice load relaxation, random ice load level variations, and continuous repeating ice load failures. Transient or random loading response calculation is an ordinary practice if the loading function is known. Continuously repeating ice load fluctuation is dependent on the response of the structure itself. A self-excited vibration model has to be adopted /22/. A conservative estimate can be calculated by assuming a saw tooth like ice force function, Fig. 8, if level ice crushing force is used as a dynamic load, and the period T chosen to be identical to one of the lowest natural modes.

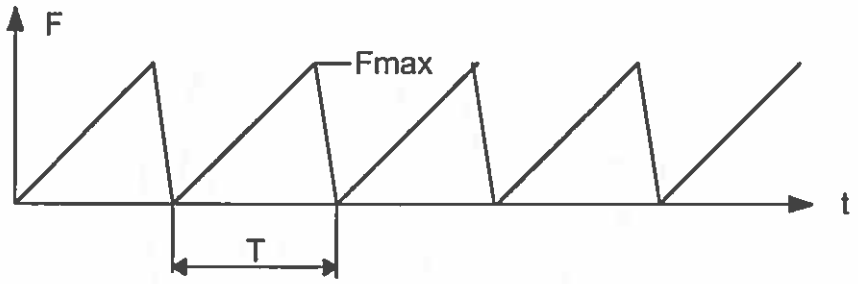

Figure 8. Assumed resonant ice force function

As an example forced dynamic response analysis results due to an assumed 1 MN saw tooth ice loading function are presented. The application pile foundation has a diameter of 4 m in 6 m water depth, it is driven down 16 m into bottom soil, the mass of 67 m high tower is 100 ton, and at the top is 78 ton nacelle and rotor. The first lowest natural frequencies are 0.38 and 2.5 Hz. The transient development of vibrations after the onset of resonance loading at the first natural frequency is given in Fig. 9 and 10. Nacelle displacement amplitude approaches 0.2 m, which is only about 20 % of maximum wind induced deflection. Acceleration levels at the nacelle also remain low at around 0.1 g. For a corresponding much stiffer caisson foundation displacement and acceleration response are only about one tenth of those of the pile foundation.

The application example indicates that dynamic ice loads do not become a restrictive factor for wind generators. With a conical section it is easy to reduce dynamic ice load fluctuations to the order of 1 MN. With cone the repetition rate of ice failures is dependent on ice thickness. Ice failure repeat after ice advances at least a distance of two times its thickness. In the Gulf of Bothnia thick ice velocity never gets over 0.3 m/s. Hence e.g. a 0.8 m thick ice will never fail

against a cone at higher frequency than 0.2 Hz. This is well below the wind generator lowest natural frequency, and hence resonant loading is possible only with thin ice and low ice forces.

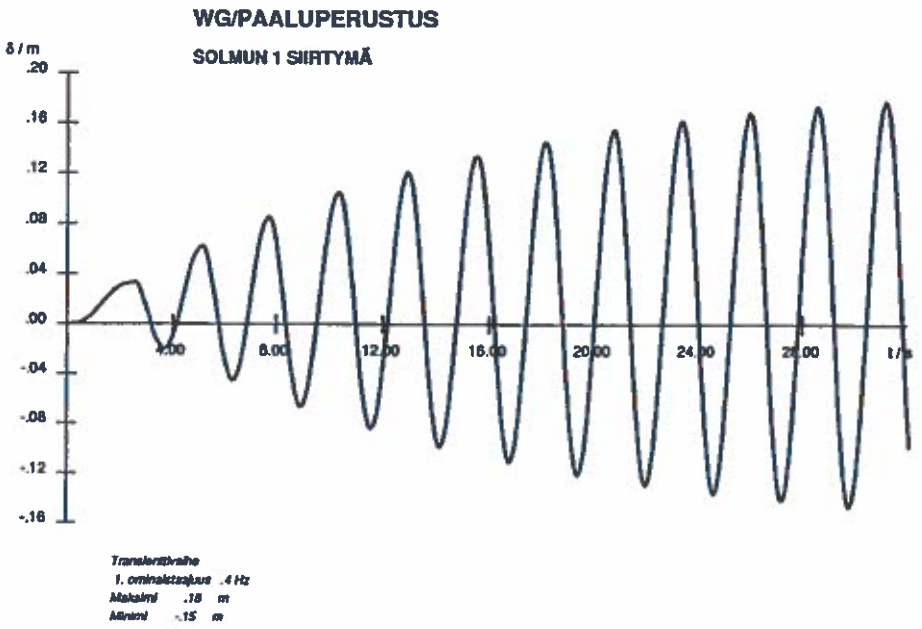

Figure 9. Transient displacement (m) vs. time (s) at the nacelle in resonant loading.

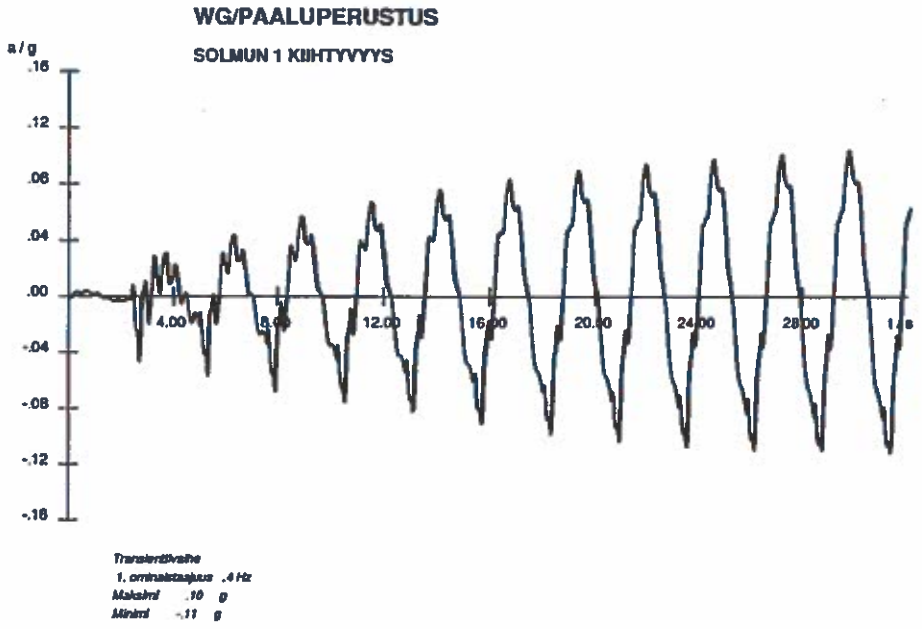

Figure 10. Transient acceleration (m/s^2) vs. time(s) at the nacelle in resonant loading.

CONCLUSIONS

Vibrations in offshore structures can be very severe while ice is moving driven by winds or current. Dynamic loading cases include transient impact loads and continuos ice failure loads. Measured dynamic load histories indicate saw tooth like functions, persistent close to harmonic

load repetition and random load variations. Most critical is the resonant type ice failure repetition.

Dynamic equations of motion of the structure are homogenous if a constant thickness level ice is moving and crushing against the structure. If the system of equations is dynamically unstable, ice-induced self-excited vibrations will emerge and tend to limit cycles.

Computational mechanics can be used efficiently to integrate numerically the dynamic response of an offshore structure to ice loads. Self-excited models predict similar response that has been observed and measured in-field.

Offshore wind energy applications need stringent dynamic analysis design both for wind- and ice-induced vibrations. Presented numerical analysis suggests that tall wind turbine towers can be designed to withstand also dynamic ice loads.

REFERENCES

1 Akagawa S., Saeki H., Takeuchi T., Sakai M., Matsushita H., Kamio Z., Terashima T. and Nakazawa N. (2001): Medium-scale field ice indentation test – Winter 1996-2000 test program. Proc. POAC '01, Canadian Hydraulics Centre, Ottawa Canada, 2001. pp. 567-576

2 Blenkarn K. A. (1970): Measurement and analysis of ice forces on Cook Inlet structures. Proc. 2nd Offshore Technology Conference, Houston, TX, OTC 1261, Vol. II, pp. 365-378.

3 Daoud N. and Lee F. (1986): Ice-induced dynamic loads on offshore structures.OMAE 1986, Tokyo, Japan, Vol IV, pp. 212-218.

4 Engelbrektson A. (1983): Observations on a Resonance Vibrating Lighthouse Structure in Moving Ice. POAC 1983, Helsinki, Finland, Vol II, pp. 855-864.

5 Izumiyama K., Wako D., and Uto S.(1998): Ice Force distribution on a flat indentor. Proc. IAHR Symposium on Ice 1998, Potrsdam, USA. pp. 917- 922.

6 Jeffries M. G. and Wright W. H. (1988): Dynamic Response of "Molikpaq" to Ice-Structure Interaction. OMAE 1988, Houston, TX, USA, Vol IV, pp. 201-220.

7 Joensuu A. and Riska K. (1988): Jään ja rakenteen välinen kosketus. (Contact between Ice and Structure, in Finnish only,). Report M-88. Helsinki University of Technology, Laboratory of Naval Architecture and Marine Engineering, Espoo, Finland.

8 Jordaan I. J., Maes M.A., and Nadreau J-P. (1988): The Crushing and Clearing of Ice in Fast Spherical Indentation tests. OMAE 1988, Houston, TX, USA, Vol IV, pp. 111-116.

9 Kärnä T. (1992): A procedure for dynamic soil-structure-ice interaction. Proc. ISOPE 1992, Vol. II, pp 764-771. International Society of Offshore and Polar Engineers, San Francisco.

10 Kärnä T. (1997): A layered flaking model for ice load determination. Proc. 6th Finnish Mechanics Days, pp. 85-101. University of Oulu, Finland.

11 Matlock H., Dawkins W. and Panak J.(1969): A model for the prediction of ice structure interaction. Journal of Engineering Mechanics, ASCE, EM4:1083-1092.

12 Michel B. and Toussaint N. (1977): Mechanisms and theory of indentation of ice plates. Journal of Glaciology, 19(81):285-300.

13 Michel B. (1978): Mechanics of Ice. Universite Laval, Quebec, Canada.

14 Montgomery C.J, Gerard R. and Lipsett A.W (1980): Dynamic Response of Bridge Piers to Ice Forces. Canadian Journal of Civil Engineering, 7:345-356.

15 Muhonen A. (1996): Evaluation of three ice-interaction models. Helsinki University of Technology. Espoo, Finland. Licenciates's thesis. 90 p.

16 Määttänen M. (1975): Experiences of ice forces against a steel lighthouse mounted on the seabed, and proposed constructional refinements. Proc. POAC'75, Fairbanks, Alaska 1975.

17 Määttänen M. (1978): On conditions for the rise of self-excited ice-induced autonomous oscillations in slender marine structures. Finnish-Swedish Winter Navigation Board, Finland, Research Report 25, 98 p.

18 Määttänen M. (1983): Dynamic ice structure interaction during continuous crushing. U. S Army Cold Regions Research and Engineering Laboratory, Hanover, NH, USA 03755, CRREL Report 83-5, 53 p.

19 Määttänen M. (1984): The effect of structural properties on ice-induced self-excited vibrations, Proc. IAHR Symposium on Ice 1984, Hamburg, West Germany, Vol II, pp. 11-20.

20 Määttänen M . (1987): Ten years of ice-induced vibration isolation in lighthouses. OMAE 1987, Houston, TX, USA, Vol IV, pp. 261-266.

21 Määttänen M. (1988):Ice-induced Vibrations in Structures - Self-Excitation. Proc. IAHR Symposium on Ice 1988, University of Hokkaido, Sapporo, Japan, Vol 2. pp. 658-665.

22 Määttänen M. (1998): Numerical Model for Ice-Induced Vibration Load Lock-in and Synchronization. Proc. IAHR Symposium on Ice 1998, Potsdam, USA. Pp. 923-930.

23 Neill C. (1976): Dynamic ice forces on piers and piles: An assessment of design guidelines in the light of recent research. Canadian Journal of Civil Engineering, 3:305-341.

24 Nevel D. E. (1986):Iceberg Impact Forces. Proc. IAHR Symposium on Ice 1986, University of Iowa, Iowa City, IO, USA, Vol III, pp 345-369.

25 Peyton H. (1968): Sea ice forces. Ice pressure against structures, National Research Council of Canada, Ottawa, Canada, Technical Memorandum 92, pp. 117-123.

26 Sanderson T. (1988): Ice Mechanics – Risks to Offshore Structures. Graham and Trotman Ltd, London.

27 Sodhi D. and Morris C. (1986): Characteristic frequency of force variations in continuous crushing of sheet ice against rigid cylindrical structures. Cold Regions Science and Technology 12:1-12.

28 Sodhi D. (1988): Ice-induced vibration of structures. Proc. IAHR Symposium on Ice 1988, Sapporo, Japan, Vol 2. pp. 625-657.

29 Sodhi D. (1994): A theoretical model for ice-structure interaction. Proc. OMAE-94, Vol. IV, pp.29-34. ASME, New York.

30 Vershinin S, Kouzmitchev K. and Tazov D. (2001) Proc POAC'01, Canadian Hydraulics Centre, Ottawa. Vol. I, pp. 403-412.

31 Wang K., Wu H., Wang C. and Liu L. (2001): Modelling sea ice ride-up and pile-up against conical caisson in Bohai Bay. Proc. IAHR Symposium on Ice 1998, Potsdam, USA. pp. 939-945.

32 Xu J. and Lingyu W. (1988): Ice force oscillator model and its numerical solutions. OMAE 1988, Houston, TX, USA, Vol IV, pp. 171-176.

33 Yue Q., Bi X. and Yu X. (2000): Effect of ice-breaking cones for mitigating ice-induced vibrations. Proc. IAHR Symposium on Ice 2000, Gdansk, Poland. pp. 127-133.

OWEMES '97
(Offshore Wind Energy in Mediterranean and other European Seas)

OFFSHORE WIND TURBINE FOUNDATIONS IN ICE INFESTED WATERS

***Erkki Haapanen, MScTech **Mauri Määttänen, D.Tech, ***Pekka Koskinen, MScTech**

*** Engineering Office Erkki Haapanen Ky, A Limited Partnership Company**
**** Helsinki University of Technical - Faculty of Mechanical Engineering**
*****Technical Research Center of Finland - Manufacturing Technology - Maritime Technology**

FINLAND

ABSTRACT

The northern coast of the Gulf of Bothnia has a great potential of wind resources and shallow waters. The majority of the wind turbines in Finland are located ashore along the coast line of the Gulf of Bothnia. The useful area is narrow making the offshore area very promising for wind energy. There are potential offshore sites for major wind parks in many locations along the 500 km coast line.

The real challenge is to develop a technology for wind turbine foundations to withstand high loads caused by up to 1.3 m thick ice during the winter time. The behaviour of ice has to be thoroughly understood. The maximum lateral ice load level can reach to an order of ten MN when high winds drive ice against the foundation structures. The larger the solid ice field the larger are the loads. Pressure ridges, which are causing a lot of trouble for marine operations, are not considered to be a major problem for wind turbines in shallow waters (max 7 m deep), because of a deep keel which will stop the ice well before the wind turbines. Ice may also cause uplift loads during water level changes. This force can reach a magnitude of one MN depending of the dimensions. The most dramatic case is caused by ice blocks piling up against the tower and foundations. This pile-up can reach a height of ten meters or even higher and cause damages to the tower structures. Thermal ice expansion can also induce lateral loads on the foundation structures.

The paper describes ice properties, ice action against structures, and presents different options for solving ice related problems in wind turbine foundations with some recommendations on how to avoid hazardous situations.

KEYWORDS

Offshore, Wind Park, Ice, Wind Energy, Foundation, Load

Introduction

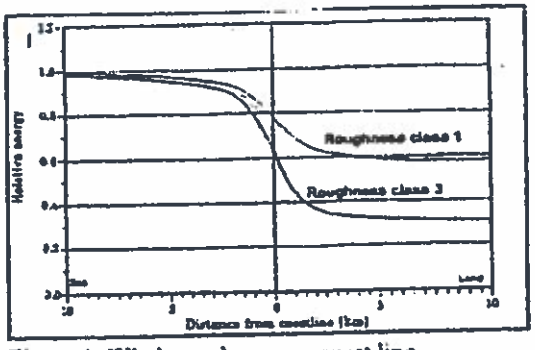

Figure 1. Wind speed across a coast line

The highest wind speeds are found in open sea areas. Figure 1 shows the wind speed change across the coast line. Wind turbines work best in open sea areas where the flow is less turbulent and the wind energy highest. Hundreds of turbines can easily be built offshore. The increase in wind speed will compensate for the higher cost of construction. The large size of modern wind turbines has brought us to a point, where the ice and rough sea can be challenged. We know from maritime winter navigation experience how to build offshore lighthouses and aids-to-navigation on an open sea even if the ice thickness is more than one metre and the sea is deeper than 10 metres. The wind society can now start to use ice infested sea areas for energy production. The technical Research Center of Finland has started a development program in which a prototype wind turbine foundation will be built in the waters of the Gulf of Bothnia.

This paper describes what can be expected from moving thick ice, presents ice load scenaria, and advises how to select a location for an offshore wind park. A practical problem in design is the uncertainty in estimating the ice loads and ice behaviour. Before a decision about the wind park site, the local environment should always be checked and discussions held with local seamen, fishermen and people who have lived years dealing with the ice and know it by heart. In the Gulf of Bothnia there are lots of excellent places for wind parks where the ice loads can be limited to a reasonable level and the production of clean energy is feasible.

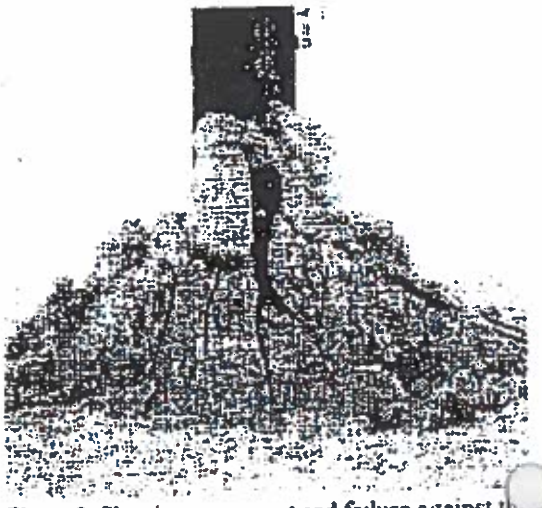
Figure 2. Slow ice movement and failure against th Kemi-1 lighthouse with a test cone

The ice load cases and their order of importance

Offshore structures will be influenced and stressed in many different ways by the ice around them. In the Gulf of Bothnia at the open sea, outside the fast ice zone, the level ice thickness is typically below 80 cm. However, the ice fields are heavily ridged. The pressure ridges are typically 4 to 6 m thick. However, an above water sail of a ridge can be more than 2 m high and an underwater keel more than 10 m deep. The ridged ice fields are often moving due to winds and currents causing high loads on offshore structures. Thus the areas, where heavy ridging occur, are not economically possible locations for wind turbines.

At the coastal region ice is moving only in autumn before the land fast zone is formed. Thus, the thickness of the moving ice is significantly lower than at the open sea area. When a strong wind drives a large ice floe, it may move at a speed up to 1 3 % of the wind speed. When such a floe meets a wind turbine foundation, it will either be stopped or broken by the structure. In the coastal area the level ice thickness may grow more than one metre thick. Temperature changes in the fast ice field will either expand or shrink the ice cover. The foundations at the coastal region have to be designed to withstand the loads due to relatively thin moving ice and thermal expansion of the thick fast ice.

In the Gulf of Bothnia the water level will rise due to storm surges from the south. The water level rise in

Kokkola can be about 1 metre and in Kemi up to 2 metres. After the storm surge, or during northerly winds the water level sinks. In winter the ice cover will reduce these maximum water level changes. When the rising water level lifts the ice, it causes uplift loads on the foundation.

Moving ice.

Shear forces created by the wind will push the ice. The driving force F [kN] is depending on the wind kinetic energy and on the surface roughness of the floe. /7/

(1a) $$F = A * \mu * q_k$$

in which

(1b) $$q_k = v_k^2/1600$$

A = the area of the ice float, m²
μ = friction factor.
= 0 0010 for smooth ice
= 0.0015 for snowy ice;
= 0.0020 ... 0,005 for rough and pack ice
q_k = wind kinetic pressure, KPa
v_k = wind speed, m/s

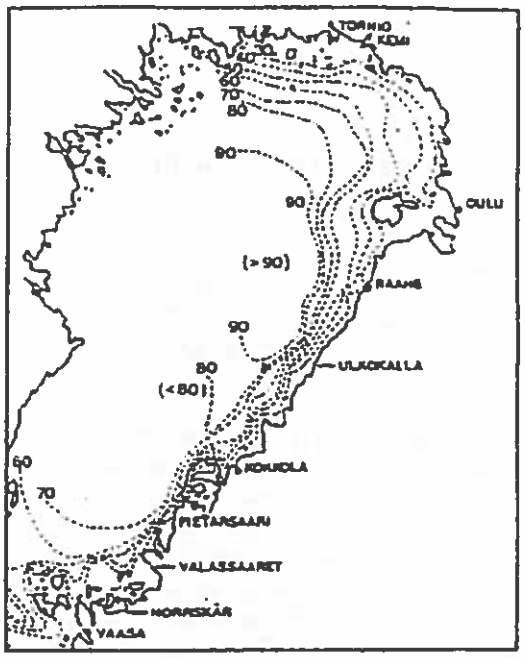

Figure 3. Moving ice thickness on the Gulf of Bothnia. Note the 0,3 m zone nearest to the coast line /10/

We can see from this formula that if the area of a floe is large enough, the force will be extremely high. In designing the maximum area in this formula should be chosen. In the Gulf of Bothnia the floe may easily be 30 x 30 km² and a 20 m/s wind will create a shear load of 0 5 ... 1.0 Pa on the surface and up to 900 MN to the whole floe. In a storm the wind speed may reach 35 m/s for few hours. It is evident that such a driving force is too large for any wind turbine foundation to resist. Practically there are two options, either the ice or the structure has to break.

Near the coastline the ice thickness in a landfast ice zone may reach 1.3 metres while further offshore in the actively moving ice zone an 0.8 m ice thickness is frequent. The structures to break such a thickness have to be extremely strong and heavy This is an obvious threat to the economy of a wind turbine structure. The site for wind turbines should be chosen in the landfast ice zone so that there are natural or man made objects to prevent too large moving floes to hit the structures. From a long experience we know that in many locations there is a few kilometre-wide zone along the coast, where only thin ice, less than 0.30 m thick, can move at the beginning of the winter before getting thicker and stabilizing, (Figure 3). In these areas the thicker ice can also move during spring, but then its strength has already detoriated. The landfast ice zone is a natural choice for wind generator foundations as maximum ice forces will

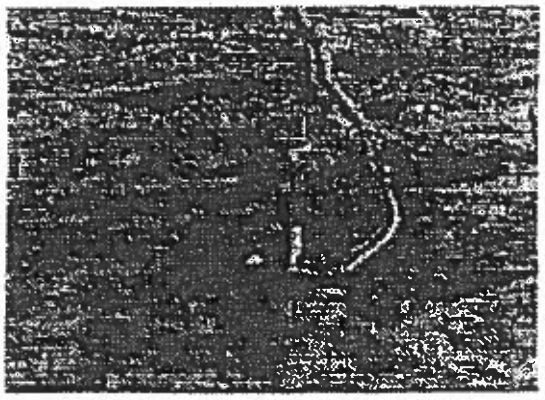

Figure 4. Wind driven ice movement at the active ice zone, Kemi-2 Lighthouse

there be limited due to the limitation of the moving ice thickness.

Forces and means to break moving ice

Ice properties will vary with time due to environmental conditions. The salt content of the water, time history of the temperature, snow coverage and consistency of ice will affect ice strength and ductility. We have to look at different load cases and then be sure that the structures are built for those requirements.

Solid ice in the autumn is the strongest and most ductile but not yet very thick. The strength in compression at a high loading rate would reach up to 10 MPa, or even higher with small test pieces. Ice strenght decreases with decreasing loading rate, and with increasing size. Thin ice cover may buckle and fail by bending before the normal stress reaches the compressive strenght limit along all the contact area. The wind friction on smooth level ice is very low and causes low pushing force. When snow covers the ice, the friction increases with the height of the snow dunes.

At the coldest time in winter, the ice has normally experienced a few temperature fluctuations which bring with thermal cracking and make the ice not homogenous any more. There may be some ridges, cracks, long leads, and other discontinuities in the ice field. Weathered cold, moving ice breaks easier than virgin autumn ice. Compressive strength is still high, but during interaction with a structure the average pressure against the whole contact area falls below 3 MPa. Later in spring when the temperature is close to the melting point the compressive strength goes down to 1.5 MPa and later to 1.0 MPa, when the ice has weakened through melting. And if the ice is moving very slowly as in the case of a thermal expansion, the compressive strength falls below 0.5 MPa and the behaviour of the ice is ductile. All these stress values are subject to arguments and may vary depending on the winter.

When ice is pushing a structure, it is compressed and possibly bent due to the eccentric or inclined contact area. Highly stressed ice will break and due to the brittle nature of the ice, the cracking will continue. Cracked pieces will be forced away, to bypass the foundation, above or below the ice cover depending on the surrounding conditions and the slope of the contact area. The ultimate load depends on the ice properties, dimensions and the geometrical shape of the obstacle.

The crushing load will be dynamic and fluctuate either

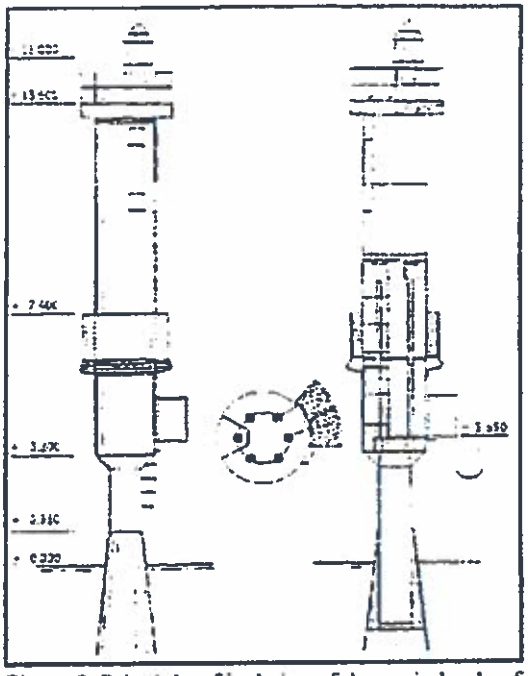

Figure 5. Principle of isolation of dynamic loads of a lighthouse. System allows lateral movement of the upper part of the tower.

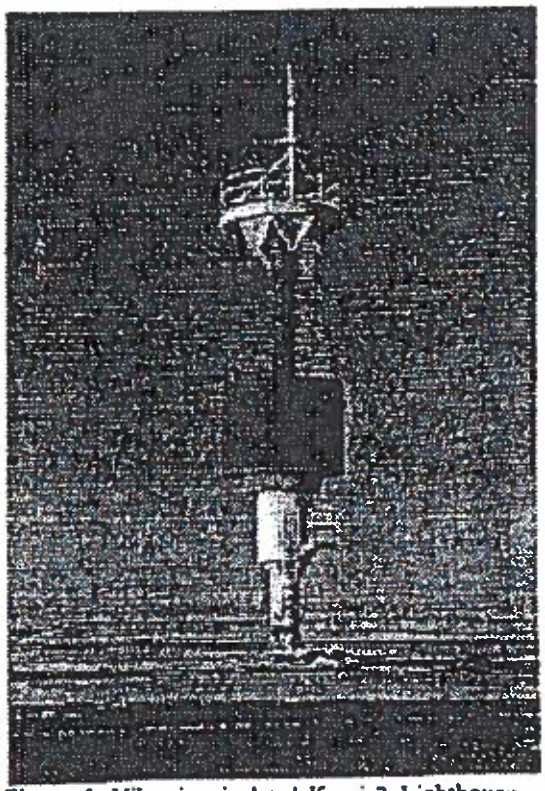

Figure 6. Vibration isolated Kemi-2 Lighthouse. Wind generator on the top has been running smoothly since construction in 1981

randomly between near zero and a certain maximum, or there is a dominant frequency depending on the ice thickness, speed, and structural response. Load amplitude also has random fluctuations. The thicker the ice, the higher the forces. Eigenfrequencies of the structure may control the ice failure frequency resulting in resonant vibrations. This situation is very dangerous for a wind turbine with a nacelle weight at the top of a narrow long tower. The foundations have to be designed in such a way that there is no chance for a resonant loading, or that the tower itself has vibration isolation to prevent oscillations and high dynamic loads. In Finnish offshore steel light houses the superstructure has been installed on top of a vibration isolation section. This concept has been proven in the field for more than twenty years in practice (Figures 5 and 6).

The initial crushing strength of ice is high if the structural shape does not stimulate bending or initiate crack propagation. To avoid extreme loads we could enhance the breaking of the ice before it reaches the wind turbine, or prevent the ice from moving by locking it in place. This is the normal situation in the landfast ice zone near the coast line, where there are natural blocks like rocks and islands to prevent ice from moving. Islands and skerries will also limit the maximum size of a floe, and prevent all but only thin ice movements. Figure 3 shows a landfast ice zone, approx. 3 - 5 km wide, in the coastal area of the Gulf of Bothnia. Here thick ice is locked by natural stoppers. By knowing the local geography and long term ice behaviour, we can approximate the maximum size and pushing force of moving floes and use this information when designing foundations.

Loads to a vertical, cylindrical foundation, when the ice starts to move or is moving.

In literature the formula for the maximum static force due to ice crushing against a vertical structure is [5], [7]:

(2)
$$P_i = k_1 * k_2 * k_3 * b * h * \sigma_{ip}$$

where k_1 = shape factor for the structure
= 0.9 for round shape
= 1.0 for rectangular shape

k_2 = ice to structure contact factor
= 1.0 when an adfrozen floe starts moving
= 1.5 when a thick ice collar has adfrozen to the structure
= 0.5 when ice is cracking continuosly

k_3 = shape ratio factor

(3)
$$k_3 = (1 + 5 * h/b)^{0.5}$$

b = width of the structure (at a level ⅛h down from the ice upper surface)
h = ice thickness
σ_{ip} = compressive strength of ice
= 3.0 MPa for intact ice moving by the wind or current at the coldest time of winter
= 2.5 MPa for intact ice moving very slowly e.g. by thermal expansion or shrinking at the coldest time of winter
= 1.5 MPa for intact ice moving in the spring and the temperature is close to melting point
= 1.0 MPa for partially weakened melting ice moving at a temperature close to melting point

This formula suggests that the worst situation is at the very moment, when a thick ice collar, adfrozen to the structure, starts to crush. Here the ice compressive strength may be σ_{ip} = 3.0 MPa and the contact factor k_2 = 1.5. However, as the ice movement starts, the loading rate is so low that the loading rate dependent ice strength is also low resulting in loads less than in the case of faster moving ice with a lower contact factor but higher strength. Hence it is the combination of all factors that has to be considered. Measurements have proven that the

initial ice failure with good contact induces the highest loads, and thereafter, the load decreases suddenly close to zero and rises again to a new maximum, which is a lot less than the initial one because of the reduced contact factor k_2.

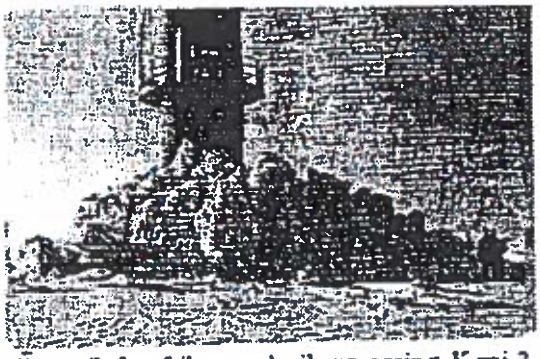

Figure 7. Ice failure and pile-up against Kemi-2 cone at active ice zone.

Loads to a conical foundation

As moving ice hits a conical foundation, both horisontal and vertical loads will develop. An ice sheet breaks easier by bending than by crushing. This makes bending failure dominant, even though crushing and shearing modes are present simultaneously to some extent. In addition the mode of ice failure depends on the shape and size of the structure. It also depends on ice properties, ice velocity and the friction between the structure and ice. In a loading cycle local crushing and shearing will occur initially, smoothening a large enough contact area, making higher ice loads possible. Increasing vertical forces first cause radial cracks and later a circumferential crack, which yields to the final bending failure. Thereafter, a new cycle can start. The ice load is at its maximum just before the formation of the circumferential crack. Clearing mechanisms involve pushing broken ice pieces upwards and aside of the structure. Figures 2 and 7.

The cone ice force calculations are based on loads needed to break the ice in the bending mode, to raise broken pieces up, and to bypass the structure. An upper bound plastic limit analysis solution can be calculated by Ralston's model. Later more refined FEM-analysis and full-scale measurements have indicated that Ralstons's model in general overpredicts maximum loads. The procedure for cone ice load calculations is too demanding to be presented here, see References /5/ and /6/.

Dynamic load

Ice failure against a structure is mostly dynamic causing dynamic load fluctuations. In dynamic ice structure interaction energy from the moving ice is being transferred and stored as elastic and kinetic energy in the structure. A dynamic crushing load P_D may have a random frequency between 0.5 Hz and 10 Hz. A resonant state may develop while an eigenmode of the structure controls the ice crushing frequency. The theoretical explanations for dynamic ice-structure interaction are based on forced or self-excited vibration models. Resulting ice force history can be solved with numerical integration of dynamic equations of motion.

In practise, however, the dynamic ice load is simply assumed to be a fraction of the static level ice load Eq 2, e.g. 50 %. If this load amplitude is applied at the frequencies of lowest eigenmodes of the structure, a conservative design against dynamic ice action is achieved. Another case is the hit of an ice edge which causes dynamic amplification of the superstructure displacements.

When ice is cracking by bending, the frequency varies from 0 to 1 Hz. The amplitude of the load varies between zero and P_D. the Conical shape of the foundations has a great importance in lowering the dynamic stresses.

Pressure ridges and ice pile-up

Pressure ridges are formed, when ice is compressed, buckled and crushed together. The pressure will lift up the crushed area. Some of the crushed ice blocks go under the water forming a keel,which typically has the depth 10 and width 30 times the height of the parent ice sheet. Pressure ridge formation takes place in the active ice zone beyond the landfast ice zone. It is not recommended to install wind generators in such areas.

Ice pile-up frequently occurs in shallow waters, or when moving ice hits the shore or the wind turbine foundations. This can occur also in the landfast ice zone before the ice thickness has grown over 0.4 m. Local loads against the structure are not too high but the threat is in the height of the pile-up, up to 14 m high formations have been recorded. The access door to the wind turbine may be blocked. Removable ladders may be required to enter the tower. The ice blocks may damage all protruding obstacles like a landing stage from the tower and foundation. The lower end of the tower must be strong enough to withstand these impacts. The impact is caused by single ice blocks sliding down and hitting against the foundation. The pressure load is low and the situation looks much worse than it really is. In the wind park area the the formation of pile-ups should be initiated on top of natural or artificial hindrances, well before the wind generators.

Rising water level makes the ice force to lift the foundations

High winds induce water level changes also during winter time even though the sea is ice covered. As ice is normally adfrozen to the foundation or tower, it results in the vertical uplift loads on structures. The surface properties of the contact area determine the maximum force. Wind turbine foundations are usually heavy enough to resist this force. The vertical load can be estimated by a formula

(7)

$$V = \tau * A$$

where A = adhesion or contact area, m²
τ = adhesion strength (e.g. at - 10°C τ = 0.1 MPa for plastics and up to 1 MPa for concrete)

How to select a proper site for offshore wind park

The wind park location should be in the landfast ice zone in a shallow place, surrounded by some islands, reef or skerries to prevent large floes from pushing the wind turbine foundations. This will limit the maximum moving ice thickness below 0.4 metres which correspondingly limits ice loads against the foundations. If some stones or rocks are seen above the water level, they are excellent stoppers and ice breakers. Shallow water depth in front of a wind park induces ice pile up preventing further ice movement closer to the coastline. However, there should be a waterway to the site for building the foundation and transporting the material.

Summary

An offshore wind park in ice infested waters is a challenge. Moving ice exerts severe loads against the foundations and ice pile-up can reach to the propeller blades or prevent access to the tower.

By choosing the wind park site inside the landfast ice zone significantly reduces the thickness of moving ice, resulting ice forces, and other adverse ice actions. By proper foundation design the ice failure mode can be controlled, which on its behalf further reduces ice loads.

Thorough knowledge of the ice dynamics history in the proposed site is essential in finding optimum solutions, which limit ice loads to a reasonable level and make offshore wind parks not only technically but also economically feasible. Large coastal areas even in ice infested waters can thus be utilized to produce wind energy efficiently

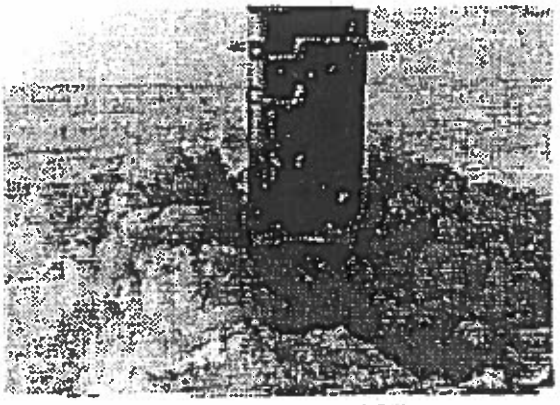

Figure 8. Slow ice movement and failure against a lighthouse at landfast zone in Kokkola

References:

1. Cammaert & Muggeridge: Ice Interaction with Offshore Structures, van Nostrand Rheinhold 1988, New York.

2. IAHR working group on "Ice Forces on Structures" State of Art Reports, 1980, 1984, 1986, 1988 and 1992.

3. Michel B: Mechanics of Ice, Les Presses de L'Universite Laval, Quebec 1978.

4. Määttänen M.: Ice Forces and constructions. Bi-lateral symposium on Ice Engineering The Chinese Hydraulic Engineering Society, The Finnish National Committee on Large Dam. Proceedings report 1989. Beijing

5. Määttänen M.: Design Recommendations for Ice Effects on Aids-to-Navigation. IALA Technical Committeee to study the Effect of Ice on Lighthouses. International Association for Lighthouse Authorities. Paris 1984

6. Ralston T. (1977):Ice Force Design Considerations for Conical Offshore Structures. POAC 1977, Memorial University of Newfoundland, St.John's, Newfoundland, Canada, Vol II, pp. 741-752.

7. RIL: Rakenteiden kuormitusmääräykset. (Finish Regulations for Structural Loads)

8. Sanderson T: Ice Mechanics, Risk to Offshore Structures, Graham & Trotman, Lontoo 1988.

9. YIT Ltd. The Vibration Isolated Lighthouse, Brochure

10. Palosuo E., et Al.: Formation, thickness and stability of fast ice along the Finnish coast. Institute of Marine research. Helsinki 1982.

ICE AND OFFSHORE WIND TURBINES IN THE GULF OF BOTHNIA

Mauri Määttänen
Helsinki University of Technology
Espoo Finland

ABSTRACT

The Gulf of Bothnia between Finland and Sweden has large relatively shallow areas with average annual wind speed above 7 m/s. In addition coastal areas in the Finnish side are gradually rising after the Ice Age creating new unpopulated land. All this makes these coastal areas good candidates for wind energy farming. Compared to existing offshore wind farms the foundations in the Gulf of Bothnia have to be designed to withstand level ice thickness up to 1.2 m. Beyond the landfast ice zone moving ice can be 0.8 m thick with significant pressure ridges.

An overview is presented on the wind energy potential in the Gulf of Bothnia, and on environment and ice conditions. Different techniques for wind turbine offshore foundations are compared with an objective how to avoid adverse effects in the turbine itself. Foundation design for both static and dynamic ice forces is addressed. Results indicate that with increasing size of the wind turbine power output the relative increase in the foundation cost due to ice action is diminishing. This, together with a possibility to produce a large number of wind turbines at same time to a vast offshore area, makes subarctic offshore wind energy a promising opportunity in near future.

1. INTRODUCTION

Wind energy has been maturing in 90's as an alternate renewable clean energy source. The wind generator propeller blades, hub and machinery have been developed to operate reliably and need less maintenance. With improved electrical energy conversion efficiency and benefits from serial production the price per produced kWh is decreasing and approaching that of conventional energy prices. The cost of coal fired power is increasing due to clean air acts. Nuclear power plants have been made unpopular due to unbelief on long duration waste treatment safety. Most of the usable hydropower is already harnessed. World oil and gas resources have limited endurance, and their energy use increases greenhouse effect. All this is making the future of wind energy brighter.

It is only few people that consider wind energy park as a decoration in the scenery. On the contrary there are becoming more and more restrictions where to construct wind generators. This is imminent already even in rural districts, e.g. in Germany, where a lot of wind energy has been installed. Another problem is that most of the present wind generators are less than 0.6 kW in capacity, and hence a great number of them are needed e.g. a multiple of nominal one thousand units to replace a 600 MW nuclear power plant. Therefore Denmark, which is a forerunner in utilizing wind energy, has started to construct wind generator parks at sea away from the population.

The trend in wind generator size is now towards larger units, to the capacity range of over 1 MW. Especially at offshore sites where foundations are more expensive it is a must to use large units. A typical 1.5 MW wind generator has its hub over 60 m level above the surface. As the diameter of the propeller is also over 60 m the blades reach to 100 m height at their topmost position. The steel tower starts with 4 m diameter and is still over 2 m at the hub level. Due to disturbance to the passing air the spacing of such generators has to be over 300 m. This allows about ten generators on a square kilometer and a nominal production of 15 kW/km^2. The blade of a 1.5 MW wind generator can be visible to a distance of 35 km at sea level and even the hub close to 30 km.

In Finland the Ministry of Trade and Industry funded a research (Holttinen et.al, 1998) to find out what is the potential of offshore wind energy in Finland and what are the implications of moving ice on wind generator foundations. By setting restrictions that water depth should be less than 10 m and annual average wind velocity over 6 m/s it was learnt that about 70 TWh, all of the annual Finnish electricity consumption, could be harvested from the Gulf of Bothnia. The potential is still significant even though only 10 %, the best and easiest locations, were utilized. Most of that area is shallow sea bottom that is gradually rising after the weight of continental ice was relieved. There is marginal use for fishing or recreation. Shallow coastline is not applicable or tempting to build summer cottages. Disadvantage is the presence of ice even for over half of the year.

In this paper wind, wave, ice and sea bottom conditions in the Gulf of Bothnia are described with an eye on establishing wind parks. Prerequisites for a good wind park are set. Different ice loading scenaria are presented. Dynamic ice forces put forward a special threat on the vulnerable propeller blades and the machinery. Principles for observing static and dynamic ice loads in foundation design are addressed.

2. OFFSHORE WIND GENERATOR PARK

Open sea is an optimal location for a wind generator. At offshore sites the wind energy production is over 10 % better than inland at the same wind speed and generator. The reason is a better shape in the wind boundary layer profile and lower turbulence level in the wind. In many cases also the average wind speed is higher at sea than inland.

Adverse effects on offshore wind generators are wave and ice loads against the foundation, and sometimes a limited access for the maintenance personnel. Atmospheric icing on the tower and propeller blades can be more intense than at inland locations.

The selection of wind generator park location is crucial to both wave and ice loads. At landfast ice zone thick ice becomes anchored on shoreline, rocks, shallows, islands, and sometimes due to grounded pressure ridges. It will not move even though storm surges cause changes in the water level. Only thin ice moves early in the winter and thick ice late in the spring when it has already become soft and detoriated. During the winter only thermal ice expansion loads are met. Hence limited ice action is excerted against the foundations in the landfast ice zone.

During ice free period at the regions of landfast ice zone, wave loads are partly reduced due to same reasons that prevent ice from moving: rocks, shallows and islands dissipate wave energy. In the Gulf of Bothnia there is no tide but a storm surge can raise water level over two meters. This allows deeper waves to proceed longer. As water depth decreases waves get higher and steeper.

Other provisions for a good wind generator site is a relatively short distance to main powerline network or local consumption. In the Gulf of Bothnia main powerlines are accessible along the whole coastline. This in addition to vast areas of landfast ice zone, Fig. 1, sparse population and limited possibilities for fishing and recreation make the Gulf of Bothnia a prospective location for harvesting wind energy.

Figure 1. Landfast ice zone along the Gulf of Bothnia. Ice map 1985-03-14

3. WIND AND WAVE LOADS

Average annual 6 m/s wind speed line follows close to the shoreline along the Finnish side of the Gulf Of Bothnia. Less than 2 km offshore average speed exceeds 7 m/s. Wind generator nominal output is usually referred to about 15 m/s wind speed. As the energy is proportional to the third power of velocity only 15 % of nominal power output is available at 7 m/s wind. At higher winds the generator RPM is limited and completely stopped during a storm. Highest measured wind speed in the Gulf of Bothnia has been 39 m/s. There is an ample safety barrier for a typical wind generator design wind gust speed of 55 m/s.

Wind load at nominal 15 m/s wind from the propeller and hub is about 280 kN. This results a bending moment of 20 MNm to sea bottom at –10 m depth. For a conical shape at waterline ice load is about 2 MN and results in the same 20 MN moment to the foundation. However, at about 25 m/s the wind load increases over twofold before the rotor is stopped. Hence the wind load will become decisive in foundation design.

Significant wave height in the Gulf of Bothnia is less than 3.5 m. For a 4 m diameter cylinder wave loads are about 0.5 MN, significantly less than ice loads. If there is a caisson or conical section underneath the wave loads will increase but the location of resultant is lower. Regardless of these possibilities wave load calculations indicate that wind loads will remain the decisive design factor in the Gulf of Bothnia.

Wave period is dependent on wave height. For significant wave heights the wave periods are always over five seconds, much longer than the longest natural periods of wind generators. Thus no wave load resonance is to be expected either. The main issue due to wave action is to furnish wind generator foundations with adequate erosion protection.

4. ICE LOADS

All possible ice loading scenaria have to be considered while designing a wind generator foundation. Environmental data from the intended location is used to judge what kind of ice movement are possible and what limiting factors might exist. Both static and dynamic ice load designs have to be made.

Uplift loads due to water level changes are insignificant for such heavy structures as wind generator tower and foundation. Also the water level changes are small and slow in the Gulf of Bothnia.

Ice adfreeze loads result after ice starts to move after a long and cold period. For a conical structure the load can be calculated e.g. by following the model of Cammaert et. al. (1986).

$$F_a = C_a C_s D h I \tau_a / \sin(\alpha) \qquad (1)$$

where C_a, C_s, and I are coefficients in Cammaert et. al. (1986). D is cone diameter at the waterline, α angle from the horizon, h ice thickness, and τ_a adhesion strength. If adhesion load for an almost cylindrical structure is compared to crushing load for the same ice, the adhesion load is typically less than half. In addition if the progressive adhesion failure is observed the load will be still lower. The experience for over 20 years in Finnish aids to navigation has proved that adhesion load is not a concern.

Level ice crushing load can be calculated from Korzhavins (1971) equation:

$$F_c = k_1 k_2 k_3 \sigma_c h d \qquad (2)$$

where coefficients k_1, k_2, and k_3 observe the plan view of the structure at the waterline, contact factor, and aspect ratio effect. σ_c is ice crushing strength, h ice thickness and d structure width. A value of 2.5 MPa for the ice crushing strength has been commonly used in the design of Finnish aids to navigation.

Thermal ice expansion induces horizontal load to an offshore structure in the landfast ice zone if ice field is fixed at one side and free to expand on the other. This situation is common close to winter navigation fairways. First one has to calculate the thermal expansion velocity that determines the strain rate at which ice is failing, and resulting ice failure stress. Then the thermal ice expansion load is calculated from Eq. 1. In Finland Noponen and Määttänen (1994) made a study to find out maximum expected thermal ice expansion loads in the landfast ice zone. By assuming optimum air temperature rise for a given ice thickness results in a simplified equation to calculate maximum expected ice expansion velocity

$$V = 12 \frac{L}{h} \cdot 10^{-9} \frac{m}{s} \qquad (3)$$

where L is distance from the fixed ice edge and h ice thickness. E.g. if an offshore structure is located 5 km from the shoreline and ice sheet is free to expand outwards, the maximum velocity with 0.3 m thick ice is only 0.20 mm/s. This is so slow that ice failure will be ductile and the corresponding ice failure strength is about 0.7 MPa, which is clearly below the average ice crushing strength.

Conical section at the waterline with ice failure by bending reduces ice loads from those of crushing. An upper bound for the cone ice loads can be calculated following Ralston (1977):

$$H = [A_1\sigma_b h^2 + A_2\rho_w g h D^2 + A_3\rho_w g h(D^2 - D_T^2)]A_4 \tag{4}$$

$$V = B_1 H + B_2\rho_w g h(D^2 - D_T^2) \tag{5}$$

The meaning of symbols and values of coefficients can be found from the original reference (Ralston 1977). In the horizontal load H the first term represents the component needed to break the ice sheet by bending and the rest stand for raising and clearing broken floes. In general Eq. 4 predicts cone ice loads about 20 % higher than what were measured in full scale by the instrumented 10 m wide cone in the Kemi-1 lighthouse in the Northern part of the Gulf of Bothnia.

In the landfast ice zone moving pressure ridge loads are not to be expected during the wintertime when ice is thickest and strongest. However, during fall ice formation and spring ice melting period moving pressure ridges can occur. The method of Dolgopolov et. al. (1975) can be used to predict a Baltic pressure ridge load:

$$\begin{cases} F_p = \mu H_e D(\frac{1}{2}\mu H_e \gamma_i + 2c)(1 + \frac{2H}{3D}) \\ \mu = \tan(\frac{\pi}{4} + \frac{\phi}{2}) \\ H < H_e < H + \frac{D}{2} \end{cases} \tag{6}$$

where H is keel depth and H_e is the design depth, D structure width, c and ϕ are ice rubble cohesion and internal friction, and γ_i is ice buoyancy body force. If pressure ridge is moving one has to add also simultaneous parent ice sheet failure load to get the maximum load.

Rubble pile-up is likely to occur on the wider and shallower foundation footing. Pile-up height over 14 m has been recorded along the cost of Gulf of Bothnia. This makes another concern for wind generator foundations. Not due to possible loads against the tower but due to blocking the access to the tower. However, if proper design and orientation of the stairways and doors are used, rubble pile-up problems can be mitigated.

There are limiting factors for the ice loading scenaria described in this chapter. Environmental thrust may not be high enough to make the ice move. In the wind generator park an array of foundations will improve the natural locking of landfast ice. Also with more fixing points the oncoming ice can buckle well ahead of the structures and form rubble piles that ground and protect structures behind. It is also possible to make artificial reefs to promote rubble pile-up formation at preferred locations. All site dependent limiting factors should be carefully considered and utilized to reduce ice action against foundations.

5. FOUNDATION PRINCIPLES

The sea bottom in the Gulf of Bothnia is silt, sand or moraine. Sufficiently high stiffness allows to use either gravity based caissons or large piles, Fig. 2. Both of these have been in-field proven in different aids to navigation applications. Both can be furnished with a conical section at the waterline to reduce ice loads and ice-induced vibrations. However, access by boat becomes more difficult with the presence of a cone.

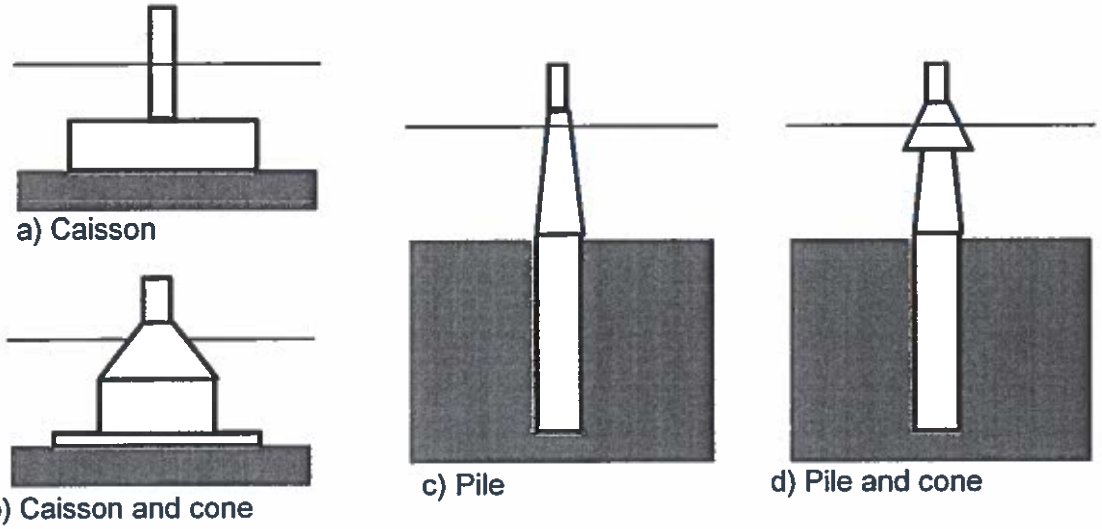

Figure 2. Caisson and pile foundation principles for wind generators

The material of a caisson foundation is normally concrete. Manufacturing can be arranged relatively close to installation sites. Caisson diameter, tentatively over 20 m, is at the same range as what has been used in offshore lighthouses. Stability of the caisson during towing phase allows to assemble also the tower, nacelle and rotor completely ashore. This reduces the required length of the weather window for installation work at sea. Bottom preparation can be made earlier and erosion protection later with less restrictions in weather conditions. The only problem is during the sinking phase when auxiliary stabilization is needed. This can be accomplished by using removable extended caisson walls or supporting winch barges. These can be reutilized while installing other wind generators in the wind park.

Steel foundation pile is manufactured in a machine shop or shipyard. The diameter is up to 4 m. As about four times the diameter is driven down into sea bottom the total length is over 20 m. The pile can be sealed and towed to the installation location where relatively small crane is needed to erect it for pile driving. Large pile can penetrate even moraine with boulders. A short fair weather window is needed at erecting the pile and beginning the driving. Another weather window is needed for installing the tower, nacelle and propeller blades. Also a large crane is needed as over 50 ton nacelle has to be lifted to over 60 m height. Compared to the caisson foundation there is more installation work at sea but the favoring factor is that neither bottom preparation nor erosion protection is needed.

The choice of foundation type depends mostly on the contractor and his course of action. The number of generators in a wind park is high enough to motivate to purchase adequate infrastructure for either of the presented foundation types. Preliminary cost estimates indicate

(Holttinen et.al. 1998) that the complete cost of foundation and installation of the wind generator is the same within few percents regardless of whether a caisson or pile foundation is chosen.

6. DYNAMIC ICE LOADS

First experiences with steel pile as a foundation for lighthouses in 1973 were disastrous. Severe vibrations destroyed their superstructures during the first winter. After the nature of ice-induced vibrations were learnt and vibration isolation for lighthouses introduced the steel foundation pile proved to be successful and replaced caisson foundations (Määttänen 1987). The same solution is not feasible for wind turbine foundations. Vibration isolation is intended to carry through high vertical and small horizontal loads between the tower and foundation. This function is hard to be combined with high horizontal wind loads.

Without vibration isolation there are two ways to mitigate the effects of dynamic ice forces. First the foundation can be made so stiff that foundation displacement response is insignificant. This requirement is likely to increase foundation cost even though with a caisson foundation the stiffness is naturally high. The second alternative is to use a conical section at the waterline that both changes ice failure from crushing to bending and reduces ice loads. Then the displacement response reduces as well. More important is that ice failure frequency falls well below the lowest natural frequencies of the complete structure. Thus the threat of resonant vibrations is avoided. The structure needs to be designed to withstand only individual ice load pulses and random fluctuations.

In design the natural frequencies and modes of the complete structure has to solved first, and if needed, structural mass and stiffness changed in such a way that resonance due to propeller blade excitation is avoided. Load cases include transients due to ice edge hit or sudden ice load relaxation, random ice load level variations, and continuous repeating ice load failures. Transient or random loading response calculation is an ordinary practice as the loading function is known. Continuously repeating ice load fluctuation is dependent on the response of the structure itself. A self-excited vibration model has to be adopted (Määttänen 1988). A conservative estimate can be calculated by assuming a saw tooth like ice forcing function.

As an example dynamic analysis response results due to an assumed 1 MN saw tooth ice loading function are presented. The pile foundation has 4 m diameter in 6 m water depth, it is driven down 16 m into bottom soil, the mass of 67 m high tower is 100 ton, and at the top is 78 ton nacelle and rotor. The first lowest natural frequencies are 0.38 and 2.5 Hz. The development of vibrations after the onset of resonance loading at the first natural frequency is given in Fig. 3 and 4. Nacelle displacement amplitude approaches 0.2 m, which is only about 20 % of maximum wind induced deflection. Acceleration levels at the nacelle also remain low at around 0.1 g. For a much stiffer corresponding caisson foundation displacement and acceleration response are only about one tenth of those of the pile foundation.

Figure 3. Transient displacement (m) vs. time (s) at the nacelle in resonant loading.

Figure 4. Transient acceleration (m/s^2) vs. time(s) at the nacelle in resonant loading.

The application example indicates that dynamic ice loads do not become a restrictive factor for wind generators. With a conical section it is easy to achieve dynamic ice load fluctuations to the order of 1 MN. With cone the repetition rate of ice failures is dependent on ice thickness. Ice failure repeat after ice advances at least a distance of two times its thickness. In the Gulf of Bothnia thick ice velocity never gets over 0.3 m/s. Hence e.g. a 0.8 m thick ice will never fail against a cone at higher frequency than 0.2 Hz. This is well below the wind generator lowest natural frequency, and hence resonant loading is possible only with thin ice and low ice forces.

7. CONCLUSIONS

The Gulf of Bothnia offers vast areas of landfast ice zone with reduced ice action against offshore structure foundations. Theoretically all the annual Finnish electrical power consumption could be harvested.

The trend in making larger wind turbine units has increased wind loads acting high above the sea level. Wind moment at the foundation becomes the most important factor in the foundation design. Wave and ice loads are of lower importance.

Pile driving or gravity caisson foundations are proven techniques in aids to navigation and are applicable for wind generator foundations as well. Both foundation types have their merits and disadvantages.

With stiff foundation and/or conical section at the waterline the dynamic response of dynamic ice forces can be made well tolerable for wind turbine nacelle and rotor.

The cost of wind energy is decreasing by serial production of wind generator components and by constructing large wind energy parks. Environmental factors on the other hand are rising the cost of conventional energy sources.

Inhabited shallow offshore sites in the Gulf of Bothnia are promising in harvesting wind energy in the future regardless of long ice covered season.

8. REFERENCES

Cammaert A.B., Kimura T., Koma N.,Yashima N., Yano S. and Matsushima Y. 1986. Adfreeze Forces on Offshore Platforms. Proc. OMAE-86, Vol IV, pp 541-548, ASME, New York

Dolgopolov Y., Afanasiev V.P., Korenkov V.A and Panfilov D.F. 1975. Effect of Hummocked Ice on the Piers of Marine Hydraulic Structures. Proc. IAHR Symposium on Ice 1975, pp. 469-478, Hanover, NH,.

Holttinen H., Liukkonen S., Furustam K-J., Määttänen M., Haapanen E. and Holttinen E.: Offshore tuulivoima Perämeren jääolosuhteissa, (Offshore wind power in the ice infested waters of the Gulf of Bothnia) Finnish only. VTT publications 828, Espoo, Finland, 1998.

Korzhavin K.: Action of Ice on Engineering Structures. Translation by U.S. Army CRREL, Hanover, NH, 1971.

Määttänen M . (1987): Ten years of ice-induced vibration isolation in lighthouses. OMAE 1987, Houston, TX, USA, Vol IV, pp. 261-266.

Noponen J and Määttänen M. 1994. Thermal Ice Load against an Isolated Structure. Proc. IAHR Symposium on Ice 1994, Vol. 1, pp.392-400. Trondheim, Norway.

Ralston T. (1977): Ice Force Design Considerations for Conical Offshore Structures. Proc. POAC-77, pp. 741-752. Memorial University of Newfoundland, St'Johns, Newfoundland, Canada.

DIMINISHING COST PENALTY DUE TO ICE LOADS ON OFFSHORE WIND TURBINE FOUNDATION

Määttänen Mauri
Helsinki University of Technology
P.O.Box 4100, FIN-02015 HUT
mauri.maattanen@hut.fi

Holttinen Esa
Electrowatt-Ekono Oy
P.O.Box 93, FIN-02151 Espoo
esa.holttinen@poyry.fi

ABSTRACT: The cost of produced wind energy is decreasing with increasing wind turbine size. Recent installations have been at 2 MW range while still larger units are at design or test phase. Expectations are that 3 MW units will be the standard after 3 years at offshore locations and later up to 5 MW generator size. In ice infested waters, depending on location, ice loads have been the decisive factor in foundation design and cost. With increasing turbine size and tower height the loads due to wind and rotor inertia are increasing while ice loads remain unchanged. Thus the share of ice load effect in the foundation cost is reducing. Case studies were made for a planned wind farm site outside Pori, West coast of Finland. The foundation cost increase due to moving first year ice was calculated by comparing foundation moment areas depending on water depth, ice failure mode, and foundation type. The results indicate that with over 3 MW unit size cost increase can be acceptable. Later even offshore areas with moving pressure ridges can become prospective wind farms opening vast ice infested offshore areas in the Baltic for wind energy harvesting.
Keywords: Off-Shore, Foundations, Ice Load, Cost Analyses

1 INTRODUCTION

The coastline of Finland is about 1300 km long. Prevailing Southwestern winds have average annual speed between 6 - 8 m/s. There is a great potential to harvest wind energy. In 1998 a study was made [2] on wind energy potential at Finnish Gulf of Bothnia offshore. It was learnt that, by restricting utilization area to less than 10 m water depth, the annual production would be at the same level as the whole annual electricity consumption in Finland, then 70 TWh. However, this far no offshore wind energy parks have been built. Feasibility studies are though in progress at several locations.

The Finnish coastal waters are ice covered for a substantial part of the year: three months in Southern and over six months in Northern parts. There is practically no tide in the Baltic but the ice is frequently moving driven by the winds at open seas. All first year ice features are present and will exert both heavy static and dynamic loads on any offshore structures. There is a lot of knowledge on ice forces and on design and construction of bottom-founded aids-to-navigation. Lighthouses with caisson foundation have a long tradition. Later steel piles driven down to sea bottom have proven to be more cost efficient. Offshore aids-to-navigation have been installed to all water depths up to 18 m. The dimensions of foundations are at same size class that is needed for large wind turbines. This experience can readily be adapted to offshore wind energy foundations in ice infested waters.

The present trend to increase the wind turbine size is increasing both wind and inertia related loads. Same time the hub has to be raised higher due to the increasing rotor diameter. The results are foundations moments increasing a bit faster than wind turbine size. Even a present 2 MW unit is causing a foundation moment that is equal to the moment due to level ice and a pressure ridge at 10 m water depth.

It is expected that in 2003 the well tested and reliable offshore wind turbine is at 3 MW class, and later on 5 MW units are emerging. This makes the wind-induced loads decisive in foundation design and cost. Thus vast new offshore areas are becoming economically viable as wind energy parks even in most severe moving ice areas in the Baltic. Another advantage is that the public much better accepts offshore locations than wind parks in the inhabited coast.

In this paper a review on ice load scenarios and ice loads on a typical Northern Baltic offshore wind turbine foundation are presented. The chosen ice conditions present a severe combination of level ice, rafted ice, and first year pressure ridge loads. A cost comparison is made on ice load effects on caisson and single pile foundations. Different water depth and ice load scenarios are compared to find out the cost effect and the potential of different foundation types.

2 ICE CONDITIONS

The records of ice thickness measurements in Finland cover over 100 years [4]. The land fast level ice maximum thickness in the Gulf of Finland, is about 80 cm, and up to 120 cm in the Northern Gulf of Bothnia. The thickness of moving ice depends on the distance from the shoreline. Close to shoreline even thin ice can stabilize. Possibility to encounter thicker moving ice gets the higher the farther offshore one goes. At narrow zone, e.g. less than 10 km from the shoreline, the moving ice is only 30 cm thick but can be further out up to 70 cm in South and 90 cm in North. The width of this transition depends on the distribution of islands, reefs and shallows that promote land fast ice stabilization. Everywhere in the moving ice zone first year pressure ridges will be encountered. Ridge keels can reach to depths more than 20 m, maximum recorded has been 28 m. At shallow locations moving ridge keels are scraping the sea bottom or grounding.

For comparisons in this study ice conditions at an offshore location near city of Pori are used. There a feasibility study was made for an intended offshore wind park. The site extends from 2 to 10 km Northwest offshore from the outermost islands. Open sea extends to West 240 km, all the way to the Swedish coast. Land fast ice zone is bounded to the extent of islands. There is practically no land fast ice beyond the outermost islands. Design ice conditions were assessed, Table 1, based on long-term data

[4], and on interviews with local fisherman and ship pilot station personnel. A general experience is that ice offshore Pori is always moving with winds. Moving pressure ridges are common and they often ground on shallow reefs.

Table 1. Design ice conditions

Moving level ice	0.70	m
Moving rafted ice	1.20	m
Ridge keel depth	12.0	m
High water, H.W.L	+0.8	m
Low water, L.W.L	-0.5	m

The sea depth varies at the planned wind energy park site from less than 10 m up to 30 m. At least 20 MW wind park can be accomplished with 2 MW units with foundations at lower than 10 m water depth. There is no tidal water level change. Storm and wind surges will either raise or lower the water level. With thick ice cover the water level changes are less than at open water. Wind driven water circulation causes slow water flow but not enough to enhance ice movement.

Wave induced bottom erosion is a concern for caisson type foundations. Wave loads against foundations are not treated here. A study in the Gulf of Bothnia [2] indicated that wave loads were significantly less than level ice crushing or ridge loads. As at Pori pressure ridge load acts simultaneously with the level ice load, the wave loads will be secondary in foundation design.

3 FOUNDATION TYPE

Full-scale measurements from lighthouses have indicated severe structural vibrations at frequencies from 0.3 to 8 Hz while ice is crushing. Ice load function is saw tooth like and can be in resonance with lowest structural natural modes. This frequency range is also critical for wind turbines. However, Kemi-1 cone full-scale measurements in the Gulf of Bothnia [3,7], Fig. 1, indicated that a conical section at the waterline reduces both global ice loads and reduces efficiently ice-induced vibrations due to ice bending failure. Wind driven ice movement velocity in the Baltic can never be so high that a resonant bending failure excitation could occur. Thus a conical section at the waterline is a desirable structural shape.

Figure 1. Pressure ridge together with 80 cm thick ice breaking against Kemi-1 cone.

The sea bottom at Pori offshore is mostly a 5 - 20 thick moraine layer on top of the rock but at some locations there is also bare rock. This suggests that most likely foundation choices are caisson, a single pile in a rock pit, or a pile driven down into moraine. Combinations with partial rock pit and moraine, and rock anchoring with caisson or tripod are also possible choices. In this study the cost comparison is made only for driven pile and caisson foundations, Fig. 2.

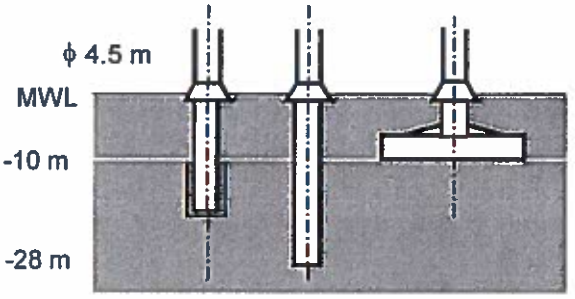

Figure 2. Pile and caisson foundations with a cone at waterline.

The major design considerations are foundations moment capacity and lateral resistance. With the driven pile the moment capacity is decisive. Using the Broms method does a simple dimensioning: the pile is assumed rigid and soil frictional capacity resists the moment. Design data includes loads, their location, pile diameter, soil density and internal friction. The caisson moment capacity is calculated from static balance: ice force moment equal to gravity load moment. Lateral sliding capacity depends only on coefficient of friction and gravity force unless no skirts under the caisson are used.

The design parameters that have direct effect on foundation cost are for a driven pile: diameter, wall thickness, and driving depth, and for caisson: diameter and mass. These parameters on their behalf depend on total load, load distribution, and water depth.

4 WIND LOADS

Wind induced loads are coming from the rotor and generator. Most severe loadings results from wind gusts, rotor unbalance and assumed generator short-circuiting. For smaller units, 0.65, 1.5 and 2.0 MW generators maximum loads to foundation were available but not yet

for a 3 MW unit. An extrapolation was made to estimate foundation loads for 3 and 5 MW units. Wind speed at 60 - 80 m height is assumed constant. Drag load resulting from energy production is then directly proportional to the unit size. At offshore locations the vertical wind profile is smoother than onshore. So the need to raise the hub height is less than at onshore locations. Thus the moment at foundation is increasing only a bit faster than to power one with generator size. The same is assumed also for abnormal maximum loadings. This way extrapolated foundation design moments at waterline are 60 and 119 MNm for 3 and 5 MW wind turbines.

5 ICE LOADS

The threat of dynamic ice loads makes cone obligatory at the waterline to induce level ice bending failure. In these cost comparisons ice load calculations include only two scenarios: level (or rafted) ice bending failure and pressure ridge shearing. Other ice load scenarios are uplift loads, thermal ice expansion loads, adfreeze loads, and dynamic loads. Compared to rafted ice breaking and pressure ridge loads these are a minor concern now.

No resonant dynamic loads are expected with the conical section at the waterline. Single level ice failures will cause a transient relaxation type vibration. Measurements and experience from Kemi-1 test cone verified only low vibration levels. The ice load fall off was about 2/3 of the level ice load, corresponding now to about 1 MN for the Pori offshore area. The resulting dynamic response is not significant. As rubble is normally piling against the cone, resulting additional damping is reducing vibration amplitudes. Eight year experience with three leading light structures at Oulu fairway having steel pile and a small cone at waterline have proven the same: there has been no problems to lantern, batteries, or solar cells due to ice-induced vibrations.

Level ice failure load against a cone is predicted using Ralston's model [5]. It is one of the oldest, best known and most referred cone ice load models. It is based on ice bending failure by plastic limit analysis upper bound solution along sectorial wedges in the ice sheet in front of the cone. The model predicts systematically about 20 % too high ice loads when compared to full-scale Kemi-1 cone measurement results. Thus foundation cost comparisons are slightly too severe for ice loads in relation to wind loads.

The conservative Ralston model predicts for a 60° cone with 5.5 m diameter at waterline a 1.4 MN horizontal ice load while 0.70 m thick ice is breaking. Respectively a 1.2 m thick consolidated layer or rafted ice will yield 2.7 MN horizontal ice load. With such a thick ice shear failure may occur at same or even lower ice load level. The reduction of ice loads using cone is significant. Without the cone the level ice design load would be 7.6 MN and about 10 MN for the rafted ice. These crushing loads would also bring with severe dynamic interactions.

Uncertainties in pressure ridge load are much higher than in cone level ice load. Scarce in-field measurements have shown that pressure ridge load is about 1.0....2.5 times the parent ices sheet crushing load. In the case of a cone this would end up from 3 to 7 times the cone ice horizontal load. The ridge load models are usually based on soil mechanics limit load approach that need knowledge of ridge keel density, cohesion and internal friction. The method of Dolgopolov et. al. [1] is now used to predict first year pressure ridge loads. The resulting ridge loads are 6.1 and 8.1 MN for a 10 m and 12 m deep ridge keels.

While the pressure ridge is moving one has to add also simultaneous parent ice sheet failure load to get the maximum load. The level ice load together with the pressure ridge present the maximum design load that determines the foundation cost. E.g. the total ice load is 10.8 MN for 1.2 m rafted ice in conjunction with 12 m pressure ridge.

6 FOUNDATION COST

The cost of a completed offshore foundation depends on its location, foundation type, manufacturing and installation techniques, etc. For the comparison of cost increase due to ice loads a simple measure is adopted. Manufacturing and installation costs are supposed to be directly proportional to the amount of steel in the pile, and on the weight of the caisson. For a 3.0 MW wind turbine a 4.5 m tower diameter is used even though a larger diameter could reduce steel weight. Hence the underwater cost of the steel pile is directly proportional to pile wall thickness that is determined from the bending moment distribution. In the case of caisson the pile moment decays fast inside the caisson. The required mass of the caisson and its diameter are determined from the overturning moment and total horizontal load at the sea bottom. After the moment distributions and loads are calculated the cost increase comparison can be made.

The results are presented for a pile driven into sea bottom moraine at 10 or 15 m water depth. The bending moment distributions are presented in Fig. 4 and 5. The horizontal axis presents depth: waterline is at left, sea bottom at the location of vertical axis, and grid interval is 1 m. The moment area above the wind only moment is directly proportional to the additional cost. It can be seen that at 10 m water depth, a penalty of about 49 % is due to the 1.2 m thick rafted ice load and 180 % due to simultaneous rafted ice and pressure ridge load. At 15 m water depth the figures are respectively 58 % and 216 %. This indicates that the presence of moving pressure ridges is a significant extra cost factor for the foundation pile. With only moving level ice the extra cost is minor, less than half of the 1.2 m thick rafted ice load.

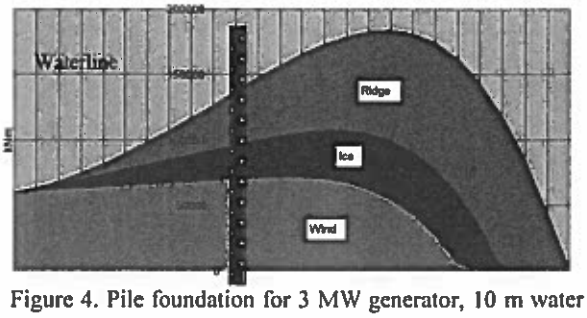

Figure 4. Pile foundation for 3 MW generator, 10 m water depth. Underwater and soil moment distributions due to wind, 1.2 m thick rafted ice, and 10 m ridge loads.

Increasing pile diameter can further reduce foundation pile cost. E.g. changing the pile diameter from the present 4.5 m to 5.5 meters reduces steel weight - and cost - about 18 %. However, there may be limitations due to transportation of large diameter piles, as well as design

constraint against buckling while wall thickness is decreasing.

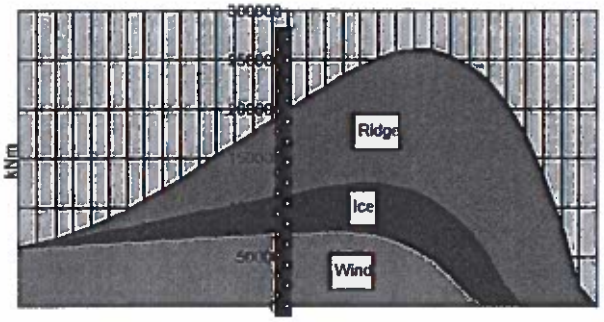

Figure 5. Pile foundation for 3 MW generator, 15 m water depth, underwater and soil moment distributions due to wind, 1.2 m thick rafted ice, and 12 m ridge loads.

For projected 5 MW wind turbines the effect of ice loads is further diminishing, Fig. 6. It is assumed a 119 MNm moment at waterline and a 5.0 m pile diameter. The 1.2 m thick rafted ice load increases moment curve area only 27 %, and with simultaneous pressure ridge load the increase is 82 %. Thus even driven pile foundation is becoming cost effective with increasing wind turbine size.

In the case of caisson foundation the foundation pile cost increase is a minor factor due to shorter exposed underwater steel pile. This can be seen in Fig. 4...6, by assuming the caisson extending 5 m above the sea bottom at 10 m water depth, and 7.5 m with 15 m water depth. The increase in the exposed foundation pile moment area is minor; the moment area due to wind is decisive.

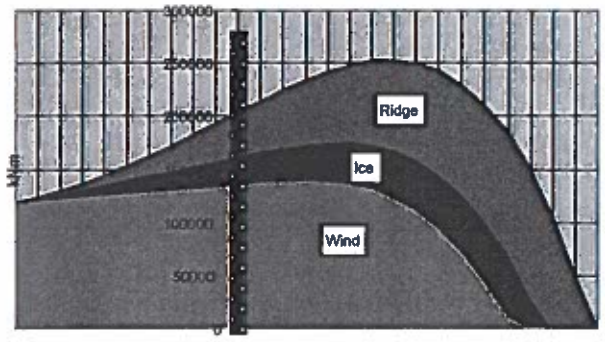

Figure 6. Pile foundation for 5 MW generator, 10 m water depth, underwater and soil moment distributions due to wind, 1.2 m thick rafted ice, and 10 m ridge loads.

The overturning moment at sea bottom can be read from Fig 4, 5, and 6. The increase at 10 m water depth is 38 % for the 1.2 m thick rafted ice and 97 % for the pressure ridge loading. For the 15 m water depth the respective figures are 54 and 167 %. If the caisson shape - diameter over height - is kept constant, the caisson mass related to that of wind only loads has to be increased to power 0.75. Thus for 10 m water depth the mass increase is 27 % for level ice and 75 % for the pressure ridge loading case. For the 15 m water depth the same figures are 38 and 109 %. If only caisson diameter is increased the mass and cost increase are to power 2/3 that would further decrease the overall cost.

The foundation cost increase has to be based on the overall cost of the wind turbine, and on better productivity at offshore location than in inland. Analysis indicates that an offshore wind turbine will produce about 15 % more wind energy per annum than its onshore neighbor at close distance. For a recent 20x2 MW wind energy park [6] the offshore foundation cost was 16.8 % of the total investment. Hence about 90 % foundation cost increase at ice infested offshore site is already compensated directly by the better productivity, e.g. investment versus MWh. In long run the better productivity is a continuous bonus. Thus at 10 m water depth driven pile is becoming cost effective and a caisson foundation even in deeper water. This result justifies developing wind energy parks also at offshore locations where ice conditions can be severe.

At ice-infested waters a good start is at land fast ice zone where no pressure ridges are present, and where the thickness of rafted ice will be much smaller. Hence the previously presented increase due to rafted ice will reduce significantly: to about 0.40 times the given values. E.g. for a driven down foundation pile the cost increase is about 25 % and with a caisson about 15 %.

In general the offshore foundations are more expensive than ashore. The difference is reducing while more efficient methods for offshore foundation construction are developed and serial production advantages utilized. Due to better public acceptance and much higher production potential offshore wind farms have an advantage. After the large units, from 3 to 5 MW, have matured also the areas with pressure ridges can become profitable.

7 CONCLUSIONS

The trend of increasing wind turbine unit size is bringing with the wind-induced loads to foundation to the same level as ice loads in the Northern Baltic. In future the wind effect will be the dominating foundation design factor.

Vast areas of shallow offshore sites are available for wind energy harvesting in ice-infested waters. Outside land fast ice zone wind is making all the first year ice features to move, including level ice, rafted ice and pressure ridges.

Ice loads for a severe offshore location are calculated. A conical section at waterline is effective in reducing both ice loads and dynamic effects.

Additional cost for a driven pile and caisson foundation is estimated. The cost increase is related to additional moment due to ice loads in foundation on top of the wind-induced moment distribution.

The comparisons at different water depths indicate that level ice has a minor effect, rafted ice significant factor, and simultaneous pressure ridge more than doubles the driven pile foundation cost. The increase is significantly less with a caisson foundation.

As the foundation cost is likely to be below 20 % of the wind turbine total cost, and while the offshore wind energy production is about 15 % better than inland, the offshore wind energy parks with 3 to 5 MW generators are becoming economically feasible also at areas where pressure ridges are moving.

REFERENCES

[1] Dolgopolov Y., Afanasiev V.P., Korenkov V.A and Panfilov D.F. 1975. Effect of Hummocked Ice on the Piers of Marine Hydraulic Structures. Proc. IAHR Symposium on Ice 1975, pp. 469-478, Hanover, NH.

[2] Holttinen H., Liukkonen S., Furustam K-J., Määttänen M., Haapanen E. and Holttinen E.: Offshore tuulivoima Perämeren jääolosuhteissa, (Offshore wind power in the ice infested waters of the Gulf of Bothnia) Finnish only. VTT publications 828, Espoo, Finland, 1998.

[3] Määttänen M. and Hoikkanen J. (1990): The Effect of Ice Pile-Up on the Ice Force of a Conical Structure. Proc. IAHR Symposium on Ice 1990, Vol. 2, pp.1010-1021. Helsinki University of Technology, Espoo, Finland.

[4] Palosuo E., Leppäranta M. ja Seinä A.: Formation, thickness and stability of fast ice along the Finnish coast. Winter Navigation Research Board, Report N:o 36, Helsinki 1982.

[5] Ralston T. (1977): Ice Force Design Considerations for Conical Offshore Structures. Proc. POAC-77, pp. 741-752. Memorial University of Newfoundland, St'Johns, Newfoundland, Canada.

[6] Sorensen H. C., Larsen J.H., Olsen F. A., Svenson J. and Hansen S. R.: Middelgrunden 40 MW Offshore Wind Farm, A Prestudy for the Danish Offshore 70 MW Wind Program. Proc. ISOPE 2000, Seattle, USA, 2000

[7] Tam G., Määttänen, M., Hoikkanen J., Nortala-Hoikkanen A., Mäkinen E., and Kivelä J. (1995): Ice Force Measurement Analysis for the Kemi-I Cone - A Joint Industry Project. Volume I and II. 127 p + ~280 p Appendices + Video + Slides + Computer Program. Kvaerner-Masa Inc, Vancouver, Canada.

POAC '01
Ottawa, Canada

Proceedings of the 16th International Conference on
Port and Ocean Engineering under Arctic Conditions
POAC'01
August 12-17, 2001
Ottawa, Ontario, Canada

ICE LOAD DESIGN RECOMMENDATIONS IN EUROPE

Mauri Määttänen, Professor
Helsinki University of Technology, Finland

ABSTRACT

A European Union funded research project LOLEIF was completed in October 2000. A rationale for lower than expected ice loads against offshore structures was presented. Two new EU funded research projects, STRICE and NEST, started in January 2001. Both of these have work packages for recommendations towards codes. The objectives are to co-ordinate interested parties, compile data for background, evaluate existing codes, and propose structure and guidelines for European ice load design code. Workshops will be arranged to create a wide international discussion and co-operation.

EXTENDED ABSTRACT

Background

Most of the Northern Europe countries have their own design codes or recommendations for ice loads for bridge piers but practically nothing for offshore structures. Only winter navigation had needs for international co-operation. One of the earliest, the first version in 1971, have been the Finnish-Swedish Ice Class Rules for ice-reinforced ships. These Rules have been later adopted by all major classification societies. IALA (International Association for Lighthouse Authorities) founded a working group in 1980 to prepare a Design Recommendations for Ice effects on Aids-to-Navigations. This working group, having representatives from Canada, Denmark, England, Finland, Sweden and USA, completed its work in 1984. Only relatively narrow structures under first year ice action were considered. Mere recommendations were presented; no design code was ratified.

Russia has a long tradition for ice design codes, SNIP 1982 and VSN 1988, originating from early ice forces research on bridge piers. Canada prepared ice design code CSA in 1992. North American oil companies together developed first API design recommendations in 1982 for arctic offshore structures. With the latest improvements along revision in 1995, the API RP 2N has become a reference guide for arctic offshore structures design.

Ice force design is not a mature discipline. Sanderson in 1988 and Croasdale 1996 proved that the top experts in different countries predicted design loads more than an order of magnitude apart by carrying through round robins for the same structure in same ice conditions. As this is the reality it is evident that only ice force design recommendations exist instead of design codes. However, as more and more full-scale ice load data has been harvested to refine and validate ice load prediction models, the time is getting ripe for an ice load design code.

European co-operation and unification during European Union expansion is spreading to engineering practice as well. Euro norms have already replaced national standards in design and manufacturing of many products. In ice load design a need for common design practice is emerging for the offshore wind energy foundations, and for the safe utilization of arctic offshore natural resources. Arctic offshore activities are still hibernating but a strong demand is foreseen in wind energy as a clean renewable source of energy. While environmentalists prevent further nuclear power plant construction by referring to safety and waste issues, over 200 wind generators are needed to replace one nuclear power plant. Environmental views also prohibit wind energy installations inland or ashore where good wind conditions prevail. The only choice left is abundant offshore wind energy production. Vast shallow offshore areas for wind energy farms can be found in the Northern Europe where, on the other hand, first year ice is a severe design consideration. Construction of thousands of new offshore wind energy foundations is planned before 2010.

Research projects

EU funded research project LOLEIF, during 1997-2000, is an acronym for Low Level Ice Forces. The project was initiated and coordinated by HSVA in Germany with partners from England, Finland, France, Norway, and Sweden. In addition collaboration with Canadian, Russian and USA research facilities was conducted. Oil companies Exxon, Statoil and Texaco were also funding the project. The project work plan included evaluating existing ice force design methods, reviewing existing full-scale data, making full-scale measurements of ice forces in a lighthouse and pressure ridge mechanical properties in the Northern Baltic. Objectives were to establish a more solid basis for ice force design in order to reduce spread in ice force prediction and to justify lower design ice loads that were anticipated earlier. Development of new or refined ice load prediction methods was initiated. A more thorough presentation of these results is given in a POAC 2001 special LOLEIF session.

A new three year EU research project STRICE, starting January 2001, will continue LOLEIF work with almost identical organization and partners. The acronym stands for Structures in Ice. STRICE objectives are to expand full-scale measurement data matrix, and to have the measured data being processed, analysed and correlated to the force effecting parameters like ice thickness, ice load area, ice velocity, ice mechanical properties, ridge properties and also to the acceleration measurements of the lighthouse. The newly measured data and analysed results will be compared with existing data from literature and also with theoretical predictions. STRICE has one of the further objectives to evaluate existing ice load design codes, and to prepare Recommendations for Ice Load Design, and a European Draft Code.

Third EU Networking project NEST during 2001-2003 has main objectives in solving problems of dynamic ice-structure interaction, but it also has a contribution towards international ice design code. This project brings together European and Chinese researchers with their own in-field data. The project organization has VTT from Finland as coordinator with four other European countries, France, Germany, Norway and Sweden as partners. Four Chinese partners are from university, research laboratory, classification society and industry. Work towards ice load design code will be looking for cooperation with experts in Canada, Japan, Russia and USA.

Work plan

Background for design code work has already been partly prepared by compiling and analysing full-scale measurement data, and by comparisons to analytical model results. The basic ice crushing against a vertical wall was thoroughly analysed from carefully conducted and well-documented panel load measurements along the peripheries of the lighthouse waterline. Scale effects have been attacked both by methods of fracture mechanics and creep analysis with material damage. Insight on the effects of micromechnisms during ice crushing at ice structure contact zone have been learnt and utilized in explaining ice load build-up and ultimate load. Data is used to correlate and validate the parameters affecting the calculated ice loads. It is expected that ice loads to vertical marine structures can be reduced, while at the same time the risk level is quantified and safety of structures is kept as first priority.

In many cases pressure ridge loads against offshore structures become the decisive ice-loading scenario. In LOLEIF project pressure ridge keel and consolidated layer mechanical properties have been measured in full-scale tests. The data proves the keel friction and cohesion to be lower than anticipated. The resolved pressure ridge mechanical properties will be used to develop a 3–D FEM analysis tool to predict nonsimultaneous ridge failure against a structure. Due to measured lower mechanical ridge strength, and nonsimultaneous progressively developing failure surface inside the ridge keel, a reduction in design ridge ice loads is expected.

The results obtained by the various STRICE and NEST work packages will be evaluated with respect to the development of recommendations on design loads for vertical structures in ice. The results will also be used as the basis for a draft of EU-Code for Ice Forces on Marine Structures. The coverage of the Draft Euro norm has not yet been decided. Main emphasize will be on first year ice loads. For industry activities outside Europe references to multi-year arctic ice loads are evidently needed.

The STRICE consortium is planning to organise a workshop early in the project, in order to introduce the user groups, such as governmental agencies, oil companies, consulting firms and classification societies, to the programme of the STRICE-project. At this workshop also experts from inside and outside Europe will be invited in order to get recommendations from end-users for the research programme, and to get also their scientific input into the project programme. An international workshop will bring together countries like Canada, Japan, Russia, and USA, that are also developing and revising ice load design codes.

Extreme Ice Properties

By Flemming Thunbo Christensen[1] and Jesper Skourup[2]

Abstract: An extreme-value analysis is carried out for ice properties in the Great Belt in Denmark. The Great Belt is an 18-km-wide body of water that connects the Baltic Sea with Kattegat and the North Sea. It divides the country of Denmark into halves of nearly equal population. The design of a bridge and tunnel system across the Great Belt called for knowledge of extreme ice properties, because dynamic ice loading governs part of the design. Because of the extremely low exceedance probability of 2×10^{-3} per year accepted for ice loading, and because of the very limited amount of data available concerning ice at the location of interest, the analysis had to depend on air-temperature records. Statistical correlation between strength and thickness of the ice was handled effectively by splitting their product in temperature dependent and independent parts and joining distributions for these by simple integration. The effect of a snow cover on the ice was also analyzed.

Introduction

The result of a preliminary extreme value analysis of ice properties in the Great Belt in Denmark was briefly described by Christensen et al. (1989) as a basis for selection of parameters for model tests. The present analysis is the final version of that for the Great Belt West Bridge. It constitutes a substantial expansion of the preliminary analysis and leads to higher compressive ice strengths. For the West Bridge, dynamic ice loads govern the design of the bridge piers.

The recurrence time of the load resulting from ice crushing is determined by the recurrence time of the product $\sigma_u h$, where σ_u = the uniaxial compressive ice strength and h = the ice sheet thickness. To determine a design value of this product, the statistical distribution of $\sigma_u h$ must be known. However, no combined values of σ_u and h exist for the Danish waters, so distributions for each parameter must be combined. This leads to the question of statistical correlation between ice strength and ice thickness. The correlation must be known to properly combine the distributions. It is clear that they are not fully uncorrelated, since cold weather will increase both strength and thickness of the ice, but it is equally clear that they are not fully correlated either, since a warm spell of, say, −2° C will weaken the ice considerably without reducing its thickness. To circumvent this problem, the product of $\sigma_u h$ is split into temperature-dependent and temperature-independent parts. Distributions for these parts can be combined safely under an assumption of no correlation.

Compressive ice strength variations have been described [e.g., Weeks and Assur (1969)] in the form

$$\sigma_u = \sigma_0 f_u(S_i, T_i) \quad \ldots\ldots (1)$$

[1]Res. Hydr. Engr., Danish Hydr. Inst., Agern Allé 5, DK-2970 Hørsholm, Denmark.

[2]Res. Hydr. Engr., Danish Hydr. Inst., Agern Allé 5, DK-2970 Hørsholm, Denmark.

Note. Discussion open until November 1, 1991. To extend the closing date one month, a written request must be filed with the ASCE Manager of Journals. The manuscript for this paper was submitted for review and possible publication on July 30, 1990. This paper is part of the *Journal of Cold Regions Engineering*, Vol. 5, No. 2, June, 1991. ©ASCE, ISSN 0887-381X/91/0002-0051/$1.00 + $.15 per page. Paper No. 25856.

where σ_0 = a constant reference strength and f_σ = a function of the mean ice temperature, T_i, and the ice salinity, S_i. In the present analysis, it was decided to describe the reference strength as a stochastic parameter. Exponential, Weibull, Gumbel, and lognormal distributions were fitted to the reference strength data described later. Goodness of fit was determined for each of these by a χ^2 test, by a Kolmogorov-Smirnov test, and by visual observation. The Weibull and Gumbel distributions both describe the data well and are clearly superior to the other distributions. The goodness of fit is equal for the Weibull and Gumbel distributions, and the Weibull distribution was selected

$$\sigma_0 \in We(\beta, k) \quad (2)$$

$$f(\sigma_0) = \frac{k}{\beta}\left(\frac{\sigma_0}{\beta}\right)^{k-1} \exp\left[-\left(\frac{\sigma_0}{\beta}\right)^k\right] \quad (3)$$

$$F(\sigma_0) = 1 - \exp\left[-\left(\frac{\sigma_0}{\beta}\right)^k\right] \quad (4)$$

where f = the probability density function; F = the distribution function; and β and k distribution parameters.

The ice thickness was calculated from a simple linear differential equation for heat conduction. The resulting expression is of the general form

$$h = f_h\left(\int T_a dt\right) \quad (5)$$

i.e., a function of the accumulated freezing-degree-day (fdd) index. A commonly used formulation of the fdd index is

$$K = \Sigma(-\bar{T}_a) \qquad \text{for } \bar{T}_a < 0^\circ\text{C} \quad (6)$$

where the index K = zero at the onset of winter; $\bar{T}_a$ = the daily average air temperature, and the summation is carried out daily. This index has many shortcomings (e.g., that the effect of thaw periods are not accounted for), but it is nevertheless widely used and reported. Wherever daily temperature records are available, the effects of thaw periods should be investigated. But the advantage of the simple index (6) is the availability of data for a larger number of years. An estimate of the thickness of the sea ice is

$$h = 0.032(K - 50)^{1/2} \text{ meter} \quad (7)$$

where K must be in Celsius degree-days. This formula is derived theoretically from an assumption of one-dimensional heat conduction, except for the subtraction of 50 degree-days, which is of empirical nature. It accounts for the freezing point being lower than 0° Celsius.

By rewriting (1) and (5) it follows that

$$\frac{\sigma_a h}{\sigma_0} = x = f_a(S_i, T_i) f_h[T_a(t), t] \quad (8)$$

$$\sigma_a h = \sigma_0 x \quad (9)$$

By defining the parameter x in (8) as the temperature-dependent part of the product $\sigma_a h$, and by letting σ_0 represent the temperature-independent part of the product, the previously mentioned split illustrated in (9) is achieved.

The methodology then entails determination of distributions for σ_0 and for x, which are eventually combined into the probability distribution function for the product $\sigma_u h$ by integration

$$F(\sigma_u h) = \int_0^\infty F(x) f(\sigma_0) d\sigma_0 \quad \ldots\ldots (10)$$

The simple integration in (10) implies that σ_0 and x are statistically independent, which was precisely the reason for the applied split of the product. In the following statistical distributions are determined for the reference strength σ_0 and for annual maximum values of the parameter x.

The compressive ice strength of sea ice is known to be strongly dependent on strain rate. It would, therefore, be desirable to determine this functional relationship and include ice velocity in the probabilistic formulation of ice-loading conditions. Because of time constraints this was not included. Instead, compressive strength in this analysis is meant to be representative of the brittle range, in which the rate effects are moderate.

Reference Strength Distribution

The specific expression defining reference strength, suggested by Weeks and Assur (1969), read

$$\sigma_u = \sigma_0 \left[1 - \left(\frac{\nu}{0.275} \right)^{1/2} \right] \quad \ldots\ldots (11)$$

where ν = the relative brine volume in the ice. This quantity may, according to Frankenstein and Garner (1967), be calculated as

$$\nu = \left(0.532 - \frac{49.185}{T_i} \right) \frac{S_i}{1{,}000} \quad \ldots\ldots (12)$$

where T_i is in negative degrees Celsius and S_i in parts per thousand. More accurate descriptions are available, e.g., Cox and Weeks (1982), but (11) and (12) give sufficient accuracy when fitted to experimental data.

It appears to be a simple matter to deterine a σ_0 distribution from a large amount of strength measurements in the area of interest. But in Danish domestic waters, only low-quality strength measurements are available. By low quality we refer to the fact that, for example, strain-rate and crystal structure have never been documented. The Danish data all stem from field programs carried out jointly by the Institute of Hydrodynamics and Hydraulic Engineering (ISVA), at the Technical University of Denmark, and by Danish Hydraulic Institute. The results have been reported by Tryde and Zorn (1979), Mortensen and Zorn (1982), and Christensen (1986). Because of the low quality of these measurements, it was decided to also use the data presented by Fransson and Elfgren (1987) from the Bay of Bothnia, provided that these data could be considered representative of reference strengths in the Great Belt some 1,000 km to the south.

The Swedish data were used as published. In the Danish data, measurements with mean ice temperatures of $-0.5°$ or warmer were discarded, leading to omission of seven of 57 measurements. These seven were all from the same location and showed unrealistic results, probably because of faulty

TABLE 1. Comparison of Danish and Swedish Measurements Regarding Reference Strength, Salinity, and Temperature

Ice parameters (1)	Mean value (2)	Standard deviation (3)	Minimum (4)	Maximum (5)
		(*a*) Reference strength		
Swedish σ_0 (MPa)	2.76	1.07	1.49	6.51
Danish σ_0 (MPa)	2.44	0.86	1.31	5.27
Joint σ_0 (MPa)	2.61	0.99	1.31	6.51
		(*b*) Salinity		
Swedish S_i (ppt)	1.85	1.00	0.00	3.78
Danish S_i (ppt)	1.69	0.95	0.8	3.5
		(*c*) Temperature		
Swedish T_i (°C)	−4.01	1.87	−10.0	−1.0
Danish T_i (°C)	−1.88	0.82	−4.1	−0.9

temperature measurements. The Danish tests were made with cubes of ice, and the resulting strength was multiplied by 0.67 to obtain the "cylinder strength." The factor 0.67 was adopted from concrete testing technology, where it varies between 0.67 and 0.80. The Swedish tests were made using cylindrical ice samples and a constant strain rate of 2×10^{-4} sec^{-1}.

The description of crystal structures in the Swedish samples offered by Fransson and Elfgren (1987) correspond well with what is expected in the Great Belt, namely, mostly columnar ice with some granular and mixed ice types as well. In Table 1 the two data sets are compared in terms of both reference strength, temperature, and salinity. The reference strengths are very close. It is tempting to raise the cylinder-to-cube-strength ratio to 0.75, and thereby achieve identical mean values in the two data sets. Because the strain rate is unknown, although brittle, in the Danish tests, it cannot be argued that the two mean values should be equal. The ratio of 0.67 remains the most commonly used value.

The salinities appear identical except perhaps for the minimum values, which is less significant. This is somewhat surprising since the water bodies have distinctly different salinities, namely, 16–20 ppt in the Great Belt versus 2–4 ppt in the Bay of Bothnia. Part of the explanation lies in the growth process. While growing, the ice rejects salt from its underside and only traps a limited amount when neighboring fingers of the skeleton layer join to form a brine pocket. Thus, as long as the water salinity exceeds typical ice salinities of, say, 2 ppt, the ice will filter out the excess salt in the growth process. According to Cox and Weeks (1988), salt entrapment during ice growth is proportional to the growth rate. In the present case, this may be balanced by the difference in water salinities. Brine drainage will also cause salinities to be similar.

The temperatures clearly show the difference in latitude, with the Bay of Bothnia having lower temperatures. This difference in ice temperatures need not be a problem if the expressions (11) and (12) are capable of extracting the effects of the temperature correctly. This is investigated in a (σ_0,T_i) bias plot (see Fig. 1). A salinity (σ_0,S_i) bias plot is also made (see Fig. 2).

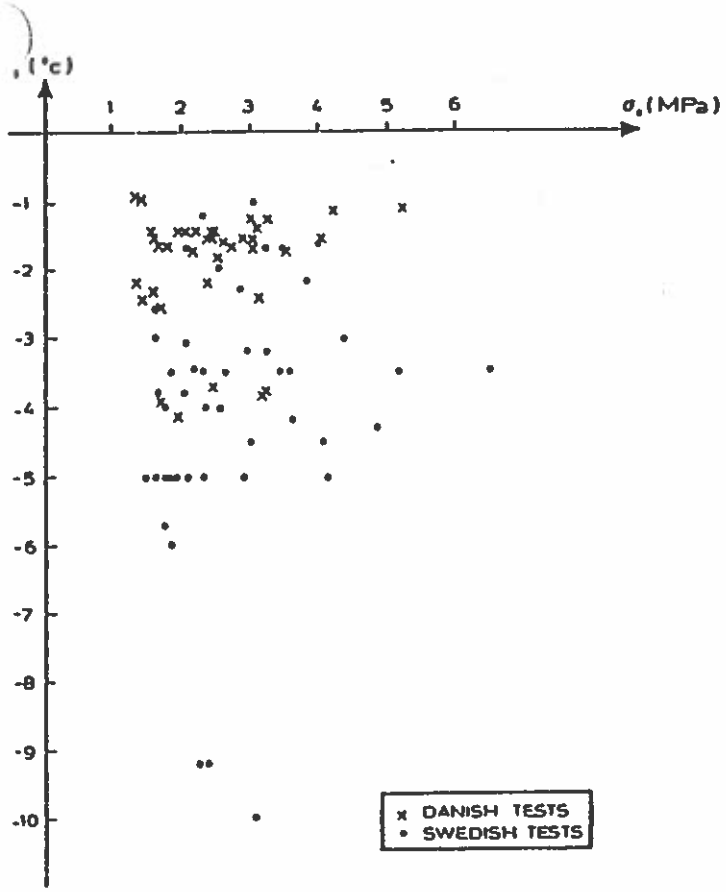

FIG. 1. Temperature T_i versus Reference Strength σ_0 for Danish and Swedish Tests

There are no visible differences in the distributions of σ_0 between the two data sets shown in the bias plots. Although the temperatures of the Swedish test samples are generally lower than the temperatures of the Danish test samples, (compare Table 1 and Fig. 1), there is no indication of differing distributions. The same holds true for the salinity plot. Note furthermore that extreme values of T_i and S_i do not coincide with extreme values of σ_0, and vice versa.

The agreement between the data sets is good for mean values. The Swedish standard deviation is slightly larger than the Danish one. This can be related to the strain rate as well as the choice of multiplication by 0.67 to obtain cylinder strengths. Because of the good agreement, it was decided to base the σ_0 distribution on the joint data set. It would be desirable to include even more data, but none were accessible within the available time frame.

The present ensemble of Danish and Swedish tests is a compromise. From a purely scientific point of view, the Danish measurements should be discarded, because the strain rates are unknown. Ideally, all scientific measurements of compressive ice strengths (meaning those with fully documented test conditions) from anywhere in the world should be included as long as they were made with appropriate ice types. The Swedish data give some confidence that the Danish measurements are reasonable. The Danish tests are included because they represent waters relatively close to the Great Belt. Through the comparisons in Table 1, they give some confidence that the Swedish data set is applicable, because of the nearly identical parameters. The agreement between the two sets of data is shown in Figs. 1 and 2.

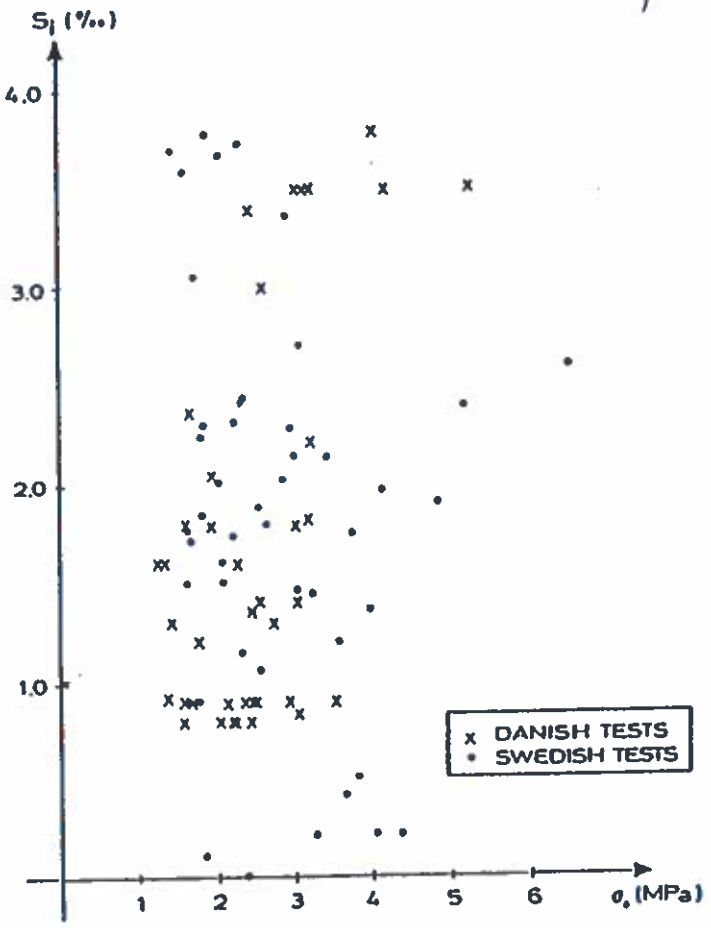

FIG. 2. Ice Salinity, S_i versus Reference Strength σ_0 for Danish and Swedish Tests

When two data sets are used to validate each other, the validation is of limited value. It is, therefore, desirable to compare with a broader spectrum of values obtained in scientific measurements. One of the best references for that purpose is an article by Timco and Frederking (1990), published shortly after the completion of this extreme value analysis. The article analyzes 283 small-scale measurements of compressive strength of first-year sea ice to formulate an empirical model that gives good results when compared with large-scale measurements. The final results of this extreme value analysis are in good agreement with the large ensemble of scientific measurements analyzed by Timco and Frederking (1990). By agreement, we mean that thicknesses, temperatures, strain rates, and strengths relate well to each other. The absolute values of extreme ice strengths in the Great Belt need obviously not equal the average values of these 283 tests.

A Weibull distribution was fitted to the joint set of data on reference strengths. Through a least-squares fit, distribution parameters of $\beta = 2.844$ and $k = 2.749$ [compare with (4)], were determined. Statistical model uncertainty has not been included in the present investigation. Only central estimates have been calculated. Distributions have been fitted by the least-squares method. This is assumed to be permissible. A comparison with maximum likelihood estimation and moment estimation results would be interesting, but the effects are assumed to be moderate, and the comparisons have therefore not been carried out.

Ice Thickness and x-Distribution

The specific expression for the x parameter corresponding to the general expression (8) becomes

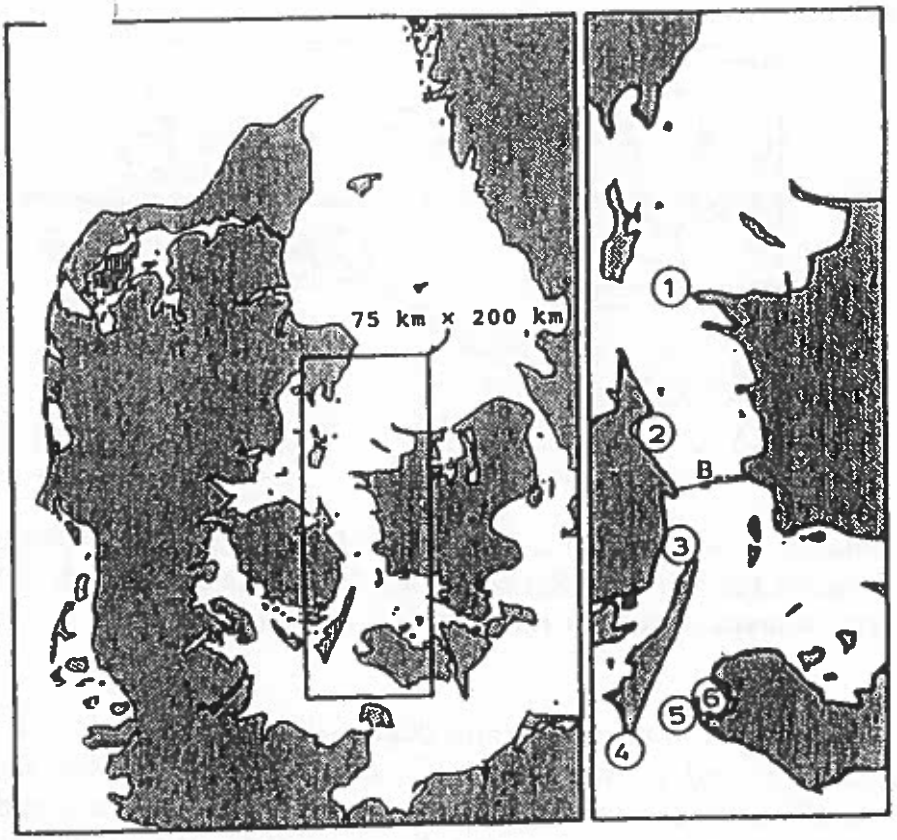

FIG. 3. Locations for Ice Thickness Observations in Entire Great Belt: (1) Røsnæs Lighthouse; (2) Kerteminde Bay; (3) Lohals; (4) Keldsnor; (5) West of Albuen; (6) Nakskov Outer Fiord; and (B) Bridge

$$x = \left(1 - \left\{\frac{\left[0.532 - \left(\frac{49.185}{T_i}\right)\right]S_i}{275}\right\}^{1/2}\right)0.032(K - 50)^{1/2} \quad \ldots\ldots\ldots\ldots \quad (13)$$

where T_i is in degrees Celsius and negative; S_i is in ppt, K is in accordance with (6); and x comes out in meters. This expression can easily be calculated day by day once $\Sigma(-\bar{T}_n)$ exceeds 50. The latter part representing thickness of the ice obviously has a direct effect on the values of x, and it consequently is important to check whether or not this theoretical expression describes nature well. This is investigated in two ways: By comparing with extreme observations from the past 80 years and by comparing with a larger amount of observations near the site of the future bridge.

Annual maximum observations of ice thickness at various locations have been reported in annual bilingual (Danish and English) publications by Statens Istjeneste in the period 1907–86. Locations of interest are shown in Fig. 3 for the entire Great Belt and in Fig. 4 for the immediate vicinity of the bridge. Observations from the five coldest winters in the 80 winters surveyed are shown in Table 2 together with theoretical thicknesses calculated from (7). A reasonable agreement is found. In the coldest winter, 1941–42, the agreement is excellent. In the other three winters, (7) appears to slightly overpredict the thickness, but since there is no guarantee of all ice thicknesses being smaller than the largest thickness observed, this has not resulted in modifications to the expression for x in (13).

Observations near the site of the future bridge have been plotted against

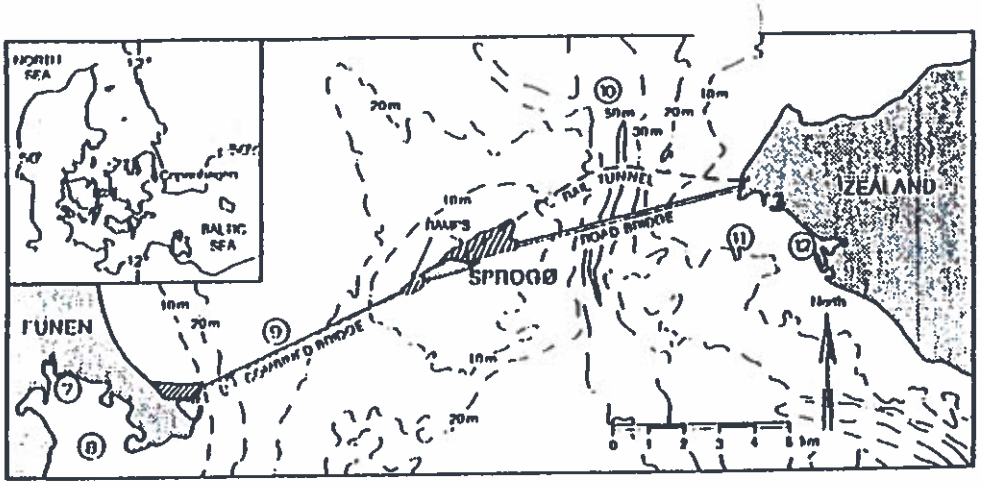

FIG. 4. Locations for Ice Thickness Observations near Site of Future Bridge: (7) Nyborg Harbour; (8) Nyborg Fiord; (9) Western Channel; (10) Eastern Channel; (11) Access to Korsør Harbour; (12) Korsør Harbour

the total amount of freezing degree-days for the relevant winters in Fig. 5. As indicated in the figure, (7) yields ice thicknesses above the best fit to the data, especially for shorter recurrence times. For longer recurrence times the difference vanishes, and this general trend may also be seen in Table 3. Furthermore, the figure shows that the best-fit curve is nonconservative with respect to the data from the Western Channel. Consequently, (7) was maintained as a reasonable estimate of the ice thickness. It is worth noting that the factor 0.032 in (7) is larger than corresponding factors used in the Arctic.

The problem is then reduced to determining the x-distribution. The development of x through the winter is of limited interest for design. The maximum value from each winter is used to determine design values. The maximum x typically occurs when K has reached about 90% of its final value for the winter. The end of the winter tends to be warmer and thus the maximum x occurs slightly before the maximum or final K.

One of the most serious shortcomings of the preliminary analysis (Christensen et al. 1989) was that the temperature records only covered 19 winters. Therefore, it was decided to use as many data as possible from nearby measurement stations in the final analysis. From the nearby Røsnæs lighthouse (see Fig. 3), eight temperature readings per day are available from 1960 on.

TABLE 2. Measured Ice Thicknesses (in cm) at Locations in Vicinity of Future Bridge during Five Coldest Winters in Period 1907–86 Compared with Results from (7)

Year (1)	K_{max} (°C-days) (2)	Location							
		Kerteminde Bay (3)	Nyborg Harbour (4)	Nyborg Fiord (5)	Lohals (6)	Keldsnor (7)	West of Albuen (8)	Nakskov outer Fiord (9)	Eq. (7) (10)
1941–42	497.5	65	60	—	—	—	65	67	64
1946–47	378.0	45	50	50	40	44	—	48	55
1939–40	368.5	—	35	50	—	—	—	30	5(
1962–63	300.3	—	—	—	—	—	—	—	47
1940–41	290.7	40	35	45	—	—	25	37	47

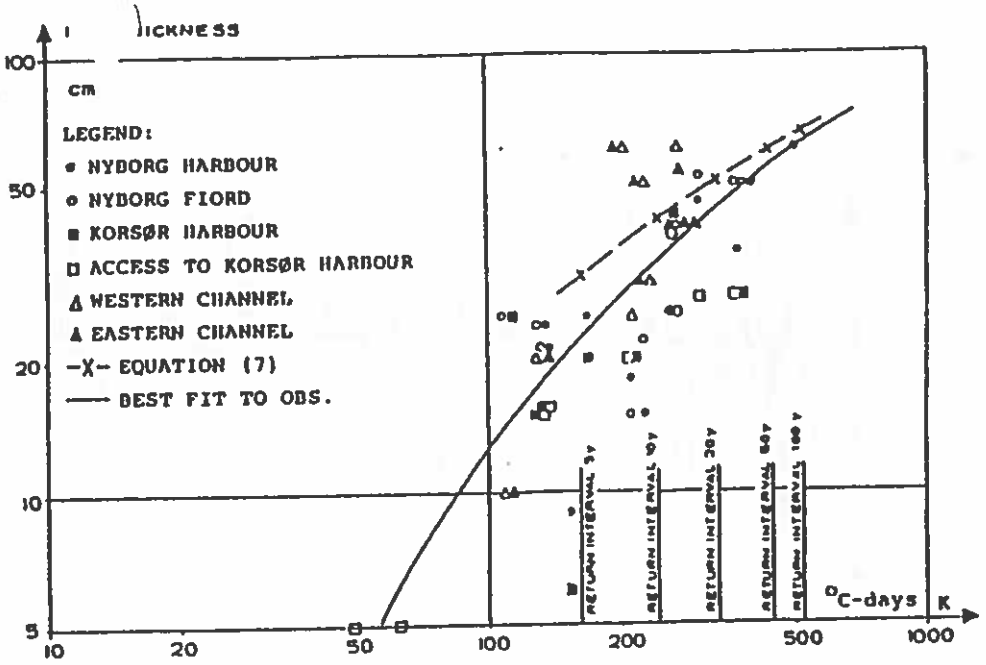

FIG. 5. Maximum Observed Ice Thicknesses (Annually) versus Number of Freezing Degree-Days, According to Statens Istjeneste

Additional data from Bogø were used for the period 1875–1960. The Bogø station is about 60 km east-southeast of the future bridge, but it is considered representative of temperature conditions at the bridge. The Bogø data contain three daily readings, plus minimum and maximum readings. The average of the latter two was used as a daily mean value.

The national mean air temperature for each of the winters 1875–1989, defined as December 1 through March 31, is shown in Fig. 6. The figure reveals a relatively mild winter climate and significant interannual variations. These variations were indeed the reason for the preliminary analysis giving unrealistically low design values. It is assumed that the temperature variations can be considered stochastic realizations of a stationary process. Hence, no trend toward a different climate is taken into account.

A 114-year temperature record may seem excessively long, but with design probabilities of exceedance in the range 2×10^{-5} to 4×10^{-5} per year this is not the case. Furthermore, calculations to obtain design values based on two different 30-year periods resulted in extreme values a factor of two

TABLE 3. Design Values of $\sigma_u h$ from POT Analysis with Weibull and Gumbel Distributions. Product $\sigma_u h$ is in MN/m

x_{th} (m) (1)	Number of data (2)	Weibull $\sigma_u h$ (MN/m) (3)	Gumbel $\sigma_u h$ (MN/m) (4)	P_W (5)	P_G (6)
0.22	29	2.60	3.32	0.0095	0.0063
0.23	26	2.66	3.35	0.0075	0.0058
0.24	23	2.80	3.42	0.0031	0.0035
0.25	17	2.71	3.33	0.0051	0.0051
0.26	14	2.65	3.21	0.0095	0.0071
0.27	12	2.60	3.04	0.0208	0.0111
0.28	11	2.65	3.08	0.0205	0.0138

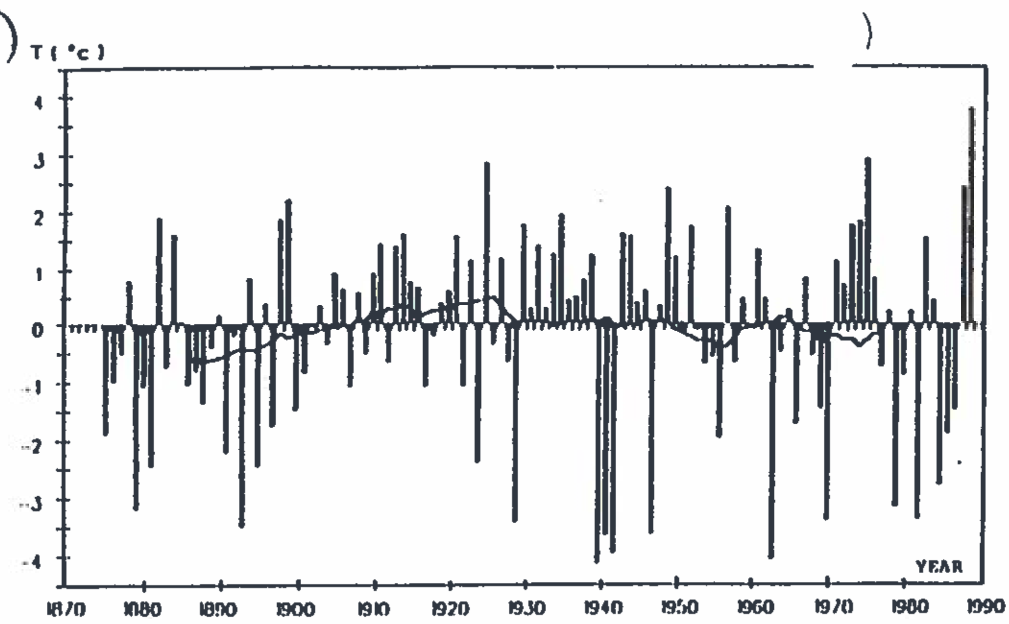

FIG. 6. Mean Air Temperature in Each Winter from 1874/75–1988/89. Solid Curve Shows Centered 30-year Average Winter Temperature (Figure Courtesy of Danish Meteorological Institute)

apart. Those calculations are not shown here. In the more severe ice winters with relatively thick ice, it normally takes about three to four days of low temperatures for the temperature profile in the ice to adjust so that the mean value corresponds to the mean of the surface and bottom temperatures of ice. Therefore, the x values were computed by using average temperatures of the last three days. This reduces the final result by about 10% compared with an analysis using individual day averages. It was decided to use a constant salinity of 1.5 ppt for the ice in the Great Belt. Timco and Frederking (1990) found decreasing gross salinities with increasing thickness. This is not taken into account in the present analysis.

Accurate temperature simulations could have been carried out, e.g., as suggested by Schwarz and Miloh (1972), but because of lack of time it was decided to use the three-day average temperatures and add a sensitivity analysis. More complex thermodynamic models of ice growth could have been used, e.g., as suggested by Maykut and Untersteiner (1971), Miller (1981), or Cox and Weeks (1988). However, the lack of the necessary data precluded use of these models.

The 114 maximum values of x were divided into groups and averaged within each group such that only about 20 points remain for determination of the distribution, as shown in Fig. 7. The grouping procedure was introduced to give equal weight to the information at either end of the curve. Without the grouping, the lower end would have a dominant effect on the best-fit distribution. In addition, Fig. 7 shows that the extreme maximum values follow another distribution than the maximum values at the lower end. The dashed line indicates the differing lower end distribution. It was also found that the extreme values of maximum x occur at low temperatures and not for temperatures close to the freezing point. Fig. 7 is a Weibull plot, but the Gumbel distribution may be just as relevant for describing the variations. The distribution functions are

$$F_W(x) = 1 - \exp\left[-\left(\frac{x}{\beta}\right)^k\right] \quad \text{(14)}$$

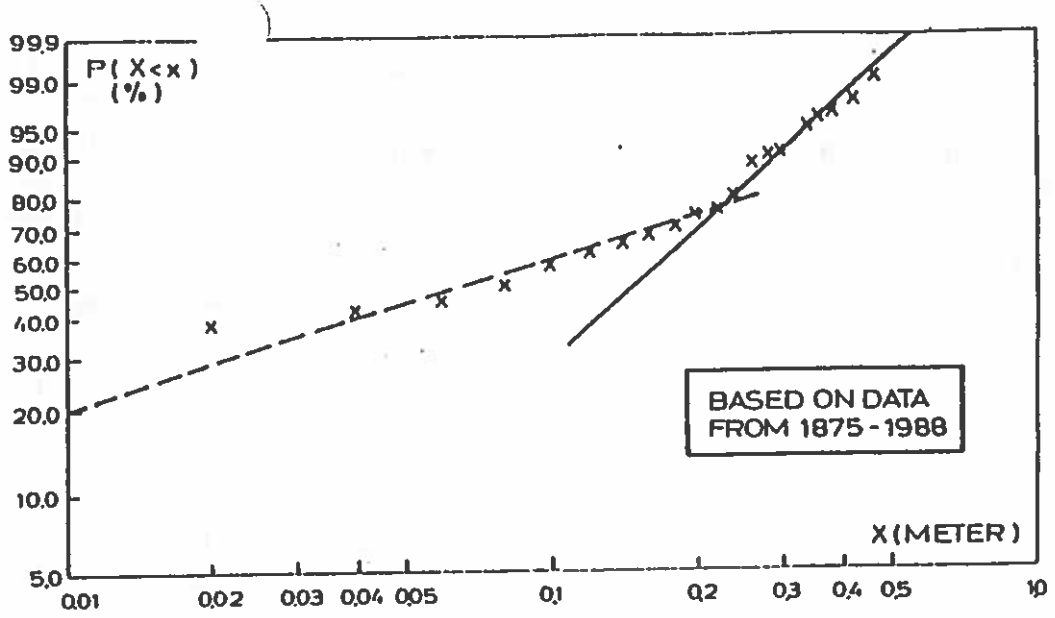

FIG. 7. Annual Exceedance Probability for x Based on Temperature Data from 1875–1988. Data Points Correspond to Upper Limits of Division Intervals

$$F_G(x) = \exp\{-\exp[-a(x-b)]\} \quad (15)$$

where the subscripts refer to the distribution names and (β, k, a, b) are distribution parameters to be determined from, for example, least-squares fit to the data. A χ^2-test is performed to determine which of the two distributions best fit the data. This means calculating a verification parameter, P, for each distribution as

$$P = \frac{1}{n-1}\sum_{i=1}^{n}(P_i - P_d)^2 \quad (16)$$

where P_i = the theoretical value according to the distribution function and P_d = the actual value based on the data. The count parameter i runs over the number of points to be fitted to. Because of the interest in extreme values, the χ^2-test is performed in conjunction with the peaks-over-threshold (POT) analysis instead of over all data points.

POT Analysis

A POT analysis is performed for the parameter x, being the standard statistic method for extreme statistics. The idea behind this analysis is that only extreme events belonging to the same family are considered. All nonextreme data are excluded.

The POT-analysis result is a function of the threshold chosen, and it is, therefore, performed with different thresholds both by use of the Weibull distribution function $F_W(x)$, and by use of the Gumbel distribution function $F_G(x)$. If the variation of the extreme values is small and nonsystematic for different thresholds, then the confidence in the results from the POT analysis will be good.

In the present analysis, the value with an exceedance probability of 2×10^{-5} per year was the one to be determined. [It was later shifted to 4×10^{-5} per year and might even shift again. The reasons behind the use of such

...treme exceedance probabilities were explained by Chr... ...sen et al. (1989).] The 2×10^{-5} per year corresponds to an average recurrence time of 50,000 years, and a distribution function value $F(\sigma_u h) = 0.99998$. This design value of $\sigma_u h$ was computed using all data points in Fig. 7 above a threshold, x_{th}, and the results are shown in Table 3 for different thresholds. Both the Weibull and the Gumbel distribution functions are used, and the χ^2-test [according to (16)] is performed to decide which of the two distribution functions are modeling the x-variation with highest accuracy.

From Table 3, it is seen that the Gumbel distribution gives results that are 10–20% larger than the results from the Weibull distribution. When the Weibull and Gumbel distribution functions are compared with the data for large values of x, it is found that the Gumbel distribution is below the actual data while the Weibull is above. It was therefore decided to base the design value of $\sigma_u h$ on a weighted average between the two distributions, and to use the values of the verification parameters as weights.

Table 3 is a good example of the importance of the theoretical expression of the distribution function when determining extreme values. At a threshold of $x_{th} = 0.28$, the two distributions give design values that are 16% apart, namely, 2.65 and 3.08 MN/m, based on the exact same data. Note also that both distributions yield $\sigma_u h$ design values that vary nonsystematically with x_{th}. This indicates that both distributions describe the general variation of the data well.

The weighted design value of $\sigma_u h$ was with $x_{th} = 0.28$ determined from

$$\frac{205}{343} F_G(\sigma_u h) + \frac{138}{343} F_W(\sigma_u h) = 2 \times 10^{-5} \quad \ldots\ldots (17)$$

where after a few iterations it was established that

$$\sigma_u h = 2.96 \text{ MN/m} \quad \ldots\ldots (18)$$

This is the central result of the extreme value analysis. It is, however, necessary to break the product into a strength and a thickness in order to continue with accurate load calculations. Eq. (7) was found to describe maximum ice thicknesses well (compare with Table 2). Christensen (1987) found that the K index for Danish domestic waters may be expressed as

$$K = 103.8[\ln(A) + 0.04]\text{°C-days} \quad \ldots\ldots (19)$$

where A = the average recurrence time in years and K is in Celsius degree-days. For the design situation, (19) gives $K = 1{,}127$ °C-days. As mentioned earlier, the maximum x typically occurs when K has reached 90% of its final value for the winter. With $K = 0.9 \times 1{,}127 = 1{,}014$ °C-days, the thickness is calculated from (7) and the strength is determined by dividing the product $\sigma_u h$ with the thickness. The results are

$$h = 0.99 \text{ m} \quad \ldots\ldots (20)$$

$$\sigma_u = 3.0 \text{ MPa} \quad \ldots\ldots (21)$$

Other breakdowns of the product in (18) are possible. The selected one agrees well with, for example, Timco and Frederking (1990); see their Fig. 10, where a thickness of 1 m and a strain rate of 2×10^{-4} sec^{-1} gives a compressive ice strength close to 3.0 MPa.

TABLE 4. Results for Various Recurrence Times, Excluding Effect of Snow Cover on Ice

Average return period (years) (1)	$\sigma_u h$ (MN/m) (2)	K (degree-days)* (3)	h (m) (4)	σ_u (MPa) (5)
50	1.26	410	0.57	2.21
100	1.48	482	0.63	2.35
1,000	2.05	721	0.78	2.63
10,000	2.58	960	0.91	2.84
25,000	2.82	1,055	0.96	2.94
50,000	2.96	1,127	0.99	2.99

*Degrees Celsius.

Results for various recurrence times are shown in Table 4. For a 10-year recurrence time, the POT-analysis method gives $\sigma_u h = 0.81$ MN/m, $h = 0.42$ m, $\sigma_u = 1.93$ MPa. The POT-analysis method, however, is suited for extreme recurrence times, and the 10-year value thus should be regarded with caution. Comparison with the preliminary results described by Christensen et al. (1989) shows that the extension of the temperature records to include 114 years resulted in a substantial increase of the design values.

Sensitivity Analyses

According to Frankenstein and Garner (1967), a more accurate estimate of the relative brine volume ν of the ice than the one given by (12) can be computed by

$$\nu = \left(1.189 - \frac{43.795}{T_i}\right)\frac{S_i}{1{,}000}, \qquad -22.9^\circ\text{ C} \le T_i \le -8.2^\circ\text{ C} \ldots\ldots\ldots (22a)$$

$$\nu = \left(0.930 - \frac{45.917}{T_i}\right)\frac{S_i}{1{,}000}, \qquad -8.2^\circ\text{ C} \le T_i \le -2.06^\circ\text{ C} \ldots\ldots\ldots (22b)$$

$$\nu = \left(-2.28 - \frac{52.56}{T_i}\right)\frac{S_i}{1{,}000}, \qquad -2.06^\circ\text{ C} \le T_i \le -0.5^\circ\text{ C} \ldots\ldots\ldots (22c)$$

When (22) is used instead of (12) to evaluate ν when the σ_0 values are computed, the relative changes in the mean value and standard deviation of the σ_0 distribution are less than 1%. Hence, it is concluded that (12) is adequate for computing ν in this analysis.

To investigate the relative importance of the largest measured σ_0 values, computations were carried out with the upper integration limit in (10) lower than infinity (which, of course, is necessary when a numerical integration is performed). The upper integration limit is chosen to be so large that the truncation error from the numerical integration is immaterial. A numerical integration of the probability density function $f(\sigma_0)$, which was given as a Weibull distribution, from 0–8 gives a difference of $1.5 \cdot 10^{-9}$ from the exact value 1. In the computations performed in this paper, the upper integration

limit is chosen as large as 20, and the numerical quadrature is performed with 10,000 points between 0 and 20.

The maximum x-values have been computed using mean air temperatures for one-, three- and five-day intervals. This gives a variation of the largest value of x computed in the period 1874/75–1988/89 between 0.5149 m for one-day intervals, 0.5108 m for three-day intervals, and 0.4911 m for a five-day averaging interval.

If the data in Fig. 7 are considered a single population, then a POT analysis is sufficient to predict the extreme values. If, on the other hand, they are considered two populations, then the extreme occurrence in both populations must be calculated. If the division point is located at the 75% fractile, then the relevant extreme value of the lower distribution is the $0.75 \cdot 50{,}000 = 37{,}500$ years event in that distribution after integration as specified in (10). This value has been computed as

$$(\sigma_u h)^* = 1.96 \text{ MN/m} \quad \ldots\ldots (23)$$

and is thus smaller than that resulting from the POT analysis. Hence, it is concluded that the results from the POT analysis are conservative with regard to the distribution of the parameter x.

Snow Cover

The effect of a snow cover on the ice has not been included in the analysis until this point. Because of the good agreement between observed and calculated thicknesses demonstrated in Table 2, it was decided not to include the snow cover in the theoretical model for ice growth. An additional reason for this is the total lack of sufficient statistics for snow layer thickness, h_s, over sea ice in Danish waters. Instead only the warming effect is included.

The presence of a snow layer will raise the mean ice temperature somewhat. Denoting the thermal conductivities of ice and snow by λ_i and λ_s, respectively, enables expression of the heat flux as a function of the thickness and temperatures, and after some simple calculations the temperature T_I at the ice-snow interface can be expressed by

$$T_I = \frac{\lambda_s h T_a + \lambda_i h_s T_w}{\lambda_s h + \lambda_i h_s} \quad \ldots\ldots (24)$$

where T_w = the temperature of the ice-water interface. The thermal conductivities of ice and snow were taken as

$$\lambda_i = 2.24 \frac{\text{W}}{(\text{m } ^\circ\text{C})} \quad \ldots\ldots (25)$$

$$\lambda_s = 2.84 \cdot 10^{-6} \rho_s^2 \frac{\text{W}}{(\text{m } ^\circ\text{C})} \qquad 140 < \rho_s < 340 \frac{\text{kg}}{\text{m}^3} \quad \ldots\ldots (26)$$

where ρ_s = the density of snow, [compare with Bergdahl (1977)]. The density ρ_s and thickness h_s of the snow cover must be estimated. The density of snow varies over a broad range [from 50 kg/m^3 (new snow in still air) to more than 400 kg/m^3 (consolidated snow)]. In this analysis, a value of 280 kg/m^3 is used. This is an average value for wind-toughened snow (Gray

TABLE 5. Design Values of $\sigma_u h$ in MN/m for Various Values of Snow Density ρ_s and Snow Thickness h_s

ρ_s (kg/m^3) (1)	h_s = 3.0 (cm) (2)	h_s = 4.0 (cm) (3)	h_s = 5.0 (cm) (4)
200	2.76	2.71	2.66
280	2.85	2.82	2.78
340	2.89	2.86	2.84

and Male 1981). Sensitivity calculations are carried out with a lower value (ρ_s = 200 kg/m^3) and a higher value (ρ_s = 340 kg/m^3) to investigate the effect of snow density. The thickness of the snow layer is estimated based on a mean value of the snow thicknesses from the 10 coldest winters in the period 1938–1988. Daily measurements of snow thicknesses (measured at 8 a.m.) are available from 1938 onward in "Meteorologisk Årbog" published by the Danish Meteorological Institute. Data from three different locations were used and a weighted mean value of the snow thicknesses was 9.7 cm.

This snow thickness was computed on the basis of measurements on open land. The retention coefficient relative to open land is for sea ice 0.4–0.5 (Gray and Male 1981), thus providing an estimate of the mean snow thickness on the ice sheet as

$$h_s = 4 \text{ cm} \quad \ldots\ldots (27)$$

This value was used in the computations. For sensitivity analyses snow thicknesses of 3 cm and 5 cm were also used as input for the computations.

The design value of $\sigma_u h$ is, as in the preceding analysis, found to be the weighted mean of the design values coming from POT analyses made with use of the Gumbel and the Weibull distributions, respectively. The results are shown in Table 5, with the central calculation giving a product of 2.82 MN/m.

A similar calculation for the 25,000-year situation using h_s = 4 cm and ρ_s = 280 kg/m^3 resulted in a product $\sigma_u h$ of 2.67 MN/m. With an ice thickness of 0.96 m (compare with Table 4), the compressive ice strength becomes 2.78 ≅ 2.8 MPa. This analysis of the effect of a snow cover on sea-ice strengths is fairly simple, and a number of questions have been left open. However, because of the complexity of the problem it is necessary to use professional judgment to some extent. Reductions in the area of 5% as indicated by Table 5 (relative to the $\sigma_u h$ = 2.96 MN/m found without snow) is seen as reasonable.

Eq. (7) gave a good estimate of ice thicknesses (compare with Table 2), even though it was based on a fairly simple model, i.e., one-dimensional heat conduction. The addition of a snow layer reduces ice growth significantly. The agreement therefore means either that there is very little snow or that other effects balance the insulating effect of the snow. Both are plausible explanations. A short warming can melt the snow or winds can deposit it in snow drifts, leaving large areas without snow. These snow-free areas would grow the largest ice thicknesses, and it is precisely those that are reported in Table 2. The bottom line, however, is that (7) gives good agreement with observations. Because of that, it was decided to only include the warming effect on strength and not on growth.

An important question is the appropriateness of the mean snow thickness. Many arguments have been weighed: (1) Extreme winters have northeasterly dry winds with little precipitation; (2) extreme winters have few or no thaw periods and, thus allow a long continuous snow accumulation without intermittent melting; (3) local spatial variations of snow thickness will leave some areas without the insulating snow cover, or at least with a reduced snow depth; and (4) can snow data from the selected locations be used as representative? All of these have been weighed, and, in the light of lack of sufficient data for a scientific approach, professional judgment was used. This led to the use of h_s = 4 cm, with only the warming effect included.

Conclusion

An extreme value analysis of ice properties in the Great Belt in Denmark has been carried out. For an annual exceedance probability of 2×10^{-5}, an ice thickness of 0.99 m and a uniaxial compressive ice strength of 2.8 MPa was found, when a snow cover was included in the analysis. Results for larger exceedance probabilities were also given.

Certain conservative assumptions mean that these values should be considered a "best-conservative" estimate rather than a central estimate. Some of these conservative assumptions are the ignoring of thaw periods when accumulating K in (6) and the assumption of a stationary stochastic process, i.e., that climatic trends are disregarded.

A method of circumventing the problem of correlation between ice thickness and ice strength was introduced by splitting their product in temperature-dependent and independent parts. The distribution of reference strength proved similar for the Great Belt and the Bay of Bothnia, which are more than 1,000 km apart. The analysis relies heavily on air temperature records and is thus well suited for areas with scarce ice information.

The effects of the testing machines on the standard deviations in the reference strength distributions have not been analyzed.

Acknowledgment

The presented analysis was carried out on behalf of the Great Belt Link Ltd. The company's permission to publish the results is gratefully acknowledged.

Appendix I. References

Bergdahl, L. (1977). "Physics of ice and snow as affects thermal pressure." *Report Series A:1*, Dept. of Hydraulics, Chalmars Univ. of Tech., Gothenburg, Sweden.

Christensen, F. T. (1986). "Sea ice strength measurements from the inner Danish Waters in early 1985." *Proc.*, First Int. Ice Technology Conf. (ITC-86), 247–253, Massachusetts Inst. of Tech., Cambridge, Mass.

Christensen, F. T. (1987). "Temporal variations of freezing degree-days in Danish domestic waters." *Proc.*, Ninth Int. Conf. on Port and Ocean Engineering under Arctic Conditions (POAC-87), Vol. 3, 201–206, Fairbanks, Alaska.

Christensen, F. T., Ottesen Hansen, N. E., Evers, K.-U., Spangenberg, S., and Vincentsen, L. J. (1989). "Design of the Great Belt Western Bridge for ice forces." *Proc.*, Eighth Int. Conf. on Offshore Mechanics and Arctic Engineering (OMAE-89), Vol. 4, 365–376, the Hague, the Netherlands.

Cox, G. F. N., and Weeks, W. F. (1982). "Equations for determining the gas and brine volumes in sea ice samples." *Report 82-30*, Cold Regions Research and Engineering Laboratory, Hanover, N.H.
Cox, G. F. N., and Weeks, W. F. (1988). "Numerical simulations of the profile properties of undeformed first-year sea ice during the growth season." *J. Geophys. Res.*, 93(c10), 12449–12460.
Frankenstein, G. E., and Garner, R. (1967). "Equations for determining the brine volume of sea ice from −0.5° C to −22.9° C." *J. Glaciol.*, 6(48), 943–944.
Fransson, L., and Elfgren, L. (1987). "Horizontal uniaxial compressive strength of low-salinity sea ice in the Gulf of Bothnia." *Proc.*, Ninth Int. Conf. on Port and Ocean Engineering under Arctic Conditions (POAC-87), Vol. 3, 21–29, Fairbanks, Alaska.
Gray, D. M., and Male, D. H., eds. (1981). *Handbook of snow*. Pergamon Press, Elmsford, N.Y.
Maykut, G. A., and Untersteiner, N. (1971). "Some results of time-dependent thermodynamic model of sea ice." *J. Geophys. Res.*, 76(6), 1550–1575.
Miller, J. D. (1981). "A simple model of seasonal sea ice growth." *Trans.*, ASME, Vol. 103, 212–218.
Mortensen, P., and Zorn, R. (1982). "Ice investigations at Farø bridge in 1982." Danish Hydraulic Institute, Hørsholm, Denmark (in Danish).
Schwarz, J., and Miloh, T. (1972). "On the time dependent temperature variations within ice sheets." *Proc.*, Int. Assoc. of Hydraulic Research Ice Symposium, 262–269, Leningrad, the Soviet Union.
"Ice and navigational conditions in the Danish waters during the winter 1985–86." (1986). Statens Istjeneste, Copenhagen, Denmark.
Timco, G. W., and Frederking, R. M. W. (1990). "Compressive strength of sea ice sheets." *Cold Reg. Sci. Tech.*, 17(3), 227–240.
Tryde, P., and Zorn, R. (1979). "Ice strength measurements in inner Danish waters during the winter of 1978–79." Danish Technical Research Council, Copenhagen, Denmark (in Danish).
Weeks, W. F., and Assur, A. (1969). "The mechanical properties of sea ice." Cold Reg. Sci. Engrg., Part II, Section C, Cold Regions Research and Engineering Laboratory, Hanover, N.H.

Appendix II. Notation

The following symbols are used in this paper:

a = parameter in Gumbel distribution;
b = parameter in Gumbel distribution;
f = probability density function;
f_h = function expressing h by k;
f_w = function of T_i and S_i;
F = probability distribution function;
F_G = Gumbel distribution function;
F_W = Weibull distribution function;
h = ice sheet thickness;
h_s = snow layer thickness;
k = parameter in Weibull distribution;
K = freezing degree-days index;
P = verification parameter;
P_d = distribution function based on data;
P_t = distribution function based on theory;
P_G = verification parameter for Gumbel distribution;
P_W = verification parameter for Weibull distribution;
S_i = gross ice salinity;

t	=	time;
T_a	=	air temperature;
$\bar{T}_a$	=	daily average air temperature;
T_i	=	mean ice temperature;
T_I	=	temperature at ice-snow interface;
T_w	=	temperature at ice-water interface;
x	=	temperature-dependent part of $\sigma_u h$;
x_{th}	=	threshold value in POT analysis;
β	=	parameter in Weibull distribution;
λ_i	=	thermal conductivity of ice;
λ_s	=	thermal conductivity of snow;
ν	=	relative brine volume in ice;
ρ_s	=	density of snow;
σ_u	=	uniaxial compressive ice strength; and
σ_0	=	reference compressive ice strength.

Danish Hydraulic Institute

Agern Allé 5
DK-2970 Hørsholm
Denmark
Telephone: +45 2 86 80 33
National 02 86 80 33
Telex: 37 402 dhicph dk
Telefax: +45 2 86 79 51

DETERMINATION OF EXTREME ICE FORCES

Notes for a Short-course at
University of Salford, England
19-21 April 1989
with corrections from june 1995

Prepared by
Flemming T. Christensen
Ph.D., Research Civil Engineer
Danish Hydraulic Institute

LIST OF CONTENTS PAGE

not included

1. INTRODUCTION

This note describes ways to determine extreme ice forces on offshore structures. The aim is to guide engineers in desk studies of ice forces on structures. The note has been logically structured in the following parts:

- Ice properties
- Driving forces
- Interaction formulas
- Selection of design forces
- Codes and standards
- Relevant literature

The present material was prepared for a short-course and it is only natural that there are many interesting aspects within ice-structure interaction, which are not covered, or only superficially covered, herein. Among subjects which are not covered are local ice pressures, multi-legged structures, ride-up and pile-up phenomena, rafting, rubble fields, remote sensing, sea ice dynamics simulation, fracture toughness of ice, friction between ice and various materials, icebreaking ships, physical and computational modelling of ice structure interaction, etc. It is the author's hope, however, that these notes will aid readers in acquiring a first insight into the problems associated with the determination of design ice loads on offshore structures.

2. ICE PROPERTIES

2.1 Crystal Structure

Ice is a polycrystalline material. The crystal lattice is formed by the oxygen atoms joined by hydrogen bonds. In the basic lattice, each oxygen is surrounded by four other oxygens to form an almost perfect tetrahedron with one hydrogen (really only a proton) between each set of oxygens. The molecules are organized in a near hexagonal pattern with an axis of symmetry called the c-axis or the optic axis. The plane perpendicular to the c-axis is called the basal plane. The lattice is illustrated in Figure 2.1.1. It is clear from the illustration that the pure (mono) crystal of ice is anisotropic with respect to most physical and mechanical parameters.

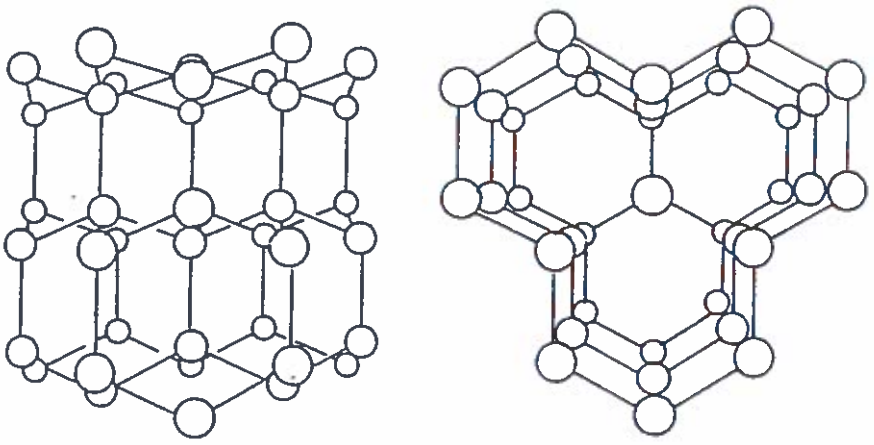

Figure 2.1.1 Crystal lattice of ice: a) View perpendicular to c-axis, b) View parallel to c-axis.

The basic crystal lattice is the same for all types of ice normally encountered by offshore structures. But the macroscopic structure of ice varies significantly with its growth history. Most ice types contain pockets of air, and sea ice also contains pockets of entrapped high salinity water called brine. The brine content is the major reason for the pronounced differences between fresh water ice and sea ice.

Typical sizes of grains in ice range from 2 mm to 50 mm, but crystals in excess of one metre have been observed. If an ice cover has reasonably uniform crystal sizes throughout the cover and a random orientation of the individual c-axes, it is referred to as isotropic. It is important to note that this term can be justified only on a macroscopic scale.

Under freezing conditions, the basic crystal lattice will grow faster in the directions of the basal plane than in the direction of the c-axis. This preferred growth results in a selective mechanism favouring crystals with their c-axis in the horizontal plane because they grow faster in the vertical direction than other crystals.

Ice formed in still water has often been found to have all horizontal c-axes of the grains more than a few centimeters below the surface, although this is far from always the case.

In sea ice the transition (with depth) to all horizontal c-axes is often very distinct but located slightly deeper, typically 10-20 cm below the surface. The preferred vertical growth results in vertically elongated crystals, and the ice is consequently referred to as columnar. Impurities, typically air and salt, are trapped at the grain boundaries as well as in the middle of grains while the crystals grow, and the columnar appearance of the polycrystalline material is thereby enhanced. Note that salt is also entrapped within each crystal. (The two terms "grain" and "crystal" are synonomous).

Because of the columnar structure, sea ice is normally anisotropic on the macroscopic scale also. Since the c-axis distribution within the horizontal plane is almost always random, the material is transversely isotropic, though.

In the remainder of this note, all properties are related to the horizontal plane in the ice. "Compressive strength" is to be understood as "compressive strength in the horizontal direction" unless something else is specifically stated. This simplifies the analyses considerably. Imagine for example the complexity arising from using six different moduli for just a monocrystal instead of using simply one Young's modulus.

Because of the temperature variation with depth and because of the strong temperature dependence of most of the mechanical properties of ice, floating ice covers are normally inhomogeneous, especially with respect to the vertical direction.

In many calculations, sea ice is still considered a homogeneous and isotropic material. For the purpose of load calculation, cf. section 4, these assumptions are adopted here.

2.2 Ice Growth

The growth of ice in nature is affected by a multitude of factors, and so an ice thickness calculated entirely on the basis of theoretical considerations cannot be used for design purposes. It is mandatory to compare with measurements from the area of concern. If such measurements do not exist, they must be carried out.

Take a column of a lake consisting of fresh water at a temperature of $+10^{o}C$. As fall moves on, the surface water is cooled, drops down, and leaves warmer water exposed to the colder atmosphere. The water is mixed and maintains an (ideally) uniform temperature profile. This continues until the lake is at $+4^{o}C$, where fresh water has its maximum of density. When cooling is continued, the colder water becomes lighter than the warmer water and forms a top layer, which eventually begins to freeze into an ice cover.

In the seas, this scenario is quite different because the temperature at which sea water has its maximum density is lower than the freezing point. This means that the mixing process will continue until the entire water column has reached the freezing point. The oceans, however, have too much heat stored in them for the atmosphere to remove it all in one winter. This is the reason why the oceans do not freeze over in winter, except of course the polar ocean.

The difference between lakes and seas is the content of dissolved salts in the sea. The oceans contain roughly 35 per thousand or 3.5 per cent salt. The freezing point of water (at atmospheric pressure) as a function of salinity is:

$$\theta_f = 0^{o}C - \frac{1.3^{o}C}{24.7\ o/oo} \times S \qquad (2.2.1)$$

where S is inserted in per thousand corresponding to the constant in the denominator. The temperature at which the density maximum occurs is:

$$\theta_{md} = 4^{o}C - \frac{5.3^{o}C}{24.7\ o/oo} \times S \qquad (2.2.2)$$

Note that the two expressions coincide at $\theta = -1.3^{o}C$ and $S = 24.7$ o/oo. Seas with a salinity above 25 o/oo will thus continue mixing all the way to the freezing point.

One of the simplest and most common formulae for calculating ice thicknesses can be derived directly from the linear differential equation of heat conduction by using constant values of the thermal properties of the ice and of the sea temperature. The formula becomes:

$$h = K^{1/2} \times 0.032 \text{ metre}/(^{\circ}\text{C-days})^{1/2} \qquad (2.2.3)$$

where K is the accumulated freezing degree-days and h the thickness. Ideally, K represents the integral of the air temperature with time, but in most practical situations each day is assigned a mean temperature, and K is increased by this amount:

$$K = \sum_{\text{days}} |\theta_{\text{mean}}(\text{day})|, \ \theta_{\text{mean}} > 0 \text{ not counted} \qquad (2.2.4)$$

Note that positive temperatures are not added. If a layer of snow is present, ice growth is slowed substantially because of the insulating effect. This would change the constant 0.032 in eq. (2.2.3), which is likely to overpredict actual ice thicknesses. In fact, a coefficient of 0.024 m/(°-days)$^{1/2}$ is used by the U.S. Army Corps of Engineers for some inland waterways in the USA.
The thermal properties applied in order to arrive at eq. (2.2.3) were: Latent heat of freezing of ice: L_i = 334 Joules/gram, thermal conductivity of ice: k_i = 2.24 Watts/(metre x Celsius degrees), and density of ice: ρ_i = 920 kilograms/m^3. These values of course change as a function of temperature and salinity. The listed values apply to near 0°C and very low salinity conditions. The purpose of showing eq. (2.2.3) is to give the reader a feel for the order of magnitudes of ice thicknesses. A scientific calculation would also account for solar radiation, reflection, wind and currents etc.

The processes of ice decay and melting are highly complex and outside the scope of these notes. The reader is referred to specialized literature, e.g. Ashton (1985).

2.3 Ice Density

The density of pure ice is 916.6 kg/m^3 at 0^{o}C and increases linearly with decreasing temperature to 920.7 kg/m^3 at -30^{o}C, see e.g. Ashton (1986) p. 32. In most practical calculations the value 920 kg/m^3 is used.

The density of natural ice is found as a weighted average of the pure ice density and the densities of impurities contained in the ice, primarily air and salt.

The basic formula for sea ice density, given e.g. by Schwerdtfeger (1963), reads:

$$\rho_i = \rho_{io} \times \frac{(1-\nu_a)}{1-(1-4.56/\theta_i)S_i/1000} \quad \text{for } -8^oC < \theta_i < \theta_f \quad (2.3.1)$$

ρ_{io} = 916.6 kg/m^3, density of pure ice
ν_a = relative volume of air bubbles in the ice
S_i = ice salinity in parts per thousand
θ_i = ice temperature in (negative) Celcius degrees
θ_f = freezing point (see eq. (2.2.1))

As an example, consider an ice with a relative air content of 0.02 by volume and a salinity of 3 o/oo at a mean temperature of -4^{o}C. The above equation then leads to a density of ρ_i = 898 kg/m^3.

2.4 Thermal Properties of Ice

The most commonly used thermal properties of ice are the latent heat, the specific heat, and the thermal conductivity. Simple formulas for the values of these parameters are given without a thorough explanation of the physics behind the formulas. Such explanations are outside the scope of these notes.

Latent Heat

The latent heat of sea ice is determined from:

$$L_i = L_{io} (1-S_i/S_w) \qquad (2.4.1)$$

L_{io} = 334 x 10^3 J/kg, the latent heat of freshwater ice
S_i = sea ice salinity ($S_i < S_w$)
S_w = sea water salinity

This formula is repeated from Schwerdtfeger (1963).

Specific Heat

For fresh water ice the specific heat, c_{io}, varies only little with the temperature. At -2^oC it is $c_{io}(-2) = 2.09 \times 10^3$ J/kg^oC and at -20^oC the value is $c_{io}(-20) = 1.97 \times 10^3$ J/kg^oC.

Saline ice, however, shows a substantial variation in specific heat near the freezing point. For S_i = 2 o/oo it is:

$$c_i = 1/(0.201n(-\theta_i)-0.049) \text{ for } -12^oC \leq \theta_i \leq -2^oC \qquad (2.4.2)$$

and for S_i = 4 o/oo it is

$$c_i = 1/(0.191n(-\theta_i)-0.084) \text{ for } -12^oC \leq \theta_i \leq -2^oC \qquad (2.4.3)$$

where θ_i is in Celsius degrees and c_i in 10^3 Joule/kg^oC.

Heat Conductivity

The thermal conductivity of sea ice is found from:

$$\lambda_i = \lambda_{io} (1-\nu_i) \qquad (2.4.4)$$

λ_{io} = 2.24 W/m^oC, conductivity of freshwater ice
ν_i = relative brine volume of sea ice
$\nu_i = (0.532-49.185/\theta_i)S_i/1000$ for $-22.9^oC \leq \theta_i \leq -0.5^oC$

The variation in conductivity with salinity and temperature is modest.

Thermal Expansion Coefficient

The last parameter of interest is the expansion coefficient. For practical reasons it is described in section 3.3.

2.5 Young's Modulus of Ice

Young's modulus, also called the elastic modulus, and Poisson's ratio are apparently not true material parameters. Researchers have attempted to measure them and describe their dependence on various other parameters since they are quite useful in simple calculations.

Estimates of the values of E and ν should be based on general experience with ice in the field and in the laboratory. It is important to realize how difficult these parameters are to measure. The values recommended here should be seen as rough estimates only. A certain amount of conservativeness should be applied when choosing a value in a design calculation.

When deforming metals at room temperature it is customary to find the elastic modulus as a constant factor of proportionality between the applied stress and the resulting strain. With ice, things become considerably more difficult. In nature ice mostly occurs at high homologuous temperatures, i.e. close to its melting point. It behaves somewhat like metals near their melting point. It has pronounced viscoelastic properties and exhibits creep for relatively small stresses. This makes it difficult to measure the elastic modulus in a simple static test.

To overcome this problem, seismic methods can be used to measure the modulus. (They are sometimes referred to as dynamic methods or ultrasonic methods also). The advantage is obviously that creep is minimized.

Monocrystals of ice seem to be temperature independent in terms of elastic modulus (Gold, 1958). On the other hand, Young's modulus of polycrystalline ice is clearly temperature dependent (Nadreau and Michel, 1984), and a general form like:

$$E = E_m(1-cT_i) \qquad (2.5.1)$$

E = elastic modulus
E_m = elastic modulus immediately below the melting point
c = constant (unit 1/celsius degree)
T_i = ice temperature in celcius degree (negative)

can be used to describe the relationship. Because of the pronounced creep properties, the measured elastic modulus becomes rather sensitive to the strain rate during measurement, with the highest values occurring at high strain rates (Trætteberg et al., 1975).

The elastic modulus of saline (sea) ice is lower than that of freshwater ice. Weeks and Assur (1967) show the dynamic modulus to be dependent on both brine volume and temperature. The general form of the relationship is:

$$E = E_o(1-e/e_o) \qquad (2.5.2)$$

E = elastic modulus
E_o = elastic modulus of pure ice
e = porosity, i.e. sum of air and brine
e_o = reference porosity ($\approx$ 0.2)

Pure freshwater ice typically has an elastic modulus in the order of 9 GPa (GigaPascals). For sea ice it is recommended to use the expression:

$$E = (1-0.011 \cdot T_i) \cdot 5.7 \text{ GPa} \qquad (2.5.3)$$

with the inherent assumption that the ice is columnar. For a mean ice temperature of $-5^{o}C$ the modulus becomes $E(-5^{o}C) = (1-0.011(-5))5.7 = 6.0$ GPa. More detailed information can be found in the literature, e.g. Lainey and Tinawi (1984). It should be remembered that both temperature, salinity, i.e. porosity, and loading rate affect the modulus. As a comparison, a typical elastic modulus for steel is in the order of 200 GPa.

It must be emphasized that sea ice is an anisotropic material essentially having six different moduli depending on which axes are considered. The values given in this section apply only to strains occurring in the direction of loading (stress).

Poisson's ratio is defined as the ratio of transverse strain (relative to loading direction) to longitudinal strain. It is often assumed to equal 0.33 and then left without attention. The anisotropy of some ice types leads to a variety of measured values. The mean value of 0.33 appears reasonable, but for columnar sea ice values up to 0.5 may apply, cf. Nadreau and Michel (1984). It is recommended to use the most conservative value.

2.6 Compressive Strength of Ice

The compressive strength of sea ice is dependent on a number of parameters. The most important ones are:

- ice type
- grain size and crystallographic orientation
- air content
- brine volume (i.e. salinity)
- loading rate
- confinement conditions
- temperature

In fact, all of these parameters must be known in order to make a strength value have any meaning. A scientist would like to know the value of each of these parameters. The designer, on the other hand, primarily wants to know what liability he has, as this may influence his judgement.

There is some disagreement among researchers whether the sample size has an effect or not. Sanderson (1986) shows a pronounced size effect of the effective contact pressure. On the other hand, Lee et al. (1986) and Petrie and Poplin (1986) found no size effect in their careful investigations.

In these notes, the effect of the ice type, grain size, and crystallographic orientation will not be described in any detail. Sea ice is normally of the S2 type in the classification system by Michel and Ramseier (1971). It has the columnar structure described in section 2.1. The effect of the latter five parameters in the list is described in the following.

Weeks and Assur (1967) developed a theory relating the ice strength to the brine volume in the ice. The brine volume, in turn, is dependent on the (gross) salinity of the ice and on the temperature. The colder the temperature, the smaller the brine volume and vice versa. Frankenstein and Garner (1967) developed an expression for the relative brine volume, ν_b, as a function of (gross) salinity and temperature:

$$\nu_b = (0.532 - \frac{49.185}{\theta_i}) \, S_i/1000 \quad -22.9^{\circ}C < \theta_i < -0.5^{\circ}C \qquad (2.6.1)$$

where θ_i must be inserted in (negative) celcius degrees and S_i in per thousand. At a temperature of $-22.9^{\circ}C$ the NaCl salts precipitate and the relationship changes substantially. The strength of the ice was described on the form:

$$\sigma = \sigma_o \, (1-(\nu_b/\nu_o)^{1/2}) \qquad (2.6.2)$$

where σ_o and ν_o are reference values of strength and relative brine volume. For first estimates ν_o = 0.275 is often used. The underlying model explains the strength variations with variations in "contact area" because of the brine pockets, and by failure planes following "weak contacts" joining the pockets. A more refined model was presented by Cox and Weeks (1983) taking into account the porosity caused by air bubbles also.

The loading rate, whether expressed in terms of strain or stress, has a very pronounced effect on the strength of ice. For low strain rates, ice fails in ductile yield, while for high strain rates it fails in a brittle manner. The overall relationship is shown in Figure 2.6.1. For strain rates lower than approximately 10^{-3} sec^{-1} there is a nearly linear relationship between the applied strain rate and the resulting strength. For strain rates above approximately 10^{-2} sec^{-1} there is not much variation in strength. In the intermediate range of strain rates from 10^{-3} to 10^{-2} sec^{-1} there is a peak strength. This is normally explained by the fact that cracks, which initially propagate in a brittle manner, do not penetrate the test sample but comes to a stop after which plastic deformation of a zone around the crack tip takes place. The "extra" peak stength is thus mobilized by the combined load requirements of crack initiation and plastic deformation. The maximum strength, and its corresponding strain rate, are found to be scale dependent by Sanderson (1984a). Against this stands the arguments of Lee et al. (1986) and Petrie and Poplin (1986).

As a comparison of compressive strengths, typical values are 2-3 MPa for sea ice, 3-5 MPa for freshwater ice, 5-10 MPa for iceberg ice, 30-60 MPa for concrete, 300-600 MPa for steel and 600-1400 MPa for high strength steel.

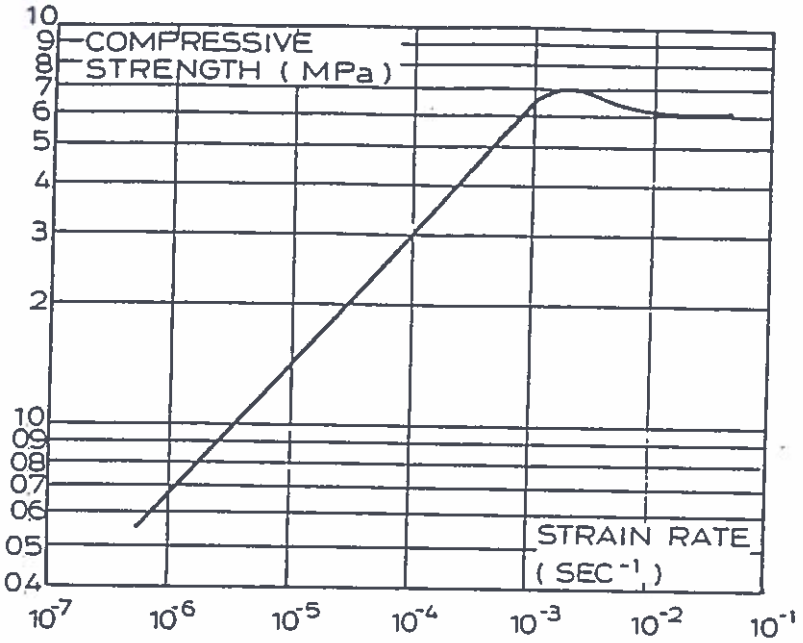

Figure 2.6.1 Examples of compressive ice strength as a function of strain rate for freshwater ice without air and salt.

One of the most recent formulas for predicting the in-plane (horizontal) unconfined compressive strength of S2 ice at low strain rates is that proposed by Timco and Frederking (1986):

$$\sigma = 39(\dot{\varepsilon})^{0.26}\,(1-(\nu/0.320)^{1/2}) \qquad 10^{-5} \leq \dot{\varepsilon} \leq 10^{-3} \qquad (2.6.3)$$

where $\dot{\varepsilon}$ is the strain rate in sec^{-1} and ν is the <u>total</u> relative porosity, $\nu = \nu_a + \nu_b$, i.e. the sum of the relative air volume and the relative brine volume. The strength is then in MegaPascals.

In confined configurations, increased strength can be found for certain types of confinements. The main types of interest for S2 sea ice are:

Type A: horizontal loading with vertical confining plates
Type B: horizontal loading with horizontal confining plates
Type D: vertical loading with vertical confining plates

The confinement types are illustrated in Figure 2.6.2. The B and D types of confinement appear to have very little effect on the measured strenghts. The A type of confinement, however, can result in strength increases by as much as a factor of four.

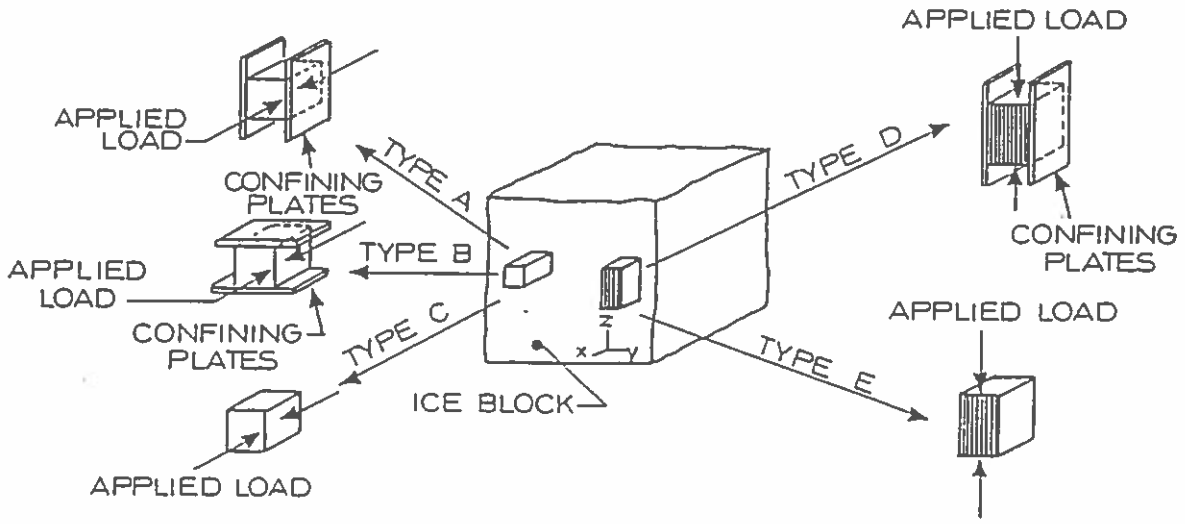

Figure 2.6.2 Types of confinement in ice strength testing.

2.7 Flexural Strength of Ice

The flexural strength of ice is most commonly determined from the breaking of beams and calculating:

$$\sigma_f = 6M/bh^2 \qquad (2.7.1)$$

where M is the breaking moment, b the beam width, and h the ice beam thickness.

The underlying assumptions, elastic behaviour and a linear stress distribution, are very coarse. Simplicity has made this formula the most widely used one, though. Flexural strength is normally expressed on the same form as compressive strength. Nadreau and Michel (1984) used:

$$\sigma_f = 0.75(1-(\nu_b/0.202)^{1/2}) \text{ MPa} \qquad (2.7.2)$$

where ν_b is determined as described in the previous section. The data supporting this formula were measured in salinity ranges from 5 to 19 o/oo, temperature ranges from -1.7°C to -12°C and with sample lengths ranging from 0.14 to 27 metres.

3. DRIVING FORCES

The driving forces, which cause movement of the ice, are wind drag, current drag, and thermal expansion forces. Each of these are briefly described in the following three sections. If these forces act simultaneously, they must obviously be added vectorially.

3.1 Wind Drag Forces

Wind over an ice surface can develop a static pressure on structures frozen into the ice cover, or impact loads in the case of moving ice sheets and floes. In large lakes, open estuaries, and oceans, wind forces are usually sufficient to cause the ice to fail against the structure, and the design ice forces are then governed by ice failure criteria. In some environments, however, the area of ice on which the wind acts may be sufficiently small that forces may be limited by the available wind drag force. Wind shear stress can be estimated from:

$$\tau_{wi} = \frac{1}{2}\rho_a C_d V_{10}^2 \qquad (3.1.1)$$

where ρ_a = density of air = 1.3 kg/m^3 at 0^{o}C

V_{10} = Wind velocity 10 metres above the surface

C_d = drag coefficient (dependent on the height at which V is determined)

The total wind drag force, F_{wi} is found from:

$$F_{wi} = \tau_{wi} A \qquad (3.1.2)$$

where τ_{wi} = wind shear stress
A = surface area of ice

The drag coefficient C_d is a function of surface roughness. Values varying from 2.8 to 5.2 x 10^{-3} have been reported for ice sheets in the Gulf of St. Lawrence, and a mean value of 4 x 10^{-3} seems to be reasonable for calculations based on V_{10}.

As a rule of thumb, it has been shown that the steady-state velocity of floating ice sheets moving under the influence of a steady wind is approximately 3% of the wind speed, when no currents are present.

3.2 Current Drag Forces

The current drag is calculated in a manner similar to that used for wind drag. The current shear stress can be estimated from:

$$\tau_{cu} = \frac{1}{2}\rho_w C_d U^2 \qquad (3.2.1)$$

where ρ_w = density of water = 1000-1020 kg/m^3

U = current velocity at a specific depth below the ice, usually 1.0 metre

C_d = drag coefficient (dependent on the depth at which U is determined)

The total current drag force F_{cu}, is found from:

$$F_{cu} = \tau_{cu} A \qquad (3.2.2)$$

where τ_{cu} = current shear stress
A = (bottom) surface area of ice

The drag coefficient C_d, is a function of the undersurface roughness of the ice, which may vary substantially. A reasonable mean for calculations is $C_d = 0.006$, when u is measured 1 m below the ice.

If an ice floe moves with the current, the relative velocity must be used, and this is normally very small. The above calculation of current drag is intended for a stationary ice cover, e.g. at rest against a structure.

3.3 Thermal Expansion Forces

Forces arising from thermal expansion and contraction of ice are very complicated to calculate in detail. This is mainly due to the complex mechanical properties of the ice. Two different scenarios are envisaged: Expansion of an ice sheet between two adjecent bridge piers (limited ice movement) and the expansion of a fast ice cover between a shore and a structure. The latter type can cause significant ice movement at the structure.

An ice sheet restricted betwen two piers will instead of actually expanding generate a force sufficient to induce a creep rate in the ice equal to the expansion rate. The net movement rate thereby becomes zero. The following discussion is based on studies by Bergdahl (1977), by Bergdahl and Wernersson (1978) and by Sanderson (1984b).

Salinity (o/oo)	0	2	4	6	8	10
$T_i = -2^oC$	1.69	-22.10	-45.89	-69.67	-93.46	-117.25
$T_i = -4^oC$	1.69	-4.12	-9.92	-15.73	-21.53	-27.34
$T_i = -6^oC$	1.69	-1.06	-3.81	-6.55	-9.30	-12.05
$T_i = -8^oC$	1.69	0.16	-1.37	-2.90	-4.43	-5.95
$T_i = -10^oC$	1.69	0.83	-0.02	-0.88	-1.73	-2.59
$T_i = -12^oC$	1.69	1.13	0.57	0.00	-0.57	-1.13
$T_i = -14^oC$	1.69	1.23	0.78	0.33	-0.13	-0.59
$T_i = -16^oC$	1.69	1.27	0.85	0.43	0.02	-0.40
$T_i = -18^oC$	1.69	1.33	0.96	0.60	0.23	-0.13
$T_i = -20^oC$	1.69	1.38	1.07	0.76	0.45	0.14
$T_i = -22^oC$	1.69	1.44	1.18	0.93	0.70	0.42

Table 3.3.1 Volumetric expansion coefficient for sea ice as a function of temperature and salinity. All values must be multiplied by 10^{-4}. A positive value indicates expansion with increasing (warmer) temperature and vice versa.

The coefficient of expansion depends strongly on both salinity and temperature. Values of the volumetric expansion coefficient, α_v, is given in Table 3.3.1. The coefficient of linear expansion, α_l, can be found from these values as:

$$\alpha_l = (1+\alpha_v)^{1/3}-1 \qquad (3.3.1)$$

or for small values and quick computations the relationship $\alpha_l = \alpha_v/3$ can be used. Note that for fresh water ice the expansion coefficient does not depend on temperature. It is interesting that the coefficients can take both positive and negative values, but the sign does not have any implications for the design forces, because both temperature increases and decreases must normally be expected.

Following the calculations of Bergdahl and Wernersson (1978) the equations become:

$$d\varepsilon = \alpha_1 d\theta \qquad (3.3.2)$$

$$\dot{\varepsilon} = \alpha_1 d\theta/dt \qquad (3.3.3)$$

For the linear expansion, and for the constitutive equation they use:

$$\dot{\varepsilon} = (\dot{\sigma}/E) + KD\sigma^n \qquad (3.3.4)$$

ε = strain
$\dot{\varepsilon}$ = strain rate
θ = temperature
t = time
σ = stress in the ice
$\dot{\sigma}$ = stress change rate
E = elastic modules of ice
n = 3.651
$K = 4.40 \cdot 10^{-26} m^{-2} (N/m^2)^{-n}$
D = coefficient of self diffusion i.e. $D_o \exp(-Q_s/RT)$
$D_o = 9.13 \cdot 10^{-4} m^2/s$
Q_s = 59.8 KJ/mol (=activation energy for self diffusion)
R = 8.31 J/mol (=universal gas constant)
T = absolute temperature in Kelvin degrees

The idea is then to set the two strain rates equal to each other. The only unknowns are then $\dot{\sigma}$ and σ.

$$\alpha d\theta/dt = (\dot{\sigma}/E) + KD\sigma^n \qquad (3.3.5)$$

This non-linear relationship can be solved by iteration on a computer. Stresses can be computed for different depths and the pressure evaluated by integration over the depth.

Calculated extreme pressures with 1000 year return periods are less than 400 kN per meter structure (Bergdahl and Wernersson, 1978), and as such the forces are substantially smaller than those resulting from impact of drifting ice floes.

The extreme pressure with a 100 year return period found for a Swedish lake at $57^{o}1'$ northern latitude was 330 kN/m.

In the case of expansion of a fast ice cover of several kilometers in size between a shore and a structure, the expansion rate is determined from a simulation of the thermal changes in the ice. The load on the structure is then determined from suitable ice failure theories with the appropriate ice movement rate.

4. INTERACTION FORMULAS

Offshore structures in ice-infested waters may be exposed to a number of different loading scenarios. Furthermore, different types of structures will cause different responses of the ice -structure system to the loading. The primary factors affecting the interaction are the structure configuration, the mechanical properties of the approaching ice and the velocity of the ice. The type of ice feature is of course also of major importance.

Ice loading on offshore structures can be divided into groups corresponding to forces from:

- landfast ice
- packice (also called drifting sheet ice)
- first-year pressure ridges
- multi-year pressure ridges
- rubble fields and blocking features
- icebergs

Structures have so far been divided into vertical and inclined structures, but with the growing activity in polar regions the list must be expanded to include some further distinctions:

- vertical vs. inclined structures
- rigid vs. flexible structures
- (bottom)fixed vs. floating structures
- narrow vs. wide structures

Only fixed, rigid structures are included in the scope of these notes. That leaves four categories, vertical and inclined, being narrow or wide.

4.1 Sheet Ice Forces on Vertical Structures

The seemingly simple problem of ice indentation forces is far from easy to solve, that is to predict the forces. This is primarily because of the complicated material behaviour of sea ice, although other factors also contribute to complicate the problem. In this chapter we shall assume that the necessary driving forces to cause ice failure are always present.

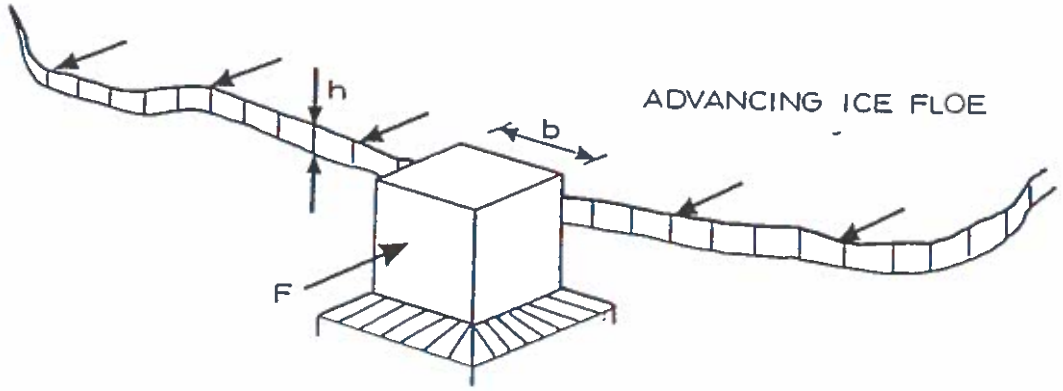

Fig. 4.1.1 Ice indentation (Type I).

Ice may fail against structures in a number of different failure modes:

- crushing
- fracture
- buckling
- creep
- bending (mostly against inclined structures)
- spalling
- cleavage
- splitting

which are mentioned here without further descriptions of each individual process. The most common failure mode against narrow vertical structures is that of crushing. Narrow structures include light-houses, bridge piers, and structures supported on columns. Early experience with offshore structures in ice has been described by Peyton (1968) and by Blenkarn (1970).

The force exerted on a structure due to ice crushing is:

$$F_c = p_e bh \qquad (4.1.1)$$

where p_e is the effective pressure over the contact area, b the structure width and h the ice sheet thickness. Naturally, p_e must depend of the ice crushing strength and the interaction conditions.

Drifting ice floes impact structures from a range of directions and within a range of different speeds. After the impact, an ice floe will fail locally as the structure "penetrates" the floe. Failure usually occurs in the form of crushing. The compressive strength of ice is very sensitive to the loading rate. For low strain rates ice behaves as a ductile material and fails by yielding. For high strain rates, say above approximately $5 \cdot 10^{-4}$ S^{-1}, it behaves in a brittle manner.

Formulas that predict loads on vertical structures from moving level ice have been presented by:

- Korzhavin (1962)
- Afanas'yev et al. (1971)
- Schwarz et al. (1974)
- Saeki et al. (1977)
- Croasdale, Morgenstern and Nuttall (1977)
- Ralston (1978)

and by a variety of authorities in the form of design codes. Most of these formulas give the horizontal force as the product of the projected contact area and the ice strength multiplied by some coefficient(s) dependent on interaction speed, geometry etc. They apply to bridge piers, lighthouses, and similar narrow structures. In the early seventies, when the first artificial islands for oil exploration were built in the Beaufort Sea, the same for-

mulas were initially used. It was quickly realized, however, that they predicted highly conservative values for the very wide structures (50-100 metres). In the following, I shall first review the formulas for narrow structures, and then move on to the wide artificial islands about which much has been learned since the mid-seventies.

Korzhavin (1962) proposed the following empirical formula:

$$p_e = Imk\ (V/V_o)^{-1/3}\sigma_u \qquad (4.1.2)$$

where the coefficients I, m, and k have physical justifications. The last factor, σ_u, is the unconfined compressive ice strength at a strain rate in the range of 10^{-3} to 10^{-2} sec^{-1}. I is an indentation coefficient accounting for confining effects as a function of the ratio of ice floe width, B, to structure width, b. The contact factor, k, accounts for the non-simultaneous contact failures occurring during continuous crushing, and the shape factor, m, accounts for the shape of the upstream face of the structure (e.g. a bridge pier). The coefficients are given as:

$I = (B/b)^{1/3}$	for $B/b < 15$	(4.1.3)
$I = 2.5$	for $B/b \geq 15$	(4.1.4)
$m = 1.0$	for flat (rectangular) indentors	(4.1.5)
$m = 0.9$	for semicircular indentors	(4.1.6)
$m = 0.85\ (\sin\alpha)^{1/2}$	for wedge-shaped piers with wedge angles of 2α between 60^o and 120^o	(4.1.7)
$0.4 \leq k \leq 0.7$	with low values for high velocities and wide structures and vice versa	(4.1.8)
$V_o = 1$ m/s	is a reference velocity	(4.1.9)

The velocity function was included in the empirical formula by Korzhavin (1962) to account for the fact that he fitted measured

forces using compressive ice strengths measured in the range of strain rates from 10^{-2} to 10^{-3} sec^{-1}. The formula is sometimes presented without the term $(V/V_o)^{-1/3}$, and in this case σ_u should be taken as the strain rate dependent unconfined compressive ice strength.

Afanas'yev et al.'s (1971) formula for crushing reads:

$$F_c = mC\sigma_u bh \qquad (4.1.10)$$

m = dimensionless shape coefficient

m = 1.0 for flat upstream face

m = 0.9 for a semicircular upstream face

C = dimensionless function of aspect ratio (4.1.11)

$C = (5(h/b)+1)^{1/2}$ for $1 < b/h < 6$

C is obtained from a linear interpolation between 4 (at b/h = 0.1) and 2.5 (at b/h = 1) for $0.1 < b/h < 1$

This formula is based on model tests with saline ice of small thickness, and it is not applicable for b/h > 6.

Schwarz et al.'s (1974) formula, which is sometimes called the Iowa-formula (it was developed partly at the University of Iowa) is based on cleavage failure. The authors saw a horizontal cleavage crack forming in the midplane of the ice in front of the pile.

Their formula can be written:

$$F = 0.564\ m^{0.4}\ \sigma_u\ b^{0.5}\ h^{1.1} \qquad (4.1.12)$$

where m is the unit meter, σ_u the uniaxial compressive strength, b the pile diameter, and h the ice thickness. The formula is supported by full-scale measurements on a b = 0.60 metre bridge pile in the Eider river in Germany and small-scale laboratory tests at the University of Iowa in the USA. The formula pertains to cleavage failure of ice within a few degrees of the freezing point against a vertical, circular structure. It should not be used for diameters in excess of two metres.

Saeki et al.'s (1977) formula is rather similar to that by Schwarz et al. It reads:

$$F = C\ \sigma_u\ b^{0.5}\ h \qquad (4.1.13)$$

where again the constant (C) must be given a dimension in order to make the equation dimensionally correct. Besides the values of C, the only other difference is in the power of h. The C values are:

$$C = 5.0\ m^{0.5} \text{ for a circular pile} \qquad (4.1.14)$$

$$C = 6.8\ m^{0.5} \text{ for a rectangular pile} \qquad (4.1.15)$$

and the failure is by cleavage as described earlier. The formula represents an upper-bound empirical fit to a combination of model test results and full-scale measurements.

Croasdale, Morgenstern and Nuttall (1977) presented the formula normally referred to as Morgenstern and Nuttall's formula. They assume an ideal elastoplastic and homogeneous ice and use a Tresca yield criterion to postulate:

$$\tau = \sigma_u/2 \qquad (4.1.16)$$

where τ is the shear strength. A truly homogeneous ice would then fail in 45^o wedges as shown in Figure 4.1.2. The formula for the corresponding force is:

$$F = \frac{1}{\cos\phi}\left(\frac{h}{4b} + \frac{1}{2\sin\phi}\right)\ \sigma_u bh \qquad (4.1.17)$$

when the indenting structure is considered frictionless. The angle ϕ, shown in Fig. 4.1.2., is close to 45^o, and using $\tau = \sigma_u/2$ the formula can also be written:

$$F = \left(\frac{\sqrt{2}}{4}\frac{h}{b} + 1\right)\ 2\tau bh \qquad (4.1.18)$$

The formula is an upper bound solution based on plastic limit theory.

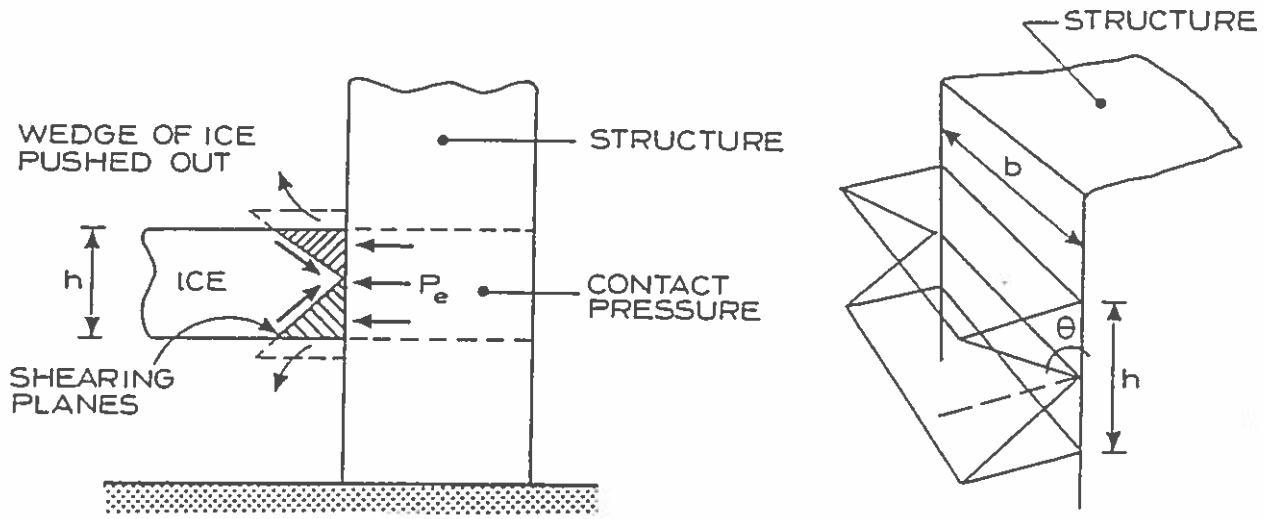

Fig. 4.1.2 Failure pattern assumed in Morgenstern and Nuttall's formula.

Ralston (1978) among others applied plastic limit analysis to the indentation problem for ice. This type of analysis is based on two theorems, viz.:

The lower bound theorem: The loads determined from a distribution of stress alone that satisfies a) the equilibrium conditions, b) stress boundary conditions, and c) nowhere violates the yield criterion are not greater than the actual collapse load.

The upper bound theorem: The loads determined by equating the external rate of work to the internal rate of dissipation in an assumed deformation mode (or velocity field) that satisfies a) velocity boundary conditions and b) strain and velocity compatibility conditions, are not less than the actual collapse load.

By suitable choice of stress and velocity fields, the above two theorems enable the required collapse load to be bracketed as closely as seems necessary for the problem under consideration.

The particular advantage of limit analysis is that it is not necessary to have a correct solution before having an answer. The correct answer, however, is revealed by identical upper and lower bounds. Thus one can start by making rough estimates that can be improved successively.

The reader is referred to the literature for a more detailed presentation of the application of plastic limit analysis to ice indentation.

Dynamic Ice Forces

The continuous crushing of ice against a bridge pier is a highly dynamic process which is both cyclic and irregular. Stresses in the ice build up in front of the pier, and microcracks begin to expand. As stresses increase the microcracks join and the ice separates into individual pieces. This pulverizing of the ice is what is usually referred to as crushing. But the formation and joining of microcracks and the possible formation and propagation of shear cracks are also part of the crushing process. At present, the ice crushing process is not fully understood (Timco and Jordaan, 1987).

Permanent deformations of a structure experiencing large loads are created over an interval of time rather than instantly. The time necessary to produce permanent deformations can be in the order of milliseconds or it can be as high as tens of seconds depending on structure material, on structure stiffness, and on foundation conditions.

The variation in load with time has been measured at high sampling rates by a number of researchers. A time series plot basically shows a number of peaks separated by drop-offs to minimum values in the range from 10% to 50% of the peak load. The duration of a peak depends on the interaction speed and the ice type among other things.

If a peak load is larger than the static design load of the structure, it may still pass without causing permanent deformations, provided that the duration of the peak is sufficiently short. The required magnitude and duration of a peak to cause permanent deformations can only be determined when a detailed structure design is available. The stiffness and natural frequency of a structure must be determined first, and then the time necessary to cause permanent deformation for the foundation is found. This normally requires detailed geotechnical investigations of the seabed material.

It is not unlikely that loads increase due to dynamic amplification if the natural frequency of the structure coincides with the typical frequency in the ice failure process. A first estimate of the typical crushing frequency, f_c, is:

$$f_c = \xi \, V/F_c$$

where F_c is the peak crushing force, V the velocity of the ice floe, and ξ the spring constant of the system. Amplification can also occur for buckling loads, see e.g. Christensen et al. (1989b).

Ice Forces on Wide Structures

As I mentioned earlier, the formulas presented above overestimate the forces on wide structures such as the artificial islands in the Beaufort Sea. Small scale ice strength tests and indentation theory resulted in global design ice pressures near 8 MPa. Even with various factors the pressure could not be lowered below approximately 4 MPa in the early island designs.

The first artificial island built in the Beaufort Sea was "Immerk" in the Canadian Beaufort Sea. It was a fill island in 3 metres of water depth. Nowadays caisson-retained-islands (CRI's) are used in water depths in excess of 30 metres. Caisson-type structures often have vertical sides.

At the time of the design of the first islands, reductions in ice forces were attempted because of:

- limited ice movement rates for the landfast ice near the coast,
- the possibility of a size effect in effective ice strength, and
- the possibility of alleviating measures in landfast ice zones.

The first limitation, that of movement rate, has been explored more over the last 16 years, and today a design ice pressure would definitely be limited by the rate-dependent ice strength if a maximum strain rate less than about 10^{-3} sec^{-1} can be ensured.

The second point, that of size effect, has been a major point of discussion among ice researchers for a number of years now. The foremost arguments are those by:

- Sanderson (1986) <u>for</u> the existence of a size effect, and
- Lee et al. (1986) and Petrie and Poplin (1986) <u>against</u> the existence of a size effect.

Sanderson (1986) uses a large number of experimental data from laboratory and field tests, full-scale measurements, and computer models of meso-scale ice mechanics to support proportionality of the upper bound indentation pressure and the contact area to the power -0.5. Lee et al. (1986) and Petrie and Poplin (1986) carried out full-scale ice strength measurements with a very carefully controlled test set-up and were unable to identify any size effects. The size effects observed by Sanderson could instead reflect other causes such as non-simultaneous failures, imperfect contact, etc. In any case, wide structures are designed for a lower global pressure than narrow structures. The reader is warned that this treatment of the ice-structure interaction problem for wide structures is very simplified. You are encouraged to study specialty literature on your own, e.g. on non-simultaneous failure (Ashby et al 1986, Kry 1981, Eranti 1990).

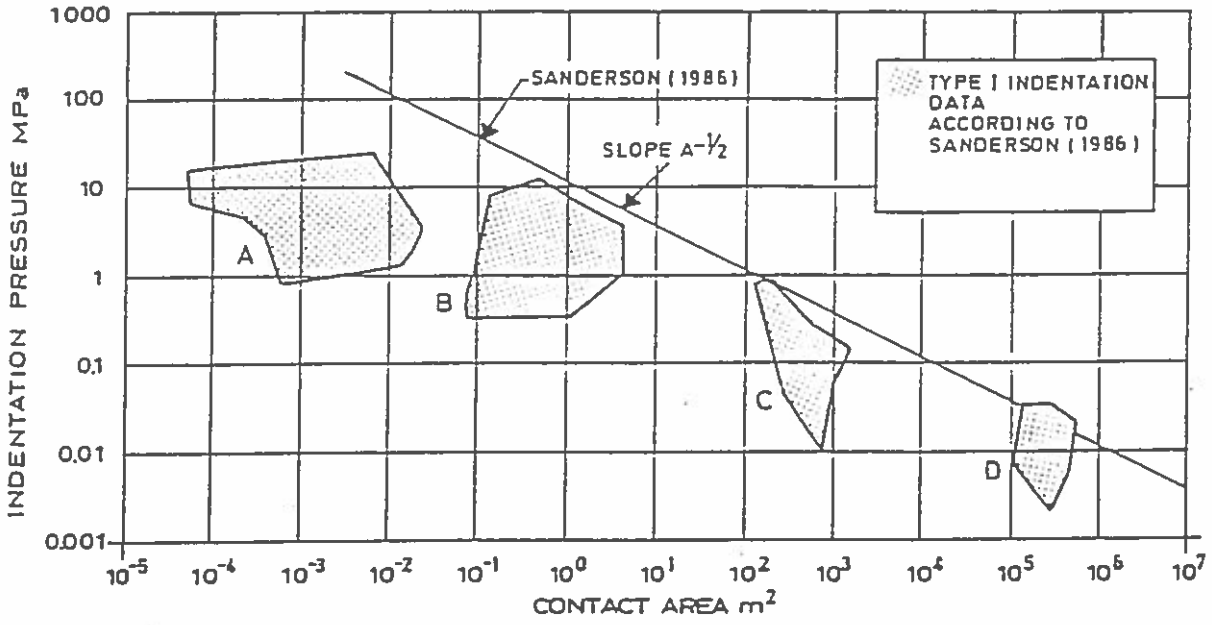

Figure 4.1.3 Pressure-Area Curve for Ice after Sanderson (1986). The four Data Groups are: A: Laboratory Tests, B: Medium-Scale Field Tests, C: Large-scale Arctic Islands measurements, D: Theoretical Mesoscale Models.

Sanderson's (1986) graph is shown in Figure 4.1.3. Other relationships than $\sigma \propto A^{-0.5}$ have been suggested for design, e.g. by Vivatrat and Slomski (1984) and by Christensen et al. (1989a).

The determination of ice loads on wide vertical structures i currently being based on three different approaches (see e.g. Croasdale (1988)), and they are:

- the indentation equation,
- the reference stress method, and
- the cut-off stress method

each of which is briefly commented on below.

The indentation equation is used with indentation factors determined from plastic limit analysis. The strength would be strain -rate dependent. Frozen-in structures subjected to ice pressure from a gradually increasing wind drag on the ice will experience "perfect contact", but a low strain rate. At higher strain rates the peak strength of the ice is used, but a contact factor less than one will apply (typically in the range from 0.3 to 0.7). The method still appears to be conservative for the widest structures.

The reference stress method described by Ponter et al. (1983) is for the creep regime, i.e. low strain rates. The results from this method are relatively close to those from the indentation equation when a rate-dependent strength and perfect contact are used. The validity of both methods ceases when fracturing begins. It appears that the onset of fracturing occurs for lower strain rates and at lower stress levels the larger the contact area becomes.

The cut-off stress method described by Walden et al. (1987b) considers the above finding, and suggests that the ice pressure has a maximum associated with the transition from ductile yield to brittle fracture. They suggested that the transition point is scale-dependent, like Sanderson (1984a) also did, and show how to determine it from full-scale data (Walden et al.; 1987a). Croasdale (1988) showed this last approach to give the best results which is natural since it is empirical.

Croasdale (1978) presented two formulas for the horizontal ice force on a conical structure.

They are normally referred to as the simple 2D theory and the adjusted 2D theory. The former theory gives the expression:

$$F = 0.68C_1\sigma_f b(\gamma_w h^5/E)^{1/4} + C_2\gamma_i Zbh \qquad (4.2.1)$$

where the first term represents the ice breaking force and the second term the ride-up force. The flexural ice strength is denoted σ_f, and γ_w and γ_i are the specific weights of water and ice, respectively. Z is the vertical height reached by the ice on the slope and C_1 and C_2 are functions of the surface slope, α, and the friction coefficient, μ, given by:

$$C_1 = \frac{\sin\alpha + \mu\cos\alpha}{\cos\alpha - \mu\sin\alpha} \qquad (4.2.2)$$

$$C_2 = \frac{(\sin\alpha + \mu\cos\alpha)^2}{\cos\alpha - \mu\sin\alpha} + \frac{\sin\alpha + \mu\cos\alpha}{\tan\alpha} \qquad (4.2.3)$$

Remember that $\cos\alpha > \sin\alpha$.

In the adjusted 2D theory an ice failure zone slightly wider than the structure is taken into account. The resulting difference is that the structure width (at the water line), b, in the ice-breaking term is replaced by a function, l', of the characteristic length, l, of the ice sheet given by:

$$l = (Eh^3/(12\gamma_w(1-\nu^2)))^{0.25} \qquad (4.2.4)$$

$$l' = (\pi^2/4)L \cong 2.47\ l \qquad (4.2.5)$$

The function l' is the approximate length of the circumferential crack in front of the structure. Since it depends only on the ice properties and not on the structure width, one should expect this theory to overestimate the breaking force on narrow structures and underestimate it on wide structures.

Ralston (1977, 1979) used plastic limit analysis for inclined structures also. Determination of ice loads on conical structures is in most cases carried out by using his theories, which have also been adopted as the recommended practice for offshore structures by the American Petroleum Institute (1982). Ralston's theory is known to be the most conservative among those predicting forces on conical structures. There is, however, no evidence that it should be too conservative. It includes both ice breaking and ice ride-up forces.

The inclination angle (with horizontal) should not exceed approximately 65^{o} in order for the theories to be applicable. This limit is given different values by various researchers, but 65^{o} is felt to be safe. It can be increased if the friction coefficient is lowered, e.g. by surface coating.

Ralston's (1977) method is based on plastic limit analysis, and the main result can be expressed as:

$$R_H = (A_1 \sigma_f h^2 + A_2 \gamma_w h b^2 + A_3 \gamma_w h (b^2 - b_t^2) A_4 \qquad (4.2.6)$$

$$R_V = B_1 R_H + B_2 \gamma_w h (b^2 - b_t^2) \qquad (4.2.7)$$

R_H = horizontal force on cone
R_V = vertical force on cone
σ_f = flexural stength of ice
γ_w = specific weight of sea water
h = ice sheet thickness
b = cone diameter at the water line
b_t = cone diameter at its top

$A_1, A_2, A_3, A_4, B_1, B_2$ = dimensionless coefficients which are functions of the ice-to-cone friction coefficient, μ and the cone inclination angle, α. Graphs for determining the coefficients are given in Fig. 4.2.2.

The global ice pressure on wide arctic offshore structures (100 metres) rarely exceeds 1.0-1.5 MegaPascals, but higher stresses cannot be excluded (Sanderson and Child; 1986) for higher strain rates.

Local Ice Pressure

The ice pressure can locally rise to values far higher than the unconfined compressive ice strength. This is in agreement with the observation of high confined compressive ice strengths for horizontal loading with vertical confining plates, cf. section 2.6, and also with the general plot by Sanderson in Figure 4.1.3. Local pressures are of importance to local structural stability and to abrasion etc. For a first estimate, it is recommended to use upper bound values from Figure 4.1.3. In special cases, however, values of twice those shown for very small areas can be achieved. The reader is referred to Cammaert and Muggeridge (1988) for a discussion of local ice pressures.

Multi-legged Structures

Ice loads on multi-legged structures are not described in these notes. This is solely in order to limit the length of the manuscript.

The reader is referred to Sodhi and Kato (1983), to Timco (1986), and to Christensen et al. (1989a). Being the most recent, the latter reference includes the most up-to-date list of literature on the problem.

4.2 Sheet Ice Forces on Inclined Structures

Typical structures classified as "narrow" and "inclined" are bridge piers with inclined noses often used in rivers where the direction of the ice floes is constant, and conical structures for lighthouses etc., which experience ice floe impact from all directions. The "philosophy" behind inclined structures is to promote bending as the dominant failure type and thereby reduce the ice forces.

Commonly appearing formulas for ice forces on inclined structures include those by:

- Croasdale (1978), simple 2D theory
- Croasdale (1978), adjusted 2D theory
- Ralston (1977, 1979), plastic limit analysis
- Edwards and Croasdale (1976), empirical
- Tryde (1975), elastic
- Bercha and Danys (1975),
- Afanas'yev et al. (1971), elastic and empirical
- Korzhavin (1962), empirical

These formulas are briefly presented in the following. Figure 4.2.1 illustrates a conical structure in ice.

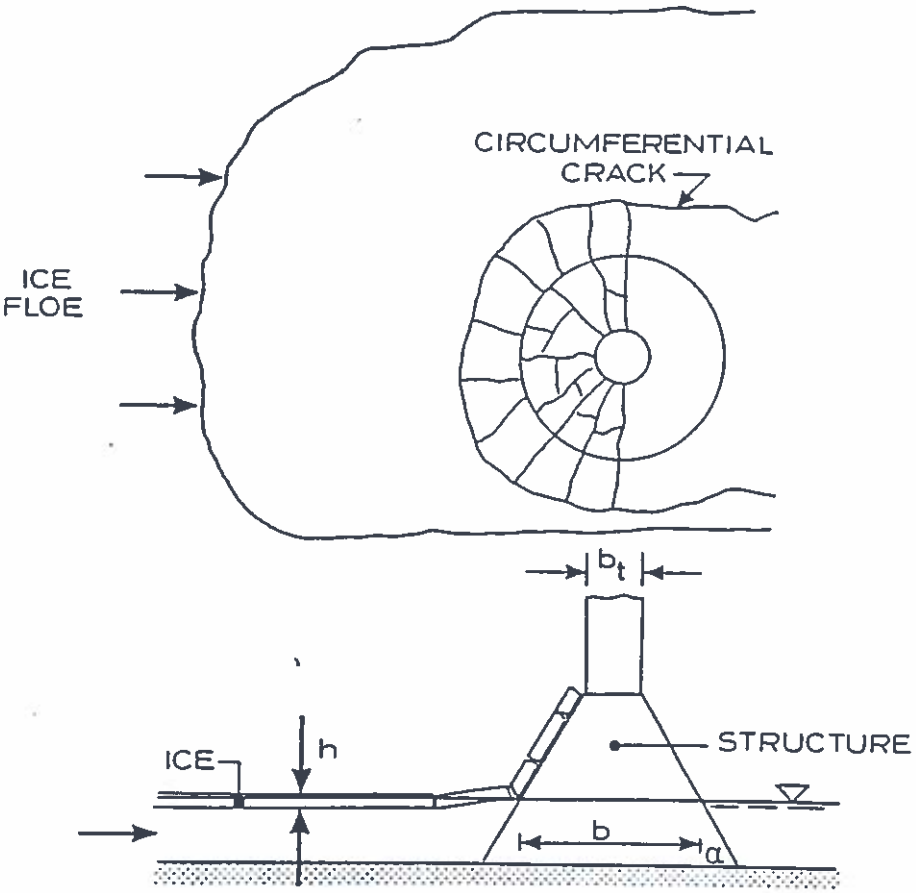

Figure 4.2.1 Sheet ice being pushed against a conical structure.

Croasdale (1978) presented two formulas for the horizontal ice force on a conical structure.

They are normally referred to as the simple 2D theory and the adjusted 2D theory. The former theory gives the expression:

$$F = 0.68 C_1 \sigma_f b (\gamma_w h^5 / E)^{1/4} + C_2 \gamma_i Z b h \qquad (4.2.1)$$

where the first term represents the ice breaking force and the second term the ride-up force. The flexural ice strength is denoted σ_f, and γ_w and γ_i are the specific weights of water and ice, respectively. Z is the vertical height reached by the ice on the slope and C_1 and C_2 are functions of the surface slope, α, and the friction coefficient, μ, given by:

$$C_1 = \frac{\sin\alpha + \mu\cos\alpha}{\cos\alpha - \mu\sin\alpha} \qquad (4.2.2)$$

$$C_2 = \frac{(\sin\alpha + \mu\cos\alpha)^2}{\cos\alpha - \mu\sin\alpha} + \frac{\sin\alpha + \mu\cos\alpha}{\tan\alpha} \qquad (4.2.3)$$

Remember that $\cos\alpha > \sin\alpha$.

In the adjusted 2D theory an ice failure zone slightly wider than the structure is taken into account. The resulting difference is that the structure width (at the water line), b, in the ice-breaking term is replaced by a function, l', of the characteristic length, l, of the ice sheet given by:

$$l = (Eh^3 / (12\gamma_w (1-\nu^2)))^{0.25} \qquad (4.2.4)$$

$$l' = (\pi^2/4) L \approx 2.47\, l \qquad (4.2.5)$$

The function l' is the approximate length of the circumferential crack in front of the structure. Since it depends only on the ice properties and not on the structure width, one should expect this theory to overestimate the breaking force on narrow structures and underestimate it on wide structures.

Ralston (1977, 1979) used plastic limit analysis for inclined structures also. Determination of ice loads on conical structures is in most cases carried out by using his theories, which have also been adopted as the recommended practice for offshore structures by the American Petroleum Institute (1982). Ralston's theory is known to be the most conservative among those predicting forces on conical structures. There is, however, no evidence that it should be too conservative. It includes both ice breaking and ice ride-up forces.

The inclination angle (with horizontal) should not exceed approximately 65^{o} in order for the theories to be applicable. This limit is given different values by various researchers, but 65^{o} is felt to be safe. It can be increased if the friction coefficient is lowered, e.g. by surface coating.

Ralston's (1977) method is based on plastic limit analysis, and the main result can be expressed as:

$$R_H = (A_1 \sigma_f h^2 + A_2 \gamma_w h b^2 + A_3 \gamma_w h (b^2 - b_t^2) A_4 \qquad (4.2.6)$$

$$R_V = B_1 R_H + B_2 \gamma_w h (b^2 - b_t^2) \qquad (4.2.7)$$

R_H = horizontal force on cone
R_V = vertical force on cone
σ_f = flexural stength of ice
γ_w = specific weight of sea water
h = ice sheet thickness
b = cone diameter at the water line
b_t = cone diameter at its top

$A_1, A_2, A_3, A_4, B_1, B_2$ = dimensionless coefficients which are functions of the ice-to-cone friction coefficient, μ and the cone inclination angle, α. Graphs for determining the coefficients are given in Fig. 4.2.2.

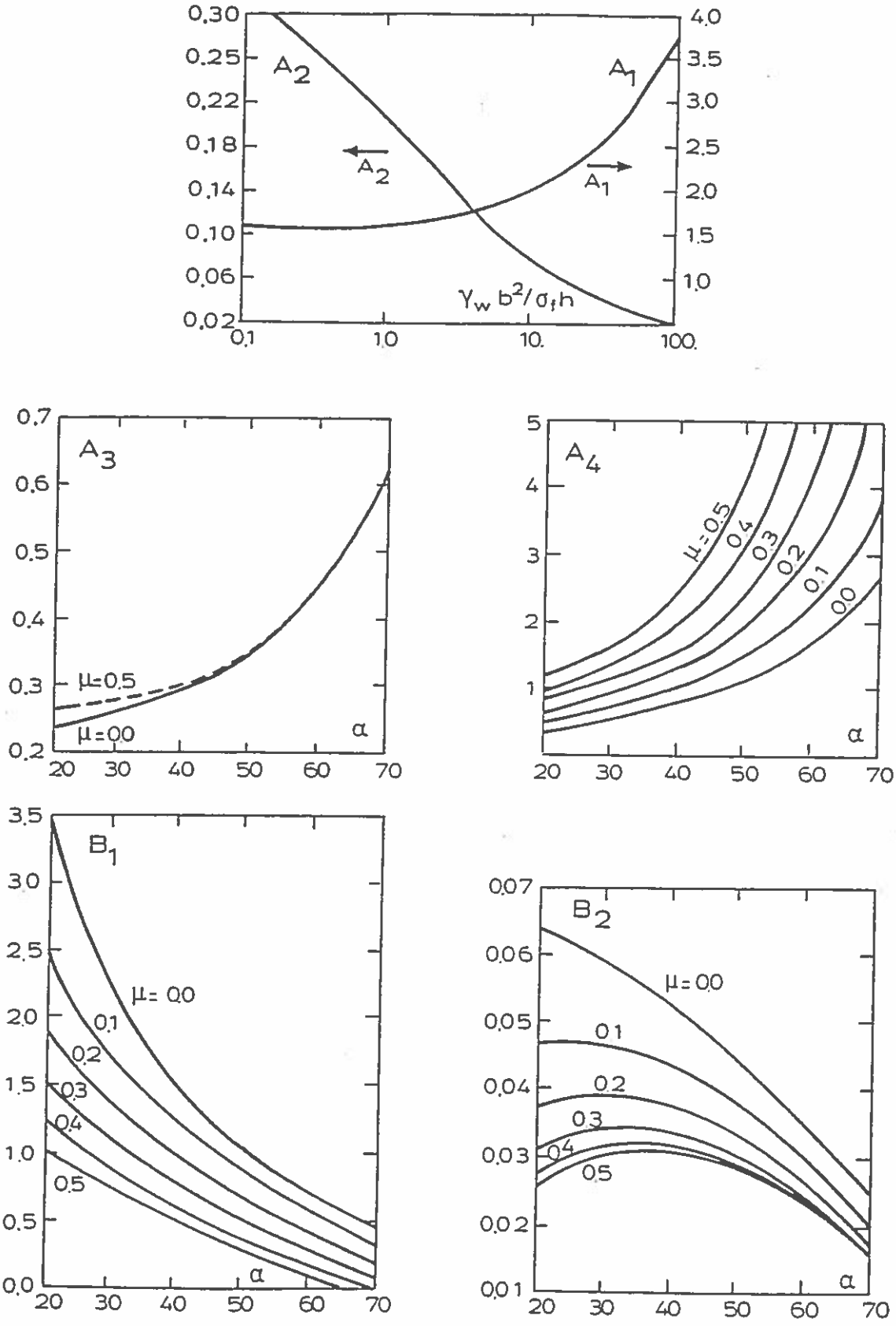

Fig. 4.2.2. Ice force coefficients for plastic limit analysis. From Ralston (1977).

The above formulas may be used when the length of the slope fro the water line to the top exceeds the size of the broken floes. It is assumed that the largest ice pieces broken off the ice sheet have a length of 1/2, where l is the characteristic length of the ice. The criterion becomes:

$$S \geq 0.5(Eh^3/12\gamma_w(1-\nu^2))^{0.25} \qquad (4.2.8)$$

S = length of slope above water
E = elastic modulus of ice
ν = Poisson's ratio

If this condition is not satisfied considerable forces may be exerted on the vertical part of the structure, and the advantage of the conical shape is partly lost. In a situation with E = 6.0 GPa, h = 0.965 m, γ_w = 10 kN/m^3 and ν = 0.5 the characteristic length becomes 15.6 m. The length of the conical surface from the water line to the top (transition to vertical pier) must therefore be about 8 m unless a more refined (dynamic) analysis is carried out. This applies to rotationally symmetric piers only. This estimate is very conservative. Refined analyses will normally show 3-4 meters to be sufficient, depending also on the tidal range at the structure.

In the above calculation it has been assumed that the cone would lift the ice sheet upon contact. A configuration with a cone inducing downward bending of the ice is also possible, and it is actually preferable because it causes smaller vertical forces. Instead of the gravity of the ice, the buoyancy becomes the source of the vertical force.

The specific weight of the ice was taken as 90% of the specific weight of the sea water (0.9 γ_w) for the calculation of the dimensionless coefficients. The buoyancy acting on depressed ice will correspond to 10% of the specific weight of the sea water (0.1 γ_w). As such, the theory may be applied to downward breaking cones by replacing γ_w with $\gamma_w/9$ and changing the sign on R_v.

The dimensionless coefficients given in the graphs can be determined semi-analytically. The procedure was described e.g. by Christensen (1988).

Example

For an example assume that the following values apply:

σ_f = 700 kPa
γ_w = 10 kN/m^3
b = 17.0 m
h = 0.965 m
α = 45 ^{o}
b_t = 5.0 m
μ = 0.15

The dimensionless parameter $(\gamma_w b^2/\sigma_f h)$ then amounts to 4.28 and the resulting values of the constants become A_1 = 1.81, A_2 = 0.12, A_3 = 0.32, A_4 = 1.40, B_1 = 0.92, and B_2 = 0.037. The horizontal and vertical forces are then found as:

R_H = 3.3 MN
R_V = 3.1 MN

These forces are substantially smaller than those for vertical piers of similar overall dimensions. Note that the vertical force introduces a stabilizing moment on the structure.

Edwards and Croasdale (1976) derived their formula on the basis of model test data. They used a surface slope angle of 45^o and a friction coefficient of about 0.1. Their formula for the horizontal force reads:

$$F = 1.6\ \sigma_f h^2 + 6.0\ \gamma_w\ bh^2 \qquad (4.2.9)$$

where b is the structure width at the water line. The two terms allegedly represent breaking and ride-up contributions to the total force. Note that the breaking term is independent of the structure width. The formula should be seen as an expression of test results rather than a tool for design.

Tryde (1975) gives a formula for the ice force on a wedge shaped structure, e.g. an upstream bridge pier face. His formula is based on a specific assumed crack pattern. Let β be half the apex angle of the wedge in the horizontal plane, and let α be the angle between the horizontal and the upstream edge of the wedge, see Figure 4.2.3. The coefficient of friction between the ice and the pier is denoted μ. Typical friction coefficients for ice on concrete piers are in the range of 0.1 to 0.2. The ice thickness is denoted h and the pier width b.

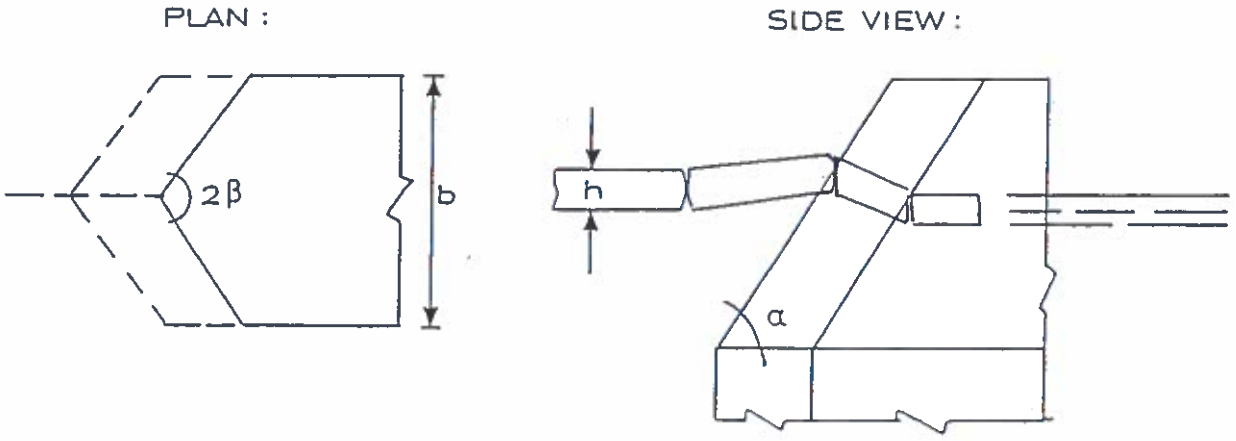

Figure 4.2.3 Definition sketch for inclined wedge piers.

The first step is to calculate the three dimensionless coefficients:

$$C_1 = 1-\mu(\tan\alpha/\sin\beta) \qquad (4.2.10)$$

$$C_2 = \mu+(\tan\alpha/\sin\beta) \qquad (4.2.11)$$

$$C_3 = 6(h/b)\cos\beta+6(C_1/C_2) \qquad (4.2.12)$$

Let furthermore E denote the elastic modulus of the ice, ρ the density of the ice, and v the velocity of the ice floe. The next step is then to calculate the combined dimensionless coefficient

$$C = 0.16(E/\rho v^2\sin^2\beta)^{1/2}(C_1/C_2)C_3^{\,2} \qquad (4.2.13)$$

Finally, let the ratio of the bending strength to the compression strength be denoted ε $(=\sigma_f/\sigma_u)$, and calculate the coefficient:

$$k = 5.2 \cdot \varepsilon^{1/3} \cdot C^{-1/2} \qquad (4.2.14)$$

The maxium horizontal force on the bridge pier may then be found by the formula:

$$F = k\sigma_u bh \quad 3.3 < b/h < 20 \qquad (4.2.15)$$

which is identical to the one for vertical piers, except that the coefficient k is calculated in an entirely different way.

Example

For an example assume that the following parameters apply:

Pier:	Ice:	
$b = 5.0$ m	$\mu = 0.15$	$v = 0.7$ m/s
$\alpha = 60^o$	$E = 6.0$ GPa	$\sigma_f = 500$ kPa
$\beta = 30^o$	$h = 0.60$ m	$\sigma_u = 1500$ kPa
	$\rho = 910$ kg/m^3	

This leads to the following coefficients:

$C_1 = 0.48$ $C_2 = 3.61$ $C_3 = 1.42$ $C = 315$ $k = 0.203$

and eventually the horizontal force:

$F = 0.203 \cdot 1500 \cdot 5 \cdot 0.60$ kN = <u>0.914 MN</u>

Note that the compression strength is used in the final formula. The ice actually fails in flexure, and this is accounted for through the parameter ε.

Piers with inclined wedges as upstream faces have been successfully used in rivers where the ice floes impact largely in the longitudinal direction of the pier. An inclined upstream face will only be effective for a limited range of directions. Consequently, it can be of interest to consider piers with a conical shape in the zone around the water line, if a range of impact directions is expected.

Bercha and Danys' (1975) formula is not explained in these notes.

Afanas'yev et al.'s (1971) formula is based on small-scale model tests with conical structures interpreted through elastic plate theory. Their formula reads:

$$F = \frac{S_c \tan\alpha}{1.93\ l}\ \sigma_f h^2 \qquad (4.2.16)$$

where α is the surface slope, l the characteristic length of the ice sheet, and S_c the length of the circumferential crack given by:

$$S_c = 0.62\ b + 1.38\ l \qquad (4.2.17)$$

where b is the structure width at the water level. The test data were obtained in ice of 3 to 3.5 cm thickness and with α-values of 30^o, 45^o, and 60^o.

Korzhavin (1962) states that the ice force is the lowest of the three forces calculated for failure in crushing, bending, and shear. His crushing formula is presented in section 4.1. The bending and shear formulas are:

$$F = C_o \tan\alpha \ \sigma_f bh \text{ for bending} \qquad (4.2.18)$$

$$F = 1.1\ k \frac{\tan\alpha}{\sin\beta} \tau bh \text{ for shear} \qquad (4.2.19)$$

where τ is the shear strength (a Tresca criterion would give $\tau = \sigma_u / 2$, albeit the Tresca criterion is simplified here), $2\beta = 80°$ is recommended), k is a contact coefficient, and C_o is a function of the angles α and β as follows:

α 2β =	45^o	60^o	75^o	90^o	120^o
45^o	0.20	0.17	0.16	0.16	0.15
60^o	0.24	0.20	0.19	0.18	0.17
70^o	0.38	0.27	0.23	0.21	0.19
75^o	0.79	0.38	0.29	0.26	0.22

Table 4.2.1 Values of Korzhavin's (1962) coefficient, C_o.

A decrease in apex angle (2β) results in an increase of C_o and thus in effective ice pressure. This is explained by the fact that a narrower structure is likely to penetrate further into an ice floe before breaking it. This means that larger pieces will break off. C_o increases with surface slope (α). This might be because of combined bending and compression failures on the steep structures.

4.3 Ice Ridge Forces on Vertical Structures

An ice ridge or pressure ridge is an accumulation of ice pieces caused by compressive ice forces in an ice cover. Pressure ridges can in arctic areas exceed drafts of 50 metres, and they are frequently a governing factor in arctic design and operations. Typical ridges have drafts in the range of 2-15 metres. The under water accumulation is referred to as the keel, and the above water part of the accumulation is called the sail. There is often a solid zone between the keel and the sail. Pressure ridges that have not (yet) undergone a melting season are called first-year ridges as opposed to multi-year ridges which are more consolidated features with a larger solid zone. Loads from first-year ridges are predicted mainly by three models, viz.:

- Croasdale (1980), plug shear
- Prodanovic (1981), spiral shear
- Rojansky and Gerwick (1981), beam bending

while loads from multi-year ridges will be substantially larger than those from first-year ridges with similar dimensions.

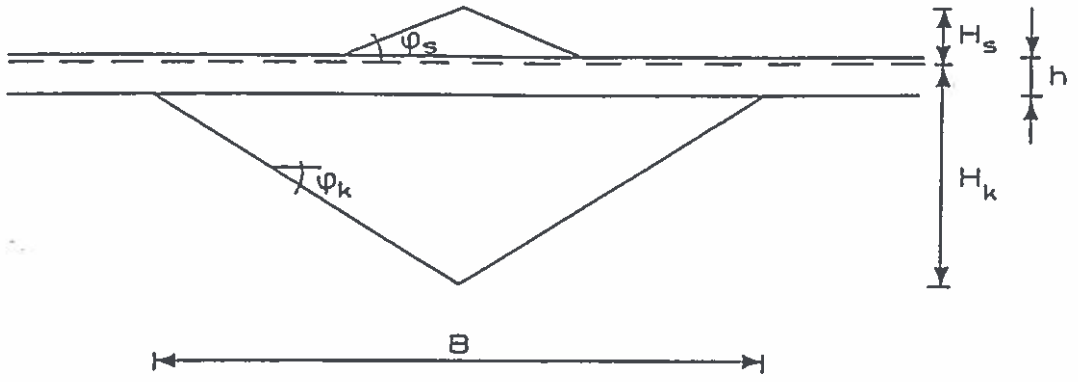

Figure 4.3.1. Definition sketch for ice pressure ridges.

Typical keel depth to sail height ratios are in the range of $H_k:H_s$ = 3:1 to 5:1 depending on how deteriorated the ridge is. Newly formed ridges can have ratios near 8:1, but then the keel has almost no structural integrity. Typical angles of repose are $\phi_s = 20^o\text{-}30^o$ and $\phi_k = 30^o\text{-}40^o$.

Croasdale (1980) assumed two plane shear failures to create a plug type shear failure stopping a section of the ridge in front of the structure. His formula reads:

$$F = F_r + F_s \qquad (4.3.1)$$

where F_r and F_s are the forces required to fail the rubble (keel and sail) and the solid zone, respectively. He suggests:

$$F_r = \frac{2}{3} B H_k^2 (\gamma_w - \gamma_i) \tan\phi_k \qquad (4.3.2)$$

where B is the ridge width, γ_w the specific weight of water, and γ_i that of the ice. He furthermore suggests determining F_s by the usual crushing formulas setting the solid zone thickness equal to the ice sheet thickness.

Prodanovic (1981) also suggests two independent terms. The rubble is assumed to fail in accordance with a Mohr-Coulomb failure criterion. This results in two spiral curved cracks, see Figure 4.3.2. The resulting rubble force, F_r, is shown graphically in Figure 4.3.3., as a function of the aspect ratio (structure width to ice thickness).

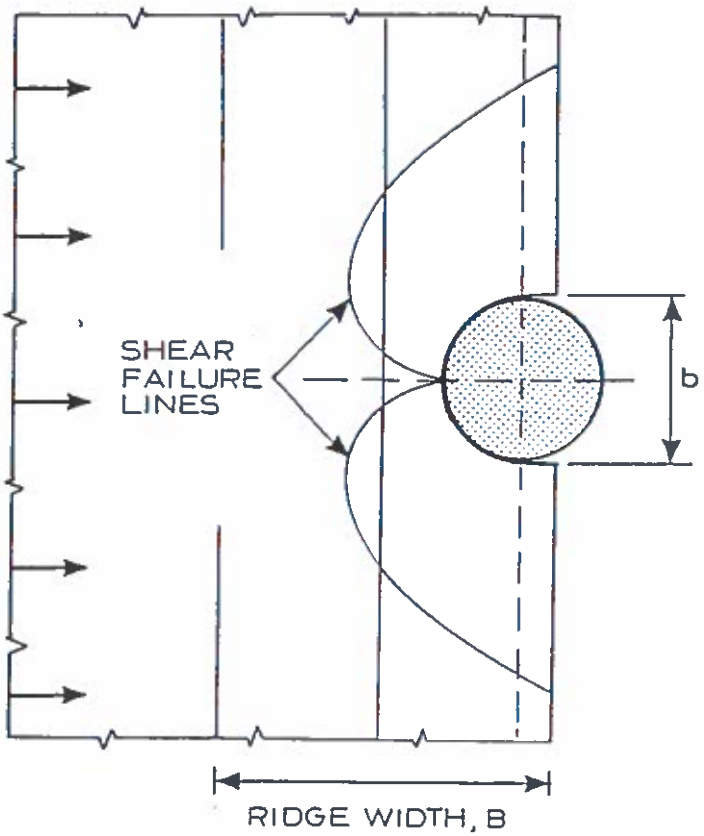

Figure 4.3.2 Failure planes from Prodanovic's model.

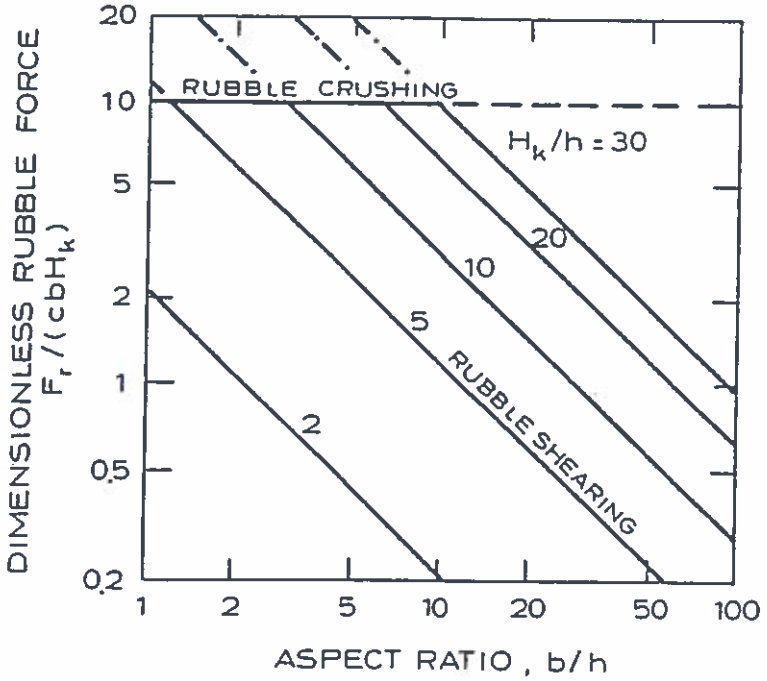

Figure 4.3.3 Rubble force as a function of aspect ratio according to Prodanovic (1981)

Multi-year ridges, which are normally stronger than first-year ridges, are also handled by Prodanovic (1981) who uses an anisotropic, pressure-sensitive yield function to predict failure of the large solid zone in the ridge. His result for multi-year ridges are illustrated in Figure 4.3.4, which shows the total ridge force as a function of aspect ratio.

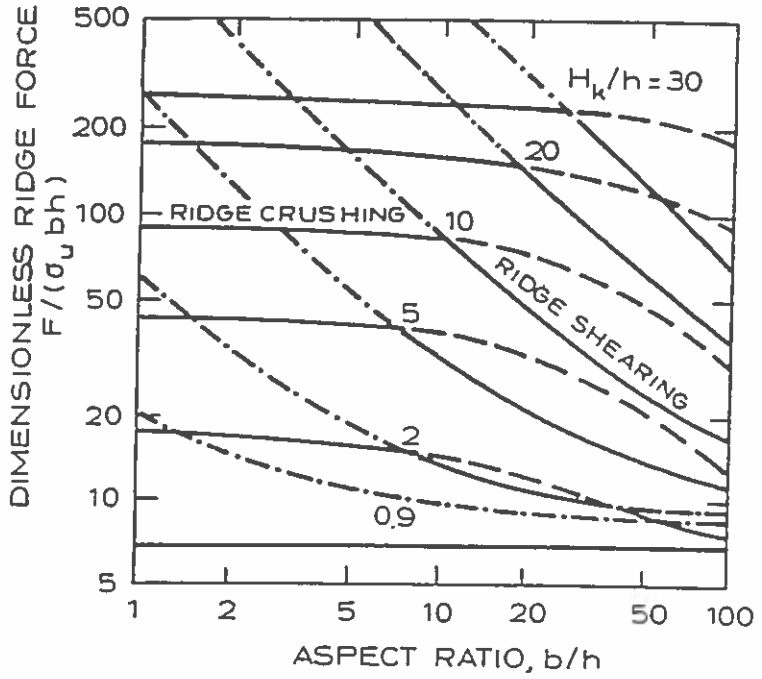

Figure 4.3.4 Multi-year ice ridge force as a function of aspect ratio according to Prodanovic (1981).

Rojansky and Gerwick's (1981) model is based on in-plane beam type bending of the ridge, and therefore likely to be better at multi-year ridge forces than at first-year ridge forces.

4.4 Ice Ridge Forces on Inclined Structures

For first-year ridges impacting inclined offshore structures, it is suggested to calculate the rubble force in the same way as for vertical structures. The solid zone (ice sheet) force, however, should be calculated according to Ralston's (1977, 1979) theories.

Multi-year ridges fail against conical structures in crushing, bending, shearing, or twisting. The preferred mode seems to be a vertical bending as the part of the ridge hitting the structure is being lifted.

Two typical bending failures have been frequently observed in model tests: initial crack formation and hinge crack formation, cf. Figure 4.4.1. Through an analogy with a floating ice beam (an elastic beam on an elastic foundation) the corresponding vertical forces on the conical structure from an infinitely long ridge become:

$$R_v = 4 \frac{\sigma_f I}{y_t l} \text{ for the initial crack, and} \qquad (4.4.1)$$

$$R_v = 6.17 \frac{\sigma_f I}{y_b l} \text{ for the hinge crack} \qquad (4.4.2)$$

where I is the moment of inertia of the ridge cross-section, y_t and y_b the distances from the top and bottom, respectively, to the neutral axis, and l the ridge characteristic length given by:

$$l = (4EI/\gamma_w B)^{0.25} \qquad (4.4.3)$$

where E is the elastic modulus of the ridge (ice blocks plus porosity). The horizontal force is simply determined as:

$$R_H = R_v \frac{\sin\alpha + \mu\cos\alpha}{\cos\alpha - \mu\sin\alpha} \qquad (4.4.4)$$

where α is the surface angle and μ the coefficient of friction.

For ridges of finite length, the reader is referred to Ralston (1977). For failure in the (probably rare) twisting mode, the reader is referred to Gershunov (1987).

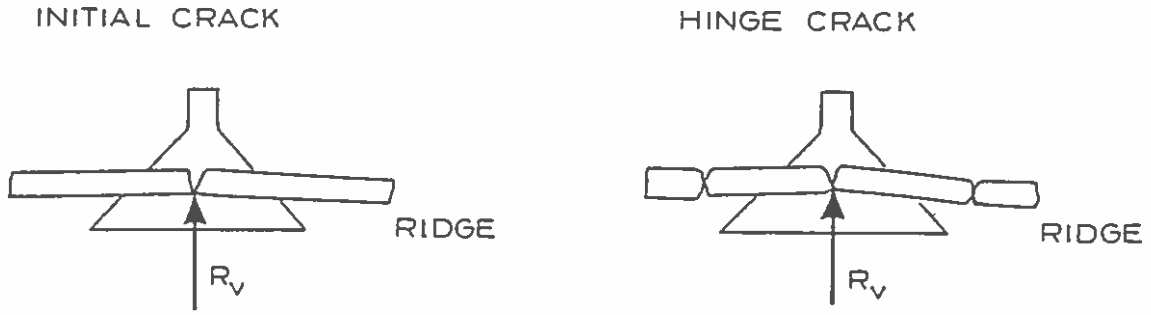

Figure 4.4.1 Initial and hinge crack formation in ridge impacting inclined structure.

4.5 Iceberg Impact Forces

Johnson and Nevel (1985) proposed a simple model for calculation of the force exerted by an impacting iceberg on an offshore structure. A vertical cylindrical structure was considered, and the iceberg was assumed to have a trapezoidal shape with a vertical front h_o = 5 m high and an angle of $\alpha = 56^o$ between the horizontal and the slant sides of the iceberg. These values are also suggested by Johnson and Nevel (1985). The impact force is calculated on the basis of a simple energy based model. The kinetic energy is dissipated by crushing of the ice, and the force can be calculated under the following conservative assumptions:

- the impact is head-on,
- the structure is rigid and immovable,
- the ice fails in crushing only,
- the ice strength is a constant,
- the structure stops the iceberg.

The structure has vertical sides and a circular cross-section with a diameter of D. For an indentation of length Δ, the width and height of the projected contact area becomes:

$$W(\Delta) = 2(\Delta(D-\Delta))^{\frac{1}{2}}, \quad \Delta \leq D/2 \qquad (4.5.1)$$

$$h(\Delta) = h_o + 2\Delta\tan\alpha \qquad (4.5.2)$$

The force is calculated as the crushing strength multiplied by the projected contact area:

$$F_c(\Delta) = 2\sigma_c(\Delta(D-\Delta))^{\frac{1}{2}}(h_o + 2\Delta\tan\alpha) \qquad (4.5.3)$$

The energy dissipated during the impact is expressed by:

$$E_c(\Delta) = \int_o^\Delta F_c(\Delta)d\Delta \qquad (4.5.4)$$

For $\Delta << D$ the expressions for F_c and E_c reduce to:

$$F_c(\Delta) \cong 2\sigma_c(\Delta D)^{\frac{1}{2}}(h_o+2\Delta\tan\alpha) \qquad (4.5.5)$$

$$E_c(\Delta) \cong 2\sigma_c D^{\frac{1}{2}} \int_o^\Delta (h_o+2\Delta\tan\alpha)\Delta^{\frac{1}{2}}d\Delta \qquad (4.5.6)$$

$$= \sigma_c D^{\frac{1}{2}}(1.33h_o\Delta^{1.5} + 1.60\tan(\alpha)\Delta^{2.5}) \qquad (4.5.7)$$

When the impacting kinetic energy is known, Δ can thus be found and the characteristic maximum force estimated.

A more refined calculation was presented by Nevel (1986), who considered rotation of the impacting iceberg. If a collision is eccentric, rotational energy may be left in the iceberg, and the largest force during the indentation will be reduced. Methods of determining probabilities associated with iceberg impact have been presented by Christensen (1989).

Note that icebergs consist of snow-ice, which is normally fine-grained, fresh and stronger than the saline sea ice.

5. DESIGN ICE FORCES

The choice of design forces from sheet ice must be based on the extreme strength and thickness together with interaction formulas, e.g. some of those described in chapter 4.

When ice floes are pushed against a structure, there are three basic limitations which may limit the load on the structure, viz.:

- limited ice strength (i.e. ice failure),
- limited driving force, and
- limited momemtum

each of which is addressed in this chapter. In order to calculate the ice loads, it is necessary to first determine the extreme (design) ice properties.

5.1 Design Ice Properties

Design criteria are normally based on the average recurrence time of a given situation, or if you will, the risk of exceeding a given situation in any one year. The first task of the (ice) design process is then to establish a relation between recurrence time and ice properties such as strength and thickness.

By looking at the formulas (2.2.3), (2.6.1), and (2.6.2) it becomes evident that both the strength and the thickness in some way increase when it becomes colder. The two parameters are not fully uncorrelated and cannot be combined if analysed separately unless the correlation is known. For this reason, the statistical analyses should be carried out of for the recurrence times of the products $\sigma_u h$ and $\sigma_f h^2$ instead. These products enter most formulas pertaining to crushing and/or bending failure of ice.

The recurrence time of the load due to ice crushing is determined by the recurrence time of the product $\sigma_u h$. In order to find this quantity the statistical distribution of $\sigma_u h$ must be known. If no combined values of σ_u and h exist for the area of interest, the statistical distribution of the product can be obtained as described below.

First the crushing strength is assumed to be given by the product of a reference strength and a function dependent on the salinity and temperature of the ice:

$$\sigma_u = \sigma_o(1-(\nu/0.275)^{1/2}) \qquad (5.1.1)$$

This formula is essentially eq. (2.6.2) with $\nu_o = 0.275$ as a first estimate except for the reference strength σ_o which is introduced as a stochastic variable (rather than a constant) in this derivation. By use of the equation together with available test data, the value of σ_o is calculated for each individual test and e.g. plotted in probability paper. A simple example is shown in Figure 5.1.1. It appears that σ_o tends to a Gaussian distribution having the probability density function:

$$f_1(\sigma_o) = \frac{1}{\sqrt{(2\pi)}\ \lambda} \cdot \exp\left(-\frac{1}{2}\left(\frac{\sigma_o-\mu}{\lambda}\right)^2\right) \qquad (5.1.2)$$

where λ is the standard deviation and μ the mean value. The following values were determined with the data in Figure 5.1.1:

$$\mu = 2.11 \text{ MPa} \qquad (5.1.3)$$

$$\lambda = 0.528 \text{ MPa} \qquad (5.1.4)$$

Hence, if combined values of temperature, salinity, and thickness of the ice are known the product $\sigma_u \cdot h$ can be determined.

In many cases such data sets do not exist, and instead some conservative assumptions are necessary. They could e.g. be:

- A constant ice salinity, S_{io}.

- The mean ice temperature is lowest at the end of the winter taking a value of half the mean air temperature of the coldest week in the winter.

- The ice thickness at the end of the winter is given by equation (2.2.3).

Based on these assumptions $\sigma_u h$ takes its maximum value at the end of the winter as both the strength and the thickness take their maximum values at that time. Evidently, the lowest air temperature in the winter is lower than the air temperature mentioned in the second assumption, but since it takes in the order of days for temperature waves to propagate to an appreciable depth, the crushing strength is determined by the mean temperature over a few days rather than the lowest temperature. The assumption that the coldest week is at the end of the winter is a conservative assumption.

The product of the maximum ice thickness and the temperature dependent part of equation (5.1.1) i.e.:

$$x = (1-(\nu/0.275)^{1/2}) \cdot 0.032\sqrt{(K-50)} \qquad (5.1.5)$$

is determined for as many winters as possible. These values can e.g. be plotted in a Weibull paper in order to obtain a distribution for x. An example is shown in Figure 5.1.2. The Weibull distribution is expressed as:

$$F_2(x) - P(X < x) = 1 - \exp\left(-\left(\frac{x}{\beta}\right)^n\right) \qquad (5.1.6)$$

The probability distribution for the product of thickness and crushing strength can now be expressed by:

$$P(Y < y) = \int_0^\infty F_2\left(\frac{y}{\sigma_o}\right) \cdot f_1(\sigma_o)\, d\sigma_o \qquad (5.1.7)$$

where

$$y = \sigma_o(1-(\nu/0.275)^{1/2}) \cdot 0.032 \,/(K-50) \qquad (5.1.8)$$
$$= \sigma_u h$$

This integral can be carried out, e.g. by means of a computer, and values of $\sigma_u h$ corresponding to various recurrence times can be determined.

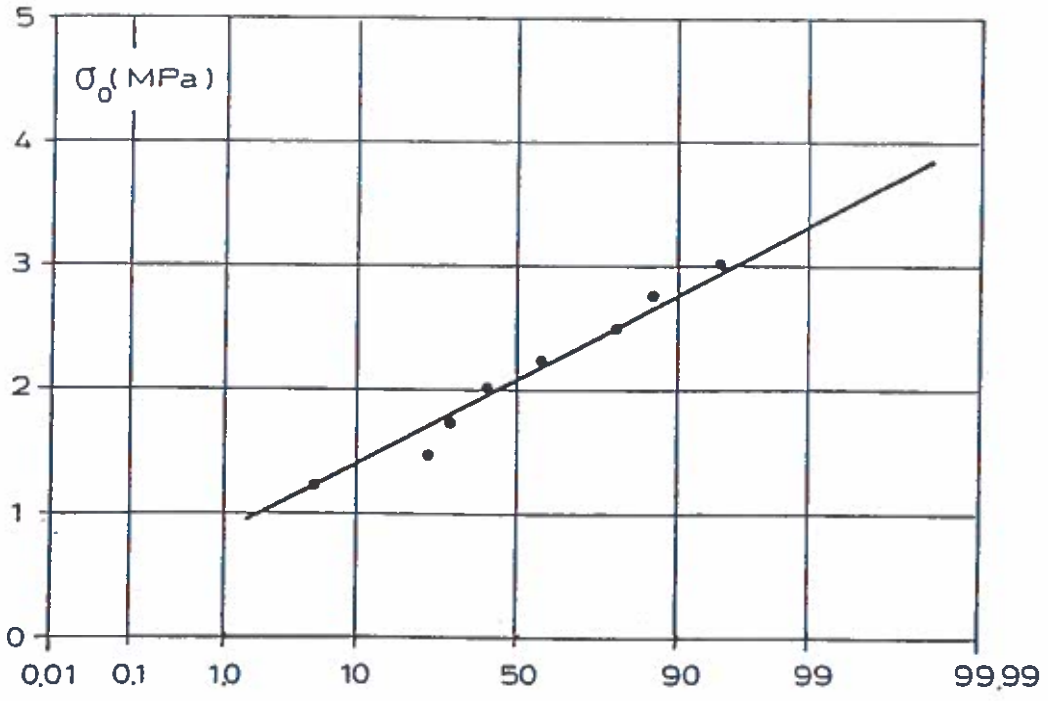

Figure 5.1.1 Gauss-plot of probability distribution of compressive reference strength of ice. (Example).

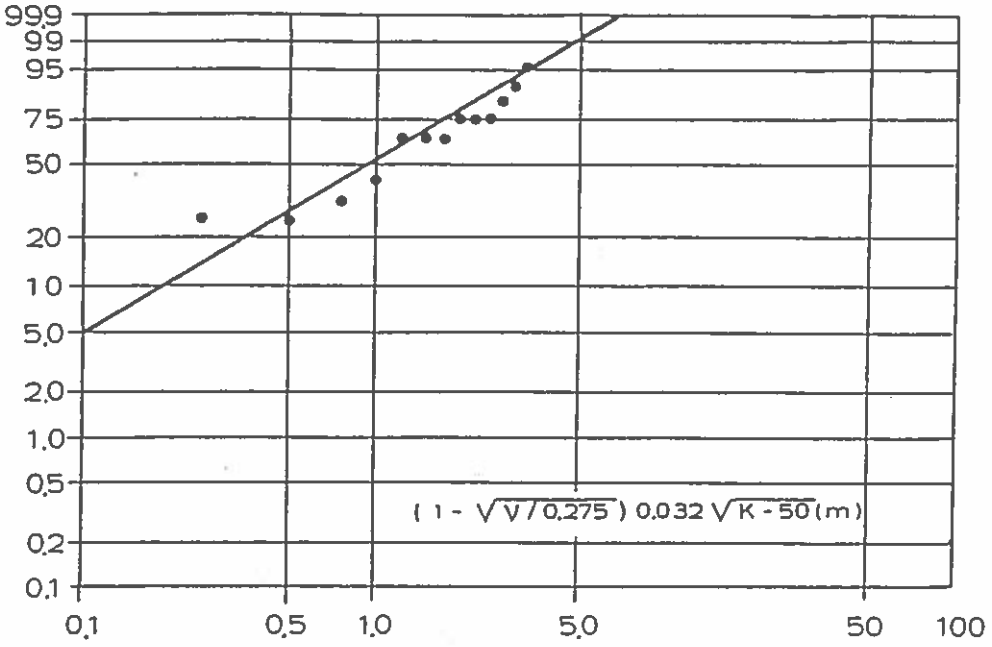

Figure 5.1.2 Weibull-plot of Non-exceedance probabilities for the temperature-dependent part of $\sigma_u h$. (Example).

The remaining problem is then to break the design value of the product $\sigma_u h$ down into a strength and a thickness. A simple way of doing this is to estimate the extreme thickness from the distribution of accumulated (over the entire winter) freezing degree -days, K. In most areas of the world it is possible to obtain an estimate of the distribution of K. A simple exponential distribution often suffice:

$$K = \bar{K} \, (\ln(A) + a) \qquad (5.1.9)$$

where $\bar{K}$ is the average value of K, A is the average recurrence time in years and a is a constant determined by fitting the expression to available data. (Since in theory h is proportional to the square-root of K, the use of a Weibull distribution for thicknesses is a natural result of using an exponential distribution, which is a Weibull distribution with the power one, for K). The value of K corresponding to the prescribed recurrence time is then used to determine the extreme thickness through equation (2.2.3). Finally, the strength is determined by dividing the product $\sigma_u h$ with the extreme thickness, h. A similar analysis can be used for the flexural strength.

It should be emphasized that the choice of distribution of the product will influence the resulting values significantly, especially for extreme recurrence times. For low return periods the density of data points is normally relatively high. These points do not reflect extreme winter conditions, however. For the long return periods, the density of data points normally is small. This is unfortunate, because these points reflect the extreme winters which produce severe ice conditions. In extrapolation to extreme values the large number of less severe data will bias the extrapolation. It appears that the bias will be in the conservative direction in mild seasonal ice climates and in the non-conservative direction in severe arctic climates.

Finally, it is pointed out that in an improved extreme value analysis, the variability within the ice sheet under given conditions and the variability of environmental conditions should preferably be separated.

5.2 Ice Loads Limited by Stress

Technically, ice loads limited by stress, i.e. failure of the ice, can be determined with design properties as described in section 5.1 and interaction formulas as described in chapter 4. The thing to remember, though, is that these notes have only covered ice forces from sheet ice, to some extent from ridges, and in a very simplifed form from iceberg impact. Furthermore, not all loading scenarios and failure types have been considered/described.

To mention but a few, the "blocking" scenario and the "rubble field" scenario have not been dealt with in these notes. Blocking occurs when a massive ice feature, e.g. a multi-year ice floe, comes to rest against a structure under conditions where failure of the multi-year floe does not occur. The limiting force may then correspond to failure of the advancing first-year ice sheet against the thicker and stronger multi-year floe. The massive multi-year floe has thereby increased the "effective diameter" of the structure. This increase can be substantial e.g. in the Beaufort Sea.

The "rubble field" scenario is a common situation around artificial islands in the Beaufort Sea, particularly in shallow waters. A field of ice rubble accumulates in front of an island, especially wide islands which make it difficult for the ice to clear around the sides. Often, though not always, the rubble pile will be grounded even in 15-20 metres of water. The rubble pile can form a vertical side against the advancing sheet ice, and in this way a wide sloping structure can become loaded by the same forces which apply to vertical structures. In most cases, however, the rubble field is believed to reduce the total force on the island, because the grounded rubble transmits some of the external force to the seabed. Attempts to quantify force transmission through rubble fields are in progress, see e.g. Sayed (1988).

5.3 Ice Loads Limited by Driving Forces

In some cases it is possible to prove that the driving forces are limited, e.g. by the floe size combined with extreme winds and currents. Physical features such as coasts or structures in some areas limit the maximum floe size. In other areas wave action might limit the floe size. Satellite data can be used to obtain floe size distributions, and maximum sizes of limited magnitude can sometimes be found. It is important, however, to consider the possibility of several floes pushing against a structure simultaneously, one behind the other.

In general, the load on the structure cannot exceed the driving forces on the ice except for cases where the ice possesses considerable momentum. If the calculated load exceeds the driving force, the limitation must be by momentum, or a mistake must be present.

When a limitation because of driving forces applies, it is very important to calculate whether the ice has sufficient momentum to cause a load larger than the driving force, or not.

5.4 Ice Loads Limited by Momentum

Ice floes with considerable kinetic energy can cause impact loads larger than the driving force on the ice itself. Icebergs are good examples of this.

The momentum limitation can be expressed by equating the kinetic energy of the ice floe, E_k, and the energy dissipated in ice crushing, E_c, and it reads:

$$E_k = \frac{1}{2} MV^2(1+C_m) = \int_0^x F(x)dx = E_c \qquad (5.4.1)$$

where $(1+C_m)$ accounts for the added mass of the ice feature, x is the indentation length (= ice movement after initial contact) and F is the interaction force which normally depends on the indentation length. From equation (5.4.1) plus the geometries of the ice feature and the structure, F(x) can be determined. If the kinetic energy is sufficient to cause development of an interaction width equal to the structure width, the force is no longer limited by the momentum, but by the failure stress.

5.5. Basic Design Rules for Ice Engineers

When you are faced with the challenge of selecting a design ice load, make sure that you always:

- calculate an upper bound design ice load, which you can thoroughly prove to be conservative. Use advanced methods and all your skills to provide the lowest possible upper bound force.

- calculate a central estimate (or even a lower bound) of the design ice force. Realistic estimates can e.g. be based on published measurements. Have a colleague review your calculation, and see if he/she also finds it realistic.

- compare the two calculated loads. If the difference is too large, search for an explanation. Your upper bound might be too conservative, or your central estimate might be unrealistic.

- repeat the process for all relevant failure types and/or limitations which are likely to occur. (This note has not given formulas for all failure types).

- have your design checked by someone with up-to-date experience in ice engineering. Being a developing field, new understandings are continuously gained, and you should naturally exploit the most recent results available from research.

These simple rules sound trivial, but they can hardly be emphasized enough.

6. CODES AND STANDARDS

Many countries and/or authorities have established design codes in the field of ice forces. Many of them are young codes, which are quickly outdated as new research yields new insight. Some of the ice codes and recommendations, which the author knows of, are listed below.

Country	Institution	Reference
USA	American Petroleum Institute	American Petroleum Institute (1982)
USA	American Association of State Highway and Transportation Officials	American Association of State Highway and Transportation Officials (1978)
Canada	Gulf, Esso and Dome Petroleum	Beaufort Sea-Mackenzie Delta Environmental Impact Statement, Vol. 3A (1982)
Canada	Canadian Standards Association Bridge Code Lighthouse practice	Canadian Standards Association (1978)
Canada	Canadian Standards Association Preliminary Standard S471, Part 1	Canadian Standards Association (1988)
USSR	State Committee of the Council of Ministers for Construction	SN-76-66 (1967)
Norway	Norwegian Petroleum Directorate	Norwegian Petroleum Directorate (1987)
Denmark	Danish Engineering Association Danish Standard, DS410	Danish Engineering Association (1982)
Sweden	Vägverket (Eng.: The Road Directorate) Istryck mot bropelare (Eng.: Ice pressure on bridge piers)	Löfquist (1987)

The various codes are briefly reviewed and compared in the following:

6.1 Codes for Vertical Structures

The Danish Code of Practice, DS410 (published by the Danish Engineering Association (1982)), is based on the same idea as the formula by Afanas'yev et al. The horizontal force is given in DS410 as:

$$F_c = k\sigma_u bh$$

$$k = 1+3/(1+b/h) \qquad 0 < b/h < 9$$

$$k = 1.75-0.05b/h \qquad 9 < b/h < 15$$

$$k = 1 \qquad 15 < b/h$$

where k is a dimensionless factor which is a function of the aspect ratio, b/h, as shown. It does not depend on the shape of the vertical pier.

In typical design situations the aspect ratio (projected structure width to ice thickness) will not fall below approximately 1, and it will probably not exceed say about 40.

This leads to coefficients from about 2.5 down to 1.0. In comparison the Swedish recommendation by Löfquist (1987), gives a coefficient of 0.8 for aspect ratios larger than four and a coefficient of 1.3 for an aspect ratio of one.

The presented formulas are reasonable for an impact parallel to the long axes of a rectangular structure, but for oblique impacts the use of a projected width will probably lead to an overestimation of the forces, as argued by Neill (1981), who states that the upstream end (nose) of e.g. bridge piers will tend to cut through the ice floe while it rotates to pass along the exposed side of the pier. Thus the failure mode (in Neill's view) is not a simultaneous crushing over the entire (projected) contact area. Correct determination of longitudinal and transverse forces resulting from an oblique impact of an ice floe requires special analyses.

Various other design codes exist, notably by the American Petroleum Institute (1982), the Canadian Standards Association (1978) and the Swedish Vägverket (Löfquist, 1987). The American Petroleum Institute recommends using $F = C\sigma_u bh$ where C is in the range from 0.3 to 0.7. For the Cook Inlet in Alaska which is characterized by a tidal flow that never leaves the ice at rest, a factor of 0.55 is recommended specifically. An application of the API code was presented by Utt et al. (1987)

The Canadian Standards Association (1978) recommends using $F = p_e bh$ where p_e is an effective ice pressure. Prior to 1974 this was given as 2.76 MPa, and after 1974 a range from 0.69 to 2.76 MPa has been suggested. The CSA has not given limits to the applicability of the formula. A new Canadian Standard is very close to being published.

The ice crushing strength is strongly dependent on salinity, temperature, and loading rate, as already mentioned. Korzhavin and Afanas'yev et al. have analysed their experiments but not suggested design values for strength. Various design codes suggest strengths in the range from as low as 0.7 MPa to as high as 3.5 MPa.

The coefficient of proportionality between F and $\sigma_u bh$ has often been split into a series of factors such as:

- an indentation coefficient taking into account the biaxial stress state in the ice in front of the structure,
- a shape factor taking into account the upstream shape of the structure,
- a contact coefficient taking into account non-simultaneous failure along the structure, and
- a correction coefficient taking into account the velocity of the ice in the interaction process.

Most design codes are in some way based on the two original formulas by Korzhavin and by Afanas'yev et al. For large ice floes with sizes exceeding say 15 times the structure width, Korzhavin's coefficient of proportionality equals 2.5 regardless of aspect ratio, b/h. Afanas'yev et al.'s coefficent, $C = 5(h/b+1)^{1/2}$ is approximately equal to Korzhavin's indentation coefficient when the aspect ratio equals unity. If the effect of the biaxial stress pattern on the force is assumed to be independent of the structure size itself, Korzhavin's formula must underestimate forces for small aspect ratios and overestimate forces for large aspect ratios. All in all, Afanas'yev et al.'s coefficient appears far more reasonable than Korzhavin's.

For aspect ratios less than approximately 11 the Danish Code of Practice, DS410, is slightly more conservative than the formula by Afanas'yev et al. For aspect ratios larger than 11 Afanas'yev et al.'s formula is the most conservative of the two, especially for aspect ratios above 15. It should be remembered, though, that Afanas'yev et al. gave $b/h < 6$ as an upper limit for applicability of their formula. The tests on which the formula is based did not cover aspect ratios higher than 6.

The most up-to-date recommendation for wide structures is contained in the Canadian "Beaufort Sea-Mackenzie Delta Environmetal Impact Statement" (1982), Vol. 3A. The EIS (which it is called for a shortname) was prepared by Dome Petroleum, Esso Resources Canada, and Gulf Canada. It expresses their experience with operations in the Canadian arctic with special emphasis on the impact on the environment. A part of it (Vol. 3A) deals with ice loads on structures. Figure 6.1.1 shows their recommendation for global ice pressure on offshore structures as a function of the aspect ratio, structure width to ice thickness. Note that the y-axis values are not dimensionless, and consequently cannot be used directly elsewhere.

This curve and the data that support it are likely to support the new Canadian Standard which is due to be published very soon, (Canadian Standards Association, 1988).

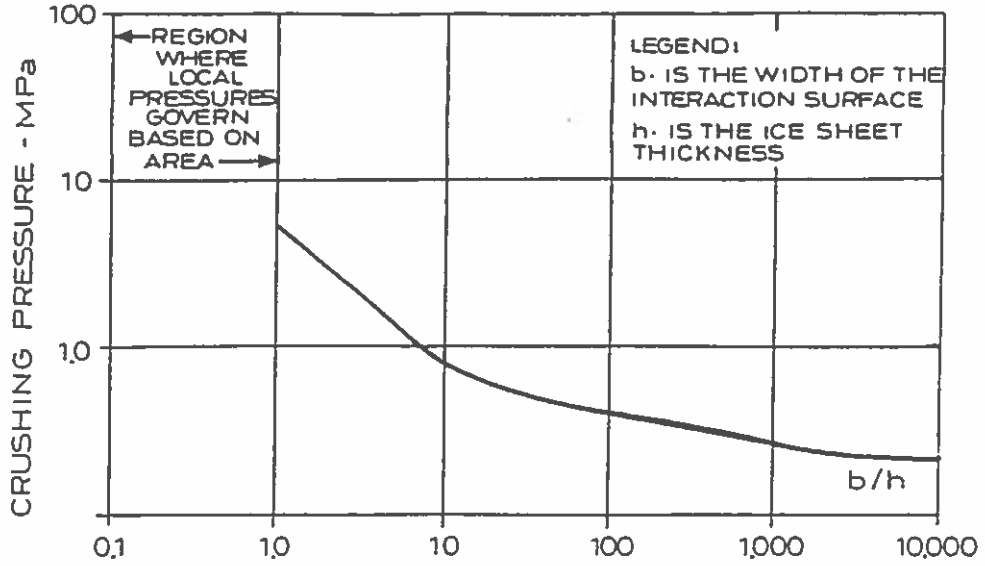

Figure 6.1.1 Pressure-aspect ratio diagram according to the Canadian Beaufort Sea-Mackenzie Delta Environmental Impact Statement (1982).

6.2 Codes for Inclined Structures

Four of the mentioned codes give formulas for ice forces on inclined structures. The Soviet code, SN-76-66 (1967) gives for the horizontal force on inclined bridge piers:

$$F = A\tan(\alpha)\sigma_f h^2 \qquad (6.2.1)$$

where α is the surface slope angle, and A is a regional climate coefficient varying between 0.75 and 2.25. The formula is independent of pier width and should only be applied where it was meant. It need not be correct under different climatic conditions.

The Canadian Standards Association in their 1974 code (CSA S6 1974) recommended reduction factors:

$$C_n = 1.00 \text{ for } 75^\circ < \alpha < 90^\circ \qquad (6.2.2)$$

$$C_n = 0.75 \text{ for } 60^\circ < \alpha < 75^\circ \qquad (6.2.3)$$

$$C_n = 0.5 \text{ for } 45^\circ < \alpha < 60^\circ \qquad (6.2.4)$$

to be multiplied with the force recommended for the corresponding vertical pier. The angle α is the angle between the upstream face and the horizontal.

The Canadian Lighthouse Practice recommends the formula:

$$F = m\sin^2\alpha\ \sigma_f bh \qquad (6.2.5)$$

where m is a combined shape and contact coefficient (dimensionless) varying between 0.4 and 0.9, see Iyer (1978).

Finally, the American Petroleum Institute (1982) recommends using Ralston's plastic limit analysis as described in section 4.2.

The wider the structure, the more important the ride-up part of the force is. The formulas considering ride-up forces are Ralstons, Edwards and Croasdale's and the 2D theories, cf. section 4.2. The other reviewed formulas were meant for bridge piers. For the very wide structures it will be necessary to consider the formation of an ice rubble field.

The formulas based on bending failure should show proportionality with h^2 and with the length of the circumferential crack. The 2D theories and Korzhavin's formula do not agree with this. They show proportionality with $h^{5/4}$ and h, respectively, making these formulas less sensitive to variations in ice thickness. The simple 2D theory and Korzhavin's formulas suggest proportionality with the structure width. This appears sensible for wide structures, but will lead to underestimation of forces on narrow structures. The adjusted 2D theory with its lack of a structure width dependence in the ice-breaking term, on the other hand, will overestimate the force on narrow structures and underestimate the force on wide structures.

The Soviet code and Edwards and Croasdale's formula lack dependence on both structure width and characteristic length of the ice. These two formulas should consequently be used only for narrow structures.

Afanas'yev et al.'s formula can be rewritten:

$$F = (0.41 + 0.46 \frac{b}{l}) \tan\alpha \, \sigma_f h^2 \qquad (6.2.6)$$

where b is the diameter of the conical structure at the water line and l the characteristic length. This illustrates the two proportionalities, one with h^2 and one with bh^2/l or $bh^{5/4}$. It is then seen that for narrow structures ($b/l \to 0$) the formula approaches the ice-breaking term of Edwards and Croasdale's formula. On the other hand an increasing width, b, results in an increased force, which makes sense.

Ralston's formula is also split in two terms, but it is far more sensitive to variations in structure width because the second term includes b^2.

Some numerical examples are given for two conical structures. Bear in mind that the formulas by Tryde and Korzhavin and the Codes, except the API recommendation, were intended for bridge piers with inclined upstream faces and vertical sides.

The following data are applied:

Narrow cone diameter at water level, b	3.0 metres
Wide cone diameter at water level, b	20.0 metres
Surface slope angle, α	45^o
Ice thickness, h	1.0 metre
Uniaxial crushing strength, σ_u	2.76 MPa
Flexural strength, σ_f	1.38 MPa
Shear strength, τ	0.69 MPa
Young's modulus, E	7.0 GPa
Poisson's ratio	0.33
Gravitational acceleration, g	9.81 m/sec^2
Friction coefficient, μ	0.1

The resulting horizontal forces are shown in the tables below:

Formula	Breaking (MN)	Ride-up (MN)	Total (MN)
Simple 2D theory	0.120	0.045	0.165
Adjusted 2D theory	1.565	0.045	1.610
Ralston	2.710	0.035	2.745
Edwards & Croasdale	2.210	0.175	2.385
Afanas'yev et al.	1.072	-	1.072
Tryde	0.900	-	0.900
Korzhavin	0.660	-	0.660
SN-76-66	0.845	-	0.845
CSA S6 1974	4.140	-	4.140
Can. Lighthouse	3.726	-	3.726

Table 6.2.1 Forces on a narrow conical structure with b = 3.0 metres.

Note how small the ride-up portion is on a narrow structure. This changes for a wide structure as seen from the other example. Of the formulas above the dashed line, Ralston's is consistently the most conservative.

Formula	Breaking (MN)	Ride-up (MN)	Total (MN)
Simple 2D theory	0.800	1.860	2.660
Adjusted 2D theory	1.565	1.860	3.425
Ralston	3.755	1.360	5.115
Edwards & Croasdale	2.210	1.175	3.385
Afanas'yev et al.	1.545	-	1.545
Tryde	7.650	-	7.650
Korzhavin	4.420	-	4.420
SN-76-66	0.845	-	0.845
CSA S6 1974	27.600	-	27.600
Can. Lighthouse	24.840	-	24.840

Table 6.2.2 Forces on a wide conical structure with b = 20.0 metres

In both examples, the Canadian codes (which were not developed for conical structures) overestimate the force.

In conclusion for inclined structures, it is suggested to use:

- simple 2D theory for wide structures when ice clearing can take place,
- formulas for vertical structures when the inclined structure is so wide that ice clearing is hindered,
- Ralston's formula for conical structures,
- the largest force of Tryde's, Korzhavin's and the one by SN-76-66 for narrow bridge piers with inclined upstream faces, and
- formulas for vertical structures when the surface slope angle exceeds 70^{o}

unless model experiments are carried out.

7. A SHORT GUIDE TO RELEVANT LITERATURE

7.1 Books

Books on ice engineering are scarce, but several good manuscripts have been published very recently. I will mention five major references:

A.B. Cammaert and D.B. Muggeridge (1988)
"Ice Interaction with Offshore Structures"
Van Nostrand Reinhold, 11 New Fetter Lane, London EC4 P4EE, England

This book is written specifically with offshore structures in mind, which gives it a well-limited scope and a clear and logical presentation. It goes relatively deep into ice properties, which is necessary for the understanding of the limitations of theories and practices. The ice-structure interaction chapters are well written, and the authors avoid too much detail where unnecessary. A more comprehensive chapter on selection of design forces would have improved it greatly, but that is strictly speaking more statistics than ice engineering.

The topic of dynamic ice loads will receive more attention in the future. This book is one of the first to address these problems. Finally, some brief chapters on physical modelling, laboratories, and on "special topics" such as uncertainty, icing, monitoring, forecasting, and ice control are included. Unfortunately, the book is brief on what concerns remote sensing, computational modelling, and forecasting.

Overall, in my personal view, this book is the best one published so far on ice-structure interaction. I bought it in 1988 for 733 Danish Kroner, which equaled about 100 US dollars.

The second book I wish to mention is by:

T.J.O. Sanderson (1988)
"Ice Mechanics, Risks to Offshore Structures"
Graham and Troman Limited, Sterling House,
66 Wilton Road, London SW1V 1DE, England

In terms of quality this book levels with that of Cammaert and Muggeridge; in fact I have not seen anything published (on ice) to parallel these two books yet.

Sanderson's chapters on ice types, ice occurrence, and morphology are particularly well written and very informative for newcomers in the field. The book concentrates on vertical-sided structures for the arctic environment, especially the wide structures in the shallow areas of the Beaufort Sea. An excellent chapter on selection of design loads completes the book.

This book is a very good reference together with the first one described. They do overlap in considerable areas, but each have their strong points. The first is written by engineers, which you can sense from the logical presentation. The second one, Sanderson's, is written by a talented designer, who had to deal with real ice (which does not always look like you draw it on paper), and who had to make some very real design decisions. The combination of these two books offers a very comprehensive understanding of ice-structure interaction.

I bought Sanderson's book in 1988 for 70 Pound Sterling.

The third book I wish to mention is by:

G.D. Ashton, editor (1986)
"River and Lake Ice Engineering"
Water Resources Publications, P.O. Box 2841, Littleton,
Colorado 80161, USA

As the title says, this is not an offshore-related book. All the physics and mechanics of ice, however, are still relevant. The book has been put together from contributions by a long list of researchers in the field of ice engineering. It includes chapters on river ice problems and ice control in waterways. It has a brief chapter on remote sensing (which is these years becomes outdated rather quickly) and a chapter on icebreaking ships. It gives a somewhat broader view of ice engineering than the first two books I have mentioned, and it does not address offshore structures as such.

I bought it in 1986 for 50 US dollar.

The fourth book I wish to mention is by:

B. Michel (1978)
"Ice Mechanics"
Les Presses de l'Université Laval, Quebec, Canada

This book seems to be available in many university libraries because it was the only textbook on ice for many years. I mention it here in order to point out that it is 11 years old, and consequently lacks many of the newer developments. It is a good book on the mechanics of ice, but unfortunately it contains quite a few printer's errors, so be careful with its equations. And if you are determining design ice loads, I would recommend acquiring a more up-to-date reference.

The fifth book I wish to mention is by:

E. Eranti and G.C. Lee (1986)
"Cold Region Structural Engineering"
McGraw-Hill

If you are dealing with a project that involves onshore operations in cold regions you will find this book of assistance.

It also includes chapters on ice-structure interaction although less comprehensive than those described above. The book is written from a contractor's point of view. If you are interested in earth works, machinery, utility lines, etc. in cold regions this book is worth looking at.

I bought it in 1986 for approximately 80 US Dollar.

Finally, I must mention the paperbacks published occasionally by the Technical Council on Cold Regions Engineering under the ASCE. They are usually advertised in "Civil Engineering" Magazine (US version). They are cheap and definitely worth the money.

7.2 Journals

Problems related to ice loads on offshore structures may appear in "ice" journals as well as in offshore journals. The "ice" journals which should be reviewed by anyone interested in this field are:

- Journal of Cold Regions Engineering, ASCE
- Cold Regions Science and Technology, Elsevier
- Journal of Offshore Mechanics and Arctic Engineering, ASME
- Journal of Hydraulic Research, IAHR
- Journal of Glaciology, Int. Glaciological Society

Also of interest with occasional ice-related articles are:

- Journal of Waterway, Port, Coastal and Ocean Eng., ASCE
- Canadian Geotechnical Journal (especially for ice mechanics)
- Journal of Energy Resources Technology, ASME

and finally I should mention:

- Iceberg Research, Scott Polar Research Institute, England.

7.3 Conference Proceedings

The following conferences result in proceedings with good quality material on ice-structure interaction:

- Offshore Mechanics and Arctic Engineering, OMAE
- Port and Ocean Engineering under Arctic Conditions, POAC
- Int. Assoc. of Hydr. Res. Symposia on Ice, IAHR
- Offshore Technology Conference, OTC
- Polartech

and there are always regional conferences of interest, such as Canadian Coastal Conference, ASCE Specialty Conferences, etc.

REFERENCES

Afanas'yev, V.P., I.V. Dologopolov and Z.I. Shvayshten (1971): "Ice Pressure on separate supporting Structures in the Sea". U.S. Army Cold Regions Research and Engineering Laboratory, Draft Translation 346.

American Association of State Highway and Transportation Officials (1978): "Interim Specifications for Highway Bridges", AASHTO, Washington DC, USA.

American Petroleum Institute (1982): "Planning, Designing and Constructing Fixed Offshore Structures in Ice Environments", Bulletin 2N, American Petroleum Institute, Washington D.C.

Ashton, G.D. (1985): "Deterioration of floating ice covers", Journal of Energy Resources Technology, 107 (June): 177-182.

Ashton, G.D., (1986): "River and Lake Ice Engineering", Water Resources Publications, Colorado, USA.

Beaufort Sea - Mackenzie Delta Environmental Impact Statement (1982), Vol. 3A, Prepared by Dome Petroleum Ltd., Esso Resources Canada Ltd. and Gulf Canada Inc. Available from: Pallister Resource Management, Bay 105, 4116-64th Ave. SE., Calgary, Alberta, Canada T2C 2B3.

Bercha, F.G. and J.V. Danys (1975): "Prediction of ice forces on conical offshore structures", Marine Science Communications, 1(5): 365-380.

Bergdahl, L. (1977): "Physics of ice and snow as affects thermal pressure", Report Series A:1, Department of Hydraulics, Chalmers University of Technology, Gothenburg, Sweden.

Bergdahl, Lars (1978): "Thermal Ice Pressure in Lake Ice Covers". Report Series A:2, Department of Hydraulics, Chalmers University of Technology, Gothenburg, Sweden.

Bergdahl, Lars and Lars Wernersson (1978): "Calculated and Expected Thermal Ice Pressures in five Swedish Lakes". Report Series B:7, Department of Hydraulics, Chalmers University of Technology, Gothenburg, Sweden.

Blenkarn, K.A. (1970): "Measurements and analysis of ice forces on Cook Inlet Structures", Proc. Offshore Technology Conference, Paper OTC 1261, Vol.2, pp. 365-378, Houston, Texas, USA.

Cammaert A.B. and D.B. Muggeridge (1988): "Ice Interaction with Offshore Structures", Van Nostrand Reinhold, London, England.

Canadian Standards Association (1978): "Design of Highway Bridges", Standard CAN3-56-M78.

Canadian Standards Association (1988): "General requirements, design criteria, environment, and loads", Preliminary Standard S471, Part 1, CSA code for the design, construction and installation of fixed offshore structures. Draft. Rexdale, Ontario, Canada.

Christensen, F.T. (1988): "Calculation of optimal dimensionless coefficients for Ralston's plastic limit analysis approach to determination of sheet ice loads on conical structures". Progress Report 66, pp. 35-38 Institute of Hydrodynamics and Hydraulic Engineering (ISVA), Technical University of Denmark, February 1988.

Christensen, F.T. (1989): "Efficiency of Detachable Platforms in the Arctic", ASCE Journal of Cold Regions Engineering, Vol. 3, No. 1, pp. 37-54, March 1989.

Christensen, F.T., N.-E. Ottesen Hansen, K.-U. Evers, S. Spangenberg and L.J. Vincentsen (1989a): "Design of the Great Belt Western Bridge for Ice Forces", 8th int. conf. on Offshore Mechanics and Arctic Engineering (OMAE-89), Vol. 4, pp. 365-376, the Hague, the Netherlands.

Christensen, F.T., N.-E. Ottesen Hansen, S. Spangenberg and L.J. Vincentsen (1989b): "Dynamic ice loads on the Great Belt Western Bridge", 10th int. conf. on Port and Ocean engineering under Arctic Conditions (POAC-89), Luleaa, Sweden, submitted.

Cox, G.F.N. and W.F. Weeks (1983): "Equations for determining the gas and brine volume in sea ice samples", Journal of Glaciology, 29(102): 306-316.

Croasdale, K.R. (1978): "Ice forces on rigid structures". Report of the Working Group on ice interaction with hydraulic structures, International Association of Hydraulic Research.

Croasdale, K.R. (1980): "Some implications of ice ridges and rubble fields on the design of Arctic Offshore Structures", Proc. Nat. Res. Council of Canada Workshop on Sea Ice Ridging, Calgary, Technical Memo 134, pp. 157-180, NRC of Canada, Ottawa, Canada.

Croasdale, K.R. (1988): "Ice Forces : Current Practices", Proc. 7th int. conf. on Offshore Mechanics and Arctic Enginering (OMAE-88), Vol. 4, pp. 133-151, Houston, Texas, USA.

Croasdale, K.R., N.R. Morgenstern and J.B. Nuttall (1977): "Indentation tests to investigate ice pressures on vertical piers", Journal of Glaciology, 19(81): 301-312.

Danish Engineering Association (1982): "Code of Practice for the Safety of Structures, DS 409 and DS 410.

Edwards, R.Y. and K.R. Croasdale (1976): "Model experiments to determine ice forces on conical structures", Preprint, Applied Glaciology Symposium, Cambridge, England.

Eranti, E. and G.C. Lee (1986): "Cold Region Structural Engineering", McGraw-Hill.

Frankenstein, G.E. and R. Garner (1967): "Linear Relationship of Brine Volume and Temperature from -0.5°C to -22°C for Sea Ice". Journal of Glaciology, 6(48): 943-944.

Gershunov, E.M. (1987): "Structure-ridge interaction", Cold Regions Science and Technology, 14(1): 85-94.

Gold, L.W. (1958): "Some observations on the dependence of strain on stress for ice", Canadian Journal of Physics, 36(10): 1265-1275.

Iyer, S.H. (1978): "Existing Ice Codes and suggested Criteria". Proc. 5'th Int. Assoc. of Hydr. Res. (IAHR) Ice Symposium, Luleaa, Sweden.

Johnson, R.C. and D.E. Nevel (1985): "Ice impact structural design loads", Proc. 8'th int. conf. on Port and Ocean engineering under Arctic Conditions (POAC-85), Vol. 2, pp. 569-578, Narssarssuaq, Greenland.

Korzhavin, K.M. (1962): "Action of Ice on Engineering Structures". U.S. Army Cold Regions Research and Engineering Laboratory, Draft Translation 260, 1971.

Lainey, L. and R. Tinawi (1984): "The mechanical Properties of Sea Ice - A Compilation of available Data", Canadian Journal of Civil Engineering, Vol. 11, No. 4, pp. 884-923.

Lee, J., T.D. Ralston and D.H. Petrie (1986): "Full-thickness sea ice strength tests". Proc. 8'th Int. Assoc. of Hydr. Res. (IAHR) Ice Symposium, Vol. 1, pp. 293-306, Iowa City, Iowa, USA.

Löfquist, Bertil (1987): "Istryck mot Bropelare" (in Swedish). Dokument 1987:43, Vägverket, Centralförrådet, Knivsta, Sweden.

Michel, B. and R.O. Ramseier (1971): "Classification of River and Lake Ice", Canadian Geotechnical Journal, 8(36): 36-45.

Michel, B. (1978): "Ice Mechanics", Les Presses de l'Université Laval, Quebec, Canada.

Nadreau, J.P. and B. Michel (1984): "Ice Properties in relation to Ice Forces". Proc. 7'th Int. Assoc. of Hydr. Res. (IAHR) Ice Symposium, Vol. 4, pp. 63-115, Hamburg, West Germany.

Neill, C.R. (editor) (1981): "Ice Effects on Bridges". Published by Roads and Transportation Association of Canada, 1765 St. Laurent Blvd., Ottawa, Canada K1G 3V4.

Nevel, D.E. (1986): "Iceberg impact forces". Proc. 8'th Int. Assoc. Hydr. Res. (IAHR) Ice Symposium, Vol. 3, pp. 345-369, Iowa City, Iowa, USA.

Norwegian Petroleum Directorate (1987): "Guidelines for the determination of loads and load effects", Stavanger, Norway. This is an appendix to the "Regulation for the structural design of load bearing structures intended for exploitation of petroleum resources" published in 1984 by the Norwegian Petroleum Directorate.

Petrie, D.H. and J.P. Poplin (1986): "Comparison of small-scale and large-scale sea ice strengths", Proc. 8'th Int. Assoc. Hydr. Res. (IAHR) Ice Symposium, Vol. 1, pp. 265-276, Iowa City, Iowa, USA.

Peyton, H.R. (1968): "Ice and Marine Structures", Part 1 in Ocean Industry, March 1968, pp. 40-44, Part 2 in Ocean Industry, September 1968, pp. 59-65, Part 3 in Ocean Industry, December 1968, pp. 51-63.

Ponter, A.R.S. et al. (1983): "The force exerted by a moving ice sheet on an offshore structure, Part 1, The creep mode", Cold Regions Science and Technology, 8(2): 109-118.

Prodanovic, A. (1981): "Upper bounds of ridge pressure on structures", Proc. 6th int. conf. on Port and Ocean Engineering under Arctic Conditions (POAC-81), Vol. 3, pp. 1288-1298, Quebec City, Quebec, Canada.

Ralston, T.D. (1977): "Ice force design considerations for conical offshore structures", Proc. 4'th int. conf. on Port and Ocean Engineering under Arctic Conditions (POAC-77), Vol. 2, pp. 741 -752, St. John's Newfoundland, Canada.

Ralston, T.D. (1978): "Analysis of ice sheet indentation", Proc. 5th Int. Assoc. of Hydr. Res. (IAHR) Ice Symposium, Vol. 1, pp. 13-31, Luleaa, Sweden.

Ralston, T.D. (1979): "Plastic limit analysis of sheet ice loads on conical structures". Proc. of IUTAM Symposium on Physics and Mechanics of Ice, pp. 289-308, Copenhagen, Denmark. (Edited by P. Tryde).

Rojansky, M. and B.C. Gerwick (1981): "Failure modes and forces of pressure ridges acting on cylindrical towers", Proc. 6th int. conf. on Port and Ocean engineering under Arctic Conditions (POAC-81), Vol. 2, pp. 663-673, Quebec City, Quebec, Canada.

Saeki, H., K. Hamanaka and A. Ozaki (1977): "Experimental study of the ice forces on a pile, Proc. 4th int. conf. on Port and Ocean engineering under Arctic Conditions (POAC -77), Vol. 2, pp. 695-706, St. John's, Newfoundland, Canada.

Sanderson, T.J.O. (1984a): "Theoretical and measured Ice Forces on wide Structures". Proc. 7'th Int. Assoc. of Hydr. Res. (IAHR) Ice Symposium, Vol. 4, pp. 151-207, Hamburg, W. Germany.

Sanderson, T.J.O. (1984b): "Thermal Ice Forces against isolated Structures". Proc. 7'th Int. Assoc. of Hydr. Res. (IAHR) Ice Symposium, Vol. 4, pp. 289-299, Hamburg, W. Germany.

Sanderson, T.J.O. (1986): "A pressure-area curve for ice". Proc. 8'th Int. Assoc. Hydr. Res. (IAHR) Ice Symposium, Vol. 2, pp. 361-384, Iowa City, Iowa, USA.

Sanderson, T.J.O. (1988): "Ice Mechanics, Risks to Offshore Structures", Graham and Trotman Limited, London, England.

Sanderson, T.J.O. and A.J. Child (1986): "Ice loads on offshore structures. The transition from creep to fracture". Cold Regions Science and Technology, 12(2):157-162.

Sayed, M. (1988): "Transmission of loads through grounded ice rubble", Proc. 9th Int. Assoc. of Hydr. Res. (IAHR) Ice Symposium, pp. 692-707, Sapporo, Japan.

Schwarz, J., K. Hirayama and H.C. Wu (1974): "Effect of ice thickness on ice forces", Proc. 6th Offshore Technology Conference, Paper OTC 2048, Volume 2, pp. 145-155, Houston, Texas, USA.

Schwerdtfeger, P. (1963): "The thermal properties of sea ice", Journal of Glaciology, Vol. 4, No. 36, pp. 789-807.

SN-76-66 (1967): "Instructions for determining ice loads on river structures", State Committee of the Council of Ministers of Construction, Published in Russian by Izdatel'stvo Literatury Po Stroitel'stvu in Moscow 1967, Translated into English by the National Research Council of Canada as their technical translation TT-1663 in 1973.

Sodhi, D.S. and K. Kato (1983): "Ice action on pairs of cylindrical and conical structures", Report 83-25, Cold Regions Research and Engineering Laboratory, New Hampshire, USA.

Timco, G.W. (1986): "Ice forces on multi-legged structures", Proc. 8'th Int. Assoc. Hydr. Res. (IAHR) Ice Symposium, Vol. 2, pp. 321-337, Iowa City, Iowa, USA.

Timco, G.W. and R.M.W. Frederking (1986): "Confined compression tests: Outlining the Failure Envelope of Columnar Sea Ice", Cold Regions Science and Technology, 12(1): 13-28.

Timco, G.W. and I.J. Jordaan (1987): "Time-series variations in ice crushing", Proc. 9'th int. conf. on Port and Ocean Engineering under Arctic Conditions (POAC-87), Fairbanks, Alaska, USA. Preprint.

Tryde, P. (1975): "Intermittent ice forces acting on inclined wedges", Proc. 4th Int. Assoc. of Hydr. Res. (IAHR) Ice Symposium, pp. 339-343, Hanover, New Hampshire, USA.

Trætteberg, A., L.W. Gold and R. Frederking (1975): "The Strain Rate and Temperature Dependence of Young's Modulus of Ice", Proc. 4'th Int. Assoc. Hydr. Res. (IAHR). Ice Symposium, pp. 479-486, Hanover, New Hampshire, USA.

Utt, M.E., K.D. Vaudrey and B.E. Turner (1987): "Design Sea Ice Load Examples using API Recommended Practice 2N" Proc. 9th int. conf. on Port and Ocean engineering under Arctic Conditions (POAC-87), Vol. 1, pp. 387-393, Fairbanks, Alaska, USA.

Vivatrat, V. and S. Slomski (1984): "Probabilistic selection of ice loads and pressures". ASCE, J. Waterway, Port Coastal and Ocean engineering, 110(4): 375-391.

Walden, J.T., J.T. Baldwin, S.D. Hallam and G.A.N. Thomas (1987a): "Prediction of Multi-year Ice Impact Loads utilizing Hans Island data", Proc. 9th int. conf. on Port and Ocean engineering under Arctic Conditions (POAC-87), Preprint, Fairbanks, Alaska, USA.

Walden, J.T., S.D. Hallam and J.T. Baldwin (1987b): "An explicit technique for calculating first-year ice loads on structures", Proc. 6th int. conf. on Offshore Mechanics and Arctic Engineering (OMAE-87), Vol. 4, pp. 267-272, Houston, Texas, USA.

Weeks, W.F. and A. Assur (1967): "The mechanical Properties of Sea Ice". Cold Regions Science and Engineering, Part II, Section C. (Old CRREL Monograph Series).

REFERENCES

McFarlane, D.S., J.A. Cherry, R.W. Gilham and E.A. Sudicky (1986). Migration of contaminants in groundwater at a landfill: A case study. 1. Groundwater flow and plume delineation. Journal of Hydrology, 63, 1-29.

Prog. Rep. 66, pp [illegible], February 1988
Inst. Hydrodyn. & Hydraulic Eng.
Tech. Univ. Denmark

4. CALCULATION OF OPTIMAL DIMENSIONLESS COEFFICIENTS FOR RALSTON'S PLASTIC LIMIT ANALYSIS APPROACH TO DETERMINATION OF SHEET ICE LOADS ON CONICAL STRUCTURES.

by

Flemming Thunbo Christensen

INTRODUCTION

The commonly used formulas derived by Ralston (1977,1979) for determining sheet ice loads on conical offshore structures involve six dimensionless coefficients. Usually, these are given in graphs. The present report very briefly outlines how these coefficients can be determined in a semi-analytical way.

CALCULATION OF COEFFICIENTS

The formulas by Ralston (1977,1979) are:

$$R_H = [A_1 \sigma_f h^2 + A_2 \gamma_w h D^2 + A_3 \gamma_w h (D^2 - D_t^2)] A_4 \quad (1)$$

$$R_V = B_1 R_H + B_2 \gamma_w h (D^2 - D_t^2) \quad (2)$$

R_H = horizontal force on cone
R_V = vertical force on cone
σ_f = flexural strength of ice
h = ice sheet thickness
γ_w = specific weight of water
D = diameter of cone at the waterline
D_t = diameter of cone at the top
A_1, A_2, A_3, A_4, B_1, B_2 = dimensionless coefficients which may be calculated in the way explained in the following.

The coefficients A_1 and A_2 are functions of the parameter ρ,

defined as:

$$\rho = A/R \quad ; \quad R < A \tag{3}$$

A = radius of deforming region
R = radius of cone at the waterline (=D/2)

and of the parameters γ_w, D, σ and h mentioned above. The solution is optimized by varying A. The parameter, ρ, that optimizes the solution may be found as the solution to the following equation

$$\rho-\ln(\rho)+0.0830(2\rho+1)(\rho-1)^2(\gamma_w D^2/\sigma_f h) = 1.369 \tag{4}$$

The solution is generally found in the range ρ = 2.1 to ρ = 1.0 for values of $(\gamma_w D^2/\sigma_f h)$ in the range from 0 to 100.

When the optimal ρ has been found, the coefficients in question may be determined as

$$A_1 = \frac{1+2.711\rho\ln(\rho)}{3(\rho-1)} \tag{5}$$

$$A_2 = 0.075(\rho^2+\rho-2) \tag{6}$$

The coefficients A_3, A_4, B_1 and B_2 are functions of the cone inclination angle, α, and the coefficient of friction, μ, between the ice and the cone surface.

Typical ranges for these parameters are 30° to 60° for α and 0.1 to 0.3 for μ. As an intermediate step it is necessary to calculate the complete elliptic integrals of the first (F) and of the second (E) kind for the argument sin(α).

$$F(\sin(\alpha)) = \int_0^{\pi/2} (1-\sin^2(\alpha)\sin^2(\theta))^{-1/2} d\theta \tag{7}$$

$$E(\sin(\alpha)) = \int_0^{\pi/2} (1-\sin^2(\alpha)\sin^2(\theta))^{+1/2} d\theta \tag{8}$$

Power series expansions for these integrals have been given by Spiegel (1968, p. 179) and by Abramowitz and Stegun (1972, p. 590). With these functions calculated, three "help" functions can be calculated

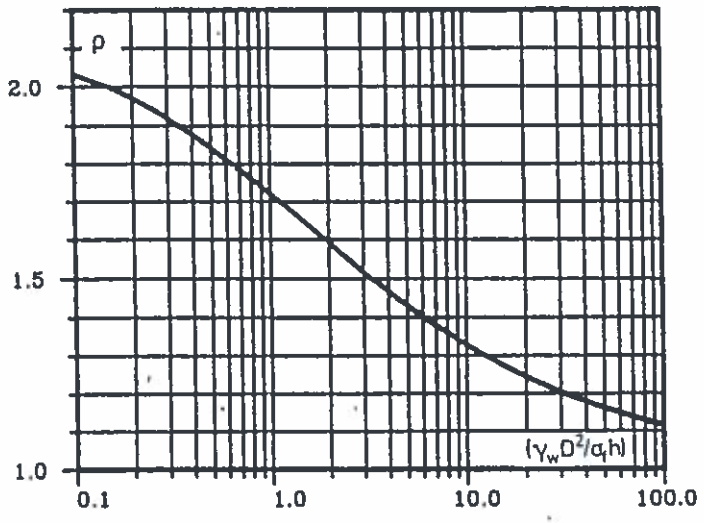

Fig. 1 The optimal ρ as a function of $(\gamma_w D^2/\sigma_f h)$, i.e. the solution to equation (4).

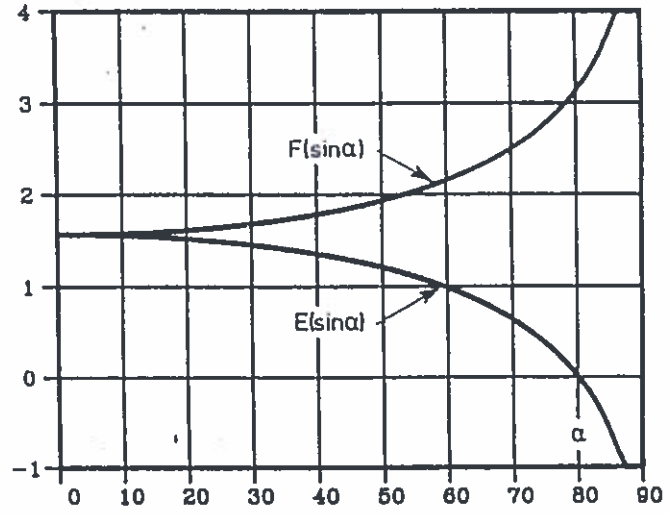

Fig. 2 Complete elliptic integrals of the first and second kind. Note that the x-axis shows α-values in degrees while the argument is sinα.

$$f(\alpha,\mu) = \sin(\alpha)+\mu\cos(\alpha)F(\sin(\alpha)) \quad (9)$$

$$g(\alpha,\mu) = \frac{1+(2\alpha/\sin(2\alpha))}{(\pi/2)\sin(\alpha)+2\alpha\mu\cot(\alpha)} \quad (10)$$

$$h(\alpha,\mu) = \cos(\alpha) -\mu[E(\sin(\alpha))-\cos^2(\alpha)F(\sin(\alpha))]/\sin(\alpha) \quad (11)$$

The purpose of the formulas (7) through (11) is merely to avoid too large expressions in the following.

The coefficients A_3, A_4, B_1 and B_2 may now be calculated from

$$A_3 = 0.225[1+\mu E(\sin(\alpha))\cot(\alpha)]/\cos(\alpha) - 0.225\mu\cot(\alpha)f(\alpha,\mu)g(\alpha,\mu) \quad (12)$$

$$A_4 = \tan(\alpha)/[1-\mu g(\alpha,\mu)] \quad (13)$$

$$B_1 = h(\alpha,\mu)/[(\pi/4)\sin(\alpha)+\mu\alpha\cot(\alpha)] \quad (14)$$

$$B_2 = 0.225[(\pi/2)\cos(\alpha)-\mu\alpha -f(\alpha,\mu)h(\alpha,\mu)/[(\pi/4)\sin(\alpha)+\mu\alpha\cot(\alpha)]] \quad (15)$$

In this analysis the specific weight in upward breaking has been taken to be $0.9\gamma_w$. On a downward breaking cone the vertical "foundation reaction" is equal to approximately $0.1\gamma_w$, namely the buoyancy. Consequently, the value $\gamma_w/9$ must be used instead of γ_w when applying this theory to downward breaking cones.

REFERENCES

Abramowitz, M. and I.A. Stegun (1972) Handbook of Mathematical Functions, Dover Publications, New York.

Ralston, T.D. (1977) Ice force design considerations for conical offshore structures, Proc. 4'th Int. Conf. on Port and Ocean Engineering under Arctic Conditions (POAC-77), Vol. 2, pp. 741-752.

Ralston, T.D. (1979) Plastic limit analysis of sheet ice loads on conical structures, Proc. IUTAM Symposium Physics and Mechanics of Ice, Copenhagen, Denmark, (Editor: P. Tryde), pp. 289-308.

Spiegel, M.R. (1968) Mathematical Handbook of Formulas and Tables, Schaum's Outline Series, McGraw-Hill, New York.

Prog. Rep. 66, pp. [illegible]5, February 1988
Inst. Hydrodyn. and [illegible]draulic Eng.
Tech. Univ. Denmark

5. THE EXCHANGE OF MOMENTUM IN THE SURF ZONE DUE TO ORGANIZED WATER MOTION

by

Rolf Deigaard[1] and Jørgen Fredsøe

INTRODUCTION

The prediction of longshore current velocity distributions often relies on a momentum exchange coefficient E to describe the shore normal momentum exchange due to the shear in the velocity. The velocity distribution is described by the momentum equation expressing the balance between the driving force, the flow resistance and the redistribution of momentum (Longuet-Higgins (1970)).

$$-\frac{\partial}{\partial x}(S_{xy}) = \tau_b - \frac{\partial}{\partial x}(\rho E D \frac{\partial V}{\partial x}) \quad (1)$$

x is the shore-normal coordinate, S_{xy} is the shear component of the radiation stress, τ_b is the bed shear stress, ρ the density of water, E the momentum exchange coefficient, D the mean water depth and V is the depth averaged longshore velocity.

Considerable uncertainty has been associated with estimates of E. The earliest approaches have been to relate E to the quantities in the organized wave motion such as the horizontal orbital excursion or the orbital velocity amplitude. Although such an approach can lead to well calibrated expressions, it is not able to account for the large differences in the momentum exchange inside and outside the surf zone. A more satisfactory principle is to relate the momentum exchange coefficient to the turbulent eddy viscosity due to the intense production of turbulence from the wave breaking (Battjes (1975)).

This note treats an additional contribution to the momentum exchange due to the organized circulation in the surf zone caused by the water carried shore-ward with the surface rollers

[1]) Present address: Danish Hydraulic Institute

Draft contribution

Last updated 1994.04.25

Ice-induced vibrations of the Sprogø NE Lighthouse

R. Zorn, M.B. Bryndum and F.T. Christensen
Danish Hydraulic Institute
Agern Alle 5
DK - 2970 Hørsholm, Denmark

Abstract

Ice-induced vibrations of the Sprogø NE Lighthouse in the Great Belt in Denmark have been measured by accellerometers located in the superstructure. The results document that ice-induced vibrations must be considered in design of marine structures in Denmark, although the ice climate is relatively mild with only about one winter in three having any ice at all. The measured accellerations were decomposed and transformed to deflections at the water level. In spite of the considerable uncertainty associated with this procedure, subsequent load estimation using an effective horizontal stiffness at water level produces very reasonable load estimates. A maximum load of 43 kN was estimated during impact of thin and warm ice. This corresponds to an effective contact pressure of 321 kPa over a 0.9 m by 0.15 m contact area.

Introduction

The Sprogø NE Lighthouse is located in the Great Belt in Denmark, a short distance north of the main navigations spans of the Great Belt Link (Christensen and Skourup, 1991). The exact location is 55°21'6" northern latitude and 11°1'36" eastern longitude. It is a channel marker, known as no W27, for the deep water route through the Great Belt, which connects the North Sea and the Baltic Sea. The lighthouse consists of a directly founded concrete caisson into which a slender, vertical, steel structure is fixed, cf Figure 1. The superstructure is placed on top of the tower at 7.5 m above water level. The water depth is about 11.3 m and the top of the caisson is located 7.25 m below mean water level.

The purpose of this investigation was to establish whether ice-induced vibrations might be responsible for damages that had occurred on other lighthouses in Danish waters. Results from other countries had shown that large accellerations may be caused by ice action, cf eg Nordlund et al (1988), and ice related damages to lighthouses have been observed eg in the Baltic Sea by Reinius et al (1971) and by Mättänen (1975,1981). Accellerometers were placed in the superstructure, and radio communication with shore-based data logging equipment was established. Accellerations were measured during March 1985, while the ice was about 15 cm thick and melting.

Owing to the relatively mild average ice climate in inner Danish waters, cf eg Christensen and Skourup (1991), it is difficult to plan and execute field measurements programmes like the one described here. Significant interannual variations in ice conditions make it necessary to continue for say 4-5 years to have one "good" ice winter. The present programme was mobilized as the ice appeared, and the resulting data are the only available measurements of ice-induced vibrations in Danish waters. The thin and warm ice does not represent typical design conditions very well, but an analysis of the data nevertheless produces interesting results.

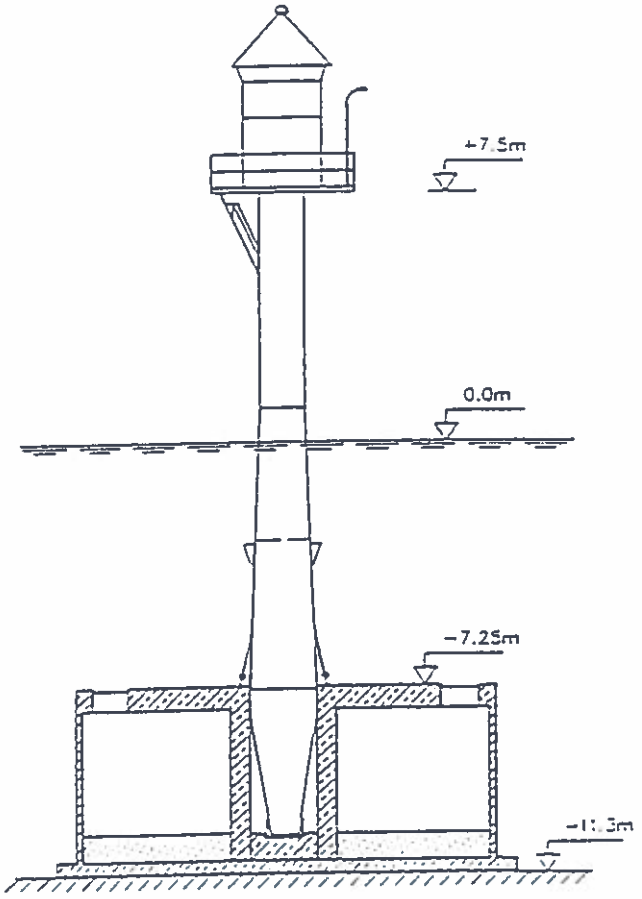

Figure 1; Sketch of the Sprogø NE Lighthouse in the Great Belt in Denmark.

Monitoring Programme

The systems for measurement and transmission of accelleration data were custom designed and built by the first author of this paper, cf Danish Hydraulic Institute (1983). Accelerations were measured in the superstructure in two horizontal directions, denoted x and z. Two Setra accellerometers, model '141A', were used, and the temperature was monitored using a sensor from Analog Devices, type 'AD 590 JF'. For the different sensors, the data interface unit was adapted to a 'DUAL VCO' modulator from Danica Electronics for telemetry. This was a double modulator with frequencies of 750 Hz and 1300 Hz.

The signal was transmitted to an onshore receiver using a 29 MHz transmitter. The mixed 730 Hz and 1300 Hz signal was sent through two parallel band filters with corresponding center frequencies. The data were subsequently stored on an ordinary two-channel analog taperecorder. In order to save power, the transmitter in the lighthouse was activated from the shore station whenever accellerations exceeded a pre-defined threshold.

The monitoring system, which is shown in Figure 2, was completed in September 1983 and subsequently installed in the Sprogø NE Lighthouse. On March 2, 1985, the sea ice in the Great Belt started moving. In the following four days, a total of 14 hours of data were recorded.

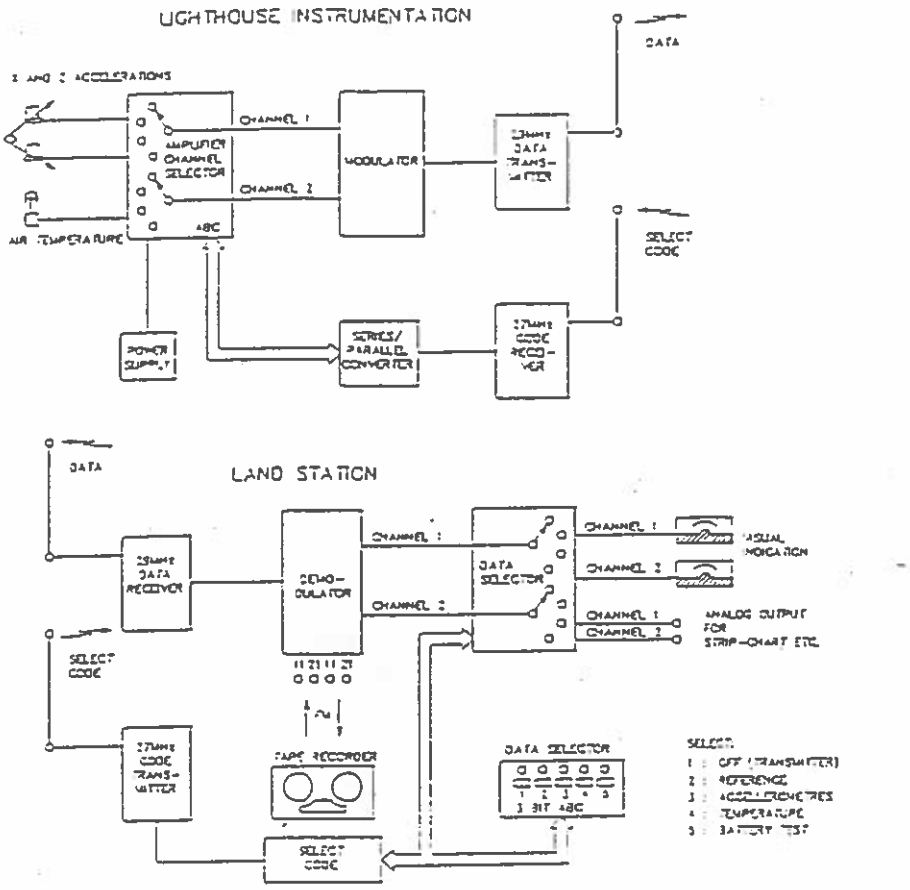

Figure 2; *Instrumentation system for the Sprogø NE Lighthouse.*

Ice conditions

The winter of 1984-85 was colder than average in Denmark. The accumulated freezing degree-day index for the entire winter was 273.4 °Celsius-days, where the average value is about 103 °Celsius-days. The corresponding statistical average recurrence period is roughly 14 years. Two periods of severe cold and wind in January and February had produced sea ice in the Danish waters. The ice conditions peaked around 20 February 1985, where the ice report from 'Statens Istjeneste' read that: *"All Danish waters are covered by fast ice or very compact pack-ice of 15-20 cm thickness with occurrences of thicker ice. In the open Seas, there are only few areas of ice free water...."*. During the period of vibration measurements 2-6 March 1985, the official ice reports said: *"In the Great Belt and the Langeland Belt, there is compact pack-ice of 15-30 cm thickness with bands of thicker ice"*. On-site observations by the first author indicated ice thicknesses of 15-30 cm and ice floe sizes in the range 5 m to 30 m. Figures 3 and 4 show the Sprogø NE Lighthouse in the moving sea ice.

Figure 3: *The Sprogø NE Lighthouse in moving sea ice in early March 1985. Photo by René Zorn.*

Eigenfrequencies

The eigenfrequencies of the lighthouse structure was calculated from beam theory by Gottschalk and Tryde (1976), assuming the tower to be hinged at the bottom, fixed against horizontal translation at the top of the caisson, and free at the top where also a lumped mass is placed to represent the superstructure. The tower structure is conical in the lower part and cylindrical in the upper part, but it was considered massless in the calculations.

The theoretical eigenfrequencies for a new and a rusted tower, respectively, are 4.1 Hz and 2.7 Hz for the first eigenmode, and 18.9 Hz and 14.8 Hz for the second eigenmode. The mode shapes of the three first eigenmodes are shown in Figure 5. A spectrum analysis of the recorded data revealed concentration of the energy around three frequencies:

$$f_1 = 3.1 \ Hz \tag{1}$$

$$f_2 = 10-12 \ Hz \tag{2}$$

$$f_3 = 18-20 \ Hz \tag{3}$$

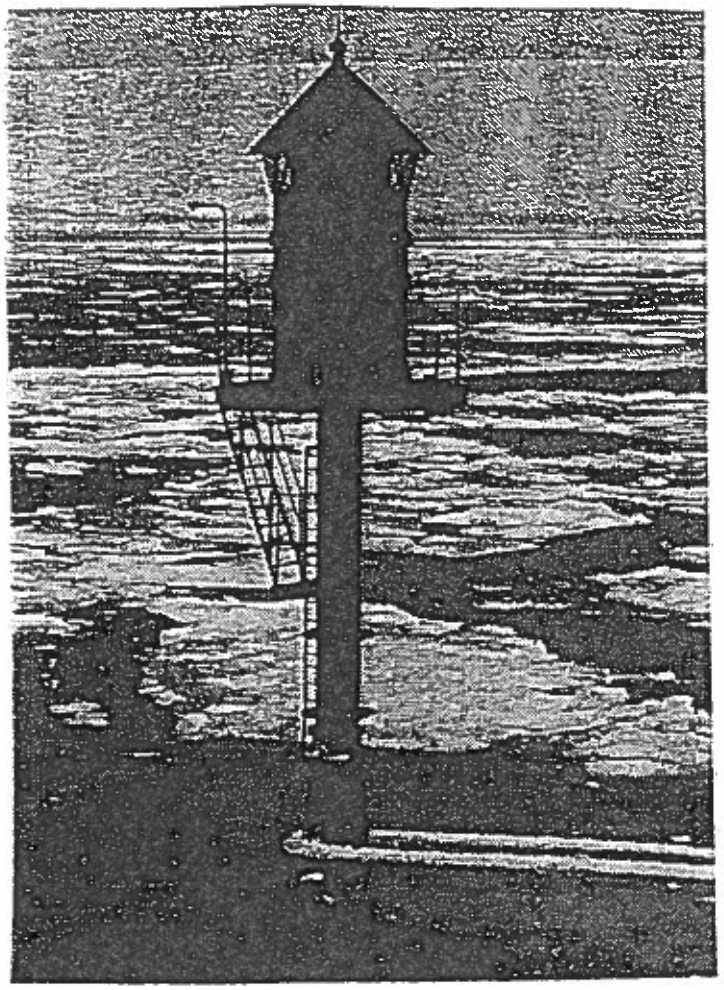

Figure 4; *Close-up of the Sprogø NE Lighthouse in moving sea ice in early March 1985. Photo by René Zorn.*

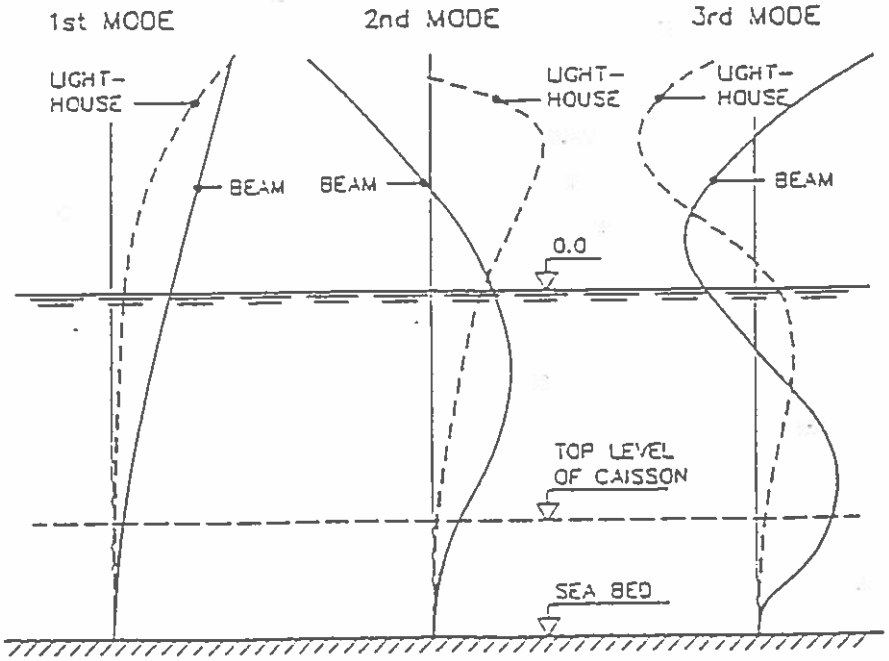

Figure 5; *The mode shapes of the first three eigenmodes for the lighthouse, and for a beam fixed at the bottom and free at the top.*

cf Figure 6. The differences between measured and calculated eigenfrequencies cannot be explained by measurement inaccuracies. The most likely explanation is that the calculated values are based on assumptions that are too idealized. The fixation of the tower structure in the caisson might not be accurately described by the stated assumptions, and also the assumption of a zero tower mass will increase the theoretical eigenfrequencies. Furthermore, as already indicated, the eigenfrequencies are lowered substantially by rusting of the tower.

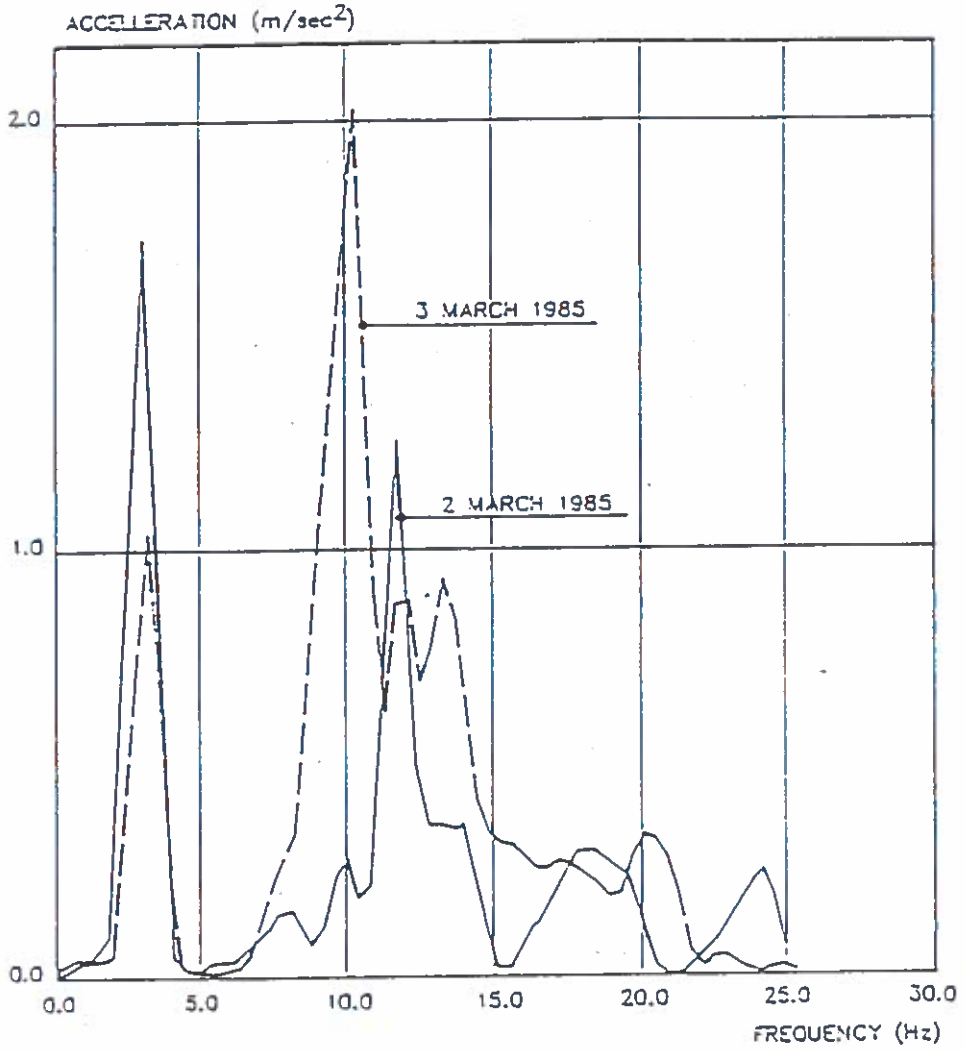

Figure 6: Power spectra of the recorded accellerations on 2 and 3 March, 1985, respectively, on the Sprogø NE Lighthouse.

It is therefore believed, without a full proof, that the peak frequencies observed in the power spectrum in Figure 6 correspond to the three lighthouse eigenmodes illustrated in Figure 5. This implies that theoretically determined eigenfrequencies are too high. The differences between the mode shapes for the lighthouse and for the "fixed-free" beam are primarily caused by the conical shape of the tower, by the support conditions and by the superstructure mass. The mode shapes for the beam do not include a superstructure mass. Full-scale measurements could help define the eigenfrequencies (Turunen and Nordlund, 1988).

Ice Load Estimation

The external load may be determined from the recorded accellerations, cf eg Thomsen (1966). The ice load was assumed to be gradually increasing until failure at which point it drops abruptly to zero. This is a simplified approach, but reasonable for very slender structures. In a brief period following the drop in load, the lighthouse will undergo free, damped oscillations. The oscillations within each eigenmode may be expressed as:

$$x = \frac{P_0}{m_n \omega_n}\left(1 - \frac{e^{-\zeta \omega_n t}}{\sqrt{1-\zeta^2}} \cos(\sqrt{1-\zeta^2}\ \omega_n t - \psi)\right) \tag{4}$$

where x is the deflection at the point of load application, P_0 is the generalized external load, m_n is the generalized mass of the oscillating system, ω_n is the cyclic eigenfrequency of the n'th eigenmode, ζ is the damping ratio, ψ is the phase angle and t represents time.

Equation (4) establishes a direct relation between the deflection and the load at the water level, influenced only by the eigenfrequency and the generalized mass. For the analyses, ω_n was determined from the spectrum analyses, and the generalized mass was determined as:

$$m_n = \int_0^L m(s)\ \phi_n^2(s)\ ds \tag{5}$$

where m(s) is the distributed mass, and $\phi_n(s)$ is the n'th normalized eigenmode.

The calculation of deflections from recorded accellerations is rather inaccurate, because very detailed and accurate determinations of the static and dynamic properties of the tower is needed. In spite of the poor knowledge of central parameters, the calculations are attempted in order to assess the applicability of the technique.

Figure 7 shows the decomposed accelleration signals. These were transformed into deflection signals by division with $(2\pi f_n)^2$, and subsequently transformed to deflections at water level by using the mode shapes in Figure 5. It is important to note how the superstructure mass causes the lighthouse top to have rather limited deflections in the second and third eigenmodes. This illustrates directly why deflections at water level inferred from the recorded deflections at the top are very inaccurate. Table 1 illustrates the calculated deflections of the tower at the water level on 2 March 1985. Similar results were obtained on 3 March 1985.

Table 1; Measured deflections in centimeters at the tower top and calculated deflections at the water level for the Sprogø NE Lighthouse on 2 March 1985.

Frequency (Hz)	Recorded accelleration (m/s^2)	Deflection tower top (cm)	Deflection water level (cm)
3.1	1.7	0.4	0.04
11.8	6.5	0.1	1
18.2	5.0	0.04	0.04
Sum	13.2	0.54	1.08

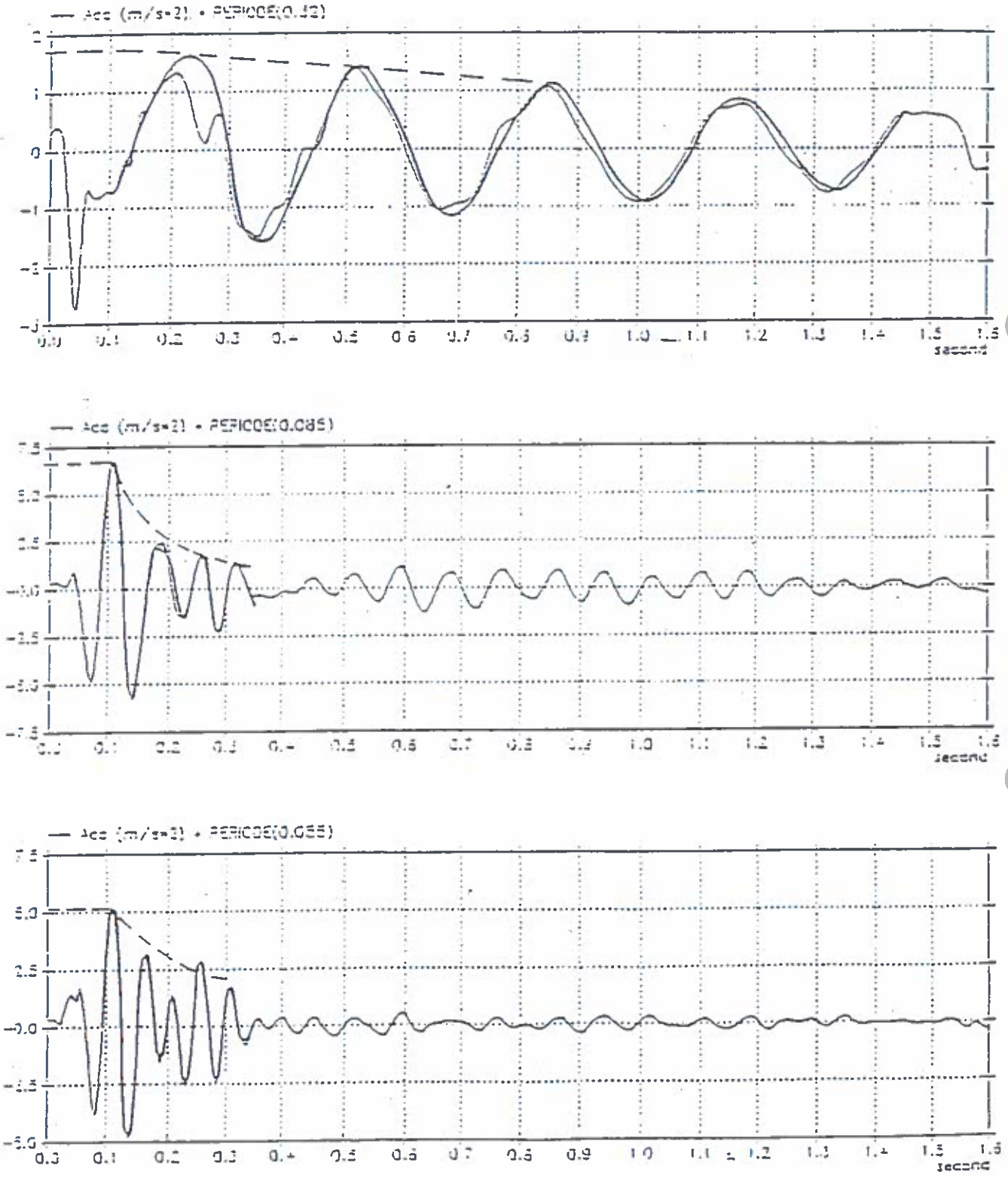

Figure 7; *Decomposed accelleration signals from 2 March 1985.*

The deflections at the water level may be transformed to loads by using the theoretical stiffness of the tower, disregarding hydrodynamic added mass:

$$P = 3 \frac{E \cdot I}{\ell^3} \delta \qquad (6)$$

where δ is the deflection, E the modulus of elasticity and I the moment of inertia for the lighthouse and ℓ the distance from the clamping to the water level. By using values of EI = 0.51 GPa, ℓ = 7.25 m and δ = 0.0108 m (=1.08 cm), the maximum external load becomes:

$$P = 43 \ kN \qquad (7)$$

The structure diameter was 0.9 m and the ice thickness 0.15 m. This result corresponds to an effective contact pressure of 321 kPa, which appears reasonable for thin ice under melting conditions. A typical aspect ratio factor, eg the one proposed by Afanasiev et al (1971), amounts to 1.35, so an unconfined, uniaxial, compressive ice strength of 237 kPa may be inferred. This is a low ice strength, but it corresponds well with the observed conditions.

Design Implications

The Danish Code of Practice for loads on structures, by the Danish Engineering Association (1982), recommends a compressive ice strength of 1250 kPa, more than five times higher, and an ice thickness of 0.6 m, four times higher than the ice that occurred on 2 March 1985. This would then indicate loads on the lighthouse in the order of 230 kN for the higher strength but the same ice thickness. If loads, deflections and accellerations are assumed to interrelate linearly, this would lead to accellerations of (1250/237)13.2 = 69.6 m/s^2 or 7 g. For larger ice thicknesses, even higher accellerations may be achieved. Vibration damping (Mättänen,1975,1977,1981) should thus be considered in lighthouse designs for the inner Danish waters.

The ice load recommended by the Danish Code of Practice is the product of an aspect ratio coefficient, k, the uniaxial compressive ice strength, σ_u, and the contact area, bh. The recommended ice thickness of 0.6 m corresponds to an average recurrence interval of 50 years. The uniaxial compressive sea ice strength for design of marine structures was set at 1.2 MPa in 1982, but subsequently raised to 1.6 MPa. This implies effective contact pressures of 3.5 MPa, and a total design load of 1.9 MN. For the 0.15 m thickness and 237 kPa inferred ice strength on 2 March 1985, the ice load expressions from the Code of Practice yield k = (1+3/(1+0.9/0.15)) = 1.43 and F = 1.43×237×0.9×0.15 = 46 kN, very close to the 43 kN inferred directly from the accelleration measurements. The low strength raises questions regarding the ice failure mode, however, and the result consequently cannot be considered a firm verification of the Code of Practice.

Engelbrektsson (1974) noted that for Swedish offshore lighthouses, a unit ice pressure of 2 MN/m was appropriate for design of moderately exposed lighthouses, and that 3-4 MN/m was needed for the heavily exposed ones. For the Sprogø NE Lighthouse, the Danish Code of Practice recommends 1.9/0.9 = 2.1 MN/m. This appears reasonable considering the much more severe ice conditions off northeastern Sweden. Engelbrektsson (1977) found smaller accellerations, 0.33g, but for large concrete lighthouses.

Although this analysis has focused on superstructure accellerations, it should be noted that dynamic ice loads can cause a significant amplification of the maximum base shear or the rotation. Engelbrektsson (1983) suggested factors as high as 2-3 for the Norströmsgrund Lighthouse, which is a massive concrete lighthouse. The amplification of base shear will most likely be smaller for a slender steel structure such as the Sprogø NE Lighthouse, whereas the amplification of superstructure excursions will be larger than for a concrete lighthouse.

It has been known for some time that the dominant ice failure frequency increases with ice velocity until it approaches the first eigenfrequency of the structure. At some point it will lock-in to this frequency, cf eg Määttänen (1984), and the external ice load is modified by the structural response. The velocity dependency appear to be related to a finite ice failure depth, ie the amount of ice that is crushed during each load cycle. The concept of a finite ice failure depth has been known for years, cf eg Matlock et al (1971) and Eranti et al (1981) who used it in models of ice interaction with slender structures. These models were not capable of reproducing the frequency lock-in, which occurs when the frequency approaches the eigenfrequency. More recent models are capable of this, eg those by Kärnä and Turunen (1989,1990), by Eranti (1992) and by Kärnä (1992). These models apply a zonal approach and account for coupling of pressures in adjacent zones. Experimental results by Kärnä (1993) and Kärnä et al (1993) have established proof for the validity of the concept of a finite ice failure depth. For the Sprogø NE Lighthouse, ice velocities were not measured, and only a modest range of velocities appear to have been present. The accellerations of the superstructure might have been larger for higher ice velocities.

It is worth remembering that slightly inclined tower surfaces can substantially lower the external ice load by causing the ice to fail in flexure rather than compression. Measured ice loads by Frederking et al (1985) and by Määttänen (1977) demonstrate this specifically for lighthouse structures.

Conclusion

Ice-induced vibrations of the Sprogø NE Lighthouse in Denmark were measured during early March 1985. This is the first time ice-induced vibrations have been documented in Danish waters.

With an ice thickness of 0.15 m, the maximum accelleration of the superstructure was 13.2 m/s^2, or 1.34 g. The effective contact pressure was 321 kPa and the inferred compressive ice strength 237 kPa. When increased damping at higher amplitudes is disregarded, use of the 1250 kPa ice strength recommended by the Danish Code of Practice leads to accelleration estimates in the order of 7 g. If furthermore the ice thickness is increased, even higher accellerations are possible.

It thus is reasonable to conclude that ice-induced vibrations can damage slender steel lighthouse structures in Danish waters, unless they are properly designed for. Design accellerations should be at least in the range of 5-10 g.

Acknowledgements

This investigation was carried out by Danish Hydraulic Institute, the Danish Maritime Authority, and the Institute of Hydrodynamics and Hydraulic Engineering at the Technical

University of Denmark. Funding was provided by the Danish Technical Research Council under grant no. 16-3527. Ødegaard & Danneskiold-Samsøe (1986) have performed parallel measurements. We are grateful to all these institutions for both cooperation and funding.

References

Afanasiev, V.P., I.V. Dolgopolov and Z.I. Shvayshten (1971), *Ice pressure on separate supporting structures in the sea*, Originally in Russian, Translated into English as: Draft Translation 346, U.S. Army Cold Regions Research and Engineering Laboratory, Hanover, New Hampshire, USA.

Christensen, F.T. and J. Skourup (1991), *Extreme ice properties*, ASCE J. of Cold Regions Engineering 5(2):51-68.

Danish Engineering Association (1982), *Danish Code of Practice for Safety Regulations for Structures, DS 409 and 410*, 3rd issue, June 1982, Danish Engineering Association, Copenhagen, Denmark.

Danish Hydraulic Institute (1983), *Iskræfter på fyrtårne, Opbygning af udstyr til måling og transmission af data*, In Danish, Report by Danish Hydraulic Institute for the Danish Technical Research Council, Copenhagen, Denmark.

Danish Hydraulic Institute (1993), *Målinger af iskræfter på fyrtårn, Sprogø NØ (W27)*, In Danish, Report by Danish Hydraulic Institute for the Danish Technical Research Council, Copenhagen, Denmark.

Engelbrektsson, A. (1974), *Istryck mot utsjöfyrar*, In Swedish, Symposium kring isfrågor, IVA-meddelande 190, pp 120-134, Ingenjörsvetenskapsakademien, Stockholm, Sweden.

Engelbrektsson, A. (1977), *Dynamic ice loads on a lighthouse structure*, Proc. 4th Int. Conf. on Port and Ocean Engineering under Arctic Conditions (POAC-77), Vol 2, pp 654-663, St. John's, Newfoundland, Canada.

Engelbrektsson, A. (1983), *Observations of a resonance vibrating lighthouse structure in moving ice*, Proc. 7th Int. Conf. on Port and Ocean Engineering under Arctic Conditions (POAC-83), Vol 2, pp 855-864, Helsinki, Finland.

Eranti, E., F.D. Haynes, M.Mättänen and T.T. Soong (1981), *Dynamic ice-structure interaction analysis for narrow vertical structures*, Proc. 6th Int. Conf. on Port and Ocean Engineering under Arctic Conditions (POAC-81), Vol 1, pp 472-479, Quebec City, Quebec, Canada.

Eranti (1992), *Dynamic ice-structure interaction, Theory and applications*, Ph.D. thesis, VTT Publications 90, Technical Research Centre of Finland, Espoo, Finland.

Frederking, R.M.W., M. Sayed, T. Hodgson and W. Berthelet (1985), *Ice force results from the modified Yamachiche Bend lightpier winter 1983-84*, Proc. Canadian Coastal Conference, pp 319-331, St.John's, Newfoundland, Canada.

Gottschalk, P. and P. Tryde (1976), *Bygningsdynamiske aspekter indenfor vandbygning*, In Danish, M.Sc. thesis by the first author under the supervision of the second author, July 1976, Institute of Hydrodynamics and Hydraulic Engineering, Technical University of Denmark, Lyngby, Denmark.

Kärnä, T. (1992), *A procedure for dynamic soil-structure-ice interaction*, Proc. 2nd International Symposium on Offshore and Polar Engineering (ISOPE-92), vol 2, pp 764-770, San Fransisco, California, USA.

Kärnä, T. (1993), *Finite ice failure depth in penetration of a vertical indentor into an ice edge*, Annals of Glaciology, Submitted for Volume 19.

Kärnä, T. and R. Turunen (1989), *Dynamic response of narrow structures to ice crushing*, Cold Regions Science and Technology, 17:173-187.

Kärnä, T. and R. Turunen (1990), *A straightforward technique for analysing structural response to dynamic ice action*, Proc. 9th Int. Conf. on Offshore Mechanics and Arctic Engineering (OMAE-90), Vol 4, pp 135-142, Houston, Texas, USA.

Kärnä, T. T. Nyman, J. Vuorio and E. Järvinen (1993), *Results from indentation tests in sea ice*, Proc. 12th Int. Conf. on Offshore Mechanics and Arctic Engineering (OMAE-93), Vol 4, pp 177-185, Glasgow, Scotland, United Kingdom.

Matlock, H., W.P. Dawkins and J.J. Panak (1971), *Analytical model for ice-structure interaction*, ASCE J. of Engineering Mechanics, EM4:1083-1092.

Määttänen, M. (1975), *Experience of ice forces against a steel lighthouse mounted on the seabed and proposed constructional refinements*, Proc. 3rd Int. Conf. on Port and Ocean Engineering under Arctic Conditions (POAC-75), Vol 2, pp 857-869, Fairbanks, Alaska, USA.

Määttänen, M. (1977), *Ice force measurements at the Gulf of Bothnia by the instrumented Kemi I lighthouse*, Proc. 4th Int. Conf. on Port and Ocean Engineering under Arctic Conditions (POAC-77), Vol 2, pp 730-740, St.John's, Newfoundland, Canada.

Määttänen, M. (1981), *Experience with vibration isolated lighthouses*, Proc. 6th Int. Conf. on Port and Ocean Engineering under Arctic Conditions (POAC-81), Vol 1, pp 491-501, Quebec City, Quebec, Canada.

Määttänen, M. (1984), *Design recommendation for ice effects on aids-to-navigation*, Final Report of the IALA Technical Committee to study the effect of ice on lighthouse structures, International Association of Lighthouse Authorities, Paris, France.

Nordlund, O.P., T. Kärnä and E. Järvinen (1988), *Measurements of ice-induced vibrations of channel markers*, Proc. 9th Int. Assoc. of Hydr. Res. (IAHR) Ice Symposium, Vol 1, pp 537-548, Sapporo, Japan.

Reinius, E., S. Haggård and E. Ernstsons (1971), *Experiences of offshore lighthouses in Sweden*, Proc. 1st Int. Conf. on Port and Ocean Engineering under Arctic Conditions (POAC-71), Vol 1, pp 657-673, Trondheim, Norway.

Thomsen, W.T. (1966), *Vibration Theory and Applications*, Published by George Allen & Unwin Ltd, London, United Kingdom. (First published in the USA in 1965 by Prentice-Hall Inc).

Turunen, R. and O.-P. Nordlund (1988), *Full-scale measurements of the dynamic properties of a channel marker*, Proc. 9th Int. Assoc. of Hydr. Res. (IAHR) Ice Symposium, Vol 1, pp 537-548, Sapporo, Japan.

Ødegaard & Danneskiold-Samsøe (1986), *Målinger af vibrationer på fyrtårnet Sprogø NE (W27)*, In Danish, Report by Ødegaard & Danneskiold-Samsøe Consulting Engineers for Farvandsdirektoratet, Copenhagen, Denmark.

Helge Gravesen

From: Helge Gravesen
Sent: 16 May 2002 11:51
To: 'michael.henriksson@nordex.nu'
Cc: Per Stenholt; Niels Lykkeberg; Jeppe Blak-Nielsen
Subject: FLADEN

Hej Michael
Vi har skønnet at de borede pæle skal være ca 2 m i diameter (3 stk pæle pr. Tripod) og med en længde på 20-25 m under fundament.
Med hensyn til spild regnede vi for Rødsand for enkeltpæle-løsningen (forsigtigt) med at det opborede materiale blev pumpet via en pram med overløb, så 50 % af det opborede materiale tilbageholdes. Vi regnede dermed med 50% spild. det vil også gælde de borede pæle.
Det er dog muligt at mindske sedimentspredningen, hvis overløbsvandet udledes vi et faldrør med diffuser. Herved vil tyngdestrømningen mindske spildet til en størrelsesorden på 10 %.
Der regnes ikke med spild ved rammede pæle.
Det kan yderligere oplyses at der ikke anvendes kunstigt bore-mudder ved enkeltpæle men at der spules med store vandmængder (700 m3//time) med normal penetration på 2 m/time som kan blive reduceret til 0,5-1 m/time i hård moræneler.

Venlig hilsen
Carl Bro as
Helge Gravesen